



V.1

This is to certify that the
dissertation entitled
UNEQUAL SEISMIC SUPPORT MOTIONS OF STEEL DECK ARCH BRIDGES

presented by

Ralph Alan Dusseau

has been accepted towards fulfillment
of the requirements for

PhD degree in Civil and Environmental
Engineering

Major professor

Date August 9, 1985



RETURNING MATERIALS:

Place in book drop to remove this checkout from your record. *FINES* will be charged if book is returned after the date stamped below.

MAY 04 1991

275

OCT 30 1991

029

FEB 26 1992

April 1st 1992

May 29th 1992

UNEQUAL SEISMIC SUPPORT MOTIONS OF STEEL DECK ARCH BRIDGES

Volume I

By

Ralph Alan Dusseau

Copyright by

Ralph Alan Dusseau

1985

A DISSERTATION

Submitted to
Michigan State University
in partial fulfillment of the requirements
for the degree of

DOCTOR OF PHILOSOPHY

Department of Civil and Environmental Engineering

1985

3846714

Copyright by

Ralph Alan Dusseau

1985

ABSTRACT

UNEQUAL SEISMIC SUPPORT MOTIONS OF STEEL DECK ARCH BRIDGES

by

Ralph Alan Dusseau

Seismic analyses were conducted on two steel deck arch bridges: the 1700 foot New River Gorge Bridge (NRGB) in West Virginia and the 700 foot Cold Springs Canyon Bridge (CSCB) in California. The analyses consisted of computer modeling using a finite element program called LINSTRUC. The LINSTRUC program performs time history analyses with either equal or unequal seismic support acceleration as input.

NRGB and CSCB were modeled using "one-plane" models derived by a synthesis of structural properties in the lateral direction. These one-plane models were analyzed under dead and wind loading and the more important of these results were generally within 10% of the values listed in the actual bridge plans.

The principal ground acceleration history was an artificially generated accelerogram called B-1 with an intensity comparable to the 1940 El Centro earthquake. The amplitude of the B-1 accelerogram was increased by 1/3 to yield a maximum ground acceleration of 0.5g. This modified B-1 accelerogram was first applied to all of the bridge supports uniformly (B1-B1 loading) and was then applied with various time lags between the ends of the arch, in particular a time lag based on a wave speed of 5600 feet per second (B1-B1' loading). Both the

B1-B1 and the B1-B1' load cases were applied in the longitudinal, the vertical and the lateral directions.

One of the most important findings involved relatively large arch axial stresses encountered under B1-B1' loading in the longitudinal direction. These stresses resulted from rapid differential arch abutment translations or "dynamic pinching" which caused large vertical inertia forces and hence large arch axial forces.

The CSCB deck design with only one expansion joint was found to be better suited to earthquake prone regions. NRCB with two deck expansion joints had deck stresses and longitudinal bracing stresses approaching or exceeding the yield stress under longitudinal B1-B1 and B1-B1' loading.

Another finding was that the CSCB lateral cable bracing could break under lateral B1-B1 or B1-B1' loading while arch and deck stresses could exceed the allowable stress. These findings confirm previous study results derived from response spectrum analyses of CSCB.

With deep gratitude and appreciation

substantial contributions were made to the

Professor of Civil and Environmental Engineering

University. In his capacity as a

advisor, Dr. Van was knowledgeable, patient, and

counselor, a devil's advocate, and a

Without the assistance and

been possible.

To my wife Ann

and my son Bob

for their love and encouragement

on this and every project.

I would also like to thank

Research and the Department

Michigan State University as well as all

their generous support. Finally, I

and colleague C. M. Lee for his

good listener.

ACKNOWLEDGEMENTS

Chapter With deep gratitude and thanks I wish to acknowledge the Page
substantial contributions made to this study by Dr. Robert K. L. Wen, 1
Professor of Civil and Environmental Engineering, Michigan State 20
University. In his official role as study coordinator and thesis 1
advisor, Dr. Wen was indispensable as a seismic and structures expert, a
counselor, a devil's advocate, a good friend and especially a teacher. 1
Without the assistance and guidance of Dr. Wen this study would not have
been possible. 1.3 1182 Summary..... 3

I would also like to thank both the Division of Engineering 3
Research and the Department of Civil and Environmental Engineering at 2
Michigan State University as well as the National Science Foundation for
their generous support. Finally, I would also like to thank my friend
and colleague C. M. Lee for his assistance as a fellow researcher and a
good listener. 1.3.2 Bridges Analysis..... 8

1.3.3 Ground Acceleration Input..... 9

1.3.4 Analysis Results..... 10

1.4 Preliminary Notes..... 10

1.4.1 Coordinate Axes..... 10

1.4.2 Glossary of Terms..... 11

II LINE ELEMENT STRUCTURAL ANALYSIS PROGRAM..... 13

2.1 Dynamic Analysis Procedures..... 16

2.1.1 Unequal Seismic Support Motion..... 16

TABLE OF CONTENTS (Continued)

Chapter		Page
	2.1.1 Newmark <u>TABLE OF CONTENTS</u>	20
	2.1.2 Sampling Matrix Approximation.....	22
Chapter 2.2	Element and Nodal Features.....	Page
	LIST OF TABLES	xi
	LIST OF FIGURES	xv
I	INTRODUCTION.....	1
1.1	Deck Arch Bridges.....	1
1.1.1	Description.....	1
1.1.2	Characteristics and Design.....	2
1.1.3	1982 Study.....	5
1.2	Objectives of the Present Study.....	5
1.2.1	Unequal Seismic Support Motion.....	6
1.2.2	Inclusion of NRGB.....	6
1.3	Steps Taken in the Present Study.....	6
1.3.1	LINSTRUC Program.....	7
1.3.2	Bridges Analyzed.....	8
1.3.3	Ground Acceleration Input.....	9
1.3.4	Analysis Results.....	10
1.4	Preliminary Notes.....	10
1.4.1	Coordinate Axes.....	10
1.4.2	Glossary of Terms.....	11
II	LINE ELEMENT STRUCTURAL ANALYSIS PROGRAM.....	15
2.1	Dynamic Analysis Procedures.....	16
2.1.1	Unequal Seismic Support Motion.....	16

TABLE OF CONTENTS (Continued)

Chapter	Page
2.1.2 Newmark's Method.....	20
2.1.3 Damping Matrix Approximation.....	22
2.2 Element and Nodal Features.....	23
2.2.1 Beam Element With Warping and Shear	24
2.2.2 Initial Yield Functions.....	24
2.2.3 Slave Nodes and Condensation.....	25
2.3 Stiffness Matrix Processing.....	26
2.3.1 Stiffness Matrix Transformation.....	26
2.3.2 Stiffness Matrix Assembly.....	27
2.4 Other Solution Procedures.....	27
III BRIDGE MODELING, PRECURSORY ANALYSES AND GROUND MOTIONS.....	32
3.1 General Modeling Notes.....	32
3.1.1 Arch and Deck Equivalent Beam Stiffnesses.....	33
3.1.2 Two Dimensional and Simplified Three	33
3.1.3 Arch and Deck Constraints.....	40
3.2 NRCB Description and Models.....	41
3.2.1 Description of NRCB.....	41
3.2.2 Final NRCB Models.....	42
3.3 CSCB Description and Models.....	43
3.3.1 Description of CSCB.....	43
3.3.2 Final CSCB Models.....	44
3.4 Dead Load Analyses.....	45

TABLE OF CONTENTS (Continued)

Chapter	Page
3.4.1	NRGB Dead Load Analysis.....45
3.4.2	CSCB Dead Load Analysis.....46
3.4.3	Dead Load Displacement Discussion.....47
3.4.4	Dead Load Stress Discussion.....48
3.5	Lateral Wind Load Analyses.....48
3.5.1	NRGB Lateral Wind Load Analyses.....49
3.5.2	CSCB Lateral Wind Load Analyses.....49
3.5.3	Wind Load Displacement Discussion.....50
3.5.4	Wind Load Stress Discussion.....51
3.6	Other Static Analyses.....52
3.6.1	Live Plus Impact Load Analyses.....52
3.6.2	Longitudinal Wind Load Analyses.....52
3.6.3	Equivalent Static Force Analyses.....53
3.7	Modal Analyses.....54
3.7.1	NRGB Mode Shapes and Natural Periods.....55
3.7.2	CSCB Mode Shapes and Natural Periods.....56
3.8	Ground Acceleration Histories.....57
3.8.1	Accelerogram Descriptions.....57
3.8.2	Ground Motion Input.....59
IV	ANALYSIS RESULTS.....93
4.1	General Observations.....93
4.1.1	Effects of Longitudinal Force Transfer
4.1.1.1	Mechanisms.....93
4.1.2	Dynamic Arch Pinching Effects.....94

TABLE OF CONTENTS (Continued)

Chapter	Page
4.1.3 Arch and Deck Bracing Responses.....	95
4.2 General Notes.....	95
4.3 X Axis Ground Acceleration Responses.....	96
4.3.1 B1-B1 Loading.....	96
4.3.2 B1-B2 Loading.....	98
4.3.3 B1-B1', B1-B1" and B1-B1"' Loading.....	100
4.3.4 B2-B2 Loading.....	102
4.4 Y Axis Ground Acceleration Responses.....	102
4.4.1 B1-B1 Loading.....	102
4.4.2 B1-B1' Loading.....	104
4.5 Z Axis Ground Acceleration Responses.....	106
4.5.1 B1-B1 Loading.....	106
4.5.2 B1-B2 Loading.....	109
4.5.3 B1-B1' Loading.....	110
4.6 Combined Results.....	111
4.6.1 Simultaneous Accelerogram Applications.....	111
4.6.2 SRSS and Summation of Maximum X, Y and Z Responses.....	113
4.7 Element Responses Versus B-1 Acceleration Levels.....	113
4.7.1 Arch Stresses at the Abutments.....	116
4.7.2 Arch Quarter Point Stresses.....	117
4.7.3 Deck Center Stresses.....	118
4.7.4 Longitudinal Bracing Resultants.....	119
V SUMMARY AND CONCLUSIONS.....	167

TABLE OF CONTENTS (Continued)

Chapter	Page
5.1 SUMMARY OF RESEARCH.....	167
5.2 ARCH, DECK AND BRACING SUMMARIES AND CONCLUSIONS.....	169
5.2.1 ARCH ELEMENTS NEAR THE ABUTMENTS.....	170
5.2.2 ARCH ELEMENTS AT THE QUARTER POINTS.....	170
5.2.3 DECK ELEMENTS NEAR THE CENTER.....	171
5.2.4 LONGITUDINAL BRACING AT THE CROWN.....	171
5.2.5 LATERAL BRACING AT THE CROWN.....	171
5.3 GENERAL CONCLUSIONS.....	172
5.3.1 ONE-PLANE MODELS.....	172
5.3.2 EFFECTS OF UNEQUAL SEISMIC SUPPORT MOTION.....	172
5.3.3 DECK LONGITUDINAL FORCE TRANSFER MECHANISMS.....	173
5.3.4 CSCB LATERAL RESPONSES.....	173
5.3.5 RESPONSE SPECTRUM ANALYSIS.....	174
5.4 FUTURE STUDIES.....	174
APPENDIX A - LINSTRUC DOCUMENTATION AND DISCUSSION.....	177
A.1 Program RESTIFF.....	184
A.1.1 Program NODDATA.....	186
A.1.2 Program ELEMENT.....	194
A.1.3 Program BAND.....	205
A.1.4 Program LOAD.....	211
A.1.5 Program MASS.....	214
A.1.6 Program DYNLOAD.....	217
A.1.7 Program TRUSSEL.....	222
A.1.8 Program SBEAMEL.....	225

TABLE OF CONTENTS (Continued)

Chapter	Page
A.1.9 Program CONDENS.....	230
A.2 Program EIGEN.....	235
A.3 Program STATDYN.....	243
A.3.1 Program LINSOLN.....	244
A.3.2 Program DYNINIT.....	249
A.3.3 Program DYSOLN.....	255
A.4 Overlay Capsules.....	261
A.4.1 Subroutine RECOVER.....	261
A.4.2 Subroutine DISPL.....	264
A.4.3 Subroutine STRESS.....	267
A.4.4 Subroutine ASEMBLE.....	273
A.4.5 Subroutine TRANSFM.....	277
APPENDIX B - BRIDGE MODELING DETAILS.....	281
B.1 NRGB Modeling Details.....	281
B.1.1 Arch Description.....	281
B.1.2 Arch Modeling.....	282
B.1.3 Arch Mass Distribution.....	283
B.1.4 Deck Description.....	284
B.1.5 Deck Modeling.....	286
B.1.6 Main Span Deck Mass Distribution.....	287
B.1.7 Bent Descriptions.....	287
B.1.8 Main Span Bent Modeling.....	289
B.1.9 Main Span Bent Mass Distribution.....	292
B.1.10 Approach Span Modeling.....	292

TABLE OF CONTENTS (Continued)

Chapter	Page
B.1.11 Approach Span Mass Distribution.....	293
B.2 CSCB Modeling Details.....	294
Table B.2.1 Arch Description.....	294
3-1 MRGB B.2.2 Arch Modeling.....	294
3-2 MRGB B.2.3 Deck Description.....	295
3-3 MRGB B.2.4 Deck Modeling.....	297
3-4 MRGB B.2.5 Column, Tower and Cable Descriptions.....	298
3-5 CSCB B.2.6 Main Span Column and Cable Modeling.....	300
3-6 CSCB B.2.7 Approach Span Modeling.....	302
3-7 CSCB B.2.8 Bridge Mass Distribution.....	305
3-8 MRGB B.3 Input Listings.....	305
3-9 CSCB B.4 B-1 and B-2 Accelerograms.....	328
3-10 LIST OF REFERENCES.....	368
3-11 CSCB Deck Wind Load Stress Comparison.....	72
3-12 CSCB Arch Wind Load Stress Comparison.....	73
3-13 CSCB Modal Period Comparison.....	74
3-14 MRGB Modal Response Spectrum Accelerations.....	75
3-15 CSCB Modal Response Spectrum Accelerations.....	76
4-1 MRGB Maximum X Direction El-B1 Responses Versus Static Responses.....	121
4-2 CSCB Maximum X Direction El-B1 Responses Versus Static Responses.....	122
4-3 CSCB Maximum Y Direction El-B1 Responses Versus 1982 Study Results.....	123

LIST OF TABLES (Continued)

Table	Page
<u>LIST OF TABLES</u>	
4-6	NRGB Maximum X Direction Bl-B1 Responses Versus Maximum Bl-B1 Responses.....124
Table	CSCB Maximum X Direction Bl-B1 Responses Versus Maximum Bl-B1 Responses.....124
3-1	NRGB and CSCB Geometric and Design Characteristics.....62
3-2	NRGB Arch Dead Load Displacement Comparison.....63
3-3	NRGB Arch Dead Load Stress Comparison.....64
3-4	NRGB Deck Dead Load Stress Comparison.....65
3-5	CSCB Vertical Arch Dead Load Displacement Comparison.....66
3-6	CSCB Arch Dead Load Stress Comparison.....67
3-7	CSCB Deck Dead Load Stress Comparison.....68
3-8	NRGB Arch Wind Load Stress Comparison.....69
3-9	CSCB Deck Wind Load Displacement Comparison.....70
3-10	CSCB Arch Wind Load Displacement Comparison.....71
3-11	CSCB Deck Wind Load Stress Comparison.....72
3-12	CSCB Arch Wind Load Stress Comparison.....73
3-13	CSCB Modal Period Comparison.....74
3-14	NRGB Modal Response Spectrum Accelerations.....75
3-15	CSCB Modal Response Spectrum Accelerations.....76
4-1	NRGB Maximum X Direction Bl-B1 Responses Versus Static Responses.....121
4-2	CSCB Maximum X Direction Bl-B1 Responses Versus Static Responses.....122
4-3	CSCB Maximum X Direction Bl-B1 Responses Versus 1982 Study Results.....123

LIST OF TABLES (Continued)

Table	Page
4-4 NRGB Maximum X Direction Bl-B1 Responses Versus Maximum Bl-B2 Responses.....	124
4-5 CSCB Maximum X Direction Bl-B1 Responses Versus Maximum Bl-B2 Responses.....	125
4-6 NRGB Static Pinching Stress and Displacement Comparisons.....	126
4-7 CSCB Static Pinching Stress and Displacement Comparisons.....	127
4-8 NRGB Dynamic Pinching Responses Due to Pulse Sine Wave Versus Static Pinching.....	128
4-9 NRGB Maximum X Direction Bl-B1 Responses Versus Maximum Bl-B1' Responses.....	129
4-10 CSCB Maximum X Direction Bl-B1 Responses Versus Maximum Bl-B1' Responses.....	130
4-11 NRGB Maximum X Direction Bl-B1 Responses Versus Maximum Bl-B1" Responses.....	131
4-12 CSCB Maximum X Direction Bl-B1 Responses Versus Maximum Bl-B1" Responses.....	132
4-13 NRGB Maximum X Direction Bl-B1 Responses Versus Maximum Bl-B1" Responses.....	133
4-14 NRGB Maximum X Direction Bl-B1 Responses Versus Maximum B2-B2 Responses.....	134
4-15 NRGB Maximum Y Direction Bl-B1 Responses Versus Static Responses.....	135
4-16 CSCB Maximum Y Direction Bl-B1 Responses Versus Static Responses.....	136

LIST OF TABLES (Continued)

Table	Page
4-17 CSCB Maximum Y Direction Bl-Bl Responses Versus 1982 Study	
Results.....	137
4-18 NRGB Maximum Y Direction Bl-Bl Responses Versus Maximum	
Bl-Bl' Responses.....	138
4-19 CSCB Maximum Y Direction Bl-Bl Responses Versus Maximum	
Bl-Bl' Responses.....	139
4-20 NRGB Maximum Z Direction Bl-Bl Responses Versus Static	
Responses.....	140
4-21 CSCB Maximum Z Direction Bl-Bl Responses Versus Static	
Responses.....	141
4-22 CSCB Maximum Z Direction Bl-Bl Responses Versus 1982 Study	
Results.....	142
4-23 NRGB Maximum Z Direction Bl-Bl Responses Versus Maximum	
Bl-B2 Responses.....	143
4-24 CSCB Maximum Z Direction Bl-Bl Responses Versus Maximum	
Bl-B2 Responses.....	144
4-25 NRGB Maximum Z Direction Bl-Bl Responses Versus Maximum	
Bl-Bl' Responses.....	145
4-26 CSCB Maximum Z Direction Bl-Bl Responses Versus Maximum	
Bl-Bl' Responses.....	146
4-27 NRGB Maximum Combined Bl-Bl Responses Versus Maximum	
Combined Bl-Bl' Responses.....	147
4-28 CSCB Maximum Combined Bl-Bl Responses Versus Maximum	
Combined Bl-Bl' Responses.....	148

LIST OF TABLES (Continued)

Table	Page
4-29 NRGB Maximum Combined Bl-Bl Responses.....	149
4-30 CSCB Maximum Combined Bl-Bl Responses.....	150
4-31 NRGB Maximum Combined Bl-Bl' Responses.....	151
4-32 CSCB Maximum Combined Bl-Bl' Responses.....	152
1-2 Pressure Vessel Analogy.....	13
1-3 Local Coordinate Axes.....	14
2-1 Multiple Degree of Freedom System Example.....	29
2-2 LINGTRUC Straight Beam Element End Displacements.....	30
2-3 LINGTRUC Stiffness Matrix Storage.....	31
3-1 NRGB Elevation View.....	37
3-2 CSCB Elevation View.....	78
3-3 Cantilevered Segment End Fixity.....	79
3-4 CSCB Cantilevered Segment End Loads.....	80
3-5 NRGB Cantilevered Segment End Loads.....	81
3-6 NRGB Typical Cross-section.....	82
3-7 NRGB One-plane Model.....	83
3-8 CSCB Typical Cross-section.....	84
3-9 CSCB One-plane Model.....	85
3-10 NRGB In-plane Modes.....	86
3-11 NRGB Out-of-plane Modes.....	87
3-12 CSCB In-plane Modes.....	88
3-13 CSCB Out-of-plane Modes.....	89
3-14 Modified B-1 Ground Motion.....	90
3-15 Modified B-2 Ground Motion.....	91

LIST OF FIGURES (Continued)

Figures

Page

3-16 Normalized Deck Types LIST OF FIGURES Pressure Vessels

Modified B-1 Types.....92

Figures Longitudinal Force Transfer Mechanisms Page

1-1	Typical Deck Arch Bridge.....	12
1-2	Pressure Vessel Analogy.....	13
1-3	Local Coordinate Axes.....	14
2-1	Multiple Degree of Freedom System Example.....	29
2-2	LINSTRUC Straight Beam Element End Displacements.....	30
2-3	LINSTRUC Stiffness Matrix Storage.....	31
3-1	NRGB Elevation View.....	77
3-2	CSCB Elevation View.....	78
3-3	Cantilevered Segment End Fixity.....	79
3-4	CSCB Cantilevered Segment End Loads.....	80
3-5	NRGB Cantilevered Segment End Loads.....	81
3-6	NRGB Typical Cross-section.....	82
3-7	NRGB One-plane Model.....	83
3-8	CSCB Typical Cross-section.....	84
3-9	CSCB One-plane Model.....	85
3-10	NRGB In-plane Modes.....	86
3-11	NRGB Out-of-plane Modes.....	87
3-12	CSCB In-plane Modes.....	88
3-13	CSCB Out-of-plane Modes.....	89
3-14	Modified B-1 Ground Motion.....	90
3-15	Modified B-2 Ground Motion.....	91

LIST OF FIGURES (Continued)

Figures	Page
3-16 Normalized Rock Spectra Versus A-1 Spectra Versus	343
B-2 Modified B-1 Spectra.....	92
4-1 Deck Longitudinal Force Transfer Mechanisms.....	153
4-2 Static Versus Dynamic Arch Pinching.....	154
4-3 Dynamic Arch Pinching Test Motion.....	155
4-4 NRGB Bl-B1 Deck Center Z Displacement.....	156
4-5 CSCB Bl-B1 Deck Center Z Displacement.....	157
4-6 Differential Bl-B2 Displacement.....	158
4-7 NRGB Arch Element 1 (of 14) - Responses at Node I To	351
B-10 Bl-B1 ⁺ Loading.....	159
4-8 CSCB Arch Element 11 (of 11) - Responses at Node J To	353
B-12 Bl-B1 ⁺ Loading.....	160
4-9 NRGB Arch Element 11 (of 14) - Responses at Node I To	355
B-14 Bl-B1 ⁺ Loading.....	161
4-10 CSCB Arch Element 4 (of 11) - Responses at Node I To	357
B-16 Bl-B1 ⁺ Loading.....	162
4-11 NRGB Deck Element 6 (of 14) - Responses at Node J To	359
B-18 Bl-B1 ⁺ Loading.....	163
4-12 CSCB Deck Element 6 (of 11) - Responses at Node I To	361
B-20 Bl-B1 ⁺ Loading.....	164
4-13 NRGB Longitudinal Bracing Truss Element 2 Responses To	363
B-22 Bl-B1 ⁺ Loading.....	165
4-14 CSCB Longitudinal Bracing Truss Element 1 Responses To	365
B-24 Bl-B1 ⁺ Loading.....	166

LIST OF FIGURES (Continued)

Figures	Page
B-1 NRGB Arch Side Trusses.....	343
B-2 NRGB Arch Lateral K-bracing.....	344
B-3 NRGB Arch Hinges.....	345
B-4 NRGB Deck Floor Stringers.....	346
B-5 NRGB Deck Side Trusses.....	347
B-6 NRGB Deck Lateral X-bracing.....	348
B-7 NRGB Deck Expansion Joint Connections.....	349
B-8 NRGB Deck Abutment Connections.....	350
B-9 NRGB Typical Bents.....	351
B-10 NRGB Bent Cap to Deck Connections.....	352
B-11 NRGB Bent 12.....	353
B-12 NRGB Bent Cantilevered Segment End Fixity and End Loads.....	354
B-13 NRGB Bent 12 Model.....	355
B-14 CSCB Arch Lateral K-bracing.....	356
B-15 CSCB Arch Hinges.....	357
B-16 CSCB Deck Lateral Bracing.....	358
B-17 CSCB Deck Expansion Connections at Panel Point 1.....	359
B-18 CSCB Deck Bearing Connections at Panel Point 20.....	360
B-19 CSCB Column Cross-section and Pedestal Connection.....	361
B-20 CSCB Tower Elevation View.....	362
B-21 CSCB Lateral Cables.....	363
B-22 CSCB Longitudinal Cables.....	364
B-23 CSCB Cable Models.....	365
B-24 NRGB Node and Element Numbers.....	366

LIST OF FIGURES (Continued)

Figures	Page
B-25 CSCB Node and Element Numbers.....	367

Long steel deck arch bridges provide key links in major highway transportation systems. Because of their size and mass, long span highway bridges face the increased risks from earthquake loading. These risks became all too apparent during the 1971 San Fernando earthquake in which highway bridges bore the brunt of the damage inflicted. As a result, a series of studies dealing with the safety of highway bridges under seismic loading have been conducted. The types of highway bridges that have been studied include long multispans highway bridges as reported by Teyssie and Douglas (ref. 1) and suspension bridge structures as reported by Abdel-Shafar (ref. 2). A similar study concerning two steel deck arch highway bridges was completed by this author in 1982 (refs. 3 and 4).

The research reported here is a more in-depth study of long span deck arch bridges. Before presenting the work, a brief discussion of deck arch bridges and their characteristics is in order.

1.1 DECK ARCH BRIDGES

1.1.1 DESCRIPTION

Figure 1-1 is a sketch of a typical steel deck arch bridge. All of the key points and segments of a deck arch are labelled in the sketch. The arch may consist of a pair of steel box ribs or a steel box truss hinged at the abutments, while the deck generally consists of a concrete

CHAPTER I

INTRODUCTION

Long span bridges often provide key links in major highway transportation networks. Because of their size and mass, long span highway bridges face heightened risks from earthquake loading. These risks became all too apparent during the 1971 San Fernando earthquake in which highway bridges bore the brunt of the damage inflicted. As a result, a series of studies dealing with the safety of highway bridges under seismic loading have been conducted. The types of highway bridges that have been studied include long multispan highway bridges as reported by Tseng and Penzien (ref. 1) and suspension bridge structures as reported by Abdel-Ghaffar (ref. 2). A similar study concerning two steel deck arch highway bridges was completed by this author in 1982 (ref. 3 and 4).

The research reported here is a more in-depth study of long span deck arch bridges. Before presenting the work, a brief discussion of deck arch bridges and their characteristics is in order.

1.1 DECK ARCH BRIDGES

1.1.1 DESCRIPTION

Figure 1-1 is a sketch of a typical steel deck arch bridge. All of the key points and segments of a deck arch are labelled in the sketch. The arch may consist of a pair of steel box ribs or a steel box truss hinged at the abutments, while the deck generally consists of a concrete

roadway slab supported by steel stringers or by another steel box truss. The deck supports can be steel columns, bents or towers while the bracing may consist of cables or truss members. The arch span can be anywhere from about 150 feet to 1500 feet while overall bridge length can vary from 300 to 3000 feet. The arch height may reach 300 feet or more while the height of the tallest columns can reach 400 feet.

As much as 60% or more of the bridge mass may be concentrated in the deck. This fact coupled with the very tall arch and column heights would seem to make steel deck arch bridges particularly vulnerable to seismic loading.

1.1.2 CHARACTERISTICS AND DESIGN

The principle behind an arch bridge is analogous to that of the cylindrical pressure vessel illustrated in Figure 1-2. Creating a vacuum in the cylinder causes a uniform external pressure as shown in Figure 1-2a that results in uniform compression in the wall of the vessel with no bending. Putting two pins in the wall of the pressure vessel (if it were possible) and removing half as depicted in Figure 1-2b causes no change in wall stress and gives rise to a situation somewhat similar to that of the arch illustrated in Figure 1-2c. The forces acting on the arch, however, are vertical loads and are not always uniform. Non-uniform loading usually causes bending in the arch. By varying the shape of the arch and/or the strength distribution along the length of the arch, the design engineer can minimize the bending stresses. For example, it is well known that an arch carrying a uniform vertical load will not be subjected to bending if it has the shape of a parabola.

The major loads that the designer of an arch bridge must contend

with in addition to dead load or self weight are as follows:

1. live plus impact loads
2. wind loads
3. thermal loads
4. earthquake loads

The live load to be designed for at a given point in an arch is the distribution of vehicular load that maximizes stress. The impact load which represents the dynamic effects of vehicle loading is determined by adding a certain percentage to the live load. This percentage is at most 30% and declines as the span of the arch increases. The worst cases for bending resulting from live plus impact loads generally occur near the quarter points of the arch (see Figure 1-1). As a result, arches often have larger cross-sections in the vicinity of the quarter points.

Wind loads are generally represented by a uniform pressure based on maximum expected wind velocities. This wind pressure is applied horizontally to the exposed surfaces of the bridge in one of two ways: laterally i.e. normal to the side of the bridge, or skewed with respect to the axis of the bridge. The lateral wind loads cause large lateral bending moments in the arch near the abutments and generally control the design of long span arches in that vicinity.

The skewed wind loads have a lateral or normal component and a longitudinal or shear component both of which act on the exposed surfaces of the bridge. The largest bending due to skewed wind loads occurs between the arch abutments and the quarter points and may surpass the live plus impact load stresses in the areas of the quarter points.

A third type of loading is thermal loading which is caused by

thermal expansion or contraction of the bridge. Most bridges are designed, fabricated and constructed based on an ambient air temperature of about 60 degrees F. Variations of about 60 degrees F plus or minus can be expected during the life of most bridges. For a 1500 foot arch, such temperature variations would be equivalent to differential arch abutment motions of plus or minus approximately 8 inches. The major responses of the arch to such loadings or motion are bending moments that are generally largest near the crown and decrease toward the abutments.

A fourth type of arch bridge loading is seismic loading. In years past, only approximate methods were used to estimate earthquake forces. One such method is the Equivalent Static Force Method in which static loads that are "equivalent" to the earthquake loads are applied to the structure. The total equivalent static load applied is a function of the maximum ground acceleration expected and the structure mass as well as other factors such as the fundamental period of the structure, the soil conditions and the structure type.

Earthquake loads can also be defined in terms of design spectra which are constructed using ground motions recorded during a number of different seismic events. Using these design spectra, the seismic effects on a given structure may be determined by a response spectrum analysis based on superposition of mode shapes. In this method, the values of the responses corresponding to each natural structure mode are combined generally by taking the square root of the sum of the squares of each modal response or some variant of this approach. Before these responses are combined a relative weight or participation factor is computed for each mode based on the design spectra acceleration and

based on other factors such as modal period, the direction in which the spectra is applied (longitudinally, laterally or vertically), the shape of the mode and the percent of critical damping. Such response spectrum analyses were the basis of the 1982 Study of two steel deck arch bridges. Seismic loading can also take the form of actual recorded ground motions applied directly to the bridge supports. The method of analysis used for this type of loading is time history analysis which is the basis of the current study.

1.1.3 1982 STUDY

The 1982 research employed response spectrum analysis as described above to study two steel deck arch bridges: the South Street Bridge (SSB) in Connecticut and the Cold Springs Canyon Bridge (CSCB) in California. The response spectra used were the Normalized Rock Spectra (NRS) (ref. 5) which assume 5% structure damping. The NRS are the basis for the American Association of State Highway and Transportation Officials' (AASHTO's) Response Coefficient "C" (RCC) curves (ref. 6) that are used in the Equivalent Static Force Method discussed above. The results of the 1982 study indicated potential problems with bracing members, bridge supports and member connections especially for CSCB. Arch and deck member stresses, however, seemed to fall safely below yield levels.

1.2 OBJECTIVES OF THE PRESENT STUDY

The two major objectives of the present study were to analyze long span steel deck arch bridges subjected to unequal seismic support motion and to include in these analyses the New River Gorge Bridge (NRGB), the worlds longest steel deck arch bridge.

1.2.1 UNEQUAL SEISMIC SUPPORT MOTION

In the 1982 Study, all bridge supports were presumed to have the same seismic motion. For bridges like CSCB that have spans of 700 feet or more, however, it is generally recognized that motions of the bridge supports could be different under seismic loading. Thus it was thought important in the present study to address the question: What effect does unequal seismic support motion have on long span steel deck arch bridge responses as opposed to the responses under equal motion of the supports?

Analyses with unequal seismic support motion can only be solved by time history analysis. Thus by including CSCB as one of the bridges analyzed, comparisons could be made between the 1982 response spectrum analysis results for CSCB and the time history results from the present analysis.

1.2.2 INCLUSION OF NRGB

A consequence of time and cost limitations encountered in the 1982 study was that NRGB was not analyzed. Being the longest of its kind in the world, NRGB should be worthy of detailed and accurate study despite its location in what is believed to be a relatively low seismic risk zone. By analyzing a very long steel deck arch bridge such as NRGB and a medium to long bridge such as CSCB, the question - What are the effects of arch span on seismic responses? - could be addressed. In addition, the differences in the bridge responses caused by the differences in certain design characteristics could also be determined.

1.3 STEPS TAKEN IN THE PRESENT STUDY

The four key steps in answering the questions posed above were:

1. writing a computer program to perform the analyses

2. choosing the bridges to be analyzed and modeling them
3. choosing the ground acceleration histories to be used in the analyses and determining how best to apply them to the bridge models
4. obtaining and analyzing the results.

1.3.1 LINSTRUC PROGRAM

The first step undertaken in the present research was evaluating available programs for possible use. Among the program features required were time history analysis with unequal seismic support motion as input, a beam element with both shear and warping deformations, condensation of structure degrees of freedom and slave nodes. After failing to find a program that included all or even most of these features, the decision was made to write a new finite-element program.

The first step in writing this program, which was called LINSTRUC, was to formulate the governing equations of motion for unequal seismic support acceleration. This derivation is presented and discussed in Section 2.1.

In using time history analysis with step-by-step numerical integration, two important choices had to be made. The first choice was whether to solve for structure displacements directly or use modal superposition. For simplicity and ease in programming, structure displacements were solved for directly. For the second choice which involved the type of numerical integration procedure to be used, the well known Newmark's Method was chosen. A detailed discussion of the solution procedure which evolved is contained in Section 2.2.

Step-by-step numerical integration can often require hundreds or even thousands of time step solutions for only 30 seconds or less of

ground motion. Thus it was imperative that the models of each structure have the fewest number of degrees of freedom possible. Analyzing complex bridges such as NRGB and CSCB with the fewest degrees of freedom possible required a somewhat new approach. This approach entailed using a so called "one-plane model" to represent each bridge. An example of a one-plane arch bridge model is provided by Figure 1-1. In a one-plane model, the properties of the bridge are lumped laterally into a single plane with the deck represented by a continuous straight beam and the arch represented by a series of straight beams connected end to end. In addition, each bent or pair of columns is represented by a single beam element. Even though the model lies in a single plane, the motions of the model are fully three dimensional.

This one-plane modeling technique required the use of certain special features in the LINSTRUC program. The most important of these special features was a straight beam element with both shear and warping deformation and with "effective" member lengths. These effective lengths were used to achieve equivalence between the stiffnesses of the arch and deck beam elements and the stiffnesses of the arch and deck assemblies they represented. Other more common programming features that helped reduce structure degrees of freedom were condensation and slave nodes. Chapter 2 discusses the major features of the LINSTRUC program while a listing of LINSTRUC itself is contained in Appendix B along with all of the documentation on the program.

1.3.2 BRIDGES ANALYZED

As discussed earlier, NRGB and CSCB were chosen for analysis and both bridges were modeled using one-plane models. These one-plane

models, however, did not include soil springs. NRGB and CSCB are both located in deep river valleys with their supports resting directly on rock. It is generally believed that such site and support conditions, which are common for most deck arch bridges, make the inclusion of soil structure interaction effects unnecessary.

Descriptions of NRGB and CSCB are presented in Chapter 3 along with the one-plane models that were developed for each. Chapter 3 also discusses the accuracy of the one-plane bridge models on the basis of static and modal analyses. Other static analyses, that were performed for comparison with dynamic analysis results, are also discussed in Chapter 3. The details on the various bridge members and how they were modeled are presented in Appendix B along with data input listings for four of the dynamic analyses performed.

1.3.3 GROUND ACCELERATION INPUT

The input for the dynamic analyses which were conducted on NRGB and CSCB were artificially generated ground acceleration histories. The two histories used are referred to as B-1 and B-2. Both were presented in the report entitled "Simulated Earthquake Motions" by Jennings, Housner and Tsai (ref. 7). These histories were chosen because they are similar to the well known El Centro earthquake of 1940 and because they are of relatively short duration (50 seconds). Thus while the B-1 and B-2 accelerograms represent large earthquakes, they are sufficiently short to provide economy in computation cost.

The B-1 accelerogram was applied simultaneously to all of the bridge supports to provide the first load case for each bridge model. In the second loading case, the B-1 accelerogram was applied to the supports on one end of the model with a time lag before application to

the supports at the other end. Finally, the B-1 accelerogram was applied at one end with the B-2 accelerogram applied at the other end. Thus two different types of unequal seismic support motion were applied to each bridge model. Section 3.8 contains detailed discussions of the B-1 and B-2 accelerograms and how they were applied to the bridge models. Appendix B contains complete listings of the B-1 and B-2 accelerograms.

1.3.4 ANALYSIS RESULTS

The responses of each bridge to the above loadings were monitored at one arch abutment, near one arch quarter point and near the center of the deck. The responses of one longitudinal bracing member and one lateral bracing member were also monitored. All of these results are presented and discussed in Chapter 4 along with some general observations that were made in the course of reviewing the results. Chapter 5 summarizes the research and presents the conclusions that were drawn from the analysis results. Areas that warrant further study are also discussed in Chapter 5.

1.4 PRELIMINARY NOTES

1.4.1 COORDINATE AXES

The global coordinate axes used throughout this report are shown in Figure 1-1 and are as follows: the global X axis is horizontal and parallel with the centerline of the bridge, the global Y axis is the vertical axis and the global Z axis is horizontal and normal to the plane of the bridge model. The X axis is often referred to as the longitudinal axis while the Z axis is often called the lateral axis.

The local coordinate axes for the straight beam elements that represent the arch and deck are depicted in Figure 1-3 and are oriented

as follows: the local z axis is along the centerline of the member, the local y axis is horizontal and coincides with the global Z axis, and the local x axis is normal to the local y and z axes and lies in the same plane as the bridge model.

1.4.2 GLOSSARY OF TERMS

The following is a list of frequently used terms and their definitions:

1. "CSCB" refers to the Cold Springs Canyon Bridge
2. "NRGB" refers to the New River Gorge Bridge
3. "longitudinal" refers to the global X direction
4. "vertical" refers to the global Y direction
5. "lateral" refers to the global Z direction
6. "main span deck" refers to that portion of the bridge deck directly over the arch as shown in Figure 1-1
7. "approach span deck" refers to the portions of the bridge deck on either side of the main span deck also as shown in Figure 1-1
8. "arch abutment" refers to the concrete supports or skewbacks at the ends of the arch
9. "panel point" refers to a point where columns or bents connect the arch and deck
10. "panel" refers to a segment of deck or arch lying between two adjacent panel points
11. "NRS" refers to Normalized Rock Spectra
12. "AASHTO" refers to American Association of State Highway and Transportation Officials

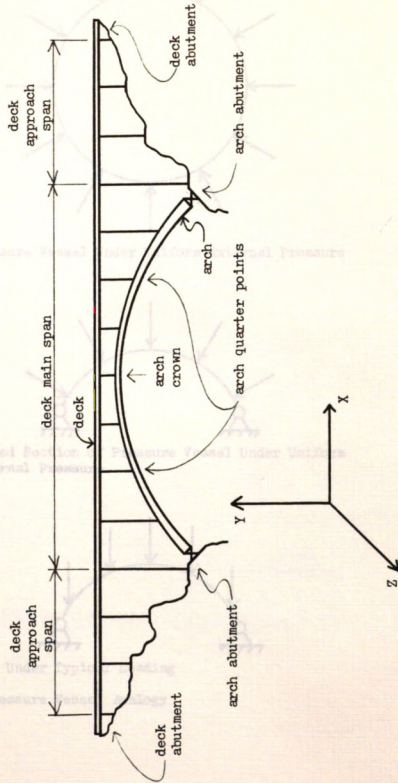
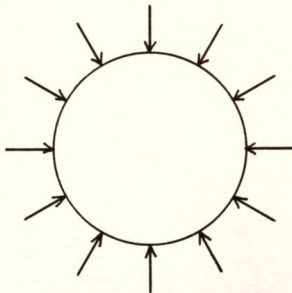
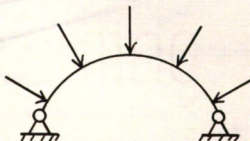


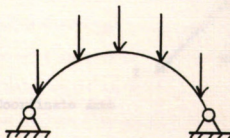
Figure 1-1 Typical Deck Arch Bridge



a) Pressure Vessel Under Uniform External Pressure



b) Pinned Section of Pressure Vessel Under Uniform External Pressure



c) Arch Under Typical Loading

Figure 1-2 Pressure Vessel Analogy

CHAPTER 11

LINE ELEMENT STRUCTURAL ANALYSIS PROGRAM

This chapter discusses the basic features of the line element structural analysis program **LINESTRUC** that was developed for this study. The program is a finite element program written in **FORTRAN V** for use on the CDC Cyber 15V computer at Sandia. **LINESTRUC** utilizes the overlay feature of **FORTRAN V** to reduce the amount of core memory used.

The first section of this chapter discusses the local coordinates and the analysis procedure used by **LINESTRUC**. This discussion includes the derivations of the basic equations of action which govern structures subjected to unequal elastic support motions. They are followed by a presentation of the solution procedure utilized by **LINESTRUC** to solve the equations of motion. Finally, the approximation used to derive the damping matrix in the equations of motion is discussed.

The second section of this chapter discusses the important element and nodal features of the **LINESTRUC** program. They include a straight beam element with warping deformation and shear deformation, initial yield functions for these beam elements, and slave node and condensation features for reducing the number of nodal degrees of freedom. In section three, coordinate transformation of the element stiffness matrices and storage of the global stiffness matrix are discussed. Finally, the last section of this chapter discusses the

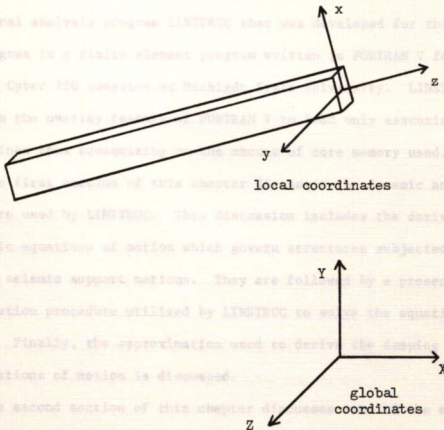


Figure 1-3 Local Coordinate Axes

CHAPTER II

LINE ELEMENT STRUCTURAL ANALYSIS PROGRAM

This chapter discusses the main features of the line element structural analysis program LINSTRUC that was developed for this study. The program is a finite element program written in FORTRAN V for use on the CDC Cyber 750 computer at Michigan State University. LINSTRUC utilizes the overlay feature of FORTRAN V to load only essential subroutines thus economizing on the amount of core memory used.

The first section of this chapter discusses the dynamic analysis procedure used by LINSTRUC. This discussion includes the derivations of the basic equations of motion which govern structures subjected to unequal seismic support motions. They are followed by a presentation of the solution procedure utilized by LINSTRUC to solve the equations of motion. Finally, the approximation used to derive the damping matrix in the equations of motion is discussed.

The second section of this chapter discusses some of the more important element and nodal features of the LINSTRUC program. They include a straight beam element with warping deformation and shear deformation, initial yield functions for these beam elements, and slave node and condensation features for reducing the number of nodal degrees of freedom. In section three, coordinate transformation of the element stiffness matrices and storage of the global stiffness matrix are discussed. Finally, the last section of this chapter discusses the

other solution procedures available with LINSTRUC. They are a static solution by matrix inversion and an eigenvalue/eigenvector solution utilizing the Jacobi Method. Presentations and discussions of the subroutines that make up the LINSTRUC program are contained in Appendix A along with the relevant documentation.

2.1 DYNAMIC ANALYSIS PROCEDURES

The LINSTRUC program uses a step-by-step numerical integration procedure to determine the responses of a structure to unequal seismic support motion. The first step in developing this procedure was the derivation of the governing equations of motion.

2.1.1 UNEQUAL SEISMIC SUPPORT MOTION

In deriving the equations of motion for a structure subjected to unequal seismic support motion, we begin by looking at a general multiple degree of freedom system such as the one illustrated in Figure 2-1. The four degrees of freedom for this system are the vertical translations at the two fixed ends (u_1 and u_2) also called the ground degrees of freedom, and the vertical translations at the two intermediate points (u_3 and u_4) also called the structure degrees of freedom. The equation of motion for a multiple degree of freedom system is:

$$M \ddot{U} + C \dot{U} + K U = 0 \quad (2-1)$$

where M = the mass matrix

\ddot{U} = the acceleration vector for ground and structure degrees

of freedom $U_1 = 0$

C = the damping matrix

\dot{U} = the velocity vector for ground and structure degrees of

freedom $\dot{U}_1 = \dot{U}_2 = 0$

K = the stiffness matrix

U = the displacement vector for ground and structure degrees of freedom

If we write out the individual terms of the matrices and vectors in (2-1) as they apply to the structure in Figure 2-1 and then partition them into ground degrees of freedom and structure degrees of freedom we obtain

$$\begin{vmatrix} m_{11} & m_{12} & m_{13} & m_{14} \\ m_{21} & m_{22} & m_{23} & m_{24} \\ \hline m_{31} & m_{32} & m_{33} & m_{34} \\ m_{41} & m_{42} & m_{43} & m_{44} \end{vmatrix} * \begin{vmatrix} u_1'' \\ u_2'' \\ \hline u_3'' \\ u_4'' \end{vmatrix} + \begin{vmatrix} c_{11} & c_{12} & c_{13} & c_{14} \\ c_{21} & c_{22} & c_{23} & c_{24} \\ \hline c_{31} & c_{32} & c_{33} & c_{34} \\ c_{41} & c_{42} & c_{43} & c_{44} \end{vmatrix} * \begin{vmatrix} u_1' \\ u_2' \\ \hline u_3' \\ u_4' \end{vmatrix} +$$

$$\begin{vmatrix} k_{11} & k_{12} & k_{13} & k_{14} \\ k_{21} & k_{22} & k_{23} & k_{24} \\ \hline k_{31} & k_{32} & k_{33} & k_{34} \\ k_{41} & k_{42} & k_{43} & k_{44} \end{vmatrix} * \begin{vmatrix} u_1 \\ u_2 \\ \hline u_3 \\ u_4 \end{vmatrix} = \begin{vmatrix} 0 \\ 0 \\ \hline 0 \\ 0 \end{vmatrix} \quad (2-2)$$

Now, writing the subgroups of terms in (2-2) as matrices yields

$$\begin{vmatrix} M_{00} & M_{01} \\ \hline M_{10} & M_{11} \end{vmatrix} * \begin{vmatrix} U_0'' \\ \hline U_1'' \end{vmatrix} + \begin{vmatrix} C_{00} & C_{01} \\ \hline C_{10} & C_{11} \end{vmatrix} * \begin{vmatrix} U_0' \\ \hline U_1' \end{vmatrix} +$$

$$\begin{vmatrix} K_{00} & K_{01} \\ \hline K_{10} & K_{11} \end{vmatrix} * \begin{vmatrix} U_0 \\ \hline U_1 \end{vmatrix} = \begin{vmatrix} 0 \\ \hline 0 \end{vmatrix} \quad (2-3)$$

The 0 in Equation 2-3 denotes the ground degrees of freedom while the 1 indicates the structure degrees of freedom. Equation 2-3 is applicable for any multiple degree of freedom system with ground supports. Writing out the last equation of (2-3) in matrix form gives

$$\begin{aligned}
 M_{10} * U_0'' + M_{11} * U_1'' + C_{10} * U_0' + C_{11} * U_1' + \\
 K_{10} * U_0 + K_{11} * U_1 = 0
 \end{aligned} \quad (2-4)$$

Rearranging (2-4) we get

$$\begin{aligned}
 M_{11} * U_1'' + C_{11} * U_1' + K_{11} * U_1 = \\
 - M_{10} * U_0'' - C_{10} * U_0' - K_{10} * U_0
 \end{aligned} \quad (2-5)$$

Defining V to be the vector of displacements U₁ resulting from a

static application of the ground displacements U_0 , we obtain from (2-4), after dropping the velocity and acceleration terms

$$K_{10} * U_0 + K_{11} * V = 0 \quad (2-6)$$

Rearranging (2-6) and differentiating we get

$$V = - K_{11}^{-1} * K_{10} * U_0 \quad (2-7)$$

$$V' = - K_{11}^{-1} * K_{10} * U_0' \quad (2-8)$$

$$V'' = - K_{11}^{-1} * K_{10} * U_0'' \quad (2-9)$$

Now, if we define W to be the displacement vector such that

$$U_1 = W + V \quad (2-10)$$

Then

$$W = U_1 - V \quad (2-11)$$

Differentiating (2-10) gives

$$U_1' = W' + V' \quad (2-12)$$

$$U_1'' = W'' + V'' \quad (2-13)$$

Substituting (2-10), (2-12) and (2-13) into (2-5) we get

$$\begin{aligned} M_{11} * (W'' + V'') + C_{11} * (W' + V') + K_{11} * (W + V) \\ = - M_{10} * U_0'' - C_{10} * U_0' - K_{10} * U_0 \end{aligned} \quad (2-14)$$

In writing the LINSTRUC program, the decision was made to use lumped nodal masses only, therefore for this study the off-diagonal submatrix M_{10} is 0. Rearranging (2-14), setting $M_{10} = 0$ and using (2-7), (2-8) and (2-9) yields

$$\begin{aligned} M_{11} * W'' + C_{11} * W' + K_{11} * W = & (M_{11} * K_{11}^{-1} * K_{10}) * U_0'' + \\ & (C_{11} * K_{11}^{-1} * K_{10} - C_{10}) * U_0' + \\ & (K_{11} * K_{11}^{-1} * K_{10} - K_{10}) * U_0 \end{aligned} \quad (2-15)$$

The last term on the right-hand side of (2-15) is 0.

The structure damping is approximated by assuming it is of the Rayleigh type, thus

$$C = \text{Alpha} * M + \text{Beta} * K \quad (2-16)$$

where C = the structure damping matrix

M = the structure mass matrix

K = the structure stiffness matrix

Alpha = parameter

Beta = parameter

Calculations of Alpha and Beta (see Section 2.1.3) based on the 1982 CSCB modal frequencies showed that both terms were of the same order of magnitude assuming units of feet and kips. With these same units, however, the typical stiffness matrix entry is 100 to 1000 times larger than the typical mass matrix term. Thus it was felt that the damping matrix C would be mainly a function of the stiffness matrix K . Dropping the mass term in (2-16) we find that

$$C_{11} = \text{Beta} * K_{11} \quad (2-17)$$

and

$$C_{10} = \text{Beta} * K_{10} \quad (2-18)$$

If we substitute (2-17) and (2-18) into the middle term on the right-hand side of (2-15) then this term vanishes and

$$M_{11} * W'' + C_{11} * W' + K_{11} * W = (M_{11} * K_{11}^{-1} * K_{10}) * U_0'' \quad (2-19)$$

Solving (2-19) yields the displacements W which are relative to the static structure responses V . To recover the absolute structure displacements U_1 we substitute (2-7) into (2-10) to obtain

$$U_1 = W - K_{11}^{-1} * K_{10} * U_0 \quad (2-20)$$

2.1.2 NEWMARK'S METHOD

The well known Newmark's Method of step-by-step numerical integration as discussed by Bathe (ref. 8) is used in the LINSTRUC program to solve the equation of motion for unequal seismic support acceleration, equation 2-19 as derived in the previous section. Writing this equation with time increment subscripts "n" yields

$$M_{11} * W''^n + C_{11} * W'^n + K_{11} * W_n = M_{11} * K_{11}^{-1} * K_{10} * U_0^n \quad (2-21)$$

The two key equations in Newmark's Method are as follows

$$W'^n = W'^o + (1 - S) * (W''^o + W''^n) * dt \quad (2-22)$$

and

$$W_n = W_o + W'^o * dt + (1/2 - S) * W''^o * dt^2 + S * W''^n * dt^2 \quad (2-23)$$

where dt = the time step increment

S = a parameter

o = subscript denoting values from last time step solution

n = subscript denoting values from current time step solution

In the present study, the parameter S was chosen to be $1/4$ because this insures that the method will be unconditionally stable (ref 8).

Rearranging (2-23) and solving for W''^n we get

$$W''^n = (W_n / (S * dt^2)) - (W_o / (S * dt^2)) - (W'^o / (S * dt)) - ((1/2 - S) / S) * W''^o \quad (2-24)$$

Substituting (2-24) into (2-22) yields

$$\begin{aligned} W'^n = & (W_n / (2 * S * dt)) - (W_o / (2 * S * dt)) \\ & + (1 - (1 / (2 * S))) * W'^o \\ & + (1 - (1/2 - S) / S) * (dt / 2) * W''^o \end{aligned} \quad (2-25)$$

Substituting (2-24) and (2-25) into (2-21) and rearranging gives

$$\begin{aligned}
& (K_{11} + C_{11} / (2 * S * dt) + M_{11} / (S * dt^{**2})) W_n \\
& = M_{11} * K_{11}^{-1} * K_{10} * U_0''^n \\
& + (C_{11} / (2 * S * dt) + M_{11} / (S * dt^{**2})) * W_o \\
& + (C_{11} * ((1 / (2 * S)) - 1) + M_{11} / (S * dt)) * W_o' \\
& + (C_{11} * ((1 / (2 * S)) - 2) * (dt / 2) * W_o'' \\
& + (M_{11} * ((1 / (2 * S)) - 1) * W_o'' \quad (2-26a)
\end{aligned}$$

The term by which W_n is multiplied on the left hand side of (2-26a) is referred as the "effective stiffness matrix" or K_e , while the right hand side of equation 2-26a is called the "effective load vector" or R_e (ref. 8). Therefore

$$K_e * W_n = R_e \quad (2-26b)$$

or

$$W_n = K_e^{-1} * R_e \quad (2-26c)$$

Writing the formula for recovering absolute structure displacements (equation 2-20 in Section 2.1.1) using time increment subscripts yields

$$U_n = W_n - K_{11}^{-1} * K_{10} * U_0^n \quad (2-27)$$

Assuming that the input is to be ground acceleration, then the ground displacement U_0^n in (2-27) may be obtained by numerical integration. If the trapezoidal rule is used, then the ground velocity is

$$U_0'^n = U_0'^o + (U_0''^o + U_0''^n) * (dt / 2) \quad (2-28)$$

and the ground displacement is

$$U_0^n = U_0^o + (U_0'^o + U_0'^n) * (dt / 2) \quad (2-29)$$

The sequence of calculations for each time step in the solution procedure is as follows:

1. Read ground acceleration at current time, $U_0''^n$.

2. Substitute $U_0''^n$, W''^o , W'^o and W_o into (2-26c) and solve for W_n .
3. Substitute W''^o , W'^o , W_o and W_n into (2-25) to get W'^n .
4. Substitute W''^o , W'^o , W_o and W_n into (2-24) to get W''^n .
5. Substitute $U_0''^n$, $U_0''^o$ and $U_0'^o$ into (2-28) to get $U_0'^n$.
6. Substitute $U_0'^n$, $U_0'^o$ and U_{0o} into (2-29) to get U_{0n} .
7. Substitute W_n and U_{0n} into (2-27) to get U_{1n} .
8. Let $W''^o = W''^n$, $W'^o = W'^n$, $W_o = W_n$, $U_0''^o = U_0''^n$, $U_0'^o = U_0'^n$ and $U_{0o} = U_{0n}$.
9. Go to step 1 for the next time increment and repeat until the analysis is complete.

2.1.3 DAMPING MATRIX APPROXIMATION

As stated above, the structure damping matrix is approximated by

$$C = \text{Alpha} * M + \text{Beta} * K \quad (2-16)$$

The parameters Alpha and Beta may be determined by first choosing two of the natural modes of vibration for the structural system and then choosing the fraction of "critical damping" for each mode. The modes chosen generally correspond to the two lowest modes. The LINSTRUC program, however, allows the user to choose any two modes for the calculation.

Letting D_1 and D_2 be the critical damping ratios for the first and second chosen modes, respectively, the constants Alpha and Beta are then computed from the following (ref. 9)

$$D_1 = (1/F_1) * \text{Alpha} + F_1 * \text{Beta} \quad (2-30)$$

$$D_2 = (1/F_2) * \text{Alpha} + F_2 * \text{Beta} \quad (2-31)$$

where F_1 = angular frequency of first chosen mode

F_2 = angular frequency of second chosen mode

2.2 ELEMENT AND NODAL FEATURES

2.2.1 BEAM ELEMENT WITH WARPING AND SHEAR DEFORMATIONS

The truss element which is used by the LINSTRUC program is a standard three-dimensional truss finite element. The straight beam element, however, includes warping deformation (ref. 10 and 11) and shear deformation (ref. 12). This beam element is illustrated in Figure 2-2 and has seven degrees of freedom at each end: translations U_x , U_y and U_z ; rotations Θ_x , Θ_y and Θ_z ; and warping displacement Θ_w .

In order to incorporate the straight beam with warping deformation into LINSTRUC, it was necessary to include a seventh degree of freedom at each node for warping. The LINSTRUC program assumes that if the warping displacement is declared to be free at a given node, then at least one beam element attached to the node must have a warping stiffness I_w . If two beam elements with warping stiffnesses are attached to a node where the warping degree of freedom is free, then LINSTRUC assumes the two beam elements are tangent and that no coordinate transformation with respect to warping is necessary.

The LINSTRUC straight beam element may be utilized as a standard straight beam finite element with six degrees of freedom at each end and no warping deformation. To specify a standard beam element, the user simply leaves the warping stiffness blank in the data input. Similarly, the user may declare the shear deformation for a given beam element to be zero by leaving the corresponding shear area blank in the data input.

2.2.2 INITIAL YIELD FUNCTIONS

In addition to standard stress calculations, LINSTRUC also provides for calculation of "initial yield function" values which are defined to

be the ratio of the total stress to the yield stress. The purpose of the initial yield functions is to provide a measure of how close a member is to yielding at a given corner of its cross-section at node I or at node J. To this end, the axial forces, bending moments and warping bimoments due to combinations of dead load and other loads (dynamic, wind, live, etc.) are each summed at node I and at node J. Then these axial force, bending moment and bimoment sums are divided by their respective yield forces, moments or bimoments to get the corresponding components of the initial yield functions at nodes I and J.

These non-dimensional force, moment and bimoment ratios are then added to or subtracted from one another depending on which corner of the member cross-section is being considered. The final initial yield function formulas are as follows

$$\begin{aligned} IYF_{ni} = & C_{1n} * (A/A_o)_i + C_{2n} * (M_x/M_{xo})_i + C_{3n} * (M_y/M_{yo})_i \\ & + C_{4n} * (M_w/M_{wo})_i \end{aligned} \quad (2-32)$$

$$\begin{aligned} IYF_{nj} = & C_{1n} * (A/A_o)_j + C_{2n} * (M_x/M_{xo})_j + C_{3n} * (M_y/M_{yo})_j \\ & + C_{4n} * (M_w/M_{wo})_j \end{aligned} \quad (2-33)$$

where IYF_{ni} = value of initial yield function n at node i
 IYF_{nj} = value of initial yield function n at node j
 C_{1n} = axial force ratio coefficient for yield function n
 $= +1$ or -1
 C_{2n} = local x - x bending moment ratio coefficient for yield function n
 $= +1$ or -1
 C_{3n} = local y - y bending moment ratio coefficient for yield function n
 $= +1$ or -1
 C_{4n} = warping bimoment ratio coefficient for yield function n
 $= +1$ or -1

$(A/A_0)_i$ = axial force sum to yield force ratio at node i

$(A/A_0)_j$ = axial force sum to yield force ratio at node j

$(M_x/M_{x0})_i$ = local x-x bending moment sum to yield moment ratio
at node i

$(M_x/M_{x0})_j$ = local x-x bending moment sum to yield moment ratio
at node j

$(M_y/M_{y0})_i$ = local y-y bending moment sum to yield moment ratio
at node i

$(M_y/M_{y0})_j$ = local y-y bending moment sum to yield moment ratio
at node j

$(M_w/M_{w0})_i$ = bimoment sum to yield bimoment ratio at node i

$(M_w/M_{w0})_j$ = bimoment sum to yield bimoment ratio at node j

In the present study, the initial yield function values at nodes I and J of a given element and at all four corners of the element cross-section were calculated. In presenting the analysis results in Chapter 4, each initial yield function value was first multiplied by the yield stress in order to recover the stress at the given element node and cross-section corner.

2.2.3 SLAVE NODES AND CONDENSATION

The LINSTRUC program features two general methods for reducing the number of structure degrees of freedom: slave nodes and condensation. The slave node feature allows the user to declare a displacement at a given node, say X translation at node 21, to be equal to the corresponding displacement at a second node, say X translation at node 26. In the assembly of the structure stiffness matrix, the X translations at nodes 21 and 26 would then represent the same degree of freedom. Unlike other finite element programs featuring slave nodes, however, if

in a Program LINSTRUC analysis node 21 is slave to node 26 with respect to X and Y translation and Z rotation for example, a rotation at node 26 will not cause corresponding X and Y translations at node 21 even if the X and Y distances between the two nodes are not zero. Thus slave nodes cannot be used to create rigid links in the LINSTRUC program.

The condensation procedure (ref. 13) allows the user to designate any nodal degree of freedom for condensation. The condensed degrees of freedom are recovered by LINSTRUC after a static solution is completed or after every nth time step is completed in a dynamic solution.

In static analyses, both the structure stiffness matrix and the structure load vector are condensed, but in dynamic analyses only the structure stiffness matrix is condensed. Thus for dynamic solutions, the user must insure that the lumped nodal masses are assigned only to those degrees of freedom that are not to be condensed. Lumped nodal masses may, however, be assigned to degrees of freedom that are slave to other degrees of freedom. In the latter case, the lumped masses at the slave and master nodes are simply added together by the program.

2.3 STIFFNESS MATRIX PROCESSING

2.3.1 STIFFNESS MATRIX TRANSFORMATION

In transforming the local straight beam element stiffness matrices into global coordinates, the LINSTRUC program utilizes the K node method (ref. 12). For this method, the user must specify a third or K node for each beam element. This K node must lie in the same plane as the element's local x and z axes but cannot lie on the element's local z (centroidal) axis. With the K node specified, LINSTRUC then uses the coordinates of the K node to orient the beam element cross-section such that the K node will lie in the local x-z plane of the cross-section.

2.3.2 STIFFNESS MATRIX ASSEMBLY

The structure stiffness matrix is assembled as illustrated in Figure 2-3a with the ground degrees of freedom first and the condensed degrees of freedom last. Before condensation, the matrix is occupied as shown by the shaded areas in Figure 2-3a. After condensation, the structure stiffness matrix is occupied as shown by the shaded area in Figure 2-3b.

The structure stiffness matrix which is symmetric is stored in banded format using three arrays: an array SG which stores the top or ground degree of freedom rows, an array S which stores the middle rows associated with the structure degrees of freedom that are not condensed and an array SC which stores the lower or condensed degree of freedom rows. The portions of the condensed structure stiffness matrix that are stored by arrays SG, S and SC are outlined by dashed lines and labelled in Figure 2-3b. Only the portions of the structure stiffness matrix in the upper left quadrants of the condensed structure stiffness matrix as indicated in Figure 2-3b are used in the static or dynamic solution procedures. The remaining portions of the arrays SG and S, and all of array SC are used only in the recovery of the condensed degrees of freedom.

2.4 OTHER SOLUTION PROCEDURES

Two additional solution procedures that are available to the LINSTRUC user are: static solutions and eigenvalue/eigenvector solutions. The static solutions allow the user to input nodal point loads in any number and order. LINSTRUC then assembles the load vector R, inverts the structure stiffness matrix K and solves for the structure displacements D using

$$D = K^{-1} * R \quad (2-34)$$

The eigenvalue/eigenvector solution routine utilizes the well known Jacobi Method that solves for all of the structure frequencies and mode shapes simultaneously. The method is therefore most efficient when only a small number of equations, say 50 or less, are being solved. The inclusion of an eigenvalue/eigenvector routine in the LINSTRUC program was solely for the secondary purpose of deriving the damping matrix constants Alpha and Beta. Therefore, no further details on the structure of this routine are presented in this report.

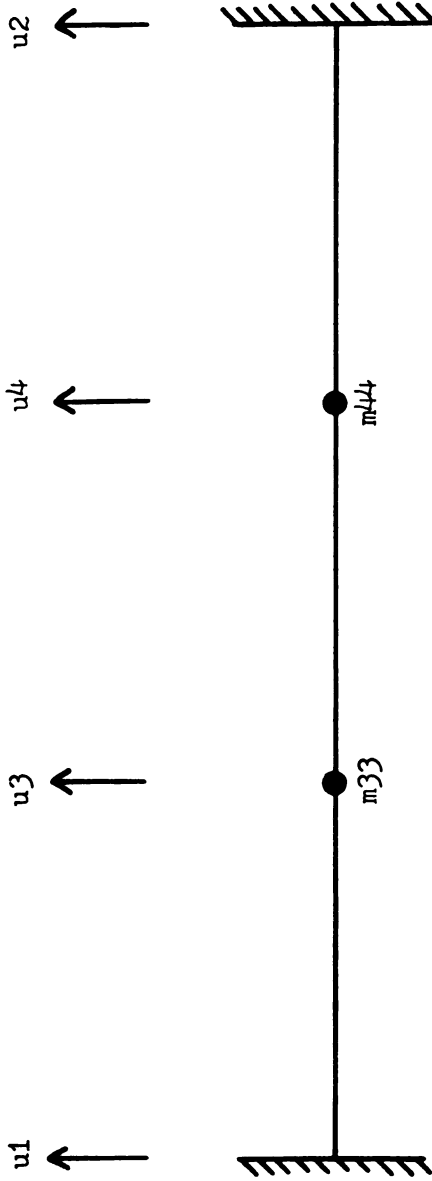


Figure 2-1 Multiple Degree of Freedom System Example

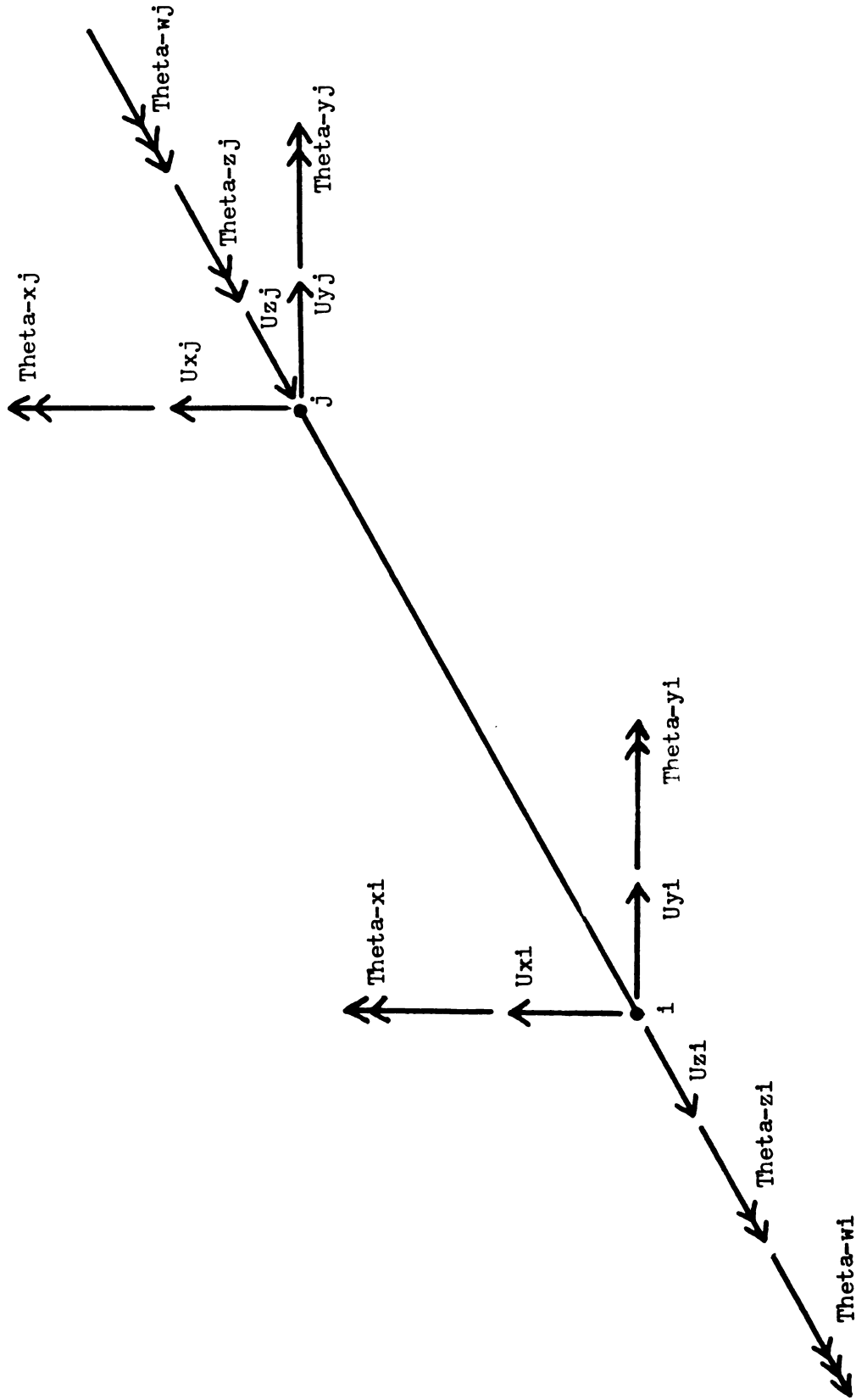
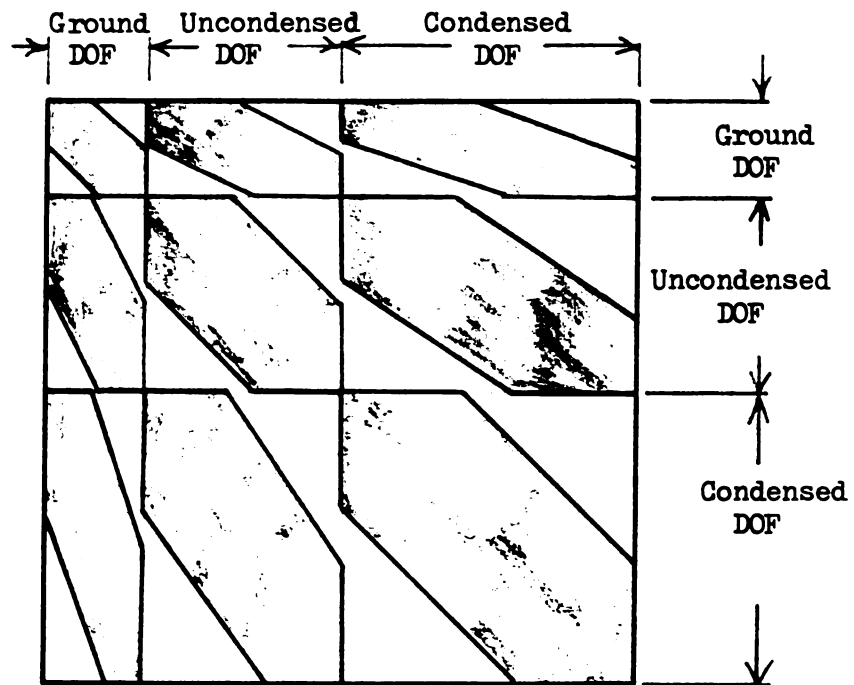
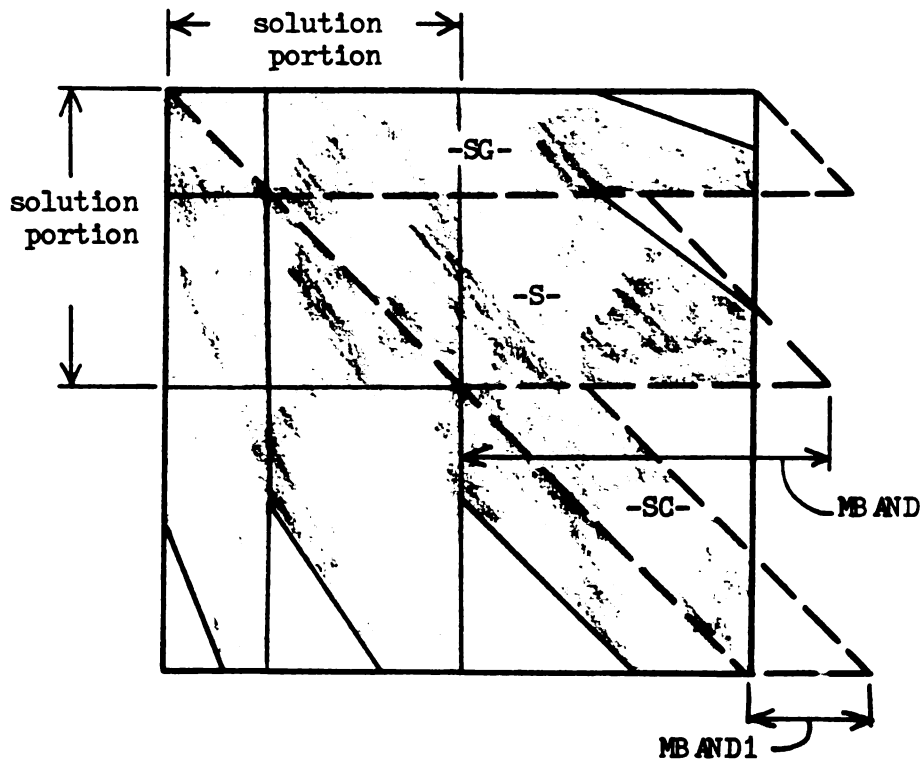


Figure 2-2 LINSTRUC Straight Beam Element End Displacements



a) Matrix Occupancy Before Condensation



b) Matrix Occupancy After Condensation

Figure 2-3 LINSTRUC Stiffness Matrix Storage

CHAPTER III

BRIDGE MODELING, PRECURSORY ANALYSES AND GROUND MOTIONS

This chapter summarizes the development of the finite element linear models of the New River Gorge Bridge (NRGB) and the Cold Springs Canyon Bridge (CSCB), the precursory analyses that were performed on these models and the ground motions employed in the dynamic analyses of these models. Table 3-1 presents a summary of the NRGB and CSCB bridge geometry and design characteristics. Figures 3-1 and 3-2 are elevation views of NRGB and CSCB, respectively. Detailed descriptions of how the bridges were modeled are presented in Appendix B.

The first section of this chapter discusses some general modeling notes that apply to both bridges. The sections that follow describe NRGB and CSCB and the one-plane models of each bridge. The static and modal analyses that were performed on the bridge models and the results of these analyses are then discussed. The static analysis results are compared with results taken from the actual bridge plans that were obtained from the bridge owners. Finally, the chapter concludes by describing the ground acceleration histories that were used in the dynamic analyses.

3.1 GENERAL MODELING NOTES

As discussed in Chapter 1, in order to reduce the number of degrees of freedom in the bridge models and thus reduce the analysis costs, NRGB and CSCB were modeled using "one-plane" models. In these models the

deck was modeled as one continuous beam while the arch was modeled as a series of straight beam elements connected end to end and all lying in one plane. In addition, each bridge was analyzed using two specialized versions of the "one-plane" model.

The first version of the one-plane model was called the "in-plane" model and was used for analyzing bridge responses to longitudinal (X) and vertical (Y) ground motions. This in-plane model was a two dimensional model with only X and Y translations and rotations about the lateral (Z) axis (see Figures 3-1 and 3-2) allowed at each node. In addition, within each in-plane model the rotation degrees of freedom about the Z axis were condensed out. The second one-plane model called the "out-of-plane" model was a specialized three dimensional version with all degrees of freedom except Z axis translation condensed out. This out-of-plane model was used for determining bridge reactions to lateral ground motion.

Further reductions in the number of degrees of freedom were made by assuming that the arch and deck at each panel point would have the same vertical Y axis translations. Still further reductions in the number of degrees of freedom were made by: modeling the approach spans as boundary elements, and by neglecting warping in the arches of both bridges. The latter assumption was based on the box truss or box shaped configuration of the NRGB and CSCB arches (discussed in more detail in Appendix B).

3.1.1 ARCH AND DECK EQUIVALENT BEAM STIFFNESSES

To permit the use of one plane models for NRGB and CSCB, it was necessary to determine the equivalent straight beam stiffnesses for the arch and deck assemblies of each bridge. For the CSCB deck, these

stiffnesses were based on the composite steel stringer and concrete slab cross-section of the deck. In order to derive the equivalent straight beam stiffnesses for the CSCB arch and the NRGB arch and deck, special "cantilevered" segments of these arch and deck assemblies were analyzed.

Each cantilevered segment of arch or deck was one panel in length and included all of the structural members that exist in the actual bridge panel. The member stiffnesses and lengths used in these cantilevered segments were determined in one of three ways. For the NRGB deck, average member stiffnesses and lengths over the entire length of the main span deck and over the lengths of the north and south approach span decks were used to generate three cantilevered segments, respectively. Member stiffnesses and lengths near the NRGB arch abutments were used to develop a cantilevered segment which represented the strongest cross-section in the arch. Similarly, member stiffnesses and lengths at the crown were used to develop a cantilevered segment to represent the weakest cross-section in the NRGB arch. Finally, for the CSCB arch, average member stiffnesses and lengths in the end panels, in the quarter point panels and in the crown panel were used to develop three cantilevered segments, respectively.

As the name implies, each cantilevered segment was "fixed" at one end and loads were applied at the other end. For the CSCB arch, which consists of two box girders connected by lateral members, "fixing" one end of each cantilevered segment meant preventing all translations and global Z axis rotations of the box girders at one end as depicted in Figure 3-3a. For the NRGB deck and arch, which each consist of four box girder chords connected by lateral and vertical truss members, "fixing" one end of each cantilevered segment meant preventing all

translations of these box girder chords at one end as shown in Figure 3-3b.

With one end fixed, a series of equivalent beam loads were then applied to the free end of each cantilevered segment and the resulting displacements were then used to determine equivalent beam stiffnesses. For the CSCB arch assembly, which contains two box girders as described above, forces and moments equivalent to the desired beam end loads were applied at the free ends of the box girder ribs as depicted in Figures 3-3a and 3-4. For the NRGB arch and deck assemblies, each of which has four box girder chords also as described above, equivalent beam end loads were derived by applying point loads to the free ends of the box girder chords as shown in Figures 3-3b and 3-5.

After fixing one end of each cantilevered segment and loading the other end, the fixed and loaded ends were reversed thus yielding two sets of end displacements for each segment. Except for lateral motions of the NRGB and CSCB arch segments, the two sets of end displacements for each cantilevered segment were the same. Equivalent straight beam stiffnesses for both the larger and smaller sets of end displacements were used in wind load analyses of CSCB (discussed in Section 3.5.2). The stiffnesses derived from the larger set of end displacements gave wind load results close to the 1982 Study responses for CSCB. Thus the equivalent straight beam stiffnesses based on the larger set of end displacements were used for all of the NRGB and CSCB analyses.

The translation T_z due to an equivalent beam axial force P applied to the free end of each cantilevered segment (see Figures 3-4a and 3-5a) was substituted into the formula $A_z = (P * L)/(E * T_z)$ in order to find the equivalent beam axial area A_z . Similarly, for the NRGB and

CSCB arches where warping was ignored, a torque M_z was applied to the free end of each cantilevered segment (see Figures 3-4b and 3-5b) and the resulting rotation Φ_z was used to calculate the torsion constant K_t utilizing the formula $K_t = (M_z * L)/(G * \Phi_z)$.

In order to determine the out-of-plane bending moment of inertia I_{xx} and the out-of-plane shear area A_y for each cantilever segment, an equivalent beam shear force P_y was applied to the free end of each cantilevered segment (see Figures 3-4c and 3-5c) resulting in a translation T_p and a rotation R_p . Similarly, an equivalent bending moment M_x was applied (see Figures 3-4d and 3-5d) resulting in a translation T_m and a rotation R_m .

The two pair of flexibility equations that govern these two types of loadings are

$$D_p = (P_y * L^3)/(3 * E * I_{xx}) + (P_y * L)/(G * A_y) \quad (3-1)$$

$$R_p = (P_y * L^2)/(2 * E * I_{xx}) \quad (3-2)$$

$$D_m = (M_x * L^3)/(2 * E * I_{xx}) \quad (3-3)$$

$$R_m = (M_x * L)/(E * I_{xx}) \quad (3-4)$$

The two apparent unknowns in these four equations are I_{xx} and A_y . Because of the symmetry of the flexibility equations, (3-2) and (3-3) will yield the same results, thus only equations 3-1, 3-2 and 3-4 need to be solved in order to achieve equivalence. Letting the length of the element L be a variable yields three equations in the three unknowns I_{xx} , A_y and L_{ex} , where L_{ex} is called the "effective" beam length with respect to out-of-plane motion.

Solving (3-1), (3-2) and (3-4) results in the following three equations for equivalent beam values of I_{xx} , A_y and L_{ex}

$$L_{ex} = (2 * R_p * M_x)/(P_y * R_m) \quad (3-5)$$

$$I_{xx} = (2 * R_p * M_x^{**2}) / (E * P_y * R_m^{**2}) \quad (3-6)$$

$$A_y = (P_y * L_{ex}) / (G * (T_p - (P_y * L_{ex}^{**3}) / (3 * E * I_{xx}))) \quad (3-7)$$

The equivalent beam in-plane bending moment I_{yy} , shear area A_x and effective length L_{ey} were also determined using the procedure described above. Loads P_x and M_y were first applied to the free end of each cantilevered segment (see Figures 3-4e, 3-4f, 3-5e and 3-5f) and the resulting translations and rotations were determined. Equations for in-plane motion, similar to (3-5), (3-6) and (3-7), were then used to determine the values of I_{yy} , A_x and L_{ey} .

For the deck in NRGB, where warping was not ignored, the equivalent beam warping constant I_w and torsion constant K_t were determined by first applying an equivalent beam torque M_z to the free end of each cantilevered segment (see Figures 3-4b and 3-5b) which resulted in an axial rotation R_t and a warping displacement W_t . In addition, a bimoment M_w was applied (see Figures 3-4g and 3-5g) resulting in a rotation R_w and a warping displacement W_w .

The two pair of stiffness equations that govern these two types of loadings are

$$M_z = ((12 * E * I_w) / (L^{**3}) + (36 * G * K_t) / (30 * L)) * R_t - ((6 * E * I_w) / (L^{**2}) + (3 * G * K_t) / (30)) * W_t \quad (3-8)$$

$$0 = (- (6 * E * I_w) / (L^{**2}) - (3 * G * K_t) / (30)) * R_t + ((4 * E * I_w) / (L) + (4 * G * K_t * L) / (30)) * W_t \quad (3-9)$$

$$0 = ((12 * E * I_w) / (L^{**3}) + (36 * G * K_t) / (30 * L)) * R_w - ((6 * E * I_w) / (L^{**2}) + (3 * G * K_t) / (30)) * W_w \quad (3-10)$$

$$M_w = (- (6 * E * I_w) / (L^{**2}) - (3 * G * K_t) / (30)) * R_w + ((4 * E * I_w) / (L) + (4 * G * K_t * L) / (30)) * W_w \quad (3-11)$$

In these four equations, the two apparent unknowns are K_t and I_w .

Equations 3-9 and 3-10 will yield the same results, however, because of the symmetry of the stiffness equations. Therefore, only (3-8), (3-9) and (3-11) need be solved in order to achieve equivalence. As in the case of bending, by letting the length of the element L be a variable in equations 3-8, 3-9 and 3-11, the result is three equations in the three unknowns K_t , I_w and L_{ew} , where L_{ew} is the "effective" beam length with respect to warping and torsion.

Solving (3-8), (3-9) and (3-11) results in the following quadratic equation for equivalent beam length L_{ew}

$$L_{ew} = (-B + (B^2 - 4 * A * C)^{(1/2)}) / (2 * A) \quad (3-12)$$

$$\text{where } A = -(R_m * W_t * M_z) + (W_m * R_t * M_z) + (M_w * W_t^2) \quad (3-12a)$$

$$B = 8 * W_t * M_w * R_t \quad (3-12b)$$

$$C = -15 * M_w * R_t^2 \quad (3-12c)$$

The resulting equation for K_t is

$$K_t = ((30 * M_z * L_{ew}) * (-3 * R_t + 2 * W_t * L_{ew})) / \\ (G * ((36 * R_t - 3 * W_t * L_{ew}) * (-3 * R_t + 2 * W_t * L_{ew}) \\ + ((6 * R_t - 3 * W_t * L_{ew}) * (3 * R_t - 4 * W_t * L_{ew}))) \quad (3-13)$$

And finally, the equation for I_w is

$$I_w = ((G * K_t * L_{ew}^2) * (3 * R_t - 4 * W_t * L_{ew})) / \\ ((60 * E) * (-3 * R_t + 2 * W_t * L_{ew})) \quad (3-14)$$

By deriving the straight beam stiffnesses and effective lengths for each cantilevered segment of arch or deck as described above, the equivalence of the arch and deck straight beam elements and the segments of deck and arch they represent is assured.

Once the equivalent beam stiffnesses for each cantilevered segment were determined, the stiffnesses of all of the straight beams representing the NRGB deck and arch and the CSCB arch were calculated.

For the NRGB deck, the stiffnesses of the main span cantilevered segment were used for all of the beams representing the main span deck.

Likewise, the stiffnesses of each approach span cantilevered segment were used for all of the beams representing that approach span.

As stated earlier, the two cantilevered segments of NRGB arch represented the strongest and weakest cross-sections in the arch. The stiffnesses of each straight beam element representing the arch were calculated using linear interpolation between the largest cross-section stiffnesses near the abutment and the smallest stiffness values at the crown. These calculations were based on two key assumptions: all of the arch panels consist of three equal subpanels and the length of each panel measured along the curve of the arch decreases linearly with the distance along the arch measured from the abutments. For each beam representing the NRGB arch, the member stiffnesses were based on interpolated values at the midpoint of the member and were assumed to be constant across the length of the member. The straight beam elements representing the end panels in the NRGB arch were a special case because each is only about $1\frac{1}{2}$ subpanels in length. For this case the equivalent lengths L_{ex} , L_{ey} and L_{ew} which were calculated for the midpoints of the end elements were simply divided by two.

For the CSCB arch, the three cantilevered segments were based on average member sizes and lengths over five of the eleven arch panels. Thus the stiffnesses for the straight beam elements representing these five panels were taken to be the same as the values calculated for the corresponding cantilevered segments. For the intermediate straight beam elements, the stiffnesses were determined using linear interpolation between the midpoints of the five elements mentioned above. For these

calculations the assumptions were made that all of the arch panels consist of four equal subpanels and that the panel lengths vary linearly.

3.1.2 TWO DIMENSIONAL AND SIMPLIFIED THREE DIMENSIONAL MODELS

As mentioned earlier, in order to further reduce the number of degrees of freedom in the bridge analyses, the full three dimensional one plane model of each bridge was reduced to a two dimensional bridge model (or in-plane model) for input motions in the vertical plane and to a simplified three dimensional bridge model (out-of-plane model) for input motions in the lateral direction. The former was accomplished by first restraining global Z axis lateral translations, longitudinal rotations about the global X axis, vertical rotations about the global Y axis and warping displacements at each node. Then all Z axis rotations were condensed out leaving only X and Y axis translations as degrees of freedom. The out-of-planes models of each bridge were derived simply by condensing out all degrees of freedom except Z axis translation.

3.1.3 ARCH AND DECK CONSTRAINTS

In CSCB, the deck and arch are connected by two columns at each panel point. Assuming that the axial deformations of these columns are minimal and that the deck and arch cross-sections do not deform, then the deck, the arch and the two columns at each panel point must maintain a parallelogram configuration under all loads.

Since the columns in CSCB are truss members which allow no shear transfer between the deck and the arch, and since the one plane model allows only one arch node and one deck node at each panel point, the pair of columns at each panel point were represented in the models by a single truss element. In order to maintain the parallelogram

configuration described above, however, it was necessary to require the arch and deck nodes at each panel point to have the same longitudinal X axis rotation. The only exceptions to this requirement occurred at the center panel points where lateral cables (discussed in more detail in Appendix B) serve to transfer Z axis shear forces. The column-cable combination at each of these center panel points was represented in the models by a single beam element.

In order to further reduce the number of degrees of freedom in the bridge models, the additional requirement that the arch and deck nodes at each panel point have the same vertical Y axis translations was imposed for each of the bridge models of NRGB and CSCB.

3.2 NRGB DESCRIPTION AND MODELS

3.2.1 DESCRIPTION OF NRGB

The New River Gorge Bridge is a four lane, box truss, steel deck arch carrying U.S. 19 over New River Gorge and Route 82 in Fayette County, West Virginia. The principal material used in the bridge is ASTM A588 grade A steel with a minimum yield stress of 50 ksi.

Figure 3-1 as mentioned earlier is an elevation view of NRGB, while Figure 3-6 is a typical bridge cross-section. As can be seen in Figures 3-1 and 3-6, both the deck and arch in NRGB are essentially box trusses consisting of four box girder chords connected by lateral and vertical truss members. Each panel in the deck is divided into 6 subpanels, while the arch panels are each divided into 1 1/2 or 3 subpanels. The deck in NRGB consists of four panels in the north approach span @ 143.5 feet each, five panels in the south approach span @ 126.5 feet each and 14 panels in the main span at 129.75 feet each for a total bridge span of 3030.5 feet. The two hinge arch consists of 12 center panels

@ 129.75 feet each and two end panels @ 71.5 feet each for a total arch span of 1700 feet.

The configuration of the arch is based on a symmetric five-centered series of circular arcs which results in a maximum arch height of 370 feet above the hinges. The deck and arch are connected at each panel point in the main span by bents consisting of two box section columns joined laterally by diagonal truss elements. Similar bents connect the deck to concrete pedestals at each panel point in the north and south approach spans. The approach span deck segments are isolated from the main span deck segment by expansion joints at the tops of bents 5 and 19. At these points, the bottom chords of the approach span deck are pinned to the top of the bents while the bottom chords of the main span deck are attached to the bents by rollers. Thus the expansion joints provide deck axial force, bending moment and warping bimoment releases at these points.

3.2.2 FINAL NRGB MODELS

The one plane models of NRGB which evolved are both illustrated by Figure 3-7. The equivalent arch beams are labelled 1 thru 14 as are the equivalent deck beams. The two truss elements which represent the truss members that transfer longitudinal loads from the deck to the arch (discussed in more detail in Appendix B) are numbered 1 and 2. The deck axial force and moment releases resulting from the expansion joints at the ends of the main span deck are also depicted in Figure 3-7.

The masses lumped at each node in the model are based on the total weights of arch, main span deck, approach span decks and individual bents as listed in the actual bridge plans. The details on how these lumped mass values were derived and on how the individual bridge members

were modeled are presented in Appendix B.

3.3 CSCB DESCRIPTION AND MODELS

3.3.1 DESCRIPTION OF CSCB

The Cold Springs Canyon Bridge, as described on pages 13-22 and 13-23 of the "Structural Steel Designer's Handbook" edited by F. S. Merritt, is a two lane, solid-ribbed steel deck arch spanning Cold Springs Canyon and Route 80 near Santa Barbara, California. All major structural steel members in CSCB are composed of A373 steel which has a minimum yield stress of 33 ksi.

Figure 3-2, which has already been presented, is an elevation view of CSCB while a typical cross-section view is shown in Figure 3-8. As can be seen in Figure 3-2, the bridge consists of 19 panels with two at 46.50 feet in length, 13 at 63.64 feet in length and four at 74.38 feet in length for an overall bridge length of 1217.8 feet. The two hinge arch, as shown in Figure 3-6, consists of two rectangular steel box girders spaced 26 feet apart and hinged at their abutments with 11 panels at 63.64 feet each for a total arch span of 700 feet.

The configuration of the arch is based on a seventh degree polynomial with the southern hinges being 46.48 feet above the northern hinges and with the rise at the highest point of the arch being 144.5 feet above the northern hinges. The use of a seventh degree polynomial was presumably to minimize dead load moments in the arch. This configuration also makes the main span column heights symmetric about the center of the arch span despite the overall deck slope of 6.64%.

The arch ribs are connected laterally by a system of crossframes with one crossframe located at each panel point and three crossframes spaced equally between panel points. This crossframe configuration thus

divides each panel into four subpanels. The ribs are also connected laterally by top and bottom lateral bracing which, along with the crossframes and the arch ribs, creates a box shaped cross-section with the arch ribs acting as the sides.

The columns located at panel points 2 to 5, 7 through 16, 18 and 19 are steel box sections with hinge connections at top and bottom. The towers at panel points 6 and 17 consist of steel box section columns that are rigidly fastened at their bases and are connected laterally by two steel box girder intermediate struts and by a composite steel box girder and concrete slab top strut.

The deck consists of a 7, inch two-way reinforced concrete slab which acts compositely with four longitudinal plate girder stringers, the latter being supported by plate girder floorbeams. The deck is divided into three continuous segments by hinged tower connections at panel points 6 and 17 which provide lateral Z axis moment releases and warping bimoment releases at these points.

Between panel points 11 and 12, systems of bridge rope cables run between the deck and the arch forming pairs of X-bracing in the longitudinal direction and pairs of V-bracing in the lateral direction.

3.3.2 FINAL CSCB MODELS

The one plane models of CSCB which evolved are both represented by Figure 3-9. The equivalent arch beams are labelled 1 thru 11 as are the equivalent deck beams. The two truss elements representing the cables which transfer longitudinal loads from the deck to the arch are numbered 1 and 2. The deck moment releases resulting from the hinge connections at the towers are also shown in Figure 3-9.

In modeling the lateral and longitudinal pairs of cable bracing,

the assumption was made that only one cable in each pair would be acting at any given time i.e. one cable's prestress is presumed to be overcome by compression while the total stress in the second cable is assumed to be below the breaking strength. Thus the stiffnesses of the members used to represent these cables (discussed in more detail in Appendix B) were based on one-half the area of each cable. In the 1982 Study two models of CSCB were used, one with cables and one without. The model with cables used the entire area of each cable which, because of the low prestressing in the cables, meant that this model was valid only for low levels of earthquake motion. The model without cables was believed to be valid only under very high levels of earthquake excitation where the cables would most likely break. Utilizing only half the cable area, the present models of CSCB represent an intermediate state of stress.

The masses lumped at the nodal points in the bridge models were based on the various material weights per foot of bridge listed for CSCB in Reference 14. The details on how these lumped mass values were calculated and on how the individual bridge members were modeled are discussed in Appendix B.

3.4 DEAD LOAD ANALYSES

Static dead load analyses of NRGB and CSCB were performed utilizing the lumped nodal masses described above multiplied by the gravitational acceleration g and applied in the negative Y direction. The results of these analyses are presented in Tables 3-2, 3-3 and 3-4 for NRGB and in Tables 3-5, 3-6 and 3-7 for CSCB.

3.4.1 NRGB DEAD LOAD ANALYSIS

In Table 3-2a a comparison is made between the dead load vertical arch displacements of NRGB as listed in the bridge plans and those

calculated in the present dead load analysis of NRGB. Table 3-2b provides a similar comparison with respect to horizontal arch dead load displacements. As can be seen in the tables, the vertical displacements differ by at most 9.3% while the horizontal displacements differ by more than 9% only near the ends.

Table 3-3 is a comparison between the design engineers estimated top and bottom arch chord stresses as presented in the actual bridge plans and the corresponding stresses calculated in the current dead load analysis. While this comparison yields a maximum difference of 18.9%, the differences in general are less than 12%.

Finally, Table 3-4 compares the top and bottom deck chord dead load stresses which are listed in the bridge plans with the corresponding stresses calculated by the present analysis. As indicated in Table 3-4, the largest difference is 40.7% and occurs near the tower at panel point 6. In most cases, however, the differences are 12% or less.

3.4.2 CSCB DEAD LOAD ANALYSIS

Table 3-5 is a three way comparison between the dead load vertical displacements of the CSCB arch which are listed in the bridge plans, the displacements presented in the 1982 Study and those calculated in the current dead load analysis of CSCB. While the differences between the current dead load displacements and those presented in the bridge plans are as high as 126.6%, the differences between the current values and the values presented in the 1982 Study are generally much smaller.

In Table 3-6 a comparison is made between the maximum arch rib stresses from the 1982 study and those calculated in the present dead load analysis. As can be seen in the table, the values differ by at most 17.2% with most values differing by less than 8%.

Finally, Table 3-7 compares the largest deck stresses as presented in the 1982 study with those determined by the current analysis. The results indicate a maximum difference of 8% near the center of the bridge, while all of the remaining differences are less than 2%.

3.4.3 DEAD LOAD DISPLACEMENT DISCUSSION

While the NRGB dead load displacements seem quite good, the CSCB results do not appear to be as good. The differences between the dead load displacements listed in the CSCB plans and the displacements from the current analysis can be better understood by breaking these differences into two components. The first component involves the differences between the dead load displacements in the bridge plans and those derived in the 1982 Study, while the second component involves the differences between the previous study displacements and those of the current analysis.

The reasons for the differences between the dead load displacements listed in the CSCB bridge plans and those presented in the 1982 Study are difficult to pinpoint because the details of the analysis used in deriving the displacements listed in the bridge plans are not known. The reasons, however, may involve differences in the assumptions made regarding deck stiffness (see Appendix B).

The differences between the CSCB dead load displacements of the 1982 study and those of the current analysis are due most likely to the fact that the arch ribs in the 1982 study were modeled using 44 straight beam elements for each rib while the current analysis utilizes 11 equivalent beam elements to represent the arch. It should be noted, however, that the largest percent differences occur near the abutments where the dead load displacements are smallest. Near the center of the

bridge where the dead load displacements are largest, the results of the present study came closer to the dead load displacements listed in the bridge plans.

3.4.4 DEAD LOAD STRESS DISCUSSION

For both the NRGB deck and arch, the dead load stress results are not as good as the displacement results. The major reason is probably the fact that the design engineers analyzed NRGB using an exact space truss model while the present study used equivalent beams with stiffnesses and section moduli derived by linear interpolation. It should be noted that except for the stresses near the ends of the main span deck, the maximum difference between the engineers' estimated stresses and those of the present study is about 3.3 ksi.

While the CSCB deck dead load stresses are remarkably good, the arch dead load stress results are not quite as good. For both the arch and the deck, however, the largest differences occur near the center where the stresses are somewhat smaller. It should also be noted that the maximum difference between the stresses calculated in the 1982 study and those of the present study is less than 1.6 ksi. This seems quite tolerable considering the current study used equivalent beams with stiffnesses and section moduli based on linear interpolation while the 1982 Study used a nearly exact three dimensional model.

3.5 LATERAL WIND LOAD ANALYSES

Lateral wind load analyses utilizing wind pressures of 60 pounds per square foot and 75 pounds per square foot were performed on NRGB and CSCB, respectively. The results of these analyses are presented in Table 3-8 for NRGB and in Tables 3-9, 3-10, 3-11 and 3-12 for CSCB.

3.5.1 NRGB LATERAL WIND LOAD ANALYSES

Table 3-8 is a comparison between the top and bottom arch chord stresses due to lateral wind loading as presented in the NRGB plans and the values calculated in the current wind load analysis. Both analyses are based on Z direction wind load pressures of 60 psf applied to all exposed surfaces. Between the quarter points and the crown the differences in the stresses are as large as 89.8%. Near the abutments, where the stresses are considerably higher, the differences are less than 11%, however.

Wind load displacements are not presented in the NRGB bridge plans, therefore no comparisons with the current study are possible. In addition, the bridge plans list the wind load forces in only those deck chord members where wind load controls the member's design and no wind load stresses are listed for the deck side truss diagonals. Therefore, the complete state of stress at the deck panel points cannot be determined from the bridge plans and hence a comparison of deck wind load stresses is not feasible.

3.5.2 CSCB LATERAL WIND LOAD ANALYSES

Table 3-9 provides a comparison between the lateral wind load deck displacements derived in the 1982 study of CSCB and those derived in the current study. Both analyses used the same Z direction wind loads based on 75 psf of wind pressure on all exposed bridge surfaces. While the largest difference in deck displacement was 13.8% and occurred near the tower at panel point 17, near the center of the bridge where the displacements are much greater the differences are less than 2.2%.

In Table 3-10 a comparison is made between the arch wind load displacements derived in the 1982 study and those calculated in the

present analysis. As can be seen in the table, the largest difference of 23.8% occurs near the south abutment. Near the center of the arch, however, where the displacements are much greater, the maximum difference is 8.2%.

Table 3-11 makes a comparison between the wind load stresses in the web plates of the exterior deck stringers in the 1982 model and those in the present model. The largest differences in Table 3-11 occur near the towers and at the center of the bridge with the largest value reaching 39%.

Finally, Table 3-12 is a comparison of the arch wind load stresses as calculated in the 1982 study and those derived in the current study. The largest differences are about 77% and occur near the quarter points while the smallest is 12.4% and occurs near the north abutment.

3.5.3 WIND LOAD DISPLACEMENT DISCUSSION

Except for the values near the towers, the percent differences between the CSCB deck wind load displacements calculated in the 1982 study and those derived in the current analysis are quite reasonable. Near the crown, where the displacements are largest, the percent differences are smallest. In all cases the maximum difference is less than 0.8 inches. All of the differences can probably be attributed to the fact that in the current analysis, continuity of warping displacement is required at all of the deck panel points, while in the previous study warping continuity at the panel points was not enforced. Therefore, the current model is stiffer with respect to lateral deck motion. Thus the deck curvature near the towers, which is large in the 1982 study, is much smaller in the current analysis causing the displacements in the present study to be larger near the towers and slightly smaller near the

crown than in the 1982 study.

The CSCB arch wind load displacements in the current study are all less than in the previous study with the largest percent differences occurring near the ends. The major reason for all of the differences is probably the fact that the previous study used a member by member model of the arch while the present study uses equivalent beams. It should be noted, however, that at all panel points the maximum difference between the previous study displacements and those of the present study is less than 0.9 inches.

3.5.4 WIND LOAD STRESS DISCUSSION

While some of the differences in the NRGB arch wind load stresses seem quite large, the results near the ends where the stresses are largest are quite good. In nearly all of the equivalent arch beam members, the stresses calculated in the present analysis fall in between the values for the top and bottom chord stresses as listed in the bridge plans. In addition, all of the differences are less than 1.4 ksi.

Some of the CSCB deck wind load stresses in the present study are much higher than in the 1982 study while others are much lower. The differences are probably caused by the same reason noted with respect to deck wind load displacements, i.e. the difference in warping continuity. In all cases, the largest difference is less than 1.5 ksi, however.

The CSCB arch wind load stresses in the present study are all much lower than in the 1982 study. Because the arch ribs in the previous study were modeled individually, they were free to rotate about their own local x axes independent from the overall arch local x axis rotation. The wind load stresses listed for the 1982 Study include both

arch rib axial stresses and arch rib local x axis bending stresses, but not local y axis bending stresses which are relatively small. The stresses in the present analysis, however, are based only on the overall bending of the arch. Therefore, the wind load stresses derived in the current study were expected to be and are less than in the 1982 Study.

3.6 OTHER STATIC ANALYSES

Three other static analyses were performed on the NRGB and CSCB models: live plus impact load analysis, longitudinal wind load analysis and equivalent static force analysis. The results of these analyses are compared in Chapter 4 with the dynamic analysis results.

3.6.1 LIVE PLUS IMPACT LOAD ANALYSES

The live plus impact load analyses that were conducted on the bridge models were in accordance with section 1.2 of the AASHTO Specifications. The AASHTO live loading used was HS 20-44 which was increased as required by the specifications to account for impact loading. The NRGB live plus impact load stresses that are presented in Chapter 4 are all within 10% of the values listed in the bridge plans. In addition, the live plus impact load stresses that are presented for CSCB are within 9% of the values calculated for the 1982 Study.

3.6.2 LONGITUDINAL WIND LOAD ANALYSES

As stated above, comparisons between live plus impact load results and Y direction dynamic analysis results are presented in Chapter 4 as are comparisons between lateral wind load results and dynamic results in the Z direction. In order to provide similar static load comparisons for X direction dynamic analysis results, longitudinal wind load analyses were conducted on the NRGB and CSCB bridge models.

Standard skewed wind load analyses generally call for wind loads to

be applied to the sides of the bridge at 60 degrees from the normal. Thus the longitudinal component is approximately 2/3 of the lateral wind load. Because the comparisons were to be with X direction dynamic results, only the longitudinal components of the skewed wind load were applied to the bridge models. In addition, no Y axis moments were applied although in the real structure the longitudinal wind load component would act on the side of the bridge thus creating Y axis moments.

3.6.3 EQUIVALENT STATIC FORCE ANALYSES

In order to provide another basis for comparison with the dynamic analysis results, the NRGB and CSCB models were also analyzed using the Equivalent Static Force Method from section 1.2.20 of the AASHTO Specifications. As mentioned in Chapter 1, this method uses a static load to determine approximate earthquake stresses. The total load applied is

$$EQ = F * W * A * R * S / Z \quad (3-15)$$

where EQ = Equivalent static force

F = Framing factor

W = The total dead weight of the structure

A = Maximum expected acceleration at bedrock at the site

R = Normalized rock response

S = Soil amplification spectral ratio

Z = Reduction for ductility and risk assessment

No distribution of this force is specified, although the resultant is required to pass through the center of gravity of the structure.

For NRGB and CSCB, Equivalent Static Force analyses were performed in the X, Y and Z directions with the distribution of the force based on

the lumped mass distribution of the structure. This loading distribution is equivalent to applying a uniform acceleration in the X, Y or Z direction. Rewriting formula (3-15) we get

$$\begin{aligned} eq &= (F * A * R * S / Z) * (m * g) \\ &= U * m * g \end{aligned} \quad (3-16)$$

where eq = Equivalent static force applied at a given node

m = Mass at the given node

g = Gravitational constant

U = Uniform acceleration applied to the structure

$$= F * A * R * S / Z$$

The values of the coefficients used in calculating the uniform acceleration U were taken to be

$$F = 1.0$$

$$A = 0.5$$

R = Value taken from the Normalized Rock Spectra (NRS)

$$S = 1.0$$

$$Z = 1.0$$

The value for R is based on the fundamental period of the structure, thus two values of U were derived for each bridge: an in-plane value for the X and Y directions and an out-of-plane value for the Z direction. The minimum value required by AASHTO for $C = A * R * S / Z$ is 0.10 and in the case of NRGB Z direction motion this is the value which controlled.

3.7 MODAL ANALYSES

In order to determine the constants Alpha and Beta in the damping matrix formula $C = \text{Alpha} * M + \text{Beta} * K$ (as discussed in Section 2.1.3), modal analyses were conducted on both the in-plane and out-of-plane

models of NRGB and CSCB. These analyses led to two sets of constants Alpha and Beta for each bridge: one set for the in-plane model and one set for the out-of-plane model. Thus one set of constants Alpha and Beta were used for longitudinal and vertical ground acceleration and one set for lateral ground acceleration.

While only two modal periods are necessary for deriving the constants Alpha and Beta, the first four mode shapes and their associated natural periods for each model of NRGB and CSCB are discussed in the following sections.

3.7.1 NRGB MODE SHAPES AND NATURAL PERIODS

The first four modes for the in-plane model of NRGB are depicted in Figure 3-10. The first mode has a natural period of 4.18 seconds and is a full wave vertical motion of the deck and arch. Mode two is a $1 \frac{1}{2}$ wave vertical deck and arch motion with a natural period of 2.00 seconds. The third mode has a natural period of 1.43 seconds and represents a two wave vertical motion of the deck and the arch. Finally, mode four is characterized by large horizontal motions of the deck toward the center of the bridge. This latter mode has a natural period of 1.21 seconds and also exhibits a small vertical deck and arch motion in the form of $1 \frac{1}{2}$ waves.

Figure 3-11 illustrates the first four modes for the out-of-plane model of NRGB. The first mode has a natural period of 6.78 seconds and is a half wave lateral motion of the deck and the arch. Mode two with a natural period of 3.48 seconds is a full wave lateral deck motion accompanied by a small full wave lateral arch motion. The third mode has a natural period of 2.40 seconds and is characterized by a large $1 \frac{1}{2}$ wave lateral motion of the deck and a small $1 \frac{1}{2}$ wave lateral

motion of the arch. Finally, mode four has a natural period of 1.89 seconds and is characterized by a large two full wave lateral motion of the deck accompanied by a small full wave lateral motion of the arch.

3.7.2 CSCB MODE SHAPES AND NATURAL PERIODS

The first four modes for the in-plane model of CSCB are depicted in Figure 3-12. The first mode has a natural period of 2.32 seconds and is a full wave vertical motion of the deck and arch. Mode two is a 1 1/2 wave vertical deck and arch motion with a natural period of 1.19 seconds. The third mode has a natural period of 0.65 seconds and is characterized by a large longitudinal translation of the deck and a moderately large two full wave vertical motion of the deck and the arch. Finally, mode four has a natural period of 0.63 seconds and is characterized by a large two full wave vertical motion of the deck and the arch and a moderately large longitudinal translation of the deck.

Figure 3-13 illustrates the first four modes for the out-of-plane model of CSCB. The first mode has a natural period of 2.67 seconds and is a half wave lateral motion of the deck and the arch. Mode two has a natural period of 1.54 seconds and is characterized by a large full wave lateral motion of the deck with a small lateral half wave motion of the arch. The third mode has a natural period of 1.01 seconds and is characterized by a large 1 1/2 wave lateral motion of the deck accompanied by a small half wave lateral motion of the arch. Finally, mode four has a natural period of 0.69 seconds and is characterized by a large half wave lateral motion of the arch accompanied by a moderately large two wave lateral motion of the deck.

Tables 3-13a and 3-13b compare the natural periods for the CSCB modes derived in the 1982 study and those presented in this report.

Table 3-13a compares the natural periods of the in-plane modes associated with the in-plane model of CSCB and Table 3-13b compares the natural periods of the out-of-plane modes associated with the out-of-plane model. The in-plane modal periods differ by less than 10% and thus the results of the current analysis with regards to the in-plane modes seem quite good. For the out-of-plane modes the differences vary from 21.1% down to as little as 0.1%. These results can also be looked at as quite good since only the first two periods were used to derive Alpha and Beta and the maximum difference for these two modes is only 7.5%.

3.8 GROUND ACCELERATION HISTORIES

3.8.1 ACCELEROGRAM DESCRIPTION

As discussed in Chapter 1, two artificially generated ground acceleration histories were utilized as input for the dynamic analyses that were conducted on NRGB and CSCB. Both are presented in the report entitled "Simulated Earthquake Motions" by Jennings, Housner and Tsai (ref. 7) and are referred to as B-1 and B-2 in their report. These accelerograms which have a duration of 50 seconds each are intended to represent shaking close to the fault line of an earthquake of Magnitude 7 on the Richter Scale. Thus B-1 and B-2 have characteristics that are similar to the El Centro Earthquake of 1940 and the Taft Earthquake of 1952. In this study, only the first 30 seconds which are the most intense portions of the type B accelerograms were used. The ground displacements during these first 30 seconds are plotted in Figures 3-14 and 3-15 for accelerograms B-1 and B-2, respectively. The B-1 and B-2 acceleration histories themselves are listed in Appendix B.

As stated in Chapter 1, the B type accelerograms were chosen

because they represent strong earthquake motions but still have relatively short durations. Thus by using the type B accelerograms, dynamic responses to large earthquakes could be determined without using more than 30 seconds of ground acceleration history thus saving greatly on computation cost.

These artificially generated accelerograms also have the advantage of having uniformly spaced time steps with 0.025 seconds ($1/40$ of a second) per step. Thus the time steps used in the analyses could be chosen to coincide with the accelerogram time steps thus insuring that no peak ground accelerations would be missed. In practice, time steps of exactly 0.025 seconds each were used in the analyses. Smaller time steps were checked and found to give maximum results within 1% of the results for 0.025 seconds. Thus $1/40$ of a second was deemed to be small enough to give accurate results. In addition, nodal displacements and element stresses were recovered at every 10th time step or every $1/4$ of a second.

It should also be noted that four types of accelerograms referred to as A through D are made available in the report by Jennings, Housner and Tsai. Of the four types, the type B accelerograms represent ground acceleration histories similar to two of the largest earthquake histories ever recorded. The type C and D accelerograms, however, represent shorter and less intense earthquakes while the type A accelerograms represent extremely long earthquakes with intensities (approximately 8 on the Richter scale) greater than any acceleration history recorded to date.

The amplitude of the B-1 and B-2 accelerograms was increased by 33.3% so that the maximum ground acceleration in either would be 0.5g.

By using accelerograms with maximum ground accelerations of 0.5g, direct comparisons could be made with the CSCB results of the 1982 Study which were derived from response spectrum analyses based on a spectra with a maximum ground acceleration of 0.5g.

Figure 3-16 is a plot of the Normalized Rock Spectrum which was used in the 1982 Study versus the response spectrum for the B-1 accelerogram increased by 33.3% and versus the spectrum for the A-1 accelerogram. As can be seen in the figure, the Normalized Rock Spectrum accelerations are smaller than nearly all of the A-1 values and most of the values for the modified B-1 spectrum. While the A-1 spectrum values are generally larger than the modified B-1 values, all of the A-1 and B-1 spectrum values are surprisingly close. Thus the 33.3% increase in the B-1 ground accelerations yields an accelerogram with a spectrum very similar at least in the lower frequency range to the spectrum for a Richter 8 earthquake.

In addition to the spectrum curves plotted in Figure 3-16, Tables 3-14a and 3-14b contain listings of the Normalized Rock Spectrum and modified B-1 spectrum accelerations for the first five modal periods of the NRGB in-plane and out-of-plane models, respectively. Similar lists are contained in Tables 3-15a and 3-15b for CSCB.

3.8.2 GROUND MOTION INPUT

The modified version of accelerogram B-1 was first applied in the X, the Y and the Z directions to the NRGB and CSCB models as follows:

1. The modified B-1 accelerogram was applied simultaneously to the north and south bridge supports (see Figures 3-7 and 3-9).

This load type is referred to as B1-B1 loading.

2. The modified version of accelerogram B-1 was then applied to

the south bridge supports while the same accelerogram with a time lag was applied to the north bridge supports. This load type is referred to as B1-B1' loading.

The time lags used for B1-B1' loading were 0.3 seconds for NRGB and 0.125 seconds for CSCB. These time lags were derived from an estimated shear wave speed in rock of about 5600 feet per second. This wave speed was based on tabulated data in the text by Newmark and Rosenblueth (ref. 15) which suggests that shock wave speeds of approximately 6000 feet per second or more are applicable for structures on rock. The time lags were also chosen to be even multiples of the 0.025 second time steps.

The following combination of accelerograms B-1 and B-2 was then applied to the NRGB and CSCB in-plane models in the X direction and to the out-of-plane models in the Z direction:

3. The modified B-1 accelerogram was applied to the south bridge supports while the modified B-2 accelerogram was applied to the north bridge supports. This type of loading is referred to as B1-B2 loading.

B1-B2 loading was only applied in the X and Z directions because the results under B1-B1 loading and under B1-B1' loading were generally much greater in the X and Z directions as opposed to the Y direction.

Since the longitudinal direction seemed to be most affected by the time lag in B1-B1' loading especially where arch axial stresses were concerned, the following loading was also applied to the NRGB and CSCB in-plane models in the X direction:

4. The modified B-1 accelerogram was applied to the south bridge supports while the same accelerogram with a longer time lag was applied to the north bridge supports. The time lag for this

load type was exactly twice the value used for B1-B1' loading.

This load type is referred to as B1-B1" loading.

The time lags for this loading correspond to a shock wave speed of about 2800 feet per second which is typical for stiff soils. Thus the time lags under B1-B1" loading are those associated with soils that are "softer" than the rock strata assumed under B1-B1' loading.

Finally, the following two types of loading were applied to the NRGB in-plane model in the X direction:

5. The modified B-2 accelerogram was applied simultaneously to the north and south bridge supports. This load type is referred to as B2-B2 loading.
6. The modified B-1 accelerogram was applied to the south bridge supports while the same accelerogram with a very long time lag was applied to the north bridge supports. The time lag for this load type was 4.2 seconds which is approximately the same as the fundamental period of the NRGB in-plane model. This load type is referred to as B1-B1"" loading.

The B2-B2 loading was applied simply to provide another sample of type B accelerogram responses. NRGB in the X direction was chosen for B2-B2 loading because NRGB is the larger bridge and the X direction generally gave the largest NRGB responses. The B1-B1"" load analysis was performed in order to consider what role, if any, the fundamental period of the in-plane model plays under differential X direction loading. NRGB was again chosen because it is the larger of the two bridges.

Table 3-1 NRGB and CSCB Geometric and Design Characteristics

Item	New River Gorge Bridge	Cold Springs Canyon Bridge
Fundamental Period	6.78 seconds	2.67 seconds
Overall Length	3030.5 feet	1217.8 feet
Arch Type	Single Cell Box Truss With Four Box Chords	Two Solid Ribs With Truss Cross-members
Arch Span	1700.0 feet	700.0 feet
Arch Panel Lengths	2 @ 71.5 feet 12 @ 129.75 feet	11 @ 63.635 feet
Arch Configuration	Five Center Series of Circular Arcs	Seventh Order Polynomial
Arch Rise to Span Ratio	1:4.59	1:4.85 for South Hinge 1:7.15 for North Hinge
Rib or Side Truss Spacing to Span Ratio	1:23.6	1:26.9
Rib or Side Truss Depth to Span Ratio	1:50 At Crown 1:32 Near Abutments	1:75 At Crown 1:73 Near Quarter Points 1:76 Near Abutments
Arch to Total Main Span Dead Load Ratio	1:2.48	1:2.41
Deck Expansion Joints	2 @ Panel Points 5 and 19	1 @ Panel Point 1
Deck Hinges	4 @ Panel Points 0, 5, 19 and 23	4 @ Panel Points 1, 6, 17 and 20
Wind Load Transfer Mechanisms	Deck To Arch Via Bents At Panel Points 6 to 18	Deck To Arch Via Cables At Panel Points 11 and 12
Longitudinal Force Transfer Mechanisms	Deck To Arch Via Truss Elements at Panel Point 12	Deck to Arch Via Cables From Panel Points 11 to 12

Table 3-2 NRGB Arch Dead Load Displacement Comparison

a) Estimated Versus One-Plane Model Vertical Arch Dead Load Displacements

Bents	Estimated Displacements inches	One-Plane Model Displacements inches	Percent Difference
6 & 18	-2.600	-2.452	-5.7
7 & 17	-6.100	-6.236	+2.2
8 & 16	-9.100	-9.300	+2.2
9 & 15	-11.000	-10.809	-1.7
10 & 14	-11.500	-10.769	-6.4
11 & 13	-11.100	-10.064	-9.3
12	-10.200	-9.811	-3.8

b) Estimated Versus One-Plane Model Horizontal Arch Dead Load Displacements

Bents	Estimated Displacements inches	One-Plane Model Displacements inches	Percent Difference
6 & 18	1.900	1.285	-32.4
7 & 17	3.000	2.732	-8.9
8 & 16	3.400	3.362	-1.1
9 & 15	3.000	3.002	+0.1
10 & 14	2.100	2.027	-3.5
11 & 13	1.000	0.958	-4.2
12	0.000	0.000	---

Table 3-3 NRGB Arch Dead Load Stress Comparison

Arch Elements and Nodes		Total Top Chord Stresses			Total Bottom Chord Stresses		
		Estimated ksi	Model ksi	% Diff.	Estimated ksi	Model ksi	% Diff.
1 & 14	I	14.45	13.87	-4.0	16.35	13.51	-17.4
	J	15.48	17.96	+16.0	16.66	16.32	-2.0
2 & 13	I	15.48	16.60	+7.2	16.66	14.96	-10.2
	J	16.87	18.25	+8.2	15.74	15.14	-3.8
3 & 12	I	16.87	17.06	+1.1	15.74	13.96	-11.3
	J	18.30	18.85	+3.0	14.32	13.95	-2.6
4 & 11	I	18.30	17.89	-2.2	14.32	12.98	-9.4
	J	18.10	18.81	+3.9	13.72	13.82	+0.7
5 & 10	I	18.10	18.10	+0.0	13.72	13.11	-4.4
	J	17.67	17.88	+1.2	13.52	15.12	+11.8
6 & 9	I	17.67	17.41	-1.5	13.52	14.64	+8.3
	J	17.47	16.80	-3.8	14.48	17.15	+18.4
7 & 8	I	17.47	16.56	-5.2	14.48	16.92	+16.8
	J	18.20	17.03	-6.4	15.59	18.53	+18.9

Table 3-4 NRGB Deck Dead Load Stress Comparison

Deck Elements and Nodes		Total Top Chord Stresses			Total Bottom Chord Stresses		
		Estimated ksi	Model ksi	% Diff.	Estimated ksi	Model ksi	% Diff.
1 & 14	I	0.00	0.00	----	0.00	0.00	----
	J	18.15	25.53	+40.7	18.76	25.53	+36.1
2 & 13	I	18.15	24.88	+37.1	18.76	24.89	+32.7
	J	14.26	14.54	+2.0	14.82	14.55	-1.8
3 & 12	I	14.26	14.54	+2.0	14.82	14.54	-1.9
	J	15.04	14.86	-1.2	15.64	14.86	-5.0
4 & 11	I	15.04	14.86	-1.2	15.64	14.86	-5.0
	J	14.93	14.60	-2.2	15.53	14.60	-6.0
5 & 10	I	14.93	14.60	-2.2	15.53	14.60	-6.0
	J	14.84	15.89	+7.1	15.47	15.89	+2.7
6 & 9	I	14.84	15.89	+7.1	15.47	15.89	+2.7
	J	14.84	17.67	+19.1	15.47	17.67	+14.2
7 & 8	I	14.84	16.57	+11.7	15.47	18.77	+21.3
	J	14.84	16.33	+10.0	15.44	18.52	+20.0

Table 3-5 CSCB Vertical Arch Dead Load Displacement Comparison

Panel Points	Estimated Displacements (1) inches	1982 Study Displacements (2) inches	One-Plane Model Displacements (3) inches	Percent Differences (3)/(1) (3)/(2)	
7	0.252	0.340	0.571	+126.6	+67.9
8	0.396	0.610	0.773	+95.2	+26.7
9	1.044	1.246	1.228	+17.6	-1.4
10	1.764	2.197	2.009	+13.9	-8.6
11	2.124	3.031	2.736	+28.8	-9.7
12	2.364	3.238	2.961	+25.2	-8.6
13	2.400	2.746	2.625	+9.4	-4.4
14	1.884	1.973	2.060	+9.3	+4.4
15	1.200	1.316	1.574	+31.2	+19.6
16	0.804	0.801	1.066	+32.6	+33.1

Table 3-6 CSCB Arch Dead Load Stress Comparison

Arch Element	1982 Study Maximum Element Stresses ksi	One-Plane Model Maximum Element Stresses ksi	Percent Difference
1	8.701	8.515	-2.1
2	7.233	7.805	+7.9
3	6.691	6.857	+2.5
4	6.969	6.165	-11.5
5	9.002	7.456	-17.2
6	NA	7.687	----
7	7.455	7.788	+4.5
8	5.960	6.333	+6.3
9	6.883	6.399	-7.0
10	9.237	8.681	-6.0
11	9.396	9.140	-2.7

Table 3-7 CSCB Deck Dead Load Stress Comparison

Deck Element	1982 Study Maximum Element Stresses ksi	One-Plane Model Maximum Element Stresses ksi	Percent Difference
1	7.948	7.812	-1.7
2	8.892	8.746	-1.6
3	7.439	7.536	+1.3
4	7.439	7.534	+1.3
5	6.172	6.288	+1.9
6	4.715	5.093	+8.0
7	5.796	5.841	+0.8
8	6.994	6.952	-0.6
9	6.994	6.949	-0.6
10	8.535	8.501	-0.4
11	7.629	7.593	-0.5

Table 3-8 NRGB Arch Wind Load Stress Comparison

Deck Elements and Nodes		Estimated Chord Stresses			One-Plane Model Maximum Element Stresses ksi	Percent Difference
		Top ksi	Bottom ksi	Average ksi		
1 & 14	I	10.453	9.295	9.874	10.757	+8.9
	J	10.640	8.060	9.350	10.365	+10.9
2 & 13	I	10.640	8.060	9.350	9.684	+3.6
	J	8.491	3.236	5.864	5.711	-2.6
3 & 12	I	8.491	3.236	5.864	5.361	-8.6
	J	5.610	0.486	3.048	2.497	-18.1
4 & 11	I	5.610	0.486	3.048	2.360	-22.6
	J	2.326	0.682	1.504	0.252	-83.2
5 & 10	I	2.326	0.682	1.504	0.153	-89.8
	J	0.538	0.728	0.633	1.020	+61.1
6 & 9	I	0.538	0.728	0.633	0.956	+51.0
	J	2.966	0.260	1.613	2.732	+69.4
7 & 8	I	2.966	0.260	1.613	2.766	+71.5
	J	4.526	0.031	2.278	2.316	+1.7

Table 3-9 CSCB Deck Wind Load Displacement Comparison

Panel Point	1982 Study Deck Lateral Displacements inches	One-Plane Model Deck Lateral Displacements inches	Percent Difference
6	5.192	5.906	+13.8
7	7.556	8.183	+8.3
8	9.754	10.215	+4.7
9	11.678	11.937	+2.2
10	13.062	13.131	+0.5
11	13.778	13.719	-0.4
12	13.830	13.744	-0.6
13	13.183	13.193	+0.1
14	11.807	11.987	+1.5
15	9.801	10.169	+3.8
16	7.407	7.923	+7.0
17	4.639	5.203	+12.2

Table 3-10 CSCB Arch Wind Load Displacement Comparison

Panel Point	1982 Study Arch Lateral Displacements inches	One-Plane Model Arch Lateral Displacements inches	Percent Difference
7	1.782	1.358	-23.8
8	4.614	3.917	-15.1
9	7.561	6.928	-8.4
10	10.052	9.412	-6.4
11	11.573	10.796	-6.7
12	11.686	10.794	-7.6
13	10.259	9.413	-8.2
14	7.805	6.954	-10.9
15	4.748	3.972	-16.3
16	1.606	1.399	-12.9

Table 3-11 CSCB Deck Wind Load Stress Comparison

Deck Element	1982 Study Deck Stresses ksi	One-Plane Model Deck Stresses ksi	Percent Difference
1	6.639	5.291	-20.3
2	2.439	3.390	+39.0
3	4.750	4.157	-12.5
4	5.829	5.552	-4.8
5	5.825	7.172	+23.1
6	5.981	7.309	+22.2
7	6.366	7.320	+15.0
8	6.366	5.912	-7.1
9	5.517	4.837	-12.3
10	3.412	2.404	-29.5
11	5.217	3.720	-28.7

Table 3-12 CSCB Arch Wind Load Stress Comparison

Arch Element	1982 Study Arch Stresses ksi	One-Plane Model Arch Stresses ksi	Percent Difference
1	11.406	8.762	-23.2
2	7.617	4.281	-43.8
3	4.470	1.849	-58.6
4	3.501	0.810	-76.9
5	2.647	1.671	-36.9
6	NA	1.691	----
7	2.672	1.658	-37.9
8	3.202	0.792	-75.3
9	5.967	1.914	-67.9
10	9.888	4.406	-55.4
11	10.308	9.028	-12.4

Table 3-13 CSCB Modal Period Comparison

a) In-Plane Modal Period Comparison

1982 Study Values		One-Plane Model Values		Percent Difference
Mode No.	Period, seconds	Mode No.	Period, seconds	
1	2.117	1	2.320	+9.6
2	1.167	2	1.191	+2.1
3	0.636	3	0.646	+1.6
4	0.611	4	0.633	+3.6

b) Out-Of-Plane Modal Period Comparison

1982 Study Values		One-Plane Model Values		Percent Difference
Mode No.	Period, seconds	Mode No.	Period, seconds	
1	2.732	1	2.729	-0.1
2	1.561	2	1.678	+7.5
3	1.182	3	1.133	-4.1
4	0.897	4	0.708	-21.1

Table 3-14 NRGB Modal Response Spectrum Accelerations

a) In-Plane Modes

Mode	Period, seconds	Normalized Rock Spectra, g	Accelerogram B-1 Spectra, g
1	4.18	0.13	0.18
2	2.00	0.29	0.32
3	1.43	0.42	0.58
4	1.21	0.49	0.54
5	1.13	0.52	0.50

b) Out-of-Plane Modes

Mode	Period, seconds	Normalized Rock Spectra, g	Accelerogram B-1 Spectra, g
1	6.78	0.06*	0.06
2	3.48	0.15	0.23
3	2.40	0.24	0.21
4	1.89	0.30	0.34
5	1.58	0.35	0.56

* approximate

Table 3-15 CSCB Modal Response Spectrum Accelerations

a) In-Plane Modes

Mode	Period, seconds	Normalized Rock Spectra, g	Accelerogram B-1 Spectra, g
1	2.32	0.25	0.23
2	1.19	0.49	0.55
3	0.65	0.88	0.90
4	0.63	0.89	0.91
5	0.43	1.30	1.25

b) Out-of-Plane Modes

Mode	Period, seconds	Normalized Rock Spectra, g	Accelerogram B-1 Spectra, g
1	2.73	0.22	0.25
2	1.68	0.34	0.55
3	1.13	0.52	0.52
4	0.71	0.80	0.96
5	0.67	0.85	0.96

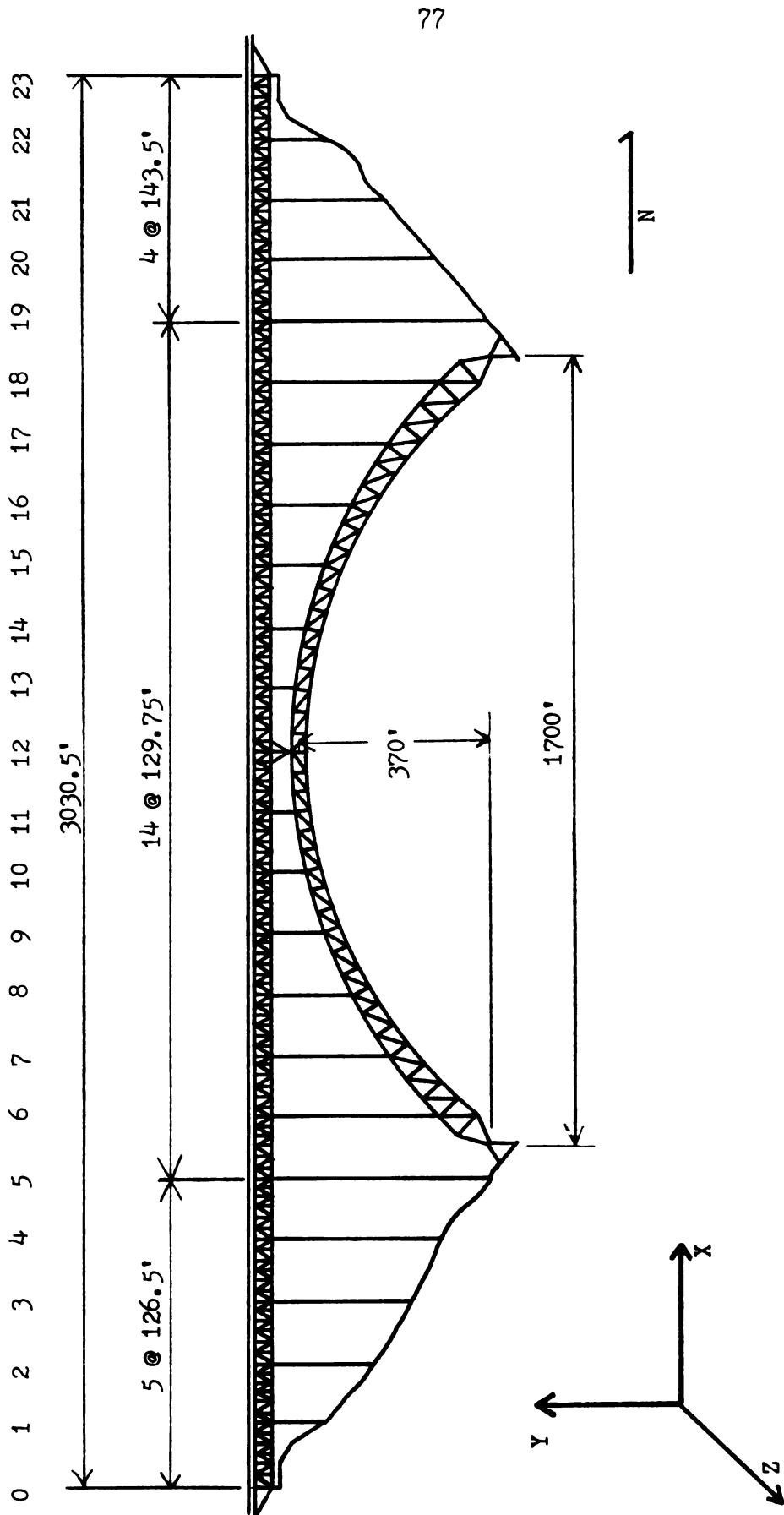


Figure 3-1 NRCB Elevation View

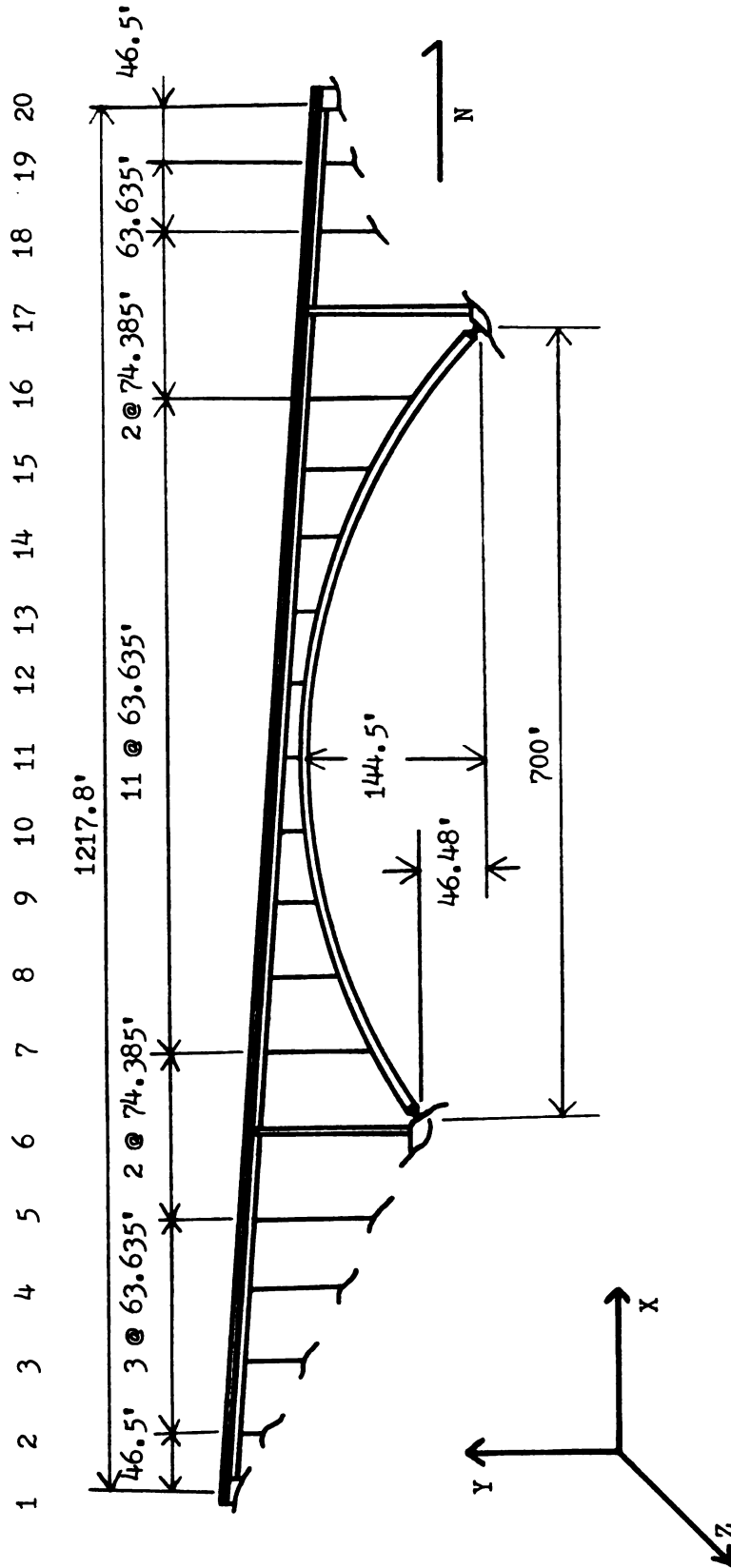


Figure 3-2 CSCB Elevation View

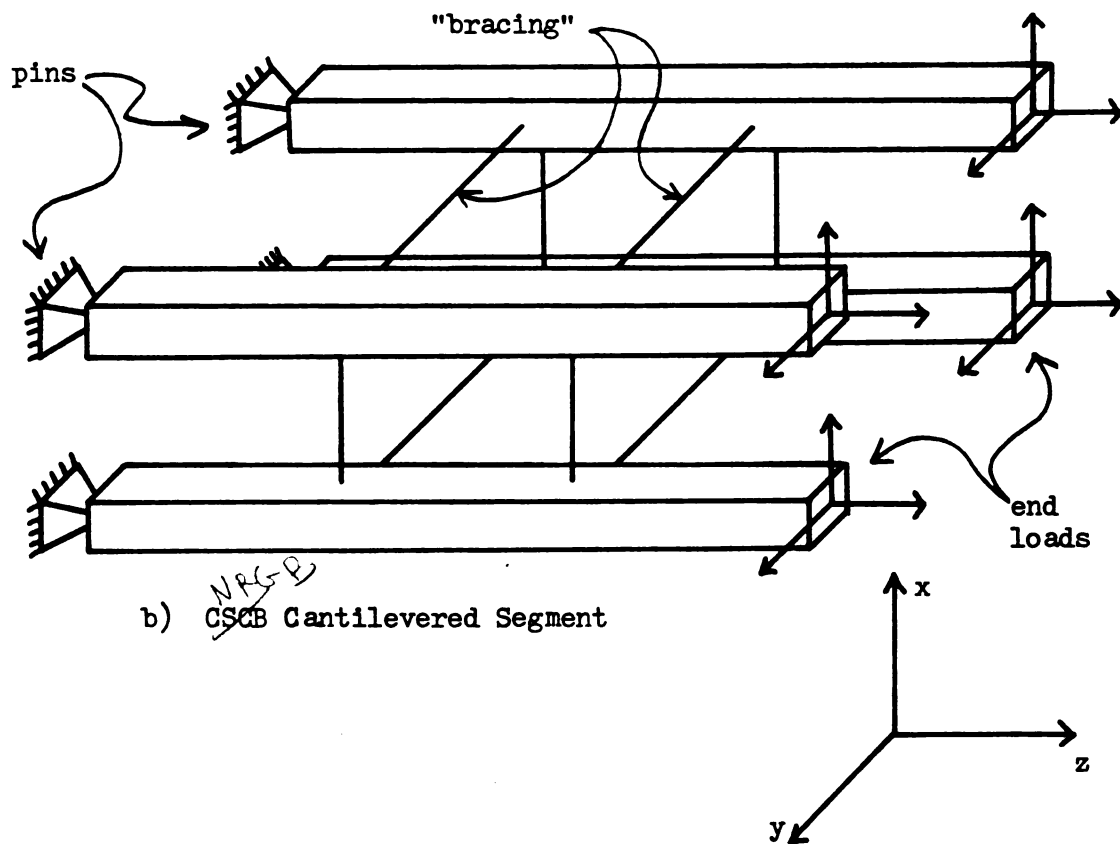
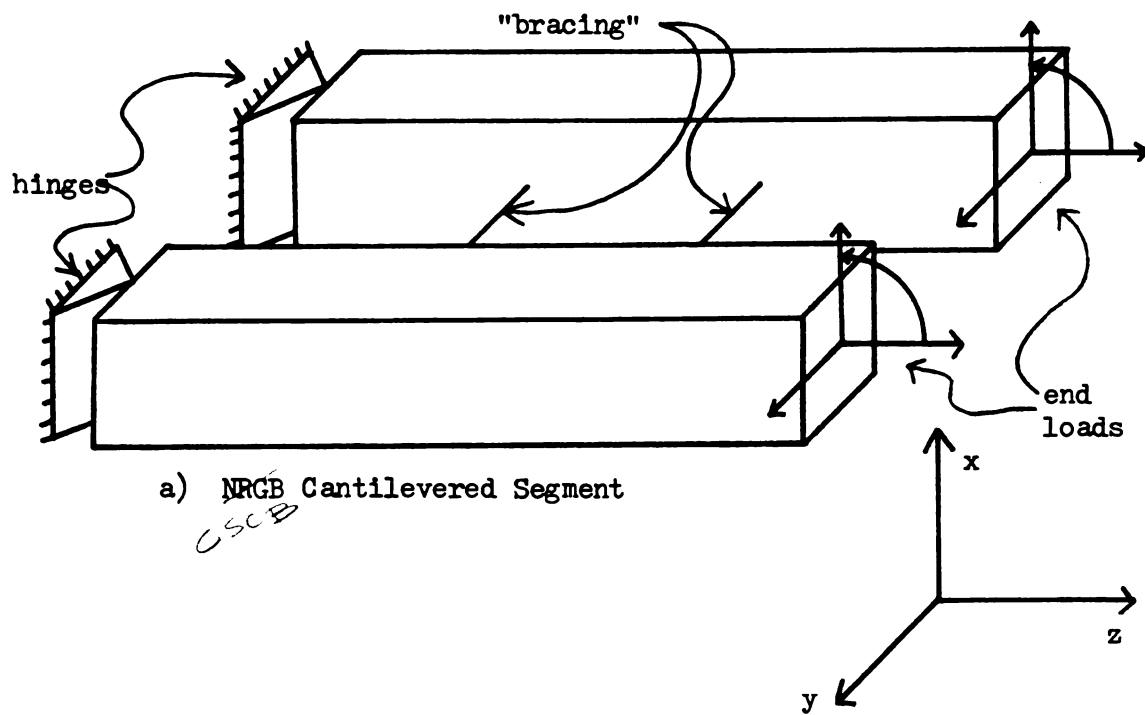


Figure 3-3 Cantilevered Segment End Fixity

[The following page contains extremely faint, illegible text, likely bleed-through from the reverse side of the document.]

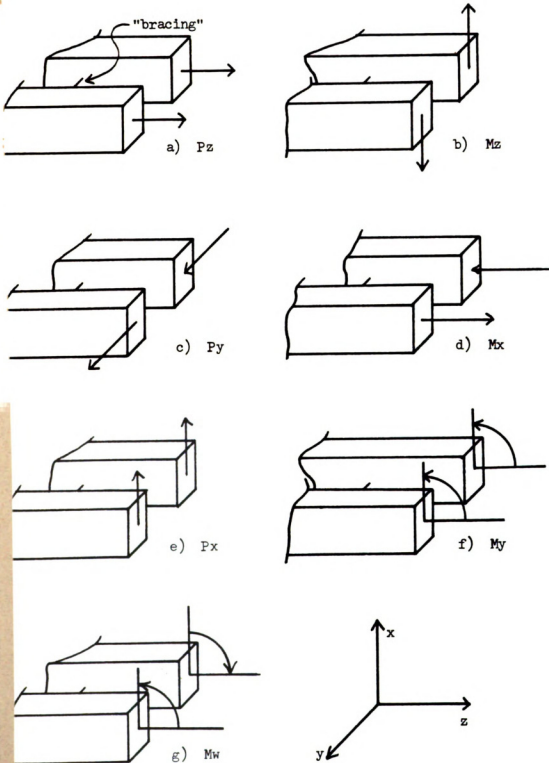


Figure 3-4 CSCB Cantilevered Segment End Loads

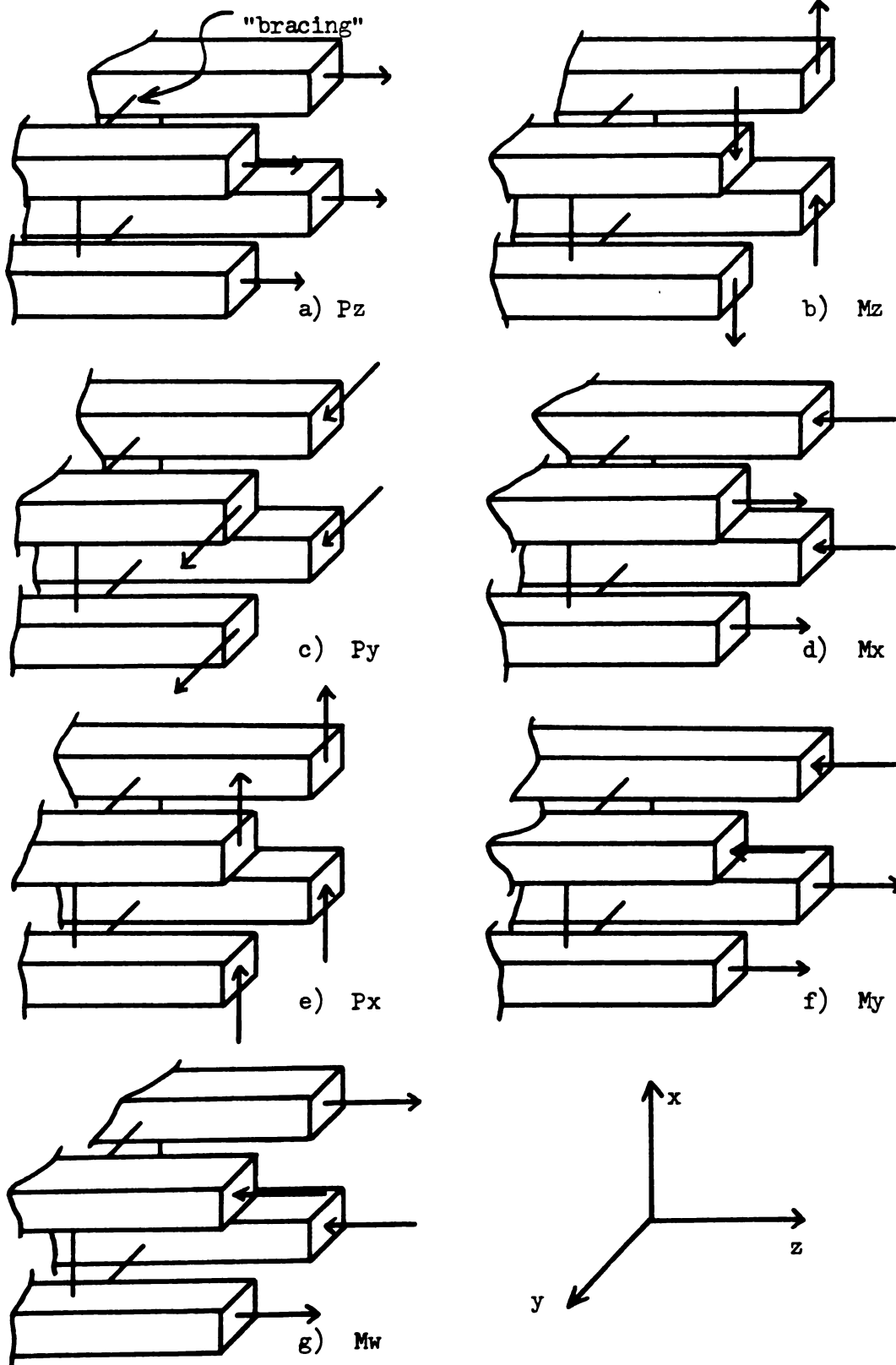


Figure 3-5 NRGB Cantilevered Segment End Loads

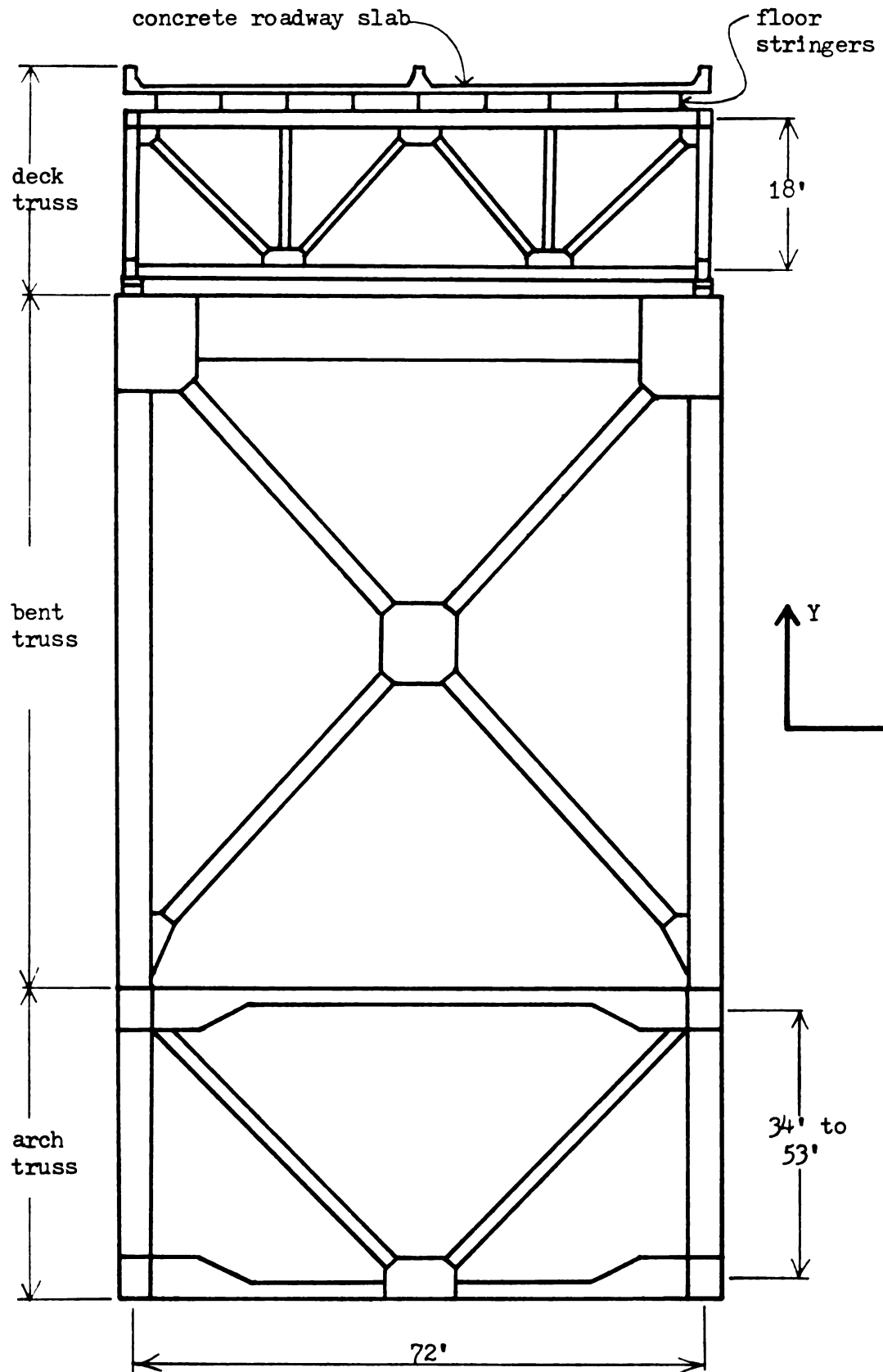


Figure 3-6 NRGB Typical Cross-section

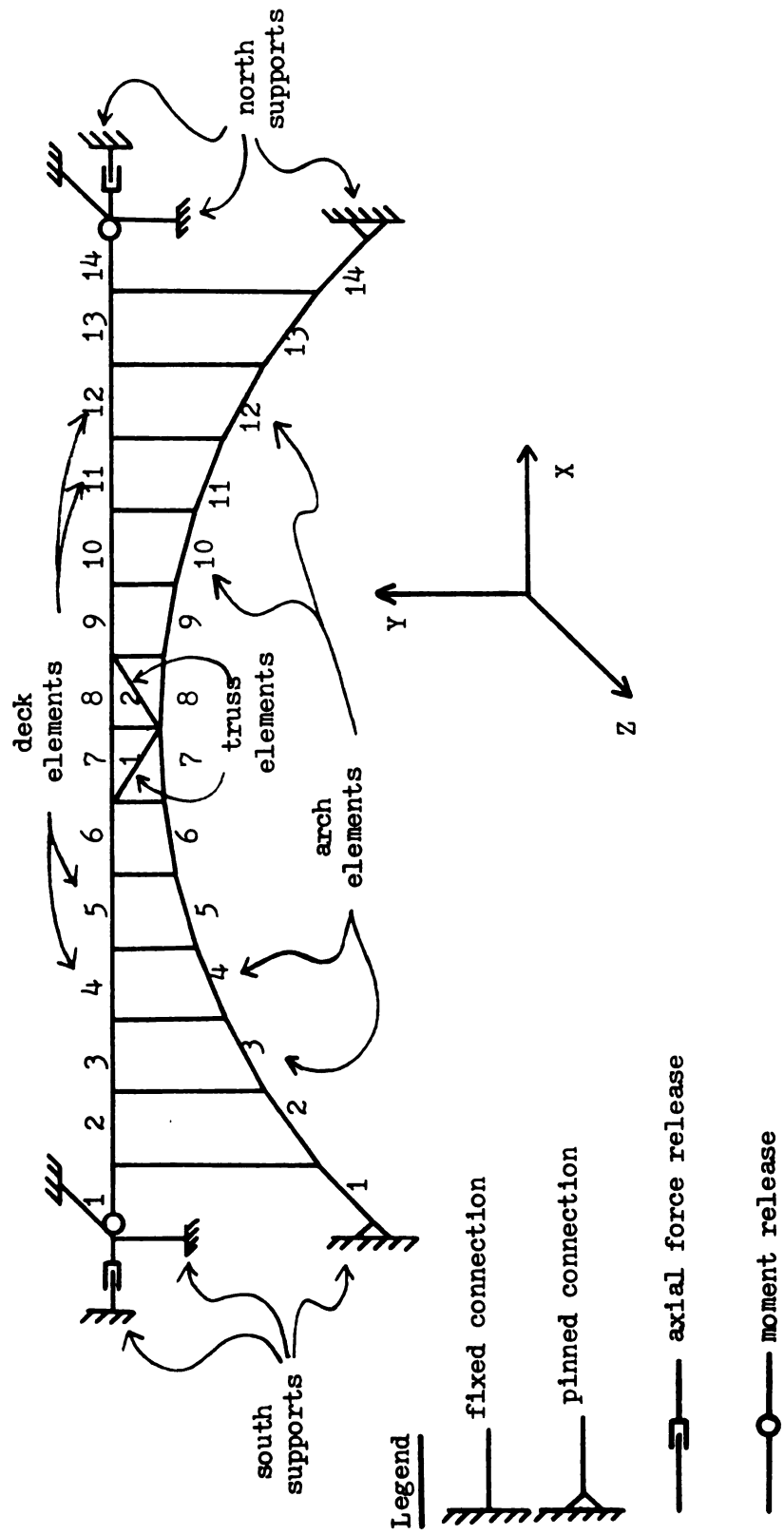


Figure 3-7 NRCB One-plane Model

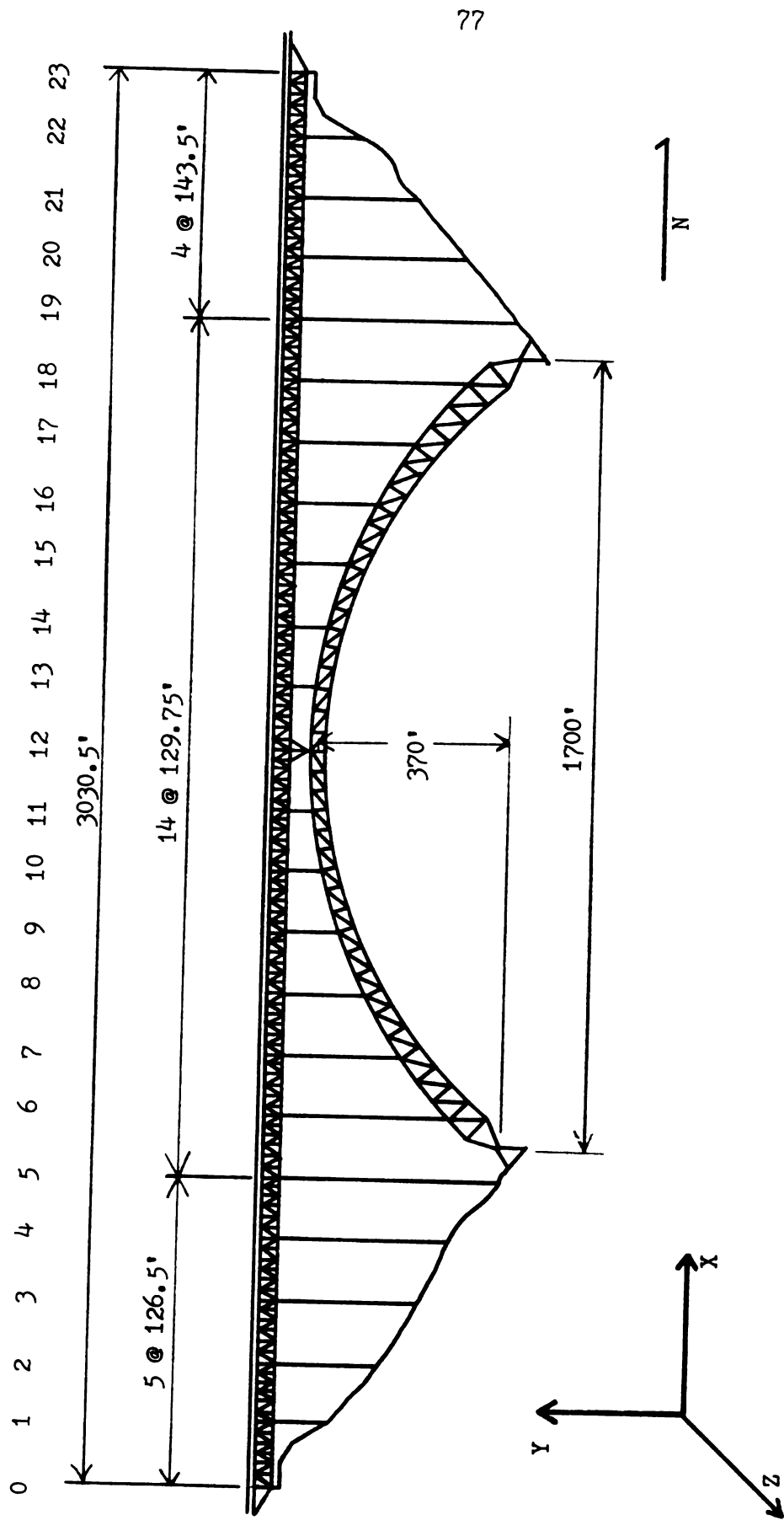


Figure 3-1 NRGB Elevation View

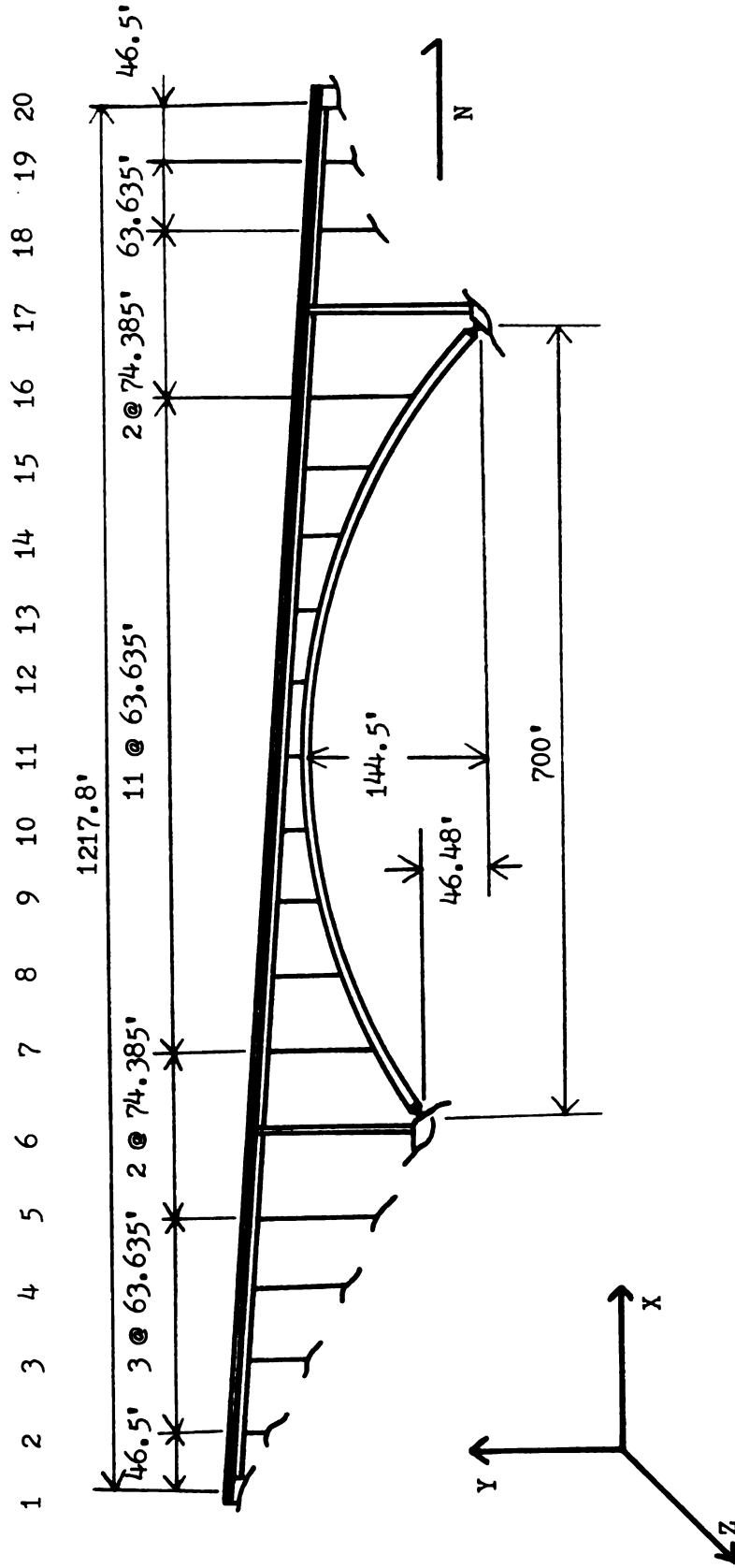


Figure 3-2 CSCB Elevation View

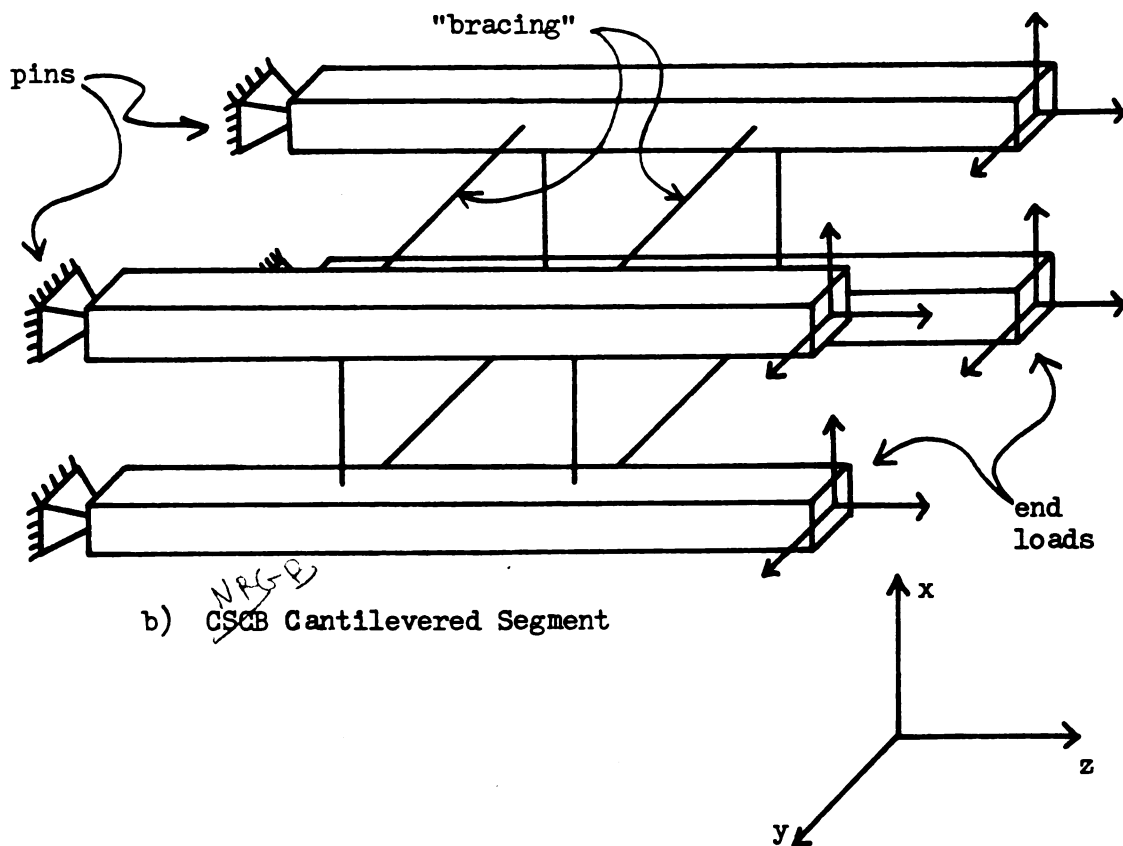
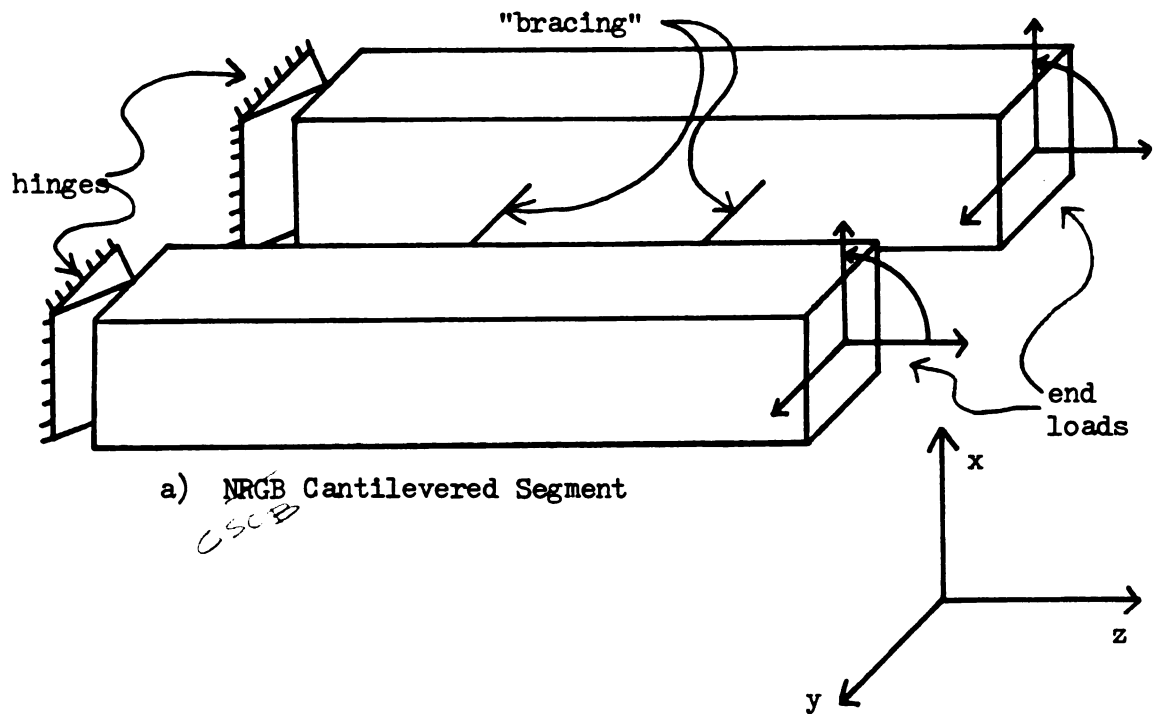


Figure 3-3 Cantilevered Segment End Fixity

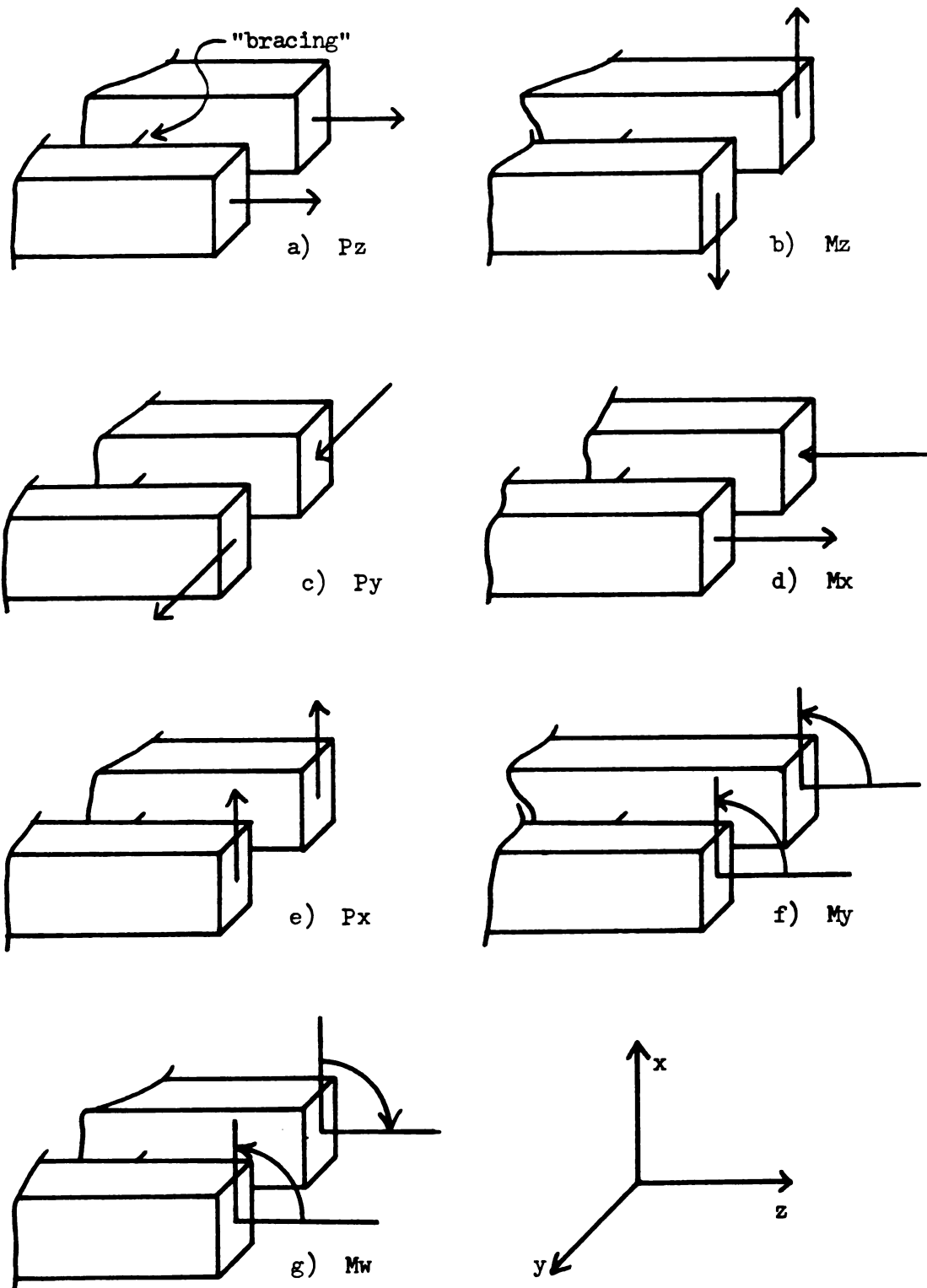


Figure 3-4 CSCB Cantilevered Segment End Loads

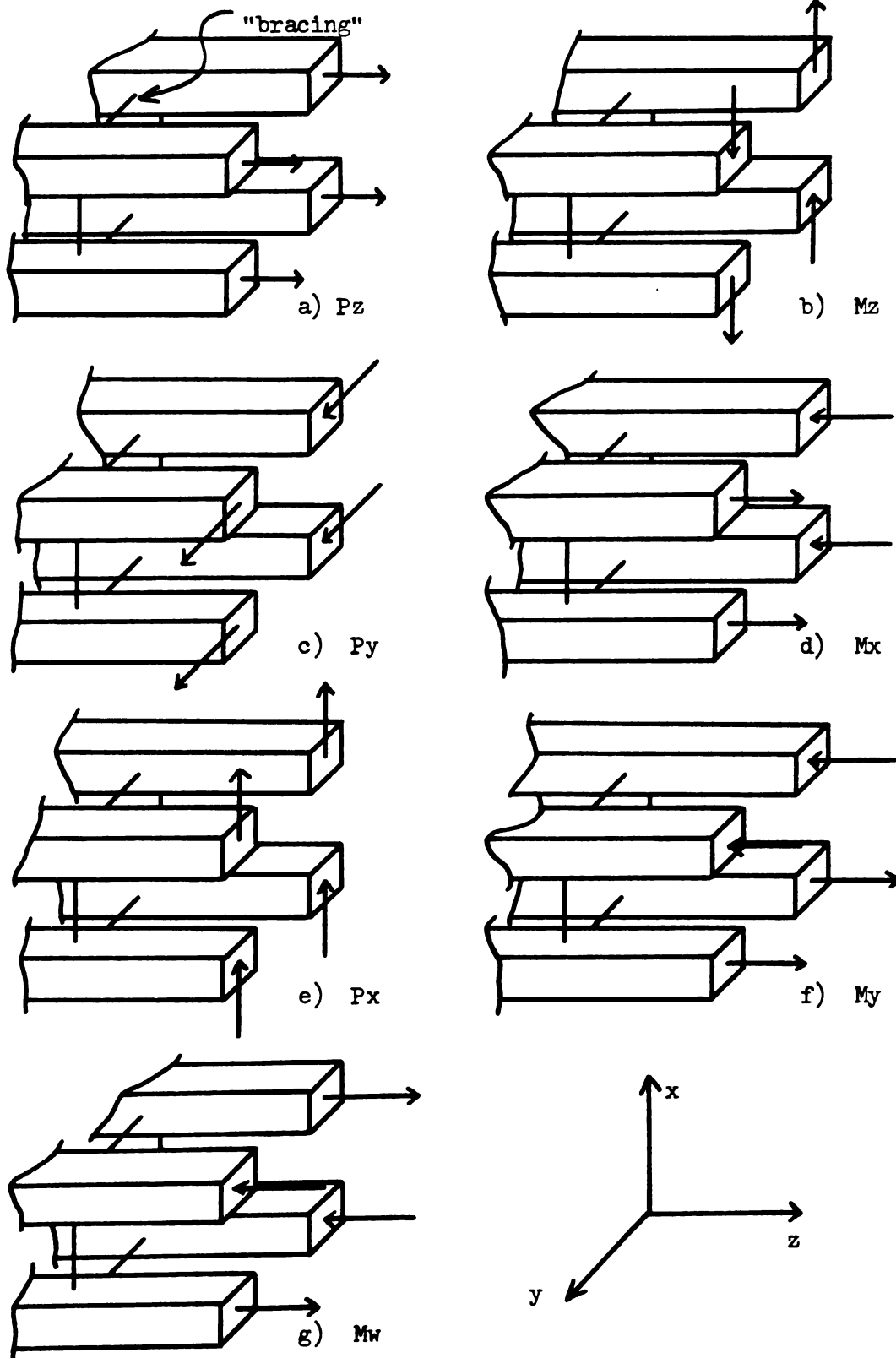


Figure 3-5 NRGB Cantilevered Segment End Loads

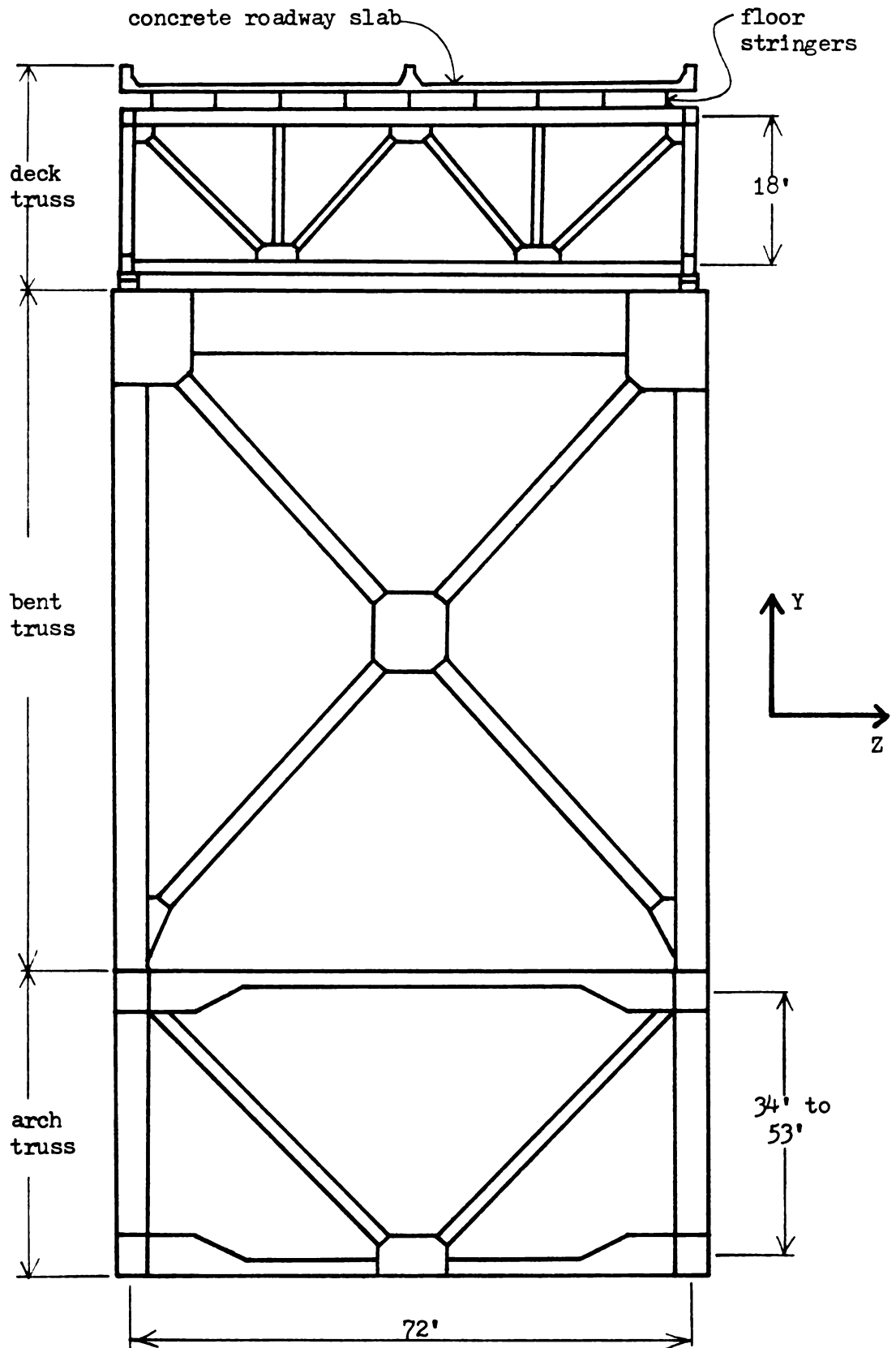


Figure 3-6 NRGB Typical Cross-section

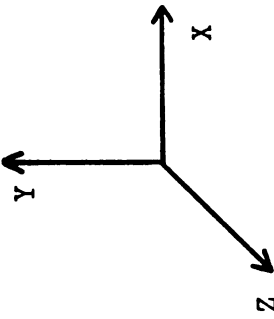


Figure 3-7 NRGB One-plane Model

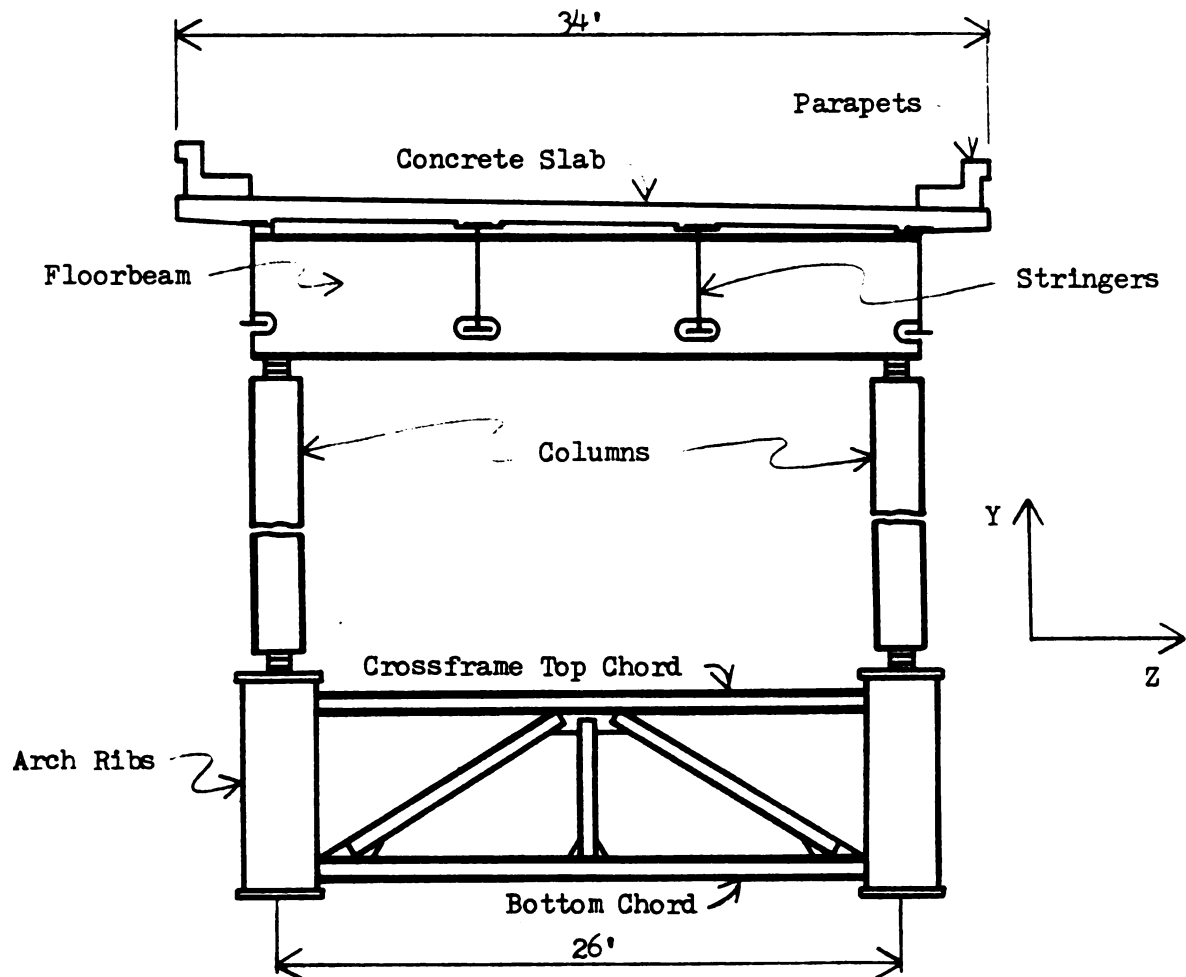


Figure 3-8 CSCB Typical Cross-section

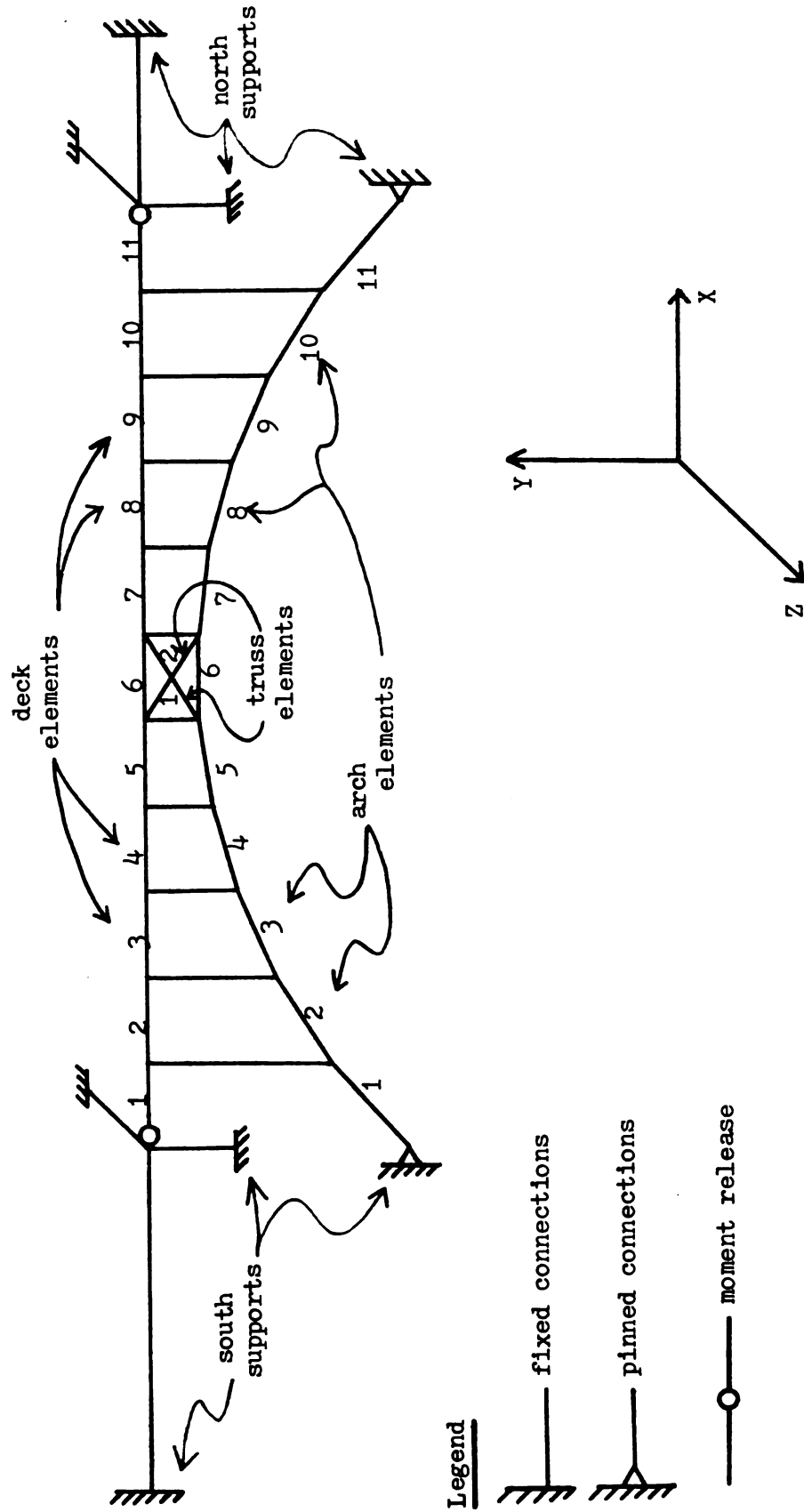


Figure 3-9 CSCB One-plane Model

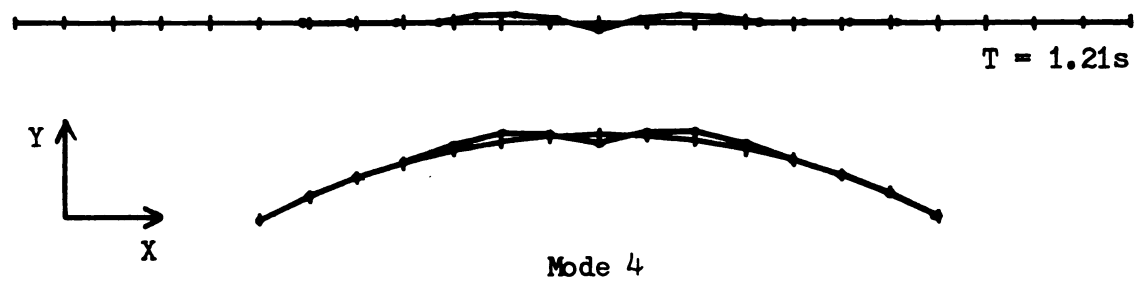
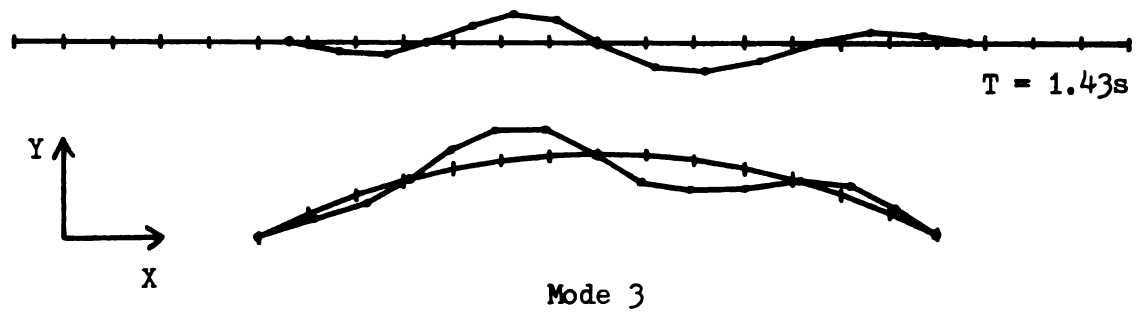
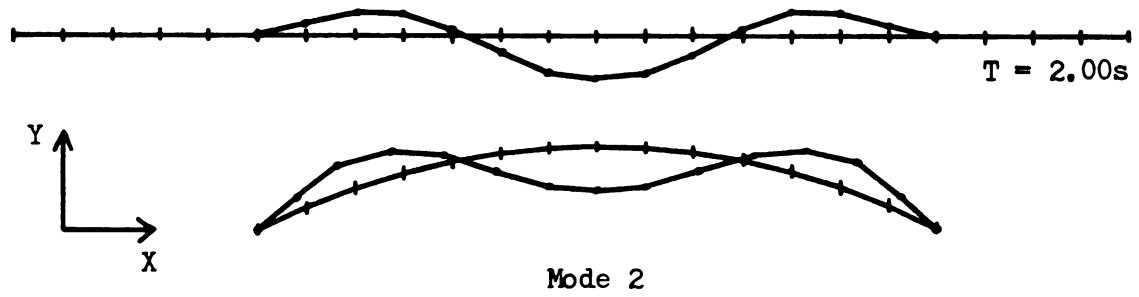
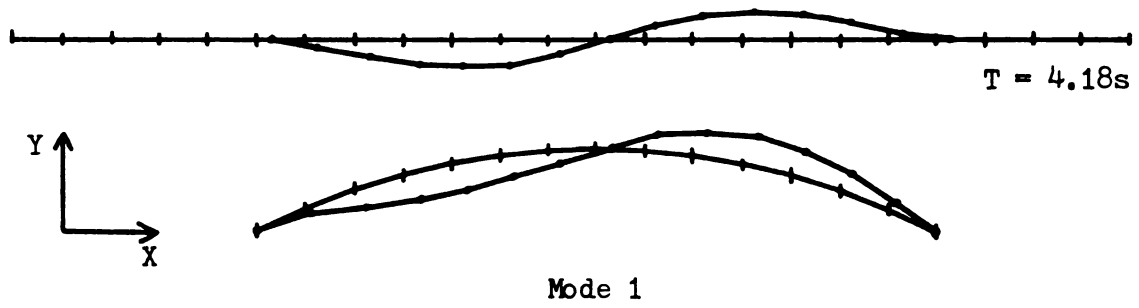


Figure 3-10 NRGB In-plane Modes

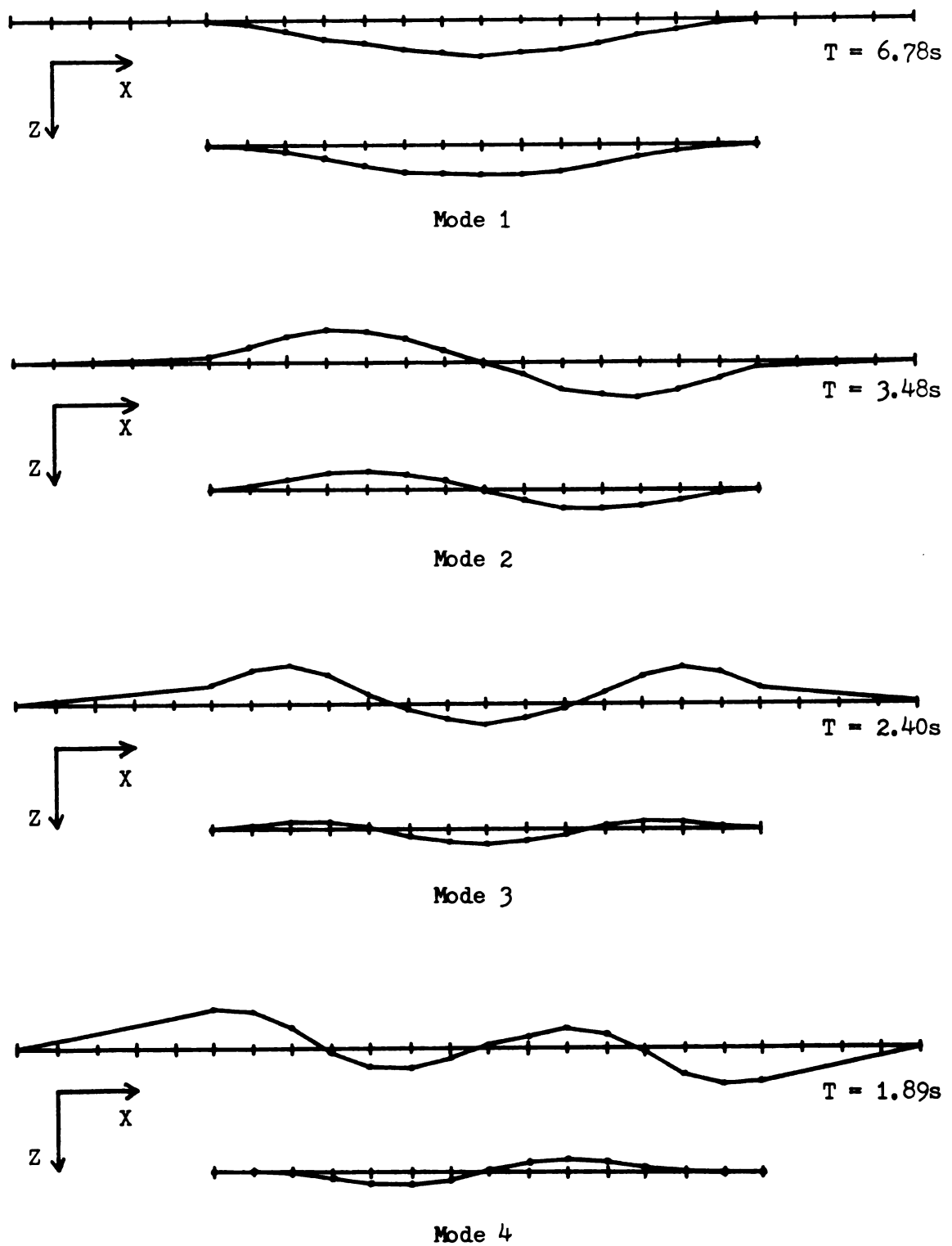


Figure 3-11 NRGB Out-of-plane Modes

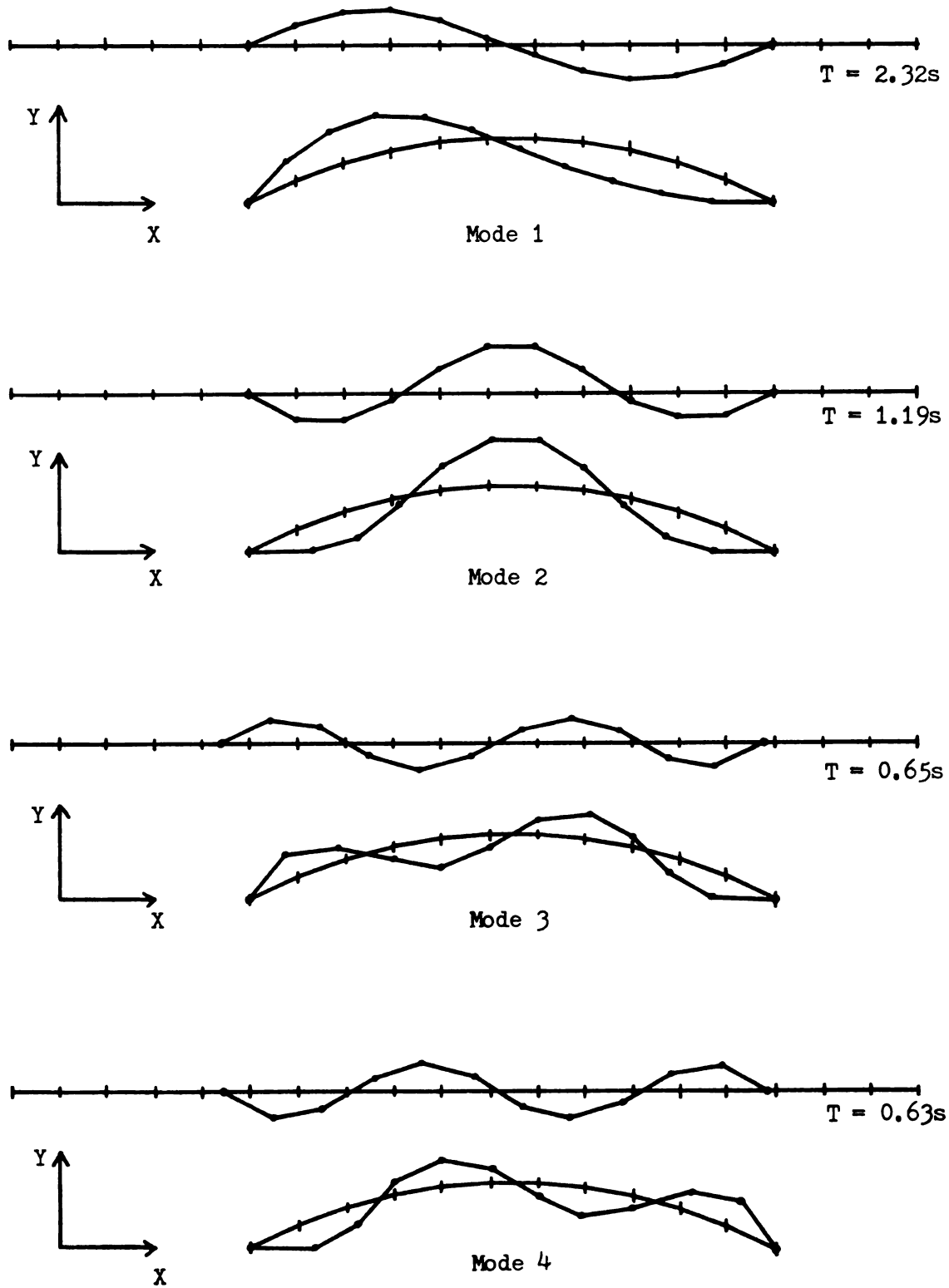


Figure 3-12 CSCB In-plane Modes

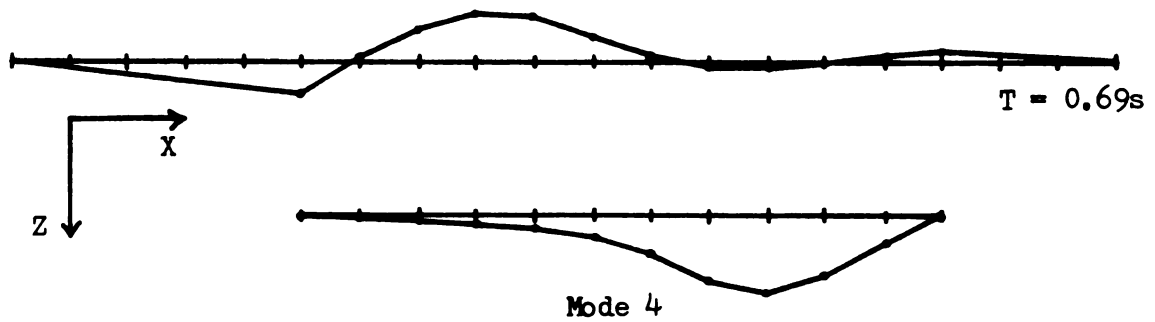
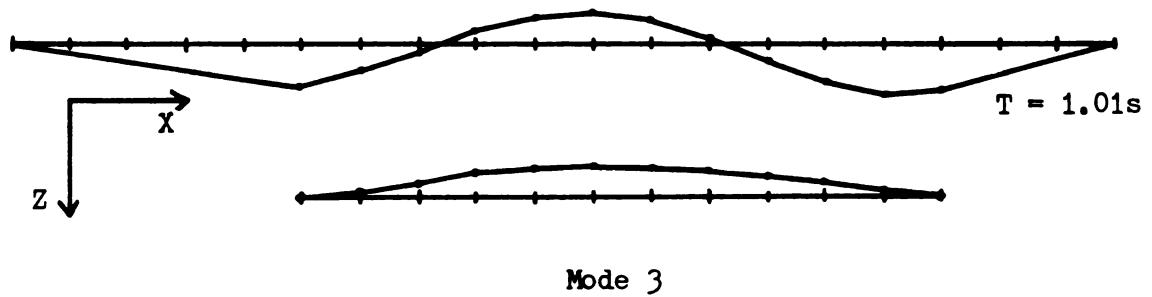
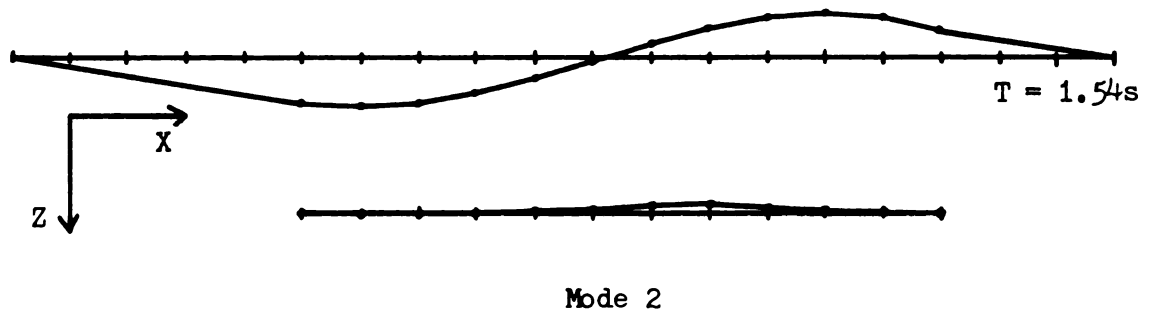
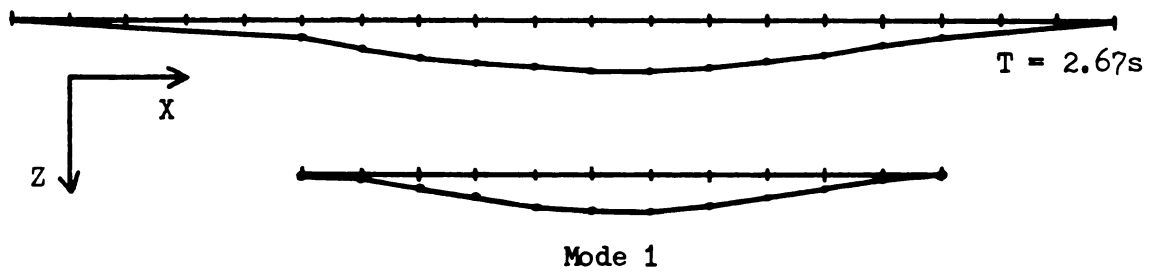


Figure 3-13 CSCB Out-of-plane Modes

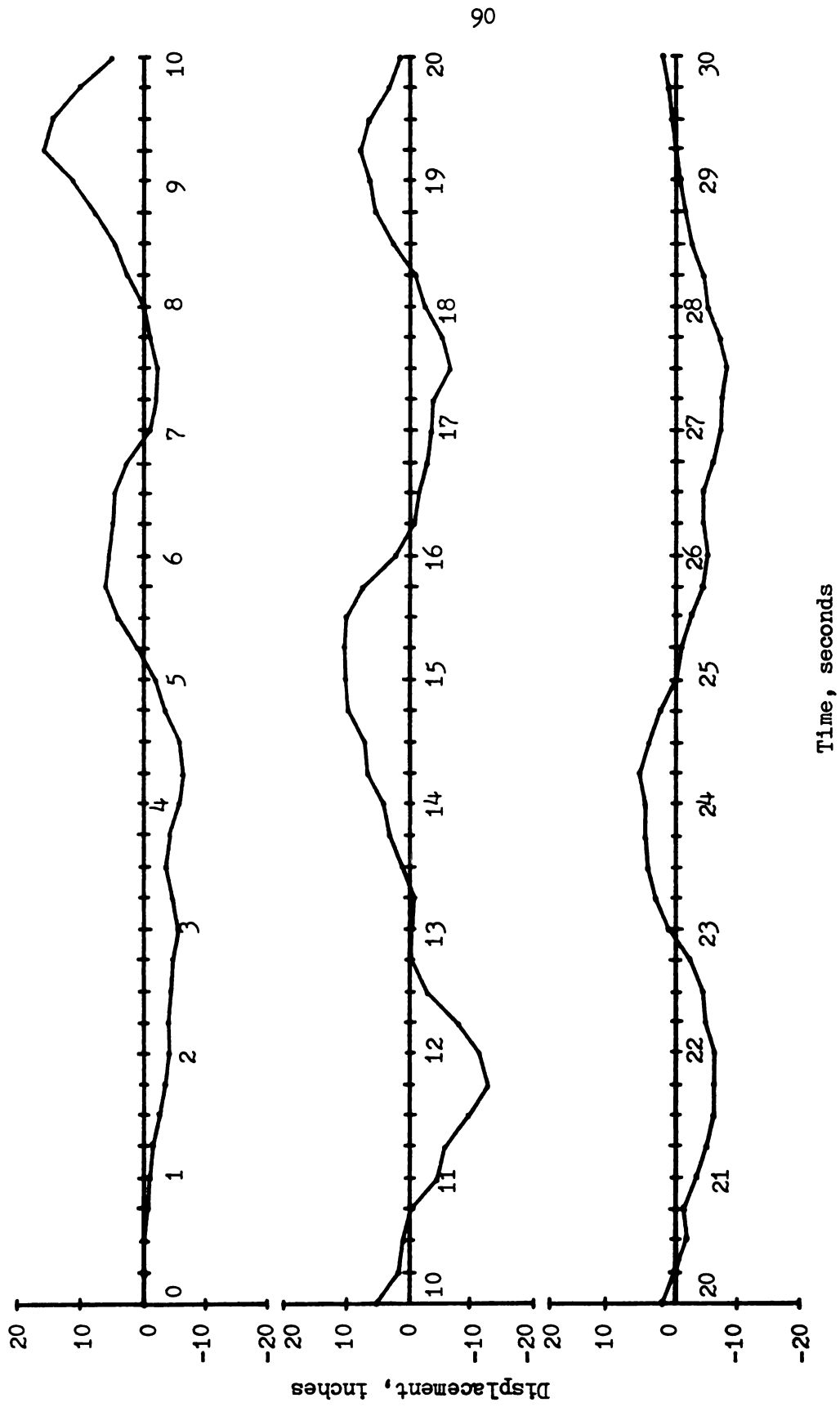


Figure 3-14 Modified B-1 Ground Motion

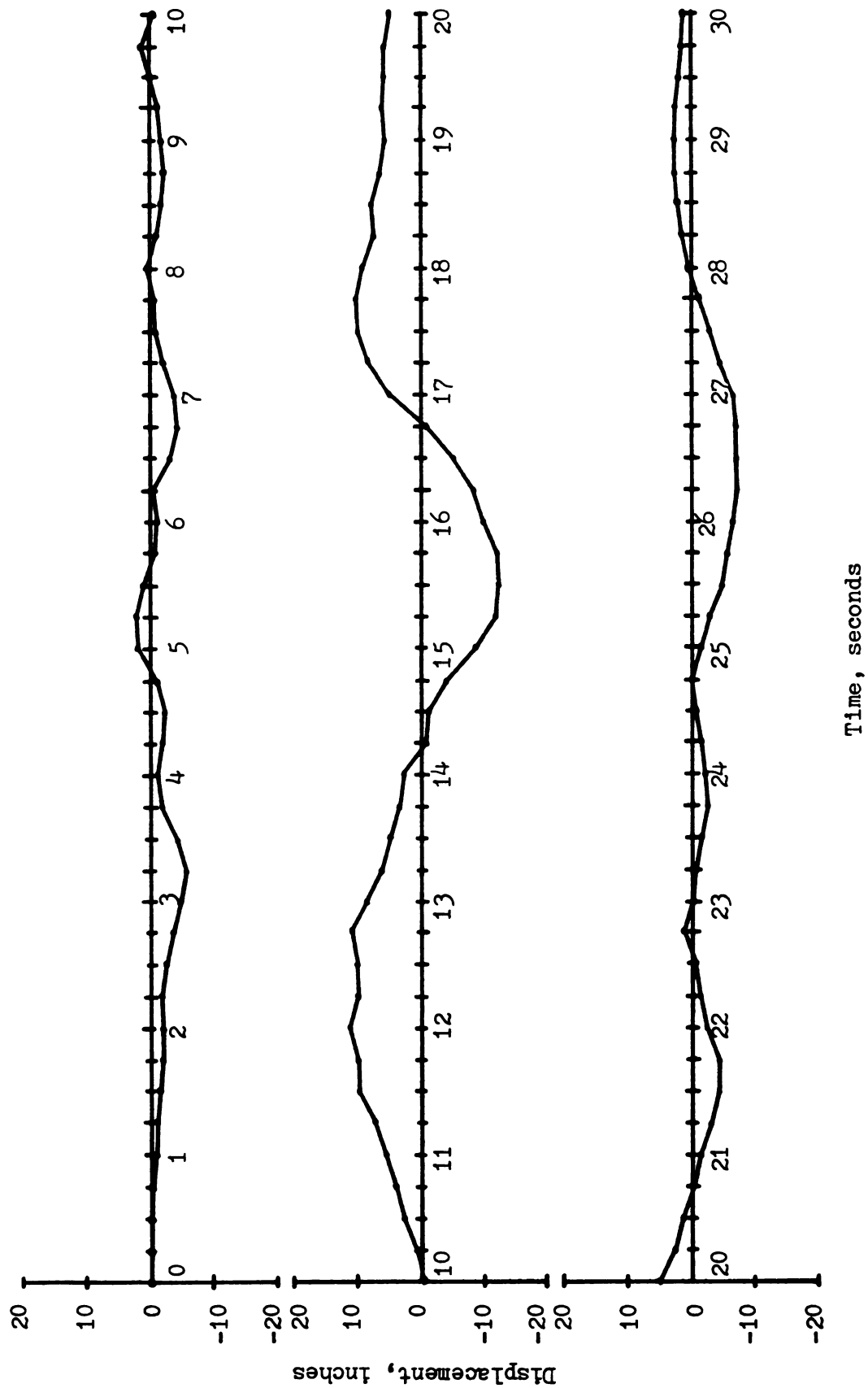


Figure 3-15 Modified B-2 Ground Motion

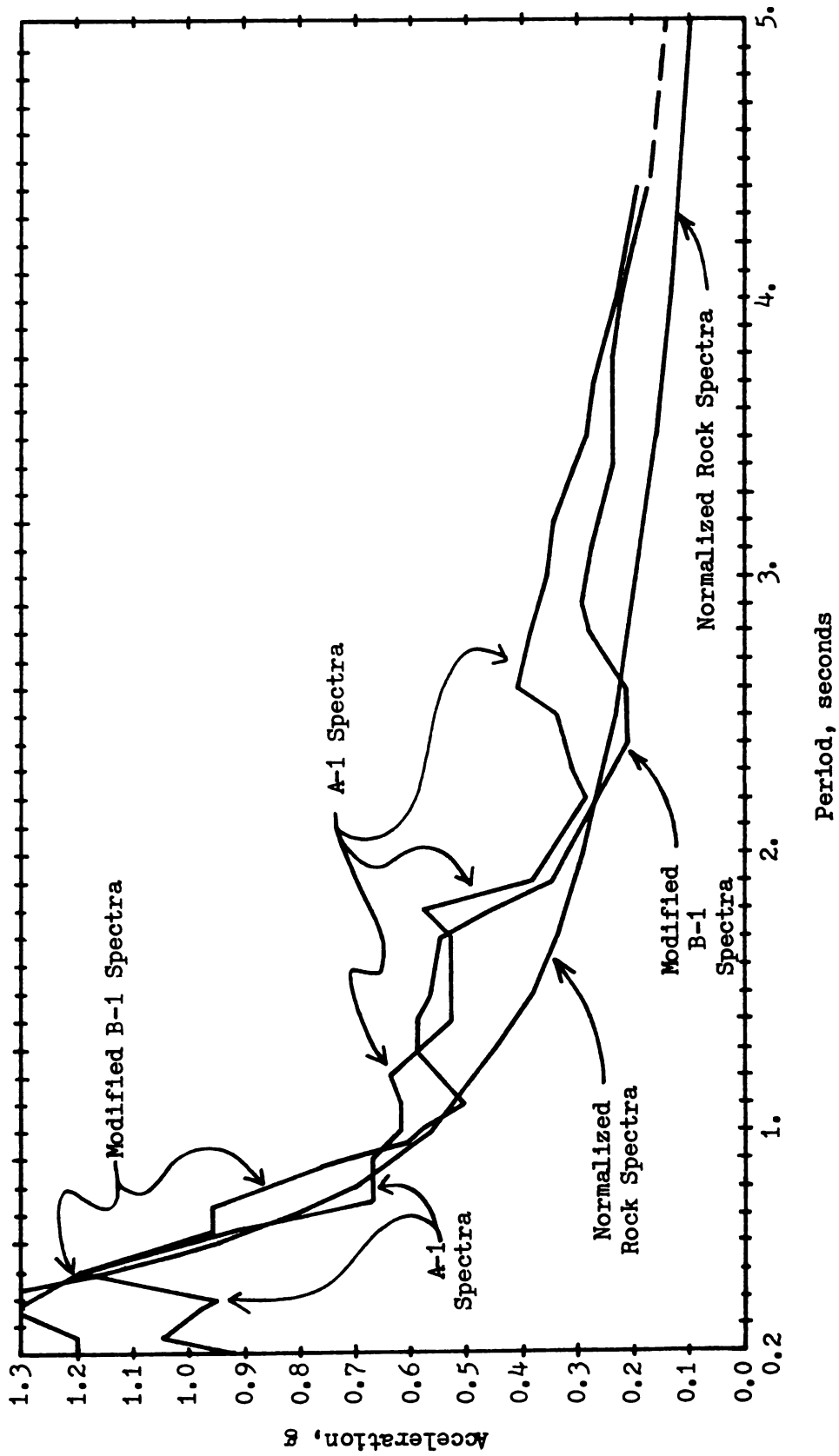


Figure 3-16 Normalized Rock Spectra Versus A-1 Spectra Versus Modified B-1 Spectra

CHAPTER IV
ANALYSIS RESULTS

4.1 GENERAL OBSERVATIONS

In reviewing the dynamic results that were obtained, certain general features were observed repeatedly. Three of the most important and interesting of these general responses are discussed in this section. Descriptions of these general responses should facilitate the presentation of the detailed results.

4.1.1 EFFECTS OF LONGITUDINAL FORCE TRANSFER MECHANISMS

The contrasts in the NRGB and CSCB responses that were caused by the differences in their deck longitudinal force transfer mechanisms were observed repeatedly. In fact this was probably the one factor which caused the greatest difference in the general characteristics of the NRGB and CSCB results.

With only one deck expansion joint at the south abutment and a pin connection at the north abutment as shown in Figure 4-1a, most of the CSCB deck longitudinal forces are transferred directly to the ground through the north abutment. The remainder of the deck longitudinal forces are transferred to the arch via the longitudinal cable bracing. The portion that may be transferred to the ground via the towers is believed to be negligible. The NRGB deck on the other hand has expansion joints at each end of the main span deck as depicted in Figure 4-1b and thus all of the main span deck longitudinal forces are

transferred to the arch via the longitudinal bracing. As a result, any type of loading that excited longitudinal deck motion had a much greater effect on the NRGB arch responses as opposed to the CSCB arch results. Such loadings included uniform and nonuniform X direction ground acceleration, nonuniform Y direction ground acceleration and X direction static loading.

4.1.2 DYNAMIC ARCH PINCHING EFFECTS

Another factor which greatly affected the dynamic results of both bridges was arch "pinching" or differential X direction translations of the arch abutment such as those that occurred under B1-B2, B1-B1' and B1-B1" loading. In all three cases substantial increases in arch axial stress were observed for both bridges in comparison with the uniform B1-B1 responses. "Static" pinching analyses or static application of differential arch abutment displacements to the bridge models showed upward motions of the arch and deck and some bending stress but very little arch axial stress. Rapid application of differential arch abutment X direction displacements or "dynamic" arch pinching, however, resulted in substantial arch axial stress with relatively little arch bending. These responses to dynamic pinching were similar to those obtained for B1-B2, B1-B1' and B1-B1" loading.

Figures 4-2a and 4-2b may help to explain the relatively large arch axial stresses due to dynamic pinching as opposed to static pinching. Static pinching assumes a slow application of differential arch abutment displacement thus giving the large deck and arch masses time to translate upward as shown in Figure 4-2a without generating inertia forces. Dynamic application of the same differential displacement is resisted by the vertical inertia of the bridge mass as depicted in

Figure 4-2b. The resulting vertical inertia forces manifest themselves as arch axial forces as dictated by the very nature of arch structures.

4.1.3 ARCH AND DECK BRACING RESPONSES

As ground motion was initially applied in the X or Z directions to the NRGB or CSCB models, the arch generally responded first and the deck then followed the motion of the arch. Later during the course of the ground motion there were times when the arch and the deck were out of phase and moving in opposite directions. Both of these cases resulted in large "differential" arch and deck displacements when compared with static load results. These large differential displacements caused large stresses in the bracing members that connect the arch and the deck.

These arch and deck bracing members take the form of longitudinal and lateral cable bracing at the crown in CSCB and bent lateral diagonal bracing and longitudinal crown bracing in NRGB. Of these four types of bracing, the two most affected by differential arch and deck motion were the CSCB lateral cables and the NRGB longitudinal bracing members. In both cases these bracing members provide the only means by which forces can be transferred from the deck to the arch in the given direction. In addition, both of these bracing types are relatively short compared with the other two kinds of bracing. Thus similar differential arch and deck displacements applied to all four types of bracing would cause greater forces in the shorter members.

4.2 GENERAL NOTES

Before presenting and discussing the dynamic analysis results, some general comments should be made. First, all of the stresses presented in this chapter, unless otherwise noted, include dead load stress while

the displacements presented are relative to the ground and do not include the dead load displacements. In addition, the total element stresses listed in the dynamic analysis results were the maximum values that occurred during the 30 seconds of dynamic loading but the components of these maximum total stresses may or may not be their respective largest values.

It should also be noted that dynamic responses were recovered for only about 1/3 of the arch and deck elements in the bridge models. Of these recovered results, the responses for two arch elements and one deck element for each bridge were chosen for presentation. One of the arch elements chosen was at an abutment while the other was near a quarter point. The deck element chosen for presentation was near the center of the bridge. Also chosen for presentation were one longitudinal bracing member and one lateral bracing member. It may be presumed that the responses of these arch, deck and bracing members were the most important ones for the structures under consideration. In addition, the displacements chosen for presentation were those deemed to be most important for the given bridge in the given direction of ground acceleration.

4.3 X AXIS GROUND ACCELERATION RESPONSES

4.3.1 B1-B1 LOADING

The dynamic analysis results presented in this section were the maximum responses of the NRGB and CSCB in-plane models under simultaneous X axis application of the modified B-1 accelerogram to the north and south bridge supports. Tables 4-1 and 4-2 compare these dynamic results for NRGB and CSCB, respectively, with the corresponding model responses to the application of longitudinal wind loads and the

application of equivalent static loads as defined in Chapter 3. These two static results were chosen for comparison because longitudinal wind load represents the largest non-seismic load in the X direction while the equivalent static load represents a simplified approach for computing seismic effects. In addition, Table 4-3 compares the current dynamic analysis results for CSCB with the values calculated during the 1982 Study.

Tables 4-1 and 4-2 show that both NRGB and CSCB exhibited considerably greater responses due to dynamic loading as opposed to longitudinal wind loading or equivalent static loading. The only major exceptions were the arch axial stresses which were nearly the same for all three types of loading. The large longitudinal bracing stresses under B1-B1 loading as opposed to static loading were the result of the larger differential arch and deck longitudinal motions under dynamic loading as discussed in Section 4.1.3. For NRGB these longitudinal bracing member stresses surpassed the 50 ksi yield stress under B1-B1 loading but failed to reach half of the yield stress under either of the static loading cases.

The relationships between dynamic and wind load responses were quite similar for the two bridge models as were the relationships between dynamic and equivalent static load responses. The ratios of total element stress to yield stress were in general much greater for NRGB, however. As mentioned above, the longitudinal bracing stresses surpassed the yield stress under B1-B1 loading and the total deck stresses near the center of NRGB under B1-B1 loading came very close to the yield value. The larger NRGB dynamic stresses relative to yield stress are an indication of the important role that the deck

longitudinal force transfer mechanisms played in the bridge responses (see Section 4.1.1.).

The general closeness exhibited in Table 4-3 between the 1982 CSCB results and the current responses seems somewhat surprising considering the differences in the bridge models and in the ground motion inputs. One major difference in the results, however, was in the longitudinal cable bracing forces. This difference may be explained by the fact that the 1982 Study used truss elements with axial areas equal to the axial areas of the longitudinal cables while the present analysis used only half of the cable area (see Section 3.3.2). Since the maximum relative arch and deck displacements for the two studies were about the same, the halved cable area in the current study caused the maximum cable forces to be halved.

4.3.2 B1-B2 LOADING

The maximum responses of both bridges to X direction application of the modified B-1 and B-2 accelerograms at the south and north bridge supports, respectively, are presented in this section. Tables 4-4 and 4-5 are comparisons of these B1-B2 dynamic responses with the results of B1-B1 loading for NRGB and CSCB, respectively. Table 4-4 indicates that except for arch rib axial stress, the NRGB responses to B1-B2 loading were the same or smaller than the B1-B1 responses. The CSCB B1-B2 results listed in Table 4-5 also show large increases in maximum arch axial stress but these are accompanied by extremely large increases in maximum X and Y axis displacements, longitudinal cable bracing forces and deck and arch bending stresses.

Tables 4-6 and 4-7 present the "static pinching" effects on the NRGB and CSCB models, respectively. These responses were based on

static application of the maximum arch abutment differential displacements under B1-B2 loading and under the three B-1 accelerogram loadings that involve time lags, namely B1-B1', B1-B1" and B1-B1"' loading. As discussed in Section 4.1.2, the static pinching results in Tables 4-6 and 4-7 indicate some arch and deck bending with very little axial stress. In addition, Table 4-7 also indicates forces in the CSCB longitudinal cable bracing due to static pinching.

Table 4-8 presents the "dynamic pinching" effects on the NRGB model that are generated by the pulse sine wave ground acceleration depicted in Figure 4-3a. This sine wave has a period of 0.4 seconds which is approximately 1/10th the fundamental in-plane period for NRGB. The resulting ground velocities and displacements are shown in Figures 4-3b and 4-3c, respectively. The wave was applied in the positive X direction to the south bridge supports and simultaneously in the negative X direction to the north supports. The responses for a similar ground motion having a period of 4.0 seconds are also presented in Table 4-8 along with the NRGB static load results. For comparison purposes, the responses for all three load cases are scaled in Table 4-8 such that the maximum arch abutment differential displacement is six inches.

The dynamic results due to a sine wave pulse of period 0.4 seconds indicated large arch axial stresses with little arch or deck bending and no deck axial stress. The results based on a much slower application of the sine pulse with $T = 4.0$ seconds come very close to the static results. It should be noted that when the sine wave pulse with $T = 0.4$ seconds was applied at one end only as opposed to both ends, greater bending stresses in the arch and deck were observed along with some deck axial stress and some additional arch axial stress.

The large axial stresses resulting from a sine wave pulse of 0.4 seconds can be looked on as dynamic pinching or high frequency responses while the bending stresses due to static pinching and those due to a sine wave pulse with $T = 4$ seconds both represent low frequency responses. For seismic loadings such as B1-B2 that have differential X direction arch abutment displacements and also contain both high and low frequency motions, both high and low frequency pinching responses exist. Thus the substantial increases in CSCB horizontal and vertical translation, longitudinal cable force, and deck and arch bending stress that occurred under B1-B2 loading compared with B1-B1 loading may be considered a result of static pinching. Similarly, the increases in NRGB and CSCB arch axial stress may be regarded as a response to dynamic pinching of the arch.

4.3.3 B1-B1', B1-B1" and B1-B1''' LOADING

This section presents the maximum responses of the bridge models to X direction application of the modified B-1 accelerogram to all of the bridge supports with time lags between the commencement of ground motion at the south supports and the beginning of ground excitation at the north supports. These time lags were based on the arch spans and on assumed speeds for seismic wave propagation as discussed in Section 3.8.2. For B1-B1' loading the time lags were 0.3 seconds for NRGB and 0.125 seconds for CSCB. Comparisons of these B1-B1' responses with the results of B1-B1 loading for NRGB and CSCB are presented in Tables 4-9 and 4-10, respectively. The time lags for B1-B1" loading were double the B1-B1' values with 0.6 seconds for NRGB and 0.25 seconds for CSCB. Tables 4-11 and 4-12 provide comparisons of these B1-B1" responses with the results of B1-B1 loading for NRGB and CSCB, respectively. Finally,

Table 4-13 compares the NRGB responses to $B1-B1'''$ loading with the $B1-B1$ results. This $B1-B1'''$ loading was based on a time lag of 4.2 seconds which is nearly the same as the fundamental NRGB in-plane period.

The results in Tables 4-9, 4-11 and 4-13 indicate the NRGB responses to $B1-B1'$, $B1-B1''$ and $B1-B1'''$ loading were generally similar to or slightly larger than the $B1-B1$ responses. The general increases in arch axial stress with increasing time lag may again be the result of dynamic pinching of the arch.

For CSCB, the $B1-B1'$ and $B1-B1''$ results presented in Tables 4-10 and 4-12 showed large increases in arch axial stress with increasing time lag. In addition, large increases in X and Y axis maximum displacements and in deck bending stress were also observed. As indicated by the results in Table 4-7, the increases in maximum displacement and in deck bending stress are probably due to the low frequency components of the ground motion input i.e. static pinching. The larger arch axial stresses, however, are very likely caused by the higher frequency components i.e. dynamic pinching.

The low value for CSCB arch bending stress at the quarter point under $B1-B1''$ loading was not the maximum bending stress that occurred during the 30 seconds of ground motion. The maximum arch total stress at time 8 seconds, however, is dominated by the large axial stress component.

NRGB deck axial stresses seemed to show substantial declines as the time lag increased while the CSCB values showed much less change. This difference in the responses of the two bridges was very likely a result of the differences in their deck longitudinal force transfer mechanisms.

As discussed in Section 4.1.1, the NRGB main span deck axial forces are transferred to the arch while most of the CSCB deck longitudinal forces go directly to the north abutment. Thus changes in the relative north and south support motions have a much greater impact on the NRGB deck responses as opposed to the CSCB results.

All of the B1-B1'' responses for NRGB were similar to the B1-B1, B1-B1' and B1-B1'' results as can be seen by comparing Tables 4-9, 4-11 and 4-13. Thus the proximity of the 4.2 second B1-B1'' time lag to the 4.18 second period of the fundamental NRGB in-plane mode played no apparent role in the B1-B1'' results.

4.3.4 B2-B2 LOADING

NRGB responses to B2-B2 loading are presented in Table 4-14 and compared with the B1-B1 results. The maximum total element stresses and maximum displacements shown in Table 4-14 were all less under B2-B2 loading. This may have been due to the fact that increasing the B-1 accelerations by 33.3% yields a maximum ground acceleration of 0.5g while increasing the B-2 values the same 33.3% yields a maximum acceleration of only 0.42g. Thus while the earthquake intensities of the B-1 and B-2 accelerograms are comparable, the modified B-2 accelerogram does have a lower maximum ground acceleration.

4.4 Y AXIS GROUND ACCELERATION RESPONSES

4.4.1 B1-B1 LOADING

The responses of the NRGB and CSCB bridge models to B1-B1 loading in the Y direction are compared respectively in Tables 4-15 and 4-16 with the static responses due to live plus "impact" loads and due to equivalent static loads. The live plus impact loading yields the largest non-seismic vertical loads (in addition to dead loads) while the

equivalent static loading provides an approximate means for determining seismic responses as discussed in Section 3.6.3. In addition, a comparison between the CSCB Bl-B1 responses in the Y direction and the results obtained in the 1982 Study is presented in Table 4-17.

For both bridges the responses to dynamic loading, live plus impact loading and equivalent static loading all exhibited high arch axial and deck bending stresses. This follows from the fact that all of these loads are uniform or nearly uniform vertical loads.

For NRGB, the total arch and deck stresses due to dynamic loading were slightly larger than the static load results with arch stresses at the abutment showing the largest difference. The CSCB results also indicated larger arch stresses at the abutment due to dynamic loading but arch quarter point and deck center stresses were dominated by the live plus impact loading. The greater importance of live plus impact loading on CSCB is not surprising since live to dead load ratios are generally larger for bridges with shorter spans.

The total deck and arch stresses for each bridge under dynamic and static loading were nearly all below half of the yield stress with only NRGB total arch quarter point stress slightly above half the yield value. Arch total stress was higher at the quarter points than at the abutments under all three load cases for NRGB and under live plus impact loading for CSCB. The equivalent static load and dynamic load results for CSCB showed higher arch stress at the abutments, however.

The larger NRGB arch quarter point stresses may have been due to the fact that the NRGB arch has its largest cross-section near the abutments. The CSCB arch on the other hand is weaker at the abutments

than it is at the quarter points and this could explain why the largest CSCB arch stresses generally occurred at the abutment. The CSCB arch is also weaker at the crown and this coupled with the fact that the worst live plus impact loading for the arch quarter point occurs when the load is applied between the arch hinge and the crown may have both contributed to the large arch bending stresses at the stronger quarter points under live plus impact loading.

Table 4-17 clearly shows that the 1982 Study results for CSCB were all greater than the results of the current study. While the arch axial stresses were modestly larger, the arch and deck bending stresses from the 1982 Study were more than double the values for the current study. In addition to the differences in bending stress, the 1982 Study results also show double the maximum Y axis displacement at the quarter points. At least part of the bending and vertical displacement differences can be attributed to the fact that the present model used only 11 straight beam elements with 10 mass points to model the CSCB arch while the 1982 Study used 44 elements with 10 mass points. Dynamic test runs on small 4 and 8 panel circular arches with only three mass points each also showed very large increases in arch quarter point bending stresses when going from the 4 to the 8 panel model. Despite the differences in the load input and in other modeling aspects, however, the arch axial stresses for the two analyses were surprisingly close.

4.4.2 B1-B1' LOADING

The responses of the one-plane models of NRGB and CSCB to B1-B1' loading in the Y direction are compared with the B1-B1 responses in Tables 4-18 and 4-19, respectively. For both bridges the B1-B1' responses were nearly all the same or smaller. The only major

exceptions were the NRGB deck axial stresses, the NRGB deck X axis displacements and the longitudinal bracing resultants for both bridges.

Under uniform Y direction support motion such as B1-B1 loading, only the symmetric in-plane modes will play a role in the overall bridge responses. Under nonuniform motion such as B1-B1' loading, however, the asymmetric in-plane modes will begin to contribute to overall bridge motion. For both NRGB and CSCB the fundamental in-plane mode was asymmetrical, but for NRGB this mode exhibited large deck longitudinal translations while the CSCB fundamental in-plane mode did not. This difference in the fundamental in-plane modes of the two bridges was another consequence of the differences in their deck longitudinal force transfer mechanisms. The net results were the large increases in NRGB deck longitudinal motion and axial stress under B1-B1' loading compared with B1-B1 loading. The CSCB increases under the same loading were very small, however.

Both bridges also showed large increases in longitudinal bracing stresses under B1-B1' loading, but the NRGB bracing stress reached half the yield stress while the CSCB bracing force was less than 1/5 the breaking strength. The fact that the NRGB increases were much greater stems from the deck longitudinal force transfer mechanisms as discussed above and in Section 4.1.1. For both bridges, however, the deck axial stresses and displacements and the longitudinal bracing resultants under B1-B1' loading in the Y direction were still much lower than the corresponding B1-B1 results in the X direction.

4.5 Z AXIS GROUND ACCELERATION RESPONSES

4.5.1 Bl-B1 LOADING

The responses of the out-of-plane NRGB and CSCB bridge models to Bl-B1 loading in the Z direction are presented in Tables 4-20 and 4-21, respectively, and are compared with the results of lateral wind loading and equivalent static loading. The choice of lateral wind load was based on the fact that it is the largest non-seismic loading which must be resisted by the bridges in the lateral direction. As in the case of X and Y direction results, equivalent static loading was used in the Z direction to provide approximate earthquake results for comparison with the Bl-B1 results. In addition to the results presented in Tables 4-20 and 4-21, the Z displacements at the center of the deck versus time under Bl-B1 loading are plotted in Figures 4-4 and 4-5 for NRGB and CSCB, respectively. Finally, the CSCB responses to Bl-B1 loading are compared with the 1982 Study results in Table 4-22.

The Bl-B1 loading results for CSCB were larger than the corresponding results for either of the static loading cases. With the exception of the arch quarter point stresses however, the equivalent static loads gave the largest responses for NRGB. The equivalent static loads used for NRGB, however, were based on the AASHTO minimum value of 0.1 for the response coefficient C while the value of this coefficient based on the Normalized Rock Spectra (NRS) acceleration was much lower. All other factors being equal, the minimum AASHTO coefficient C governs only where the fundamental structure frequency is low. This would seem to imply that in the opinion of AASHTO the NRS do not contain enough sample motions with low frequency components.

The most crucial result obtained for either bridge under Bl-B1

loading in the Z direction was the maximum CSCB lateral cable force being more than double the 96 ton breaking strength of the cables. This result is not surprising since, as discussed in Section 4.1.3, the only means by which lateral forces can be transferred between the deck and the arch in CSCB is via the two pairs of lateral cables at the crown. The story for NRGB which has laterally braced bents at every panel point was quite different. In fact the largest stress in any NRGB bent diagonal under Bl-Bl loading was the value for the crown bent which is listed in Table 4-20 and was just over half the yield stress.

For NRGB the maximum Z displacement at the ends of the main span deck were much larger under dynamic loading than under static loading. In fact this maximum displacement at the ends of the main span deck occurred at the same time as the maximum displacement at the center but in the opposite direction. The reason that such a deck deformation can occur in NRGB is because the moment releases about the vertical axis at the ends of the main span deck give the approach spans much greater freedom for independent motion than is the case with the CSCB approach spans. This deformation of the deck resulted in a more than 50 inch differential displacement between the ends of the main span deck and its middle which also helps to explain the larger deck lateral bending stresses under dynamic loading as opposed to those under wind loading. These larger deck lateral bending stresses occurred even though the maximum displacements at the center of the bridge were very nearly the same for Bl-Bl loading and lateral wind loading.

Another result worth noting is that arch quarter point stresses were quite small for both bridges under dynamic and static loads. This clearly indicates that under simultaneous lateral support motion and

under wind loads and equivalent static loads the arch acts like a uniformly loaded fixed ended beam. The low arch lateral bending stresses near the quarter points thus correspond to the low bending stresses near the moment inflection points in a fixed ended beam under uniform load.

One final note about the results in Tables 4-20 and 4-21 is the fact that the CSCB arch and deck lateral bending stresses and deck warping stresses caused by Bl-Bl loading in the Z direction were actually larger than the NRGB values. The arch abutment bending stress may have been larger because the CSCB arch is weaker at the abutments while the stresses at the quarter points were low for both bridges as discussed above. Taken together, however, the dynamic results seem to indicate greater CSCB responses under Bl-Bl loading in the Z direction. Such a conclusion is corroborated by the modified B-1 spectrum accelerations of the fundamental out-of-plane modes for CSCB and NRGB as listed in Tables 3-14 and 3-15. For NRGB this acceleration is 0.06g while the CSCB value is 0.25g.

Figures 4-4 and 4-5 show the displacements relative to the ground at the center of the deck due to Bl-Bl loading for NRGB and CSCB, respectively, versus time. The largest absolute displacements at the center of the deck were 40.08 inches (at 17.00 seconds) for NRGB and 36.00 inches (at 9.75 seconds) for CSCB. In the region of maximum relative displacement in Figure 4-4, the period of the NRGB motion was about 5.8 seconds which is approximately 15% lower than the fundamental out-of-plane modal period. For CSCB the period of the largest motion in Figure 4-5 was about 3.0 seconds which is approximately 10% greater than the period of the fundamental mode. Thus the responses of both bridges

demonstrate the importance of the fundamental out-of-plane mode under uniform lateral support excitation.

The results in Table 4-22 indicate that the CSCB responses to Bl-B1 loading were in general larger in the present analysis than the 1982 results. The only exceptions were lateral bending stresses at the arch quarter point and deck center which were slightly larger in the 1982 study. The generally lower 1982 results may have been due to the lower spectrum acceleration for the fundamental out-of-plane mode. The Normalized Rock Spectra value is 0.22g while the modified B-1 spectra acceleration is 0.25g.

4.5.2 Bl-B2 LOADING

Tables 4-23 and 4-24 compare the NRGB and CSCB responses to Z direction Bl-B2 loading, respectively, with the Bl-B1 responses. All of the CSCB responses were lower under Bl-B2 loading while the NRGB results were mixed. The deck stresses and bent diagonal stresses near the center of the bridge and the lateral displacements at the deck center and arch crown were all lower for NRGB under Bl-B2 loading. The total arch stresses and the deck end displacements were somewhat larger, however.

The larger arch stresses that occurred in the NRGB out-of-plane model may have been related to the frequency content of the differential arch abutment displacements under Bl-B2 loading. Figure 4-6 is a plot of differential arch abutment displacement under Bl-B2 loading. As can be seen in the figure, the largest differential motion occurs in the 8 to 18 second range with a period of motion in this range of about 6.0 seconds. This 6 second period is very close to the 6.8 second fundamental period of the NRGB out-of-plane model. In addition, this 6

second period for the differential B1-B2 arch abutment motion was nearer to the period of the second NRGB out-of-plane mode (3.5 seconds) than to the period of the CSCB first and second modes (2.7 and 1.5 seconds). Thus the much closer proximity of the NRGB first and second modal periods to the period of the largest differential arch abutment displacements may account for the larger NRGB arch stresses under B1-B2 loading. This may also explain why NRGB arch stresses increased under B1-B2 loading while CSCB arch stresses decreased.

Under B1-B1 loading, the symmetric out-of-plane modes will play the major role in determining overall bridge motion. Under B1-B2 loading the asymmetric modes start to contribute to overall bridge motion while the symmetric modes begin to contribute less. For NRGB, modes 4 and 6 which were the 2nd and 3rd asymmetric out-of-plane modes each had their largest lateral displacements at the ends of the main span deck. The CSCB asymmetric out-of-plane modes, however, had much smaller lateral displacements at the ends of the main span deck. This would explain why the lateral displacements at the ends of the main span deck increased for NRGB under B1-B2 loading but decreased for CSCB.

It should also be noted that the asymmetric modes for both bridges had virtually no lateral displacements at the center of the deck and the crown of the arch. Thus the substantially lower lateral displacements that occurred under B1-B2 loading at these points for both bridges can be expected because of the increased role of the asymmetric modes in overall bridge motion.

4.5.3 B1-B1' LOADING

Tables 4-25 and 4-26 are comparisons of the Z direction B1-B1' responses and the B1-B1 responses for NRGB and CSCB, respectively. For

both bridges the results were generally the same or slightly greater under Bl-Bl' loading. In many instances in fact the results of Bl-B1 and Bl-B1' loading were indistinguishable. The only changes worth mentioning were the increases in NRGB arch abutment stresses and deck end displacements. The reasons for these increases may have been the same as the reasons discussed in Section 4.5.2.

4.6 COMBINED RESULTS

The purpose of this section is to present combined results due to Bl-B1 loading and due to Bl-B1' loading. For the following two reasons, combined responses for Bl-B2 loading were not derived. First, as explained in Section 3.8.2, Bl-B2 loading was not applied to the bridge models in the Y direction. Secondly, the possibility of either bridge being subjected to two different ground acceleration histories as in the case of Bl-B2 loading seems much less likely than Bl-B1 loading which is uniform or Bl-B1' loading which involves a time lag.

For the arch and deck total stresses, maximum combinations of X and Z direction (X-Z) responses and X, Y and Z direction (X-Y-Z) responses are presented while maximum combined X and Y direction (X-Y) responses are presented for the longitudinal bracing. The X-Z combination was chosen for presentation of deck and arch stresses because X and Z responses were larger than Y responses in 9 of the 12 results which are presented (NRGB versus CSCB, Bl-B1 versus Bl-B1' loading, and deck center, arch abutment, and arch quarter point stresses).

4.6.1 SIMULTANEOUS ACCELEROGRAM APPLICATIONS

Tables 4-27 and 4-28 present combined NRGB and CSCB responses, respectively, based on simultaneous application of loading in the directions specified. For Bl-B1 loading this means that the same ground

motion was input at each bridge support in the X and Y, the X and Z or the X, Y and Z directions simultaneously. For Bl-Bl' loading, the ground motion was applied in the X and Y, the X and Z or the X, Y and Z directions simultaneously at the south bridge supports with a time lag before simultaneous application at the north supports.

For both bridges the combined results were generally the same or greater for Bl-Bl' loading as opposed to Bl-Bl loading. The only exceptions were the maximum arch quarter point stress under combined X-Y-Z input for both bridges and the maximum NRGB deck center stress under X-Z input. Even for these exceptions, the Bl-Bl' stresses were less than 12% lower than the Bl-Bl results.

The major consequence of the differences in NRGB and CSCB deck longitudinal force transfer mechanisms was that the NRGB X direction responses were generally larger than the Z direction results while the reverse was true for CSCB. This fact combined with the greater arch stiffness near the abutments caused the NRGB arch quarter point combined stresses to be much greater than the arch combined stresses near the abutments. Similarly, the greater dominance of Z direction loads combined with the greater arch strength near the quarter points caused the CSCB arch combined stresses near the abutments to be larger than the arch quarter point combined stresses. For both bridges the largest combined arch stresses exceeded 80% of the yield stress with the largest CSCB values approaching 90%.

The two most important results presented in Tables 4-27 and 4-28, however, are the deck center stresses and longitudinal bracing stresses for NRGB which both exceeded the 50 ksi yield stress. The corresponding values for CSCB were less than 75% and 85% of the yield levels,

respectively. These differing results are one more effect caused by the differences in the deck longitudinal force transfer mechanisms.

4.6.2 SRSS AND SUMMATION OF MAXIMUM X, Y and Z RESPONSES

The simultaneous combined results discussed in the previous section are compared with results of other combination techniques in this section. The two combination methods introduced in this section are the square root of the sum of the squares (SRSS) of the maximum X and Y, the maximum X and Z or the maximum X, Y and Z responses and the summation of the absolute values of these maximum direction results. Tables 4-29 and 4-30 compare the simultaneous combined results discussed in Section 4.5.1 with the SRSS results and with the summation results for NRGB and CSCB, respectively, under B1-B1' loading. Similar comparisons for B1-B1' responses are contained in Tables 4-31 and 4-32.

While summation of the maximum direction results gave the largest combined stresses, the SRSS combinations of these direction maximums gave results that were lower than the simultaneous maximum results in 26 of 28 cases. Thus the SRSS method does not appear to be conservative in general.

Of the results presented in Tables 4-29 to 4-32, only the CSCB arch at the abutments, the NRGB deck near the center and the NRGB longitudinal bracing had summation stresses that exceeded the yield stress. In addition, only the NRGB deck near the center and the NRGB longitudinal bracing had simultaneous combined stresses or SRSS combined stresses exceeding the yield stress.

4.7 ELEMENT RESPONSES VERSUS B-1 ACCELERATION LEVELS

Figures 4-7 to 4-14 are presented for two purposes: to summarize the dynamic results for B1-B1' loading and to relate these results to

current design practice. These figures depict the dynamic and static responses of the arch abutment members, the arch quarter point members, the deck center members and the longitudinal bracing members versus two different measures of ground acceleration: the B-1 amplitude factor and the maximum ground acceleration. With the exception of CSCB longitudinal cable bracing forces, all of the results presented in these figures are stresses.

The bottom scale in Figures 4-7 to 4-14 runs from 0 indicating no ground excitation to 1.333 which was the factor used in the dynamic analyses to modify the amplitude of the B-1 accelerogram. The left and right scales are measures of the element stresses or forces while the top scale is a measure of the maximum ground acceleration. The top scale runs from 0.0g again indicating no ground motion and continues up to 0.5g which was the maximum ground acceleration under the modified B-1 accelerogram.

The B1-B1' loading was chosen for presentation in Figures 4-7 to 4-14 because the results were in general larger for this type of loading than for B1-B1 loading. The abbreviations used in the figures are defined as follows:

1. DL = dead load response
2. LL-Max = live plus impact load response ($\times 1.333/1.000$)
3. WL-Lat = lateral wind load response ($\times 1.333 / 1.250$)
4. WL-Lon = longitudinal wind load response ($\times 1.333 / 1.250$)
5. X-Max = maximum X direction responses
6. Y-Max = maximum Y direction responses
7. Z-Max = maximum Z direction responses
8. ESL-X = X direction equivalent static load responses

- 9. ESL-Y = Y direction equivalent static load responses
- 10. ESL-Z = Z direction equivalent static load responses
- 11. ESL-XYZ = sum of X, Y and Z equivalent static load responses
- 12. SIM-XY = maximum simultaneous X and Y direction responses
- 13. SIM-XZ = maximum simultaneous X and Z direction responses
- 14. SIM-XYZ = maximum simultaneous X, Y and Z direction responses
- 15. SRSS-XY = SRSS combined maximum X and Y direction responses
- 16. SRSS-XZ = SRSS combined maximum X and Z direction responses
- 17. SRSS-XYZ = SRSS combined maximum X, Y and Z responses
- 18. SUM-XY = sum of maximum X and Y direction responses
- 19. SUM-XZ = sum of maximum X and Z direction responses
- 20. SUM-XYZ = sum of maximum X, Y and Z direction responses

All of the responses depicted in Figures 4-3 to 4-10 include the dead load responses. In addition, the dynamic responses in the figures vary linearly with the B-1 amplitude factor while the static responses are constant. The only exceptions are the equivalent static load responses which are functions of the maximum ground acceleration.

The factors of 1.333/1.000 and 1.333/1.250 used to modify the live plus impact load responses and the wind load responses, respectively, are based on the AASHTO allowable stresses for these static load cases and for earthquake loading. For dead plus live plus impact loading, the allowable stress for steel members is 55% of the yield stress. This allowable stress is increased by 25% and 33.3% for dead plus wind loading and dead plus earthquake loading, respectively. Thus in order to compare the responses in Figures 4-7 to 4-14 and determine which loading will govern the design of given member, the LL-Max responses were increased by a factor of 1.333/1.000 while the WL-Lat and WL-Lon

responses were increased by a factor of 1.333/1.250. Hence all of the responses in the figures are scaled with respect to the allowable stress for dead plus earthquake loading.

4.7.1 ARCH STRESSES AT THE ABUTMENTS

Figures 4-7 and 4-8 depict the arch stresses at the abutments versus ground acceleration for NRGB and CSCB, respectively. Disregarding seismic loading, the lateral wind load stresses for both bridges would appear to control the design of the arch near the abutment. Taking the simultaneous X-Y-Z stresses (SIM-XYZ) as a measure of dynamic stress, this stress exceeded the lateral wind load stress at about 0.42g for NRGB and 0.25g for CSCB. These values correspond to B-1 amplitude factors of approximately 1.12 and 0.67 for NRGB and CSCB, respectively. Thus at higher levels of ground acceleration, the seismic loading would govern the design of the arch near the abutment.

The B1-B1' stresses for both bridges were largest in the Z direction and smallest in the Y direction. All of the CSCB B1-B1' responses, however, were larger relative to the yield stress than the NRGB values. As a result, the only combined stresses that exceeded the yield stress were the CSCB X-Z and X-Y-Z summation values.

The equivalent static load results in each direction were all much lower than their dynamic analysis counterparts except for NRGB in the Z direction. As discussed earlier, this exception was most likely due to the fact that the value of the coefficient C which was used to derive the NRGB Z direction equivalent static load stress was the minimum allowed by AASHTO and not the value calculated using the Normalized Rock Spectra which yielded a much lower value.

One last note, for both bridges the equivalent static load stress

in the Y direction exceeded the X direction value while the dynamic analysis stresses had the reverse order. This was due to the large increases in arch axial stress caused by dynamic pinching under B1-B1' loading in the X direction. Thus, while the Y direction stresses were larger than the X direction stresses under B1-B1 loading, the increases in arch axial stress under X direction B1-B1' loading propelled the X responses past the Y responses.

4.7.2 ARCH QUARTER POINT STRESSES

The NRGB and CSCB arch quarter point responses are depicted in Figures 4-9 and 4-10, respectively. Maximum live plus impact load stresses would appear to control the design of the arches near the quarter points for both bridges. Again taking the maximum simultaneous X-Y-Z stresses as a gage of dynamic stress, the maximum live plus impact load stress was exceeded at a maximum ground acceleration of about 0.28g for NRGB which corresponds to a B-1 amplitude factor of about 0.75. The CSCB maximum simultaneous X-Y-Z stresses, however, never exceeded the maximum live plus impact load stress at maximum ground accelerations less than 0.5g. In addition, none of the combined stresses for either bridge surpassed the yield stress.

The much larger NRGB combined stresses relative to the yield stress were due to the differences in the NRGB and CSCB X direction force transfer mechanisms which result in greater X direction stresses for NRGB. Thus, even though the X direction responses were largest for both bridges and the Z direction responses were smallest, the X, Y and Z responses were all relatively close for CSCB, while the X direction responses far exceeded the Y and Z responses for NRGB. In addition, the longitudinal wind load stress for NRGB came much closer to the maximum

live plus impact load stress than in the case of CSCB.

While the equivalent static load responses for NRGB were in the same order as the dynamic responses, the X direction B1-B1' stresses far exceeded the equivalent static load values. For CSCB the equivalent static load responses were largest in the Y direction and smaller in the X direction while the dynamic results had the reverse order. Thus both bridges exhibited X direction dynamic stresses considerably higher than the equivalent static load values. This was due mainly to the increased arch axial stresses caused by dynamic arch pinching under B1-B1' loading.

4.7.3 DECK CENTER STRESSES

Figures 4-11 and 4-12 depict the deck center stresses versus ground acceleration for NRGB and CSCB, respectively. Disregarding the seismic loads, the lateral wind load would seem to dictate the design of the deck near the center of both bridges. Once again using simultaneous X-Y-Z stress as a gage, the lateral wind load stress was exceeded at ground accelerations of about 0.14g for NRGB and 0.18g for CSCB. These values correspond to B-1 amplitude factors of approximately 0.37 and 0.48, respectively. Thus seismic loading would begin to govern the design at these acceleration levels. In addition, the NRGB simultaneous maximum X-Y-Z stress exceeded the yield stress at about 0.43g or a B-1 amplitude factor of 1.15. For CSCB, however, none of the combined stresses exceeded the yield stress.

The larger NRGB combined stresses were mainly a result of the greater influence of X direction ground excitation on NRGB which resulted in very large X direction dynamic stresses for NRGB. In addition, the NRGB Y direction dynamic stresses were also much larger

than the CSCB values due mainly to the much greater NRGB deck axial stresses which occurred under B1-B1' loading. Together, these two factors led to NRGB combined stresses considerably larger than the CSCB values. Moreover, these differences in the NRGB and CSCB responses under X direction loading and under Y direction loading are both directly related to the differences in the deck longitudinal force transfer mechanisms.

For NRGB, the X direction dynamic stress far exceeded the Y and Z stresses while the Z direction stress was largest in CSCB with X stress second and Y stress a distant third. For both bridges, the equivalent static load stresses in the Z direction far exceeded the X or Y direction values. Except for CSCB Y direction stresses, however, all of the B1-B1' responses were much larger than the equivalent static load stresses.

4.7.4 LONGITUDINAL BRACING RESULTANTS

Stresses versus ground acceleration are plotted for the NRGB longitudinal bracing members in Figure 4-13, while forces versus ground acceleration are plotted in Figure 4-14 for the CSCB cable bracing members. While the design of these bracing members may be controlled by the longitudinal wind load stresses, these stresses were exceeded by simultaneous X-Y stresses at very low levels of ground acceleration. For NRGB this level was only about 0.04g while 0.02g was the approximate level for CSCB. These values correspond to B-1 amplitude factors of 0.11 and 0.05, respectively. The NRGB simultaneous X-Y stresses exceeded the yield stress at about 0.42g or a B-1 amplitude factor of approximately 1.12. In addition, the NRGB X direction stress alone exceeded the yield stress at a ground acceleration of about 0.49g or a

B-1 amplitude factor of about 1.31. None of the CSCB individual direction forces or combined forces exceeded the cable breaking force of 162 tons, however.

The much larger NRGB stresses as discussed earlier were caused by the fact that all of the deck main span longitudinal inertia forces are transferred through the longitudinal bracing to the arch and then to the ground. For both bridges, however, the B1-B1' X and Y component responses were considerably larger than the equivalent static load resultants. This was a consequence of the large arch and deck differential X direction translations that occurred under dynamic loading as discussed in Section 4.1.3

Table 4-1 NRGB Maximum X Direction Bl-Bl Responses Versus Static Responses (Yield Stress = 50 ksi)

Response	Units	Accelerograms Bl and Bl	Longitudinal Wind Load	Equivalent Static Load
Arch Beam Stresses at Abutment Element 1 of 14 Node I				
Axial (and Total)	ksi	16.34	14.16	14.89
Arch Beam Stresses at Quarter Point Element 11 of 14 Node I				
Axial	ksi	17.81	15.75	17.84
Local y-y Bending	ksi	15.33	4.92	3.98
Total	ksi	33.14	20.67	21.82
Longitudinal Bracing Axial Stresses Truss Element 2	ksi	55.67	5.59	23.27
Deck Beam Stresses near Center Element 6 of 14 Node J				
Axial	ksi	24.81	3.60	9.92
Local y-y Bending	ksi	21.53	16.58	11.27
Total	ksi	46.34	20.18	21.19
X Translation at Ends of Deck Panel Point 5	inches	13.06	3.34	8.44
X Translation at Quarter Point of Arch Panel Point 9	inches	17.47	4.09	10.24
Y Translation at Quarter Point of Deck and Arch Panel Point 9	inches	26.47	5.27	13.16

Table 4-2 CSCB Maximum X Direction B1-B1 Responses Versus Static Responses (Yield Stress = 33 ksi)

Response	Units	Accelerograms B1 and B1	Longitudinal Wind Load	Equivalent Static Load
Arch Beam Stresses at Abutment Element 11 of 11 Node J				
Axial (and Total)	ksi	9.78	9.24	9.38
Arch Beam Stresses at Quarter Point Element 4 of 11 Node I				
Axial	ksi	5.07	5.25	4.98
Local y-y Bending	ksi	4.13	1.38	2.19
Total	ksi	9.20	6.63	7.17
Longitudinal Bracing Axial Forces (Breaking Strength = 162 tons) Truss Element 1	tons	105.2	8.6	21.0
Deck Beam Stresses near Center Element 6 of 11 Node I				
Axial	ksi	8.76	1.02	3.06
Local y-y Bending	ksi	6.42	4.73	4.44
Total	ksi	15.18	5.75	7.50
X Translation at Ends of Deck Panel Point 6	inches	3.41	0.46	1.32
Y Translation at Quarter Point of Deck and Arch Panel Point 9	inches	4.19	2.21	4.36

Table 4-3 CSCB Maximum X Direction Bl-Bl Responses Versus 1982 Study Results (Yield Stress = 33 ksi)

Response	Units	Accelerograms Bl and Bl	1982 Study
Arch Beam Stresses at Abutment Element 11 of 11 - Node J			
Axial (and Total)	ksi	9.78	9.46
Time	seconds	(17.25)	
Arch Beam Stresses at Quarter Point Element 4 of 11 - Node I			
Axial	ksi	5.07	5.97
Local y-y Bending	ksi	4.13	5.97
Total	ksi	9.20	11.29
Time	seconds	(17.00)	
Longitudinal Bracing Axial Forces Truss Element 1			
Time	seconds	(15.00)	206.7
Deck Beam Stresses near Center Element 6 of 11 - Node I			
Axial	ksi	8.76	11.08
Local y-y Bending	ksi	6.42	11.11
Total	ksi	15.18	17.51
Time	seconds	(15.00)	
X Translation at Ends of Deck Panel Point 6			
Time	seconds	(15.00)	4.11
Y Translation at Quarter Point of Deck and Arch Panel Point 9			
Time	seconds	(17.00)	4.84

Table 4-4 NRGB Maximum X Direction B1-B1 Responses Versus Maximum B1-B2 Responses (Yield Stress = 50 ksi)

Response	Units	Accelerograms B1 and B1	Accelerograms B1 and B2
Arch Beam Stresses at Abutment Element 1 of 14 - Node I			
Axial (and Total)	ksi	16.34	20.11
Time	seconds	(14.25)	(7.50)
Arch Beam Stresses at Quarter Point Element 11 of 14 - Node I			
Axial	ksi	17.81	20.39
Local y-y Bending	ksi	15.33	10.69
Total	ksi	33.14	31.08
Time	seconds	(12.75)	(17.25)
Longitudinal Bracing Axial Stresses Truss Element 2			
Time	seconds	(13.50)	(10.50)
Deck Beam Stresses near Center Element 6 of 14 - Node J			
Axial	ksi	24.81	13.71
Local y-y Bending	ksi	21.53	23.07
Total	ksi	46.34	36.78
Time	seconds	(11.00)	(9.75)
X Translation at Ends of Deck Panel Point 5			
Time	seconds	(11.00)	(9.25)
X Translation at Quarter Point of Arch Panel Point 9			
Time	seconds	(12.75)	(16.75)
Y Translation at Quarter Point of Deck and Arch Panel Point 9			
Time	seconds	(12.75)	(9.25)

Table 4-5 CSCB Maximum X Direction B1-B1 Responses Versus Maximum B1-B2 Responses (Yield Stress = 33 ksi)

Response	Units	Accelerograms B1 and B1	Accelerograms B1 and B2
Arch Beam Stresses at Abutment Element 11 of 11 - Node J			
Axial (and Total)	ksi	9.78	15.40
Time	seconds	(17.25)	(8.00)
Arch Beam Stresses at Quarter Point Element 4 of 11 - Node I			
Axial	ksi	5.07	8.13
Local y-y Bending	ksi	4.13	8.72
Total	ksi	9.20	16.85
Time	seconds	(17.00)	(16.00)
Longitudinal Bracing Axial Forces (Breaking Strength = 162 tons) Truss Element 1			
Time	seconds	(15.00)	(11.75)
Deck Beam Stresses near Center Element 6 of 11 - Node I			
Axial	ksi	8.76	5.21
Local y-y Bending	ksi	6.42	9.25
Total	ksi	15.18	14.46
Time	seconds	(15.00)	(14.50)
X Translation at Ends of Deck Panel Point 6			
Time	seconds	(15.00)	(11.75)
Y Translation at Quarter Point of Deck and Arch Panel Point 9			
Time	seconds	(17.00)	(12.00)

Table 4-6 NRGB Static Pinching Stress and Displacement Comparisons
(Yield Stress = 50 ksi)

Response	Units	Acceler- ograms B1-B2	Acceler- ograms B1-B1'	Acceler- ograms B1-B1''	Acceler- ograms B1-B1'''
Maximum Differential Arch Abutment X Direction Displacement	inches	21.39	5.91	10.14	16.95
Maximum X Displacement at the End of the Deck Panel Point 5	inches	10.68	2.95	5.07	8.48
Maximum Y Displacement of Arch and Deck at Quarter Point Panel Point 9	inches	14.45	3.99	6.85	11.46
Arch Beam Stresses at Abutment Element 1 of 14 Node I					
Axial (and Total)	ksi	0.06	0.02	0.03	0.05
Arch Beam Stresses at Quarter Point Element 11 of 14 Node I					
Axial	ksi	0.12	0.03	0.06	0.10
Local y-y Bending	ksi	1.88	0.52	0.89	1.49
Total	ksi	2.00	0.55	0.95	1.59
Deck Beam Stresses near Center Element 6 of 14 Node J					
Axial	ksi	0.00	0.00	0.00	0.00
Local y-y Bending	ksi	1.96	0.54	0.93	1.56
Total	ksi	1.96	0.54	0.93	1.56

Table 4-7 CSCB Static Pinching Stress and Displacement Comparisons
(Yield Stress = 33 ksi)

Response	Units	Acceler- ograms Bl-B2	Acceler- ograms Bl-B1'	Acceler- ograms Bl-B1''
Maximum Differential Arch Abutment X Direction Displacement	inches	21.39	2.30	4.97
Maximum X Displacement at the End of the Deck Panel Point 6	inches	21.39	2.30	4.97
Maximum Y Displacement of Arch and Deck at Quarter Point Panel Point 9	inches	23.78	2.55	5.53
Arch Beam Stresses at Abutment Element 11 of 11 Node J				
Axial (and Total)	ksi	0.82	0.09	0.19
Arch Beam Stresses at Quarter Point Element 4 of 11 Node I				
Axial	ksi	0.74	0.08	0.17
Local y-y Bending	ksi	7.80	0.84	1.81
Total	ksi	8.54	0.92	1.98
Longitudinal Bracing Axial Forces (Breaking Strength = 162 tons) Truss Element 1	tons	276.1	29.6	64.2
Deck Beam Stresses near Center Element 6 of 11 Node I				
Axial	ksi	1.68	0.18	0.39
Local y-y Bending	ksi	3.50	0.38	0.81
Total	ksi	5.18	0.56	1.20

Table 4-8 NRGB Dynamic Pinching Responses Due to Pulse Sine Wave Versus Static Pinching (Yield Stress = 50 ksi)

Response	Units	Dynamic Pinching T = 0.4 seconds	Dynamic Pinching T = 4.0 seconds	Static Pinching
Maximum Differential Arch Abutment X Direction Displacement	inches	6.00	6.00	6.00
Maximum Y Displacement of Arch and Deck at Quarter Point Panel Point 9	inches	3.91	4.07	4.05
Maximum Y Displacement of Arch and Deck at Crown Panel Point 12	inches	4.22	5.47	5.43
Arch Beam Stresses at Abutment Element 1 of 14 Node I				
Axial (and Total)	ksi	2.38	0.06	0.02
Arch Beam Stresses at Quarter Point Element 11 of 14 Node I				
Axial	ksi	3.74	0.05	0.03
Local y-y Bending	ksi	0.11	0.53	0.53
Total	ksi	3.85	0.58	0.56
Deck Beam Stresses near Center Element 6 of 14 Node J				
Axial	ksi	0.03	0.01	0.00
Local y-y Bending	ksi	0.21	0.56	0.55
Total	ksi	0.24	0.57	0.55

Table 4-9 NRGB Maximum X Direction Bl-Bl Responses Versus Maximum Bl-Bl' Responses (Yield Stress = 50 ksi)

Response	Units	Accelerograms Bl and Bl	Accelerograms Bl and Bl'
Arch Beam Stresses at Abutment Element 1 of 14 - Node I			
Axial (and Total)	ksi	16.34	17.66
Time	seconds	(14.25)	(16.25)
Arch Beam Stresses at Quarter Point Element 11 of 14 - Node I			
Axial	ksi	17.81	20.19
Local y-y Bending	ksi	15.33	16.73
Total	ksi	33.14	36.92
Time	seconds	(12.75)	(13.25)
Longitudinal Bracing Axial Stresses Truss Element 2	ksi	55.67	50.39
Time	seconds	(13.50)	(12.25)
Deck Beam Stresses near Center Element 6 of 14 - Node J			
Axial	ksi	24.81	17.58
Local y-y Bending	ksi	21.53	25.36
Total	ksi	46.34	42.94
Time	seconds	(11.00)	(11.25)
X Translation at Ends of Deck Panel Point 5	inches	13.06	12.30
Time	seconds	(11.00)	(12.50)
X Translation at Quarter Point of Arch Panel Point 9	inches	17.47	17.99
Time	seconds	(12.75)	(12.75)
Y Translation at Quarter Point of Deck and Arch Panel Point 9	inches	26.47	31.74
Time	seconds	(12.75)	(12.75)

Table 4-10 CSCB Maximum X Direction Bl-Bl Responses Versus Maximum Bl-Bl' Responses (Yield Stress = 33 ksi)

Response	Units	Accelerograms Bl and Bl	Accelerograms Bl and Bl' 0.125
Arch Beam Stresses at Abutment Element 11 of 11 - Node J			
Axial (and Total)	ksi	9.78	15.40
Time	seconds	(17.25)	(17.75)
Arch Beam Stresses at Quarter Point Element 4 of 11 - Node I			
Axial	ksi	5.07	7.31
Local y-y Bending	ksi	4.13	3.52
Total	ksi	9.20	10.83
Time	seconds	(17.00)	(8.25)
Longitudinal Bracing Axial Forces (Breaking Strength = 162 tons) Truss Element 1			
Time	seconds	(15.00)	(21.00)
Deck Beam Stresses near Center Element 6 of 11 - Node I			
Axial	ksi	8.76	6.54
Local y-y Bending	ksi	6.42	6.99
Total	ksi	15.18	13.53
Time	seconds	(15.00)	(21.00)
X Translation at Ends of Deck Panel Point 6			
Time	seconds	(15.00)	(11.50)
Y Translation at Quarter Point of Deck and Arch Panel Point 9			
Time	seconds	(17.00)	(16.00)

Table 4-11 NRGB Maximum X Direction Bl-Bl Responses Versus Maximum Bl-Bl" Responses (Yield Stress = 50 ksi)

Response	Units	Accelerograms Bl and Bl	Accelerograms Bl and Bl"
Arch Beam Stresses at Abutment Element 1 of 14 - Node I			
Axial (and Total)	ksi	16.34	18.50
Time	seconds	(14.25)	(7.50)
Arch Beam Stresses at Quarter Point Element 11 of 14 - Node I			
Axial	ksi	17.81	21.02
Local y-y Bending	ksi	15.33	16.22
Total	ksi	33.14	37.24
Time	seconds	(12.75)	(13.50)
Longitudinal Bracing Axial Stresses Truss Element 2	ksi	55.67	36.28
Time	seconds	(13.50)	(12.25)
Deck Beam Stresses near Center Element 6 of 14 - Node J			
Axial	ksi	24.81	5.13
Local y-y Bending	ksi	21.53	28.00
Total	ksi	46.34	33.13
Time	seconds	(11.00)	(13.25)
X Translation at Ends of Deck Panel Point 5	inches	13.06	12.67
Time	seconds	(11.00)	(12.75)
X Translation at Quarter Point of Arch Panel Point 9	inches	17.47	16.09
Time	seconds	(12.75)	(12.75)
Y Translation at Quarter Point of Deck and Arch Panel Point 9	inches	26.47	28.79
Time	seconds	(12.75)	(12.75)

Table 4-12 CSCB Maximum X Direction Bl-Bl Responses Versus Maximum Bl-Bl" Responses (Yield Stress = 33 ksi)

Response	Units	Accelerograms Bl and Bl	Accelerograms Bl and Bl"
Arch Beam Stresses at Abutment Element 11 of 11 - Node J			
Axial (and Total)	ksi	9.78	19.06
Time	seconds	(17.25)	(8.00)
Arch Beam Stresses at Quarter Point Element 4 of 11 - Node I			
Axial	ksi	5.07	10.97
Local y-y Bending	ksi	4.13	0.68
Total	ksi	9.20	11.65
Time	seconds	(17.00)	(8.00)
Longitudinal Bracing Axial Forces (Breaking Strength = 162 tons) Truss Element 1			
Time	seconds	(15.00)	(11.00)
Deck Beam Stresses near Center Element 6 of 11 - Node I			
Axial	ksi	8.76	7.57
Local y-y Bending	ksi	6.42	9.47
Total	ksi	15.18	17.04
Time	seconds	(15.00)	(15.25)
X Translation at Ends of Deck Panel Point 6			
Time	seconds	(15.00)	(16.00)
Y Translation at Quarter Point of Deck and Arch Panel Point 9			
Time	seconds	(17.00)	(16.00)

Table 4-13 NRGB Maximum X Direction Bl-Bl Responses Versus Maximum Bl-Bl^{''} Responses (Yield Stress = 50 ksi)

Response	Units	Accelerograms Bl and Bl	Accelerograms Bl and Bl ^{''}
Arch Beam Stresses at Abutment Element 1 of 14 - Node I			
Axial (and Total)	ksi	16.34	18.38
Time	seconds	(14.25)	(10.25)
Arch Beam Stresses at Quarter Point Element 11 of 14 - Node I			
Axial	ksi	17.81	19.98
Local y-y Bending	ksi	15.33	13.99
Total	ksi	33.14	33.97
Time	seconds	(12.75)	(17.25)
Longitudinal Bracing Axial Stresses Truss Element 2			
Time	seconds	(13.50)	(16.50)
Deck Beam Stresses near Center Element 6 of 14 - Node J			
Axial	ksi	24.81	14.56
Local y-y Bending	ksi	21.53	23.91
Total	ksi	46.34	38.47
Time	seconds	(11.00)	(11.25)
X Translation at Ends of Deck Panel Point 5			
Time	seconds	(11.00)	(16.50)
X Translation at Quarter Point of Arch Panel Point 9			
Time	seconds	(12.75)	(12.75)
Y Translation at Quarter Point of Deck and Arch Panel Point 9			
Time	seconds	(12.75)	(12.75)

Table 4-14 NRGB Maximum X Direction B1-B1 Responses Versus Maximum B2-B2 Responses (Yield Stress = 50 ksi)

Response	Units	Accelerograms B1 and B1	Accelerograms B2 and B2
Arch Beam Stresses at Abutment Element 1 of 14 - Node I			
Axial (and Total)	ksi	16.34	15.96
Time	seconds	(14.25)	(4.75)
Arch Beam Stresses at Quarter Point Element 11 of 14 - Node I			
Axial	ksi	17.81	16.30
Local y-y Bending	ksi	15.33	8.42
Total	ksi	33.14	24.72
Time	seconds	(12.75)	(20.25)
Longitudinal Bracing Axial Stresses Truss Element 2	ksi	55.67	37.90
Time	seconds	(13.50)	(10.50)
Deck Beam Stresses near Center Element 6 of 14 - Node J			
Axial	ksi	24.81	17.50
Local y-y Bending	ksi	21.53	22.21
Total	ksi	46.34	39.71
Time	seconds	(11.00)	(5.50)
X Translation at Ends of Deck Panel Point 5	inches	13.06	8.48
Time	seconds	(11.00)	(19.00)
X Translation at Quarter Point of Arch Panel Point 9	inches	17.47	11.87
Time	seconds	(12.75)	(18.50)
Y Translation at Quarter Point of Deck and Arch Panel Point 9	inches	26.47	18.07
Time	seconds	(12.75)	(18.50)

Table 4-15 NRGB Maximum Y Direction Bl-Bl Responses Versus Static Responses (Yield Stress = 50 ksi)

Response	Units	Accelerograms Bl and Bl	Live Plus Impact Load	Equivalent Static Load
Arch Beam Stresses at Abutment Element 1 of 14 Node I				
Axial (and Total)	ksi	18.54	14.86	15.40
Arch Beam Stresses at Quarter Point Element 11 of 14 Node I				
Axial	ksi	21.18	17.31	18.36
Local y-y Bending	ksi	4.87	5.49	2.81
Total	ksi	26.05	22.80	21.17
Longitudinal Bracing Axial Stresses Truss Element 2	ksi	9.27	1.89	2.13
Deck Beam Stresses near Center Element 6 of 14 Node J				
Axial	ksi	1.89	0.00	0.00
Local y-y Bending	ksi	19.92	19.74	18.44
Total	ksi	21.81	19.74	18.44
X Translation at Ends of Deck Panel Point 19	inches	0.62	0.00	0.00
Y Translation at Quarter Point of Arch and Deck Panel Point 9	inches	4.77	6.63	12.16
Y Translation at Crown of Arch and Center of Deck Panel Point 12	inches	4.76	3.17	11.04

Table 4-16 CSCB Maximum Y Direction Bl-Bl Responses Versus Static Responses (Yield Stress = 33 ksi)

Response	Units	Accelerograms Bl and Bl	Live Plus Impact Load	Equivalent Static Load
Arch Beam Stresses at Abutment Element 11 of 11 Node J				
Axial (and Total)	ksi	16.12	10.92	11.35
Arch Beam Stresses at Quarter Point Element 4 of 11 Node I				
Axial	ksi	8.48	5.67	6.46
Local y-y Bending	ksi	1.79	7.03	1.24
Total	ksi	10.27	12.70	7.70
Longitudinal Bracing Axial Forces (Breaking Strength = 162 tons) Truss Element 1	tons	7.4	5.2	6.6
Deck Beam Stresses near Center Element 6 of 11 Node I				
Axial	ksi	0.23	0.03	0.04
Local y-y Bending	ksi	5.78	8.62	6.40
Total	ksi	6.01	8.59	6.36
X Translation at Ends of Deck Panel Point 6	inches	0.10	0.00	0.01
Y Translation at Quarter Point of Deck and Arch Panel Point 9	inches	1.67	5.91	1.54
Y Translation at Crown of Arch and Center of Deck Panel Point 11	inches	1.47	2.88	3.42

Table 4-17 CSCB Maximum Y Direction Bl-B1 Responses Versus 1982 Study Results (Yield Stress = 33 ksi)

Response	Units	Accelerograms Bl and B1	1982 Study
Arch Beam Stresses at Abutment Element 11 of 11 - Node J			
Axial (and Total)	ksi	16.12	19.85
Time	seconds	(7.75)	
Arch Beam Stresses at Quarter Point Element 4 of 11 - Node I			
Axial	ksi	8.48	11.76
Local y-y Bending	ksi	1.79	11.34
Total	ksi	10.27	18.35
Time	seconds	(4.50)	
Longitudinal Bracing Axial Forces (Breaking Strength = 162 tons) Truss Element 1			
Time	seconds	(7.50)	17.0
Deck Beam Stresses near Center Element 6 of 11 - Node I			
Axial	ksi	0.23	0.60
Local y-y Bending	ksi	5.78	11.76
Total	ksi	6.01	11.83
Time	seconds	(8.00)	
X Translation at Ends of Deck Panel Point 6			
Time	seconds	(11.75)	0.18
Y Translation at Quarter Point of Deck and Arch Panel Point 9			
Time	seconds	(7.75)	3.72
Y Translation at Crown of Arch and Center of Deck Panel Point 11			
Time	seconds	(4.50)	2.15

Table 4-18 NRGB Maximum Y Direction Bl-Bl Responses Versus Maximum Bl-Bl' Responses (Yield Stress = 50 ksi)

Response	Units	Accelerograms Bl and Bl	Accelerograms Bl and Bl'
Arch Beam Stresses at Abutment Element 1 of 14 - Node I			
Axial (and Total)	ksi	18.54	17.22
Time	seconds	(9.50)	(7.50)
Arch Beam Stresses at Quarter Point Element 11 of 14 - Node I			
Axial	ksi	21.18	18.58
Local y-y Bending	ksi	4.87	4.93
Total	ksi	26.05	23.51
Time	seconds	(13.50)	(13.50)
Longitudinal Bracing Axial Stresses Truss Element 2			
Time	seconds	(17.50)	(13.50)
Deck Beam Stresses near Center Element 6 of 14 - Node J			
Axial	ksi	1.89	12.08
Local y-y Bending	ksi	19.92	18.05
Total	ksi	21.81	30.13
Time	seconds	(17.50)	(14.00)
X Translation at Ends of Deck Panel Point 19			
Time	seconds	(15.00)	(10.00)
Y Translation at Quarter Point of Deck and Arch Panel Point 9			
Time	seconds	(7.50)	(9.75)
Y Translation at Crown of Arch and Center of Deck Panel Point 12			
Time	seconds	(9.50)	(9.75)

Table 4-19 CSCB Maximum Y Direction Bl-Bl Responses Versus Maximum Bl-Bl' Responses (Yield Stress = 33 ksi)

Response	Units	Accelerograms Bl and Bl	Accelerograms Bl and Bl'
Arch Beam Stresses at Abutment Element 11 of 11 - Node J			
Axial (and Total)	ksi	16.12	13.63
Time	seconds	(7.75)	(8.00)
Arch Beam Stresses at Quarter Point Element 4 of 11 - Node I			
Axial	ksi	8.48	7.76
Local y-y Bending	ksi	1.79	1.73
Total	ksi	10.27	9.49
Time	seconds	(4.50)	(8.00)
Longitudinal Bracing Axial Forces (Breaking Strength = 162 tons) Truss Element 1			
Time	seconds	(7.50)	(11.50)
Deck Beam Stresses near Center Element 6 of 11 - Node I			
Axial	ksi	0.23	0.36
Local y-y Bending	ksi	5.78	6.40
Total	ksi	6.01	6.04
Time	seconds	(8.00)	(9.75)
X Translation at Ends of Deck Panel Point 6			
Time	seconds	(11.75)	(16.00)
Y Translation at Quarter Point of Deck and Arch Panel Point 9			
Time	seconds	(7.75)	(17.50)
Y Translation at Crown of Arch and Center of Deck Panel Point 11			
Time	seconds	(4.50)	(19.50)

Table 4-20 NRGB Maximum Z Direction Bl-Bl Responses Versus Static Responses (Yield Stress = 50 ksi)

Response	Units	Accelerograms Bl and Bl	Lateral Wind Load	Equivalent Static Load
Arch Beam Stresses at Abutment Element 1 of 14 Node I				
Local x-x Bending	ksi	8.53	10.76	15.54
Total	ksi	22.22	24.45	29.23
Arch Beam Stresses at Quarter Point Element 11 of 14 Node I				
Local x-x Bending	ksi	1.76	0.25	0.57
Total	ksi	20.58	19.07	19.39
Bent Diagonal Bracing Axial Stresses Panel Point 12	ksi	27.18	25.38	45.12
Deck Beam Stresses near Center Element 6 of 14 Node J				
Warping	ksi	3.00	2.48	2.42
Local x-x Bending	ksi	11.89	6.93	17.42
Total	ksi	31.28	25.80	34.46
Z Translation at Ends of Deck Panel Point 5	inches	7.98	1.04	1.51
Z Translation at Center of Deck Panel Point 12	inches	43.33	42.34	61.63
Z Translation at Crown of Arch Panel Point 12	inches	37.22	37.40	54.29

Table 4-21 CSCB Maximum Z Direction Bl-Bl Responses Versus Static Responses (Yield Stress = 33 ksi)

Response	Units	Accelerograms Bl and Bl	Lateral Wind Load	Equivalent Static Load
Arch Beam Stresses at Abutment Element 11 of 11 Node J				
Local x-x Bending	ksi	16.51	9.03	13.95
Total	ksi	25.59	18.11	23.02
Arch Beam Stresses at Quarter Point Element 4 of 11 Node I				
Local x-x Bending	ksi	2.00	0.24	0.69
Total	ksi	8.16	6.40	6.86
Lateral Cable Bracing Axial Forces (Breaking Strength = 96 tons) Panel Point 12	tons	221.6	44.4	106.6
Deck Beam Stresses near Center Element 6 of 11 Node I				
Warping	ksi	6.17	2.53	4.69
Local x-x Bending	ksi	12.31	4.65	6.21
Total	ksi	23.56	12.27	15.99
Z Translation at Ends of Deck Panel Point 6	inches	10.45	5.91	8.82
Z Translation at Center of Deck Panel Point 11	inches	26.16	13.72	20.99
Z Translation at Crown of Arch Panel Point 11	inches	19.55	10.80	15.98

Table 4-22 CSCB Maximum Z Direction Bl-Bl Responses Versus 1982 Study Results (Yield Stress = 33 ksi)

Response	Units	Accelerograms Bl and Bl	1982 Study
Arch Beam Stresses at Abutment Element 11 of 11 - Node J			
Local x-x Bending	ksi	16.51	13.70
Total	ksi	25.59	22.74
Time	seconds	(11.25)	
Arch Beam Stresses at Quarter Point Element 4 of 11 - Node I			
Local x-x Bending	ksi	2.00	4.15
Total	ksi	8.16	9.52
Time	seconds	(11.50)	
Lateral Cable Bracing Axial Forces (Breaking Strength = 96 tons) Panel Point 12	tons	221.6	152.8
Time	seconds	(11.50)	
Deck Beam Stresses near Center Element 6 of 11 - Node I			
Warping	ksi	6.17	0.00
Local x-x Bending	ksi	12.31	14.83
Total	ksi	23.56	19.59
Time	seconds	(11.00)	
Z Translation at Ends of Deck Panel Point 6	inches	10.45	6.94
Time	seconds	(9.75)	
Z Translation at Center of Deck Panel Point 11	inches	26.16	22.18
Time	seconds	(9.75)	
Z Translation at Crown of Arch Panel Point 11	inches	19.55	17.92
Time	seconds	(11.00)	

Table 4-23 NRGB Maximum Z Direction B1-B1 Responses Versus Maximum
B1-B2 Responses (Yield Stress = 50 ksi)

Response	Units	Accelerograms B1 and B1	Accelerograms B1 and B2
Arch Beam Stresses at Abutment Element 1 of 14 - Node I			
Local x-x Bending	ksi	8.53	10.20
Total	ksi	22.22	23.89
Time	seconds	(19.25)	(20.25)
Arch Beam Stresses at Quarter Point Element 11 of 14 - Node I			
Local x-x Bending	ksi	1.76	2.39
Total	ksi	20.58	21.21
Time	seconds	(16.25)	(14.25)
Bent Diagonal Bracing Axial Stresses Panel Point 12			
Time	seconds	(17.00)	(21.25)
Deck Beam Stresses near Center Element 6 of 14 - Node J			
Warping	ksi	3.00	1.32
Local x-x Bending	ksi	11.89	6.74
Total	ksi	31.28	24.45
Time	seconds	(17.00)	(21.25)
Z Translation at Ends of Deck Panel Point 5			
Time	seconds	(17.00)	(12.25)
Z Translation at Center of Deck Panel Point 12			
Time	seconds	(17.00)	(21.25)
Z Translation at Crown of Arch Panel Point 12			
Time	seconds	(17.00)	(21.25)

Table 4-24 CSCB Maximum Z Direction B1-B1 Responses Versus Maximum B1-B2 Responses (Yield Stress = 33 ksi)

Response	Units	Accelerograms B1 and B1	Accelerograms B1 and B2
Arch Beam Stresses at Abutment Element 11 of 11 - Node J			
Local x-x Bending	ksi	16.51	11.38
Total	ksi	25.59	20.46
Time	seconds	(11.25)	(11.00)
Arch Beam Stresses at Quarter Point Element 4 of 11 - Node I			
Local x-x Bending	ksi	2.00	1.90
Total	ksi	8.16	8.06
Time	seconds	(11.50)	(11.75)
Lateral Cable Bracing Axial Forces (Breaking Strength = 96 tons) Panel Point 12			
Time	seconds	(11.50)	(11.25)
Deck Beam Stresses near Center Element 6 of 11 - Node I			
Warping	ksi	6.17	5.02
Local x-x Bending	ksi	12.31	4.67
Total	ksi	23.57	14.78
Time	seconds	(11.00)	(10.75)
Z Translation at Ends of Deck Panel Point 6			
Time	seconds	(9.75)	(13.00)
Z Translation at Center of Deck Panel Point 11			
Time	seconds	(9.75)	(11.00)
Z Translation at Crown of Arch Panel Point 11			
Time	seconds	(11.00)	(11.00)

Table 4-25 NRGB Maximum Z Direction Bl-Bl Responses Versus Maximum Bl-Bl' Responses (Yield Stress = 50 ksi)

Response	Units	Accelerograms Bl and Bl	Accelerograms Bl and Bl'
Arch Beam Stresses at Abutment Element 1 of 14 - Node I			
Local x-x Bending	ksi	8.53	9.89
Total	ksi	22.22	23.58
Time	seconds	(19.25)	(16.50)
Arch Beam Stresses at Quarter Point Element 11 of 14 - Node I			
Local x-x Bending	ksi	1.76	1.77
Total	ksi	20.58	20.59
Time	seconds	(16.25)	(16.50)
Bent Diagonal Bracing Axial Stresses Panel Point 12			
Time	seconds	(17.00)	(17.00)
Deck Beam Stresses near Center Element 6 of 14 - Node J			
Warping	ksi	3.00	2.80
Local x-x Bending	ksi	11.89	11.47
Total	ksi	31.28	30.66
Time	seconds	(17.00)	(17.25)
Z Translation at Ends of Deck Panel Point 5			
Time	seconds	(17.00)	(9.75)
Z Translation at Center of Deck Panel Point 12			
Time	seconds	(17.00)	(17.00)
Z Translation at Crown of Arch Panel Point 12			
Time	seconds	(17.00)	(17.00)

Table 4-26 CSCB Maximum Z Direction Bl-Bl Responses Versus Maximum Bl-Bl' Responses (Yield Stress = 33 ksi)

Response	Units	Accelerograms Bl and Bl	Accelerograms Bl and Bl'
Arch Beam Stresses at Abutment Element 11 of 11 - Node J			
Local x-x Bending	ksi	16.51	18.08
Total	ksi	25.59	27.15
Time	seconds	(11.25)	(11.25)
Arch Beam Stresses at Quarter Point Element 4 of 11 - Node I			
Local x-x Bending	ksi	2.00	2.17
Total	ksi	8.16	8.33
Time	seconds	(11.50)	(11.50)
Lateral Cable Bracing Axial Forces (Breaking Strength = 96 tons) Panel Point 12	tons	221.6	203.8
Time	seconds	(11.50)	(11.00)
Deck Beam Stresses near Center Element 6 of 11 - Node I			
Warping	ksi	6.17	4.89
Local x-x Bending	ksi	12.31	12.91
Total	ksi	23.56	22.89
Time	seconds	(11.00)	(11.00)
Z Translation at Ends of Deck Panel Point 6	inches	10.45	10.85
Time	seconds	(9.75)	(9.75)
Z Translation at Center of Deck Panel Point 11	inches	26.16	26.43
Time	seconds	(9.75)	(10.00)
Z Translation at Crown of Arch Panel Point 11	inches	19.55	19.57
Time	seconds	(11.00)	(10.00)

Table 4-27 NRGB Maximum Combined Bl-Bl Responses Versus Maximum
Combined Bl-Bl' Responses (Yield Stress = 50 ksi)

Response	Units	Accelerograms Bl and Bl	Accelerograms Bl and Bl'
Arch Beam Stresses at Abutment			
Element 1 of 14 - Node I			
X + Z Directions	ksi	23.09	25.94
Time	seconds	(16.25)	(16.25)
X + Y + Z Directions	ksi	26.24	28.29
Time	seconds	(16.25)	(16.50)
Arch Beam Stresses at Quarter Point			
Element 11 of 14 - Node I			
X + Z Directions	ksi	33.71	37.08
Time	seconds	(12.75)	(13.25)
X + Y + Z Directions	ksi	40.45	39.62
Time	seconds	(12.75)	(13.00)
Longitudinal Bracing Axial Stresses			
Truss Element 2			
X + Y Directions	ksi	60.64	59.22
Time	seconds	(13.50)	(13.50)
Deck Beam Stresses near Center			
Element 6 of 14 - Node J			
X + Z Directions	ksi	54.69	48.33
Time	seconds	(11.00)	(11.25)
X + Y + Z Directions	ksi	55.59	56.72
Time	seconds	(11.00)	(11.25)

Table 4-28 CSCB Maximum Combined Bl-Bl Responses Versus Maximum Combined Bl-Bl' Responses (Yield Stress = 33 ksi)

Response	Units	Accelerograms Bl and Bl	Accelerograms Bl and Bl'
Arch Beam Stresses at Abutment Element 11 of 11 - Node J			
X + Z Directions	ksi	25.87	29.16
Time	seconds	(11.25)	(11.25)
X + Y + Z Directions	ksi	28.89	29.61
Time	seconds	(11.00)	(11.25)
Arch Beam Stresses at Quarter Point Element 4 of 11 - Node I			
X + Z Directions	ksi	10.06	11.09
Time	seconds	(17.25)	(8.25)
X + Y + Z Directions	ksi	13.53	11.91
Time	seconds	(7.75)	(8.00)
Longitudinal Bracing Axial Forces (Breaking Strength = 162 tons) Truss Element 1			
X + Y Directions	tons	106.7	119.3
Time	seconds	(15.00)	(11.50)
Deck Beam Stresses near Center Element 6 of 11 - Node I			
X + Z Directions	ksi	26.69	27.04
Time	seconds	(10.75)	(11.00)
X + Y + Z Directions	ksi	26.97	27.88
Time	seconds	(10.75)	(11.00)

Table 4-29 NRGB Maximum Combined Bl-Bl Responses
(Yield Stress = 50 ksi)

Response	Units	Simultaneous Maximum Responses	SRSS Combined Maximum Responses	Sum of Maximum Responses
Arch Beam Stresses at Abutment Element 1 of 14 Node I				
X + Z Directions	ksi	23.09	22.62	24.87
Time	seconds	(16.25)		
X + Y + Z Directions	ksi	26.24	23.85	29.72
Time	seconds	(16.25)		
Arch Beam Stresses at Quarter Point Element 11 of 14 Node I				
X + Z Directions	ksi	33.71	33.25	34.90
Time	seconds	(12.75)		
X + Y + Z Directions	ksi	40.45	34.96	42.14
Time	seconds	(12.75)		
Longitudinal Bracing Axial Stresses Truss Element 2				
X + Y Directions	ksi	60.64	56.17	63.05
Time	seconds	(13.50)		
Deck Beam Stresses near Center Element 6 of 14 Node J				
X + Z Directions	ksi	54.69	49.85	61.26
Time	seconds	(11.00)		
X + Y + Z Directions	ksi	55.59	50.29	66.69
Time	seconds	(11.00)		

Table 4-30 CSCB Maximum Combined Bl-B1 Responses
(Yield Stress = 33 ksi)

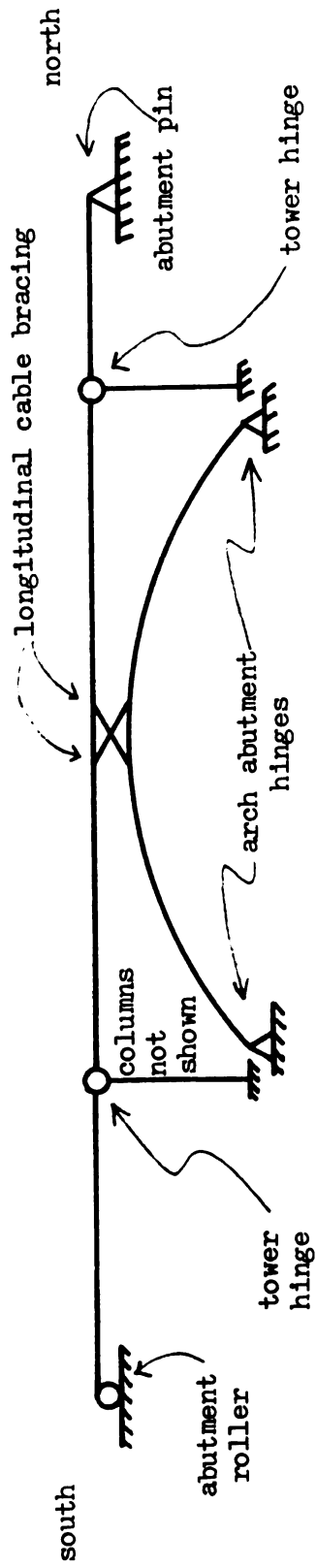
Response	Units	Simultaneous Maximum Responses	SRSS Combined Maximum Responses	Sum of Maximum Responses
Arch Beam Stresses at Abutment Element 11 of 11 Node J				
X + Z Directions	ksi	25.87	25.60	26.29
Time	seconds	(11.25)		
X + Y + Z Directions	ksi	28.89	27.04	33.34
Time	seconds	(11.00)		
Arch Beam Stresses at Quarter Point Element 4 of 11 Node I				
X + Z Directions	ksi	10.06	9.80	11.20
Time	seconds	(17.25)		
X + Y + Z Directions	ksi	13.53	11.65	15.31
Time	seconds	(7.75)		
Longitudinal Bracing Axial Forces (Breaking Strength = 162 tons) Truss Element 1				
X + Y Directions	tons	106.7	105.2	107.3
Time	seconds	(15.00)		
Deck Beam Stresses near Center Element 6 of 11 Node I				
X + Z Directions	ksi	26.69	26.14	33.66
Time	seconds	(10.75)		
X + Y + Z Directions	ksi	26.97	26.16	34.58
Time	seconds	(10.75)		

Table 4-31 NRGB Maximum Combined Bl-Bl' Responses
(Yield Stress = 50 ksi)

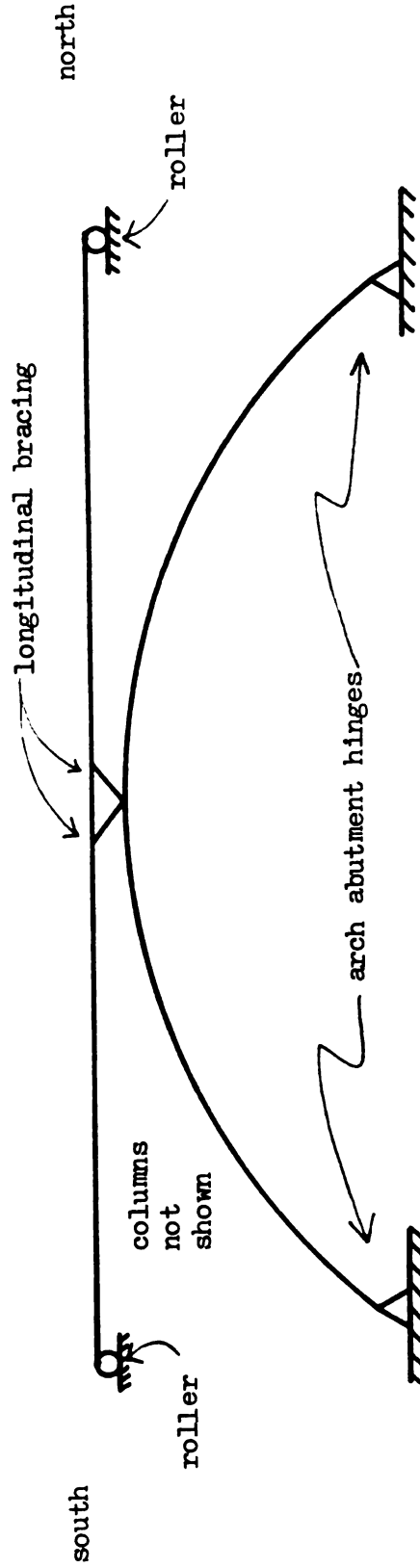
Response	Units	Simultaneous Maximum Responses	SRSS Combined Maximum Responses	Sum of Maximum Responses
Arch Beam Stresses at Abutment Element 1 of 14 Node I				
X + Z Directions	ksi	25.94	24.35	27.55
Time	seconds	(16.25)		
X + Y + Z Directions	ksi	28.29	24.92	31.08
Time	seconds	(16.50)		
Arch Beam Stresses at Quarter Point Element 11 of 14 Node I				
X + Z Directions	ksi	37.08	37.01	38.69
Time	seconds	(13.25)		
X + Y + Z Directions	ksi	39.62	37.60	43.39
Time	seconds	(13.00)		
Longitudinal Bracing Axial Stresses Truss Element 2				
X + Y Directions	ksi	59.22	55.74	73.79
Time	seconds	(13.50)		
Deck Beam Stresses near Center Element 6 of 14 Node J				
X + Z Directions	ksi	48.33	46.54	57.23
Time	seconds	(11.25)		
X + Y + Z Directions	ksi	56.72	49.53	70.98
Time	seconds	(11.25)		

Table 4-32 CSCB Maximum Combined Bl-Bl' Responses
(Yield Stress = 33 ksi)

Response	Units	Simultaneous Maximum Responses	SRSS Combined Maximum Responses	Sum of Maximum Responses
Arch Beam Stresses at Abutment Element 11 of 11 Node J				
X + Z Directions	ksi	29.16	28.23	33.48
Time	seconds	(11.25)		
X + Y + Z Directions	ksi	29.61	28.76	38.03
Time	seconds	(11.25)		
Arch Beam Stresses at Quarter Point Element 4 of 11 Node I				
X + Z Directions	ksi	11.09	11.31	13.00
Time	seconds	(8.25)		
X + Y + Z Directions	ksi	11.91	12.29	16.33
Time	seconds	(8.00)		
Longitudinal Bracing Axial Forces (Breaking Strength = 162 tons) Truss Element 1				
X + Y Directions	tons	119.3	100.5	121.9
Time	seconds	(11.50)		
Deck Beam Stresses near Center Element 6 of 11 Node I				
X + Z Directions	ksi	27.04	24.79	31.33
Time	seconds	(11.00)		
X + Y + Z Directions	ksi	27.88	24.81	32.29
Time	seconds	(11.00)		

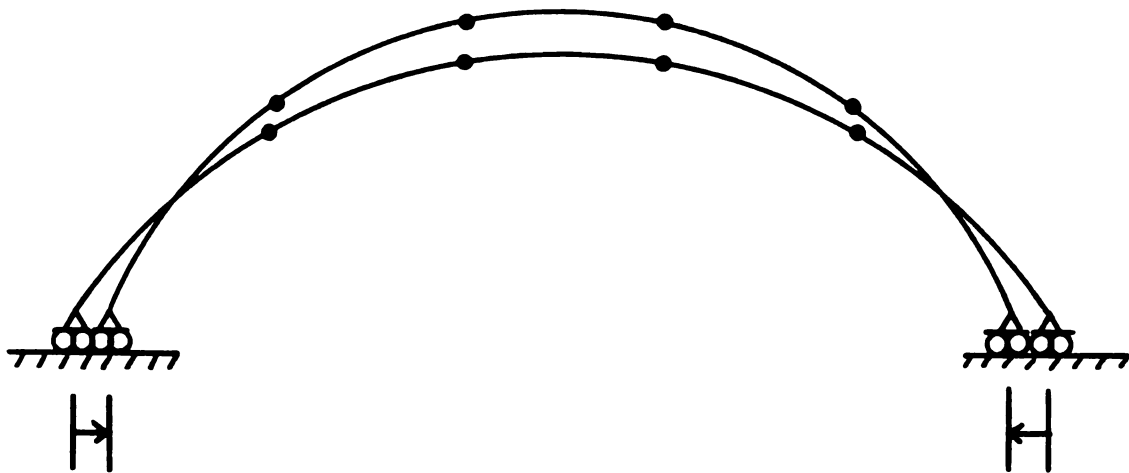


a) CSCB Transfer Mechanisms

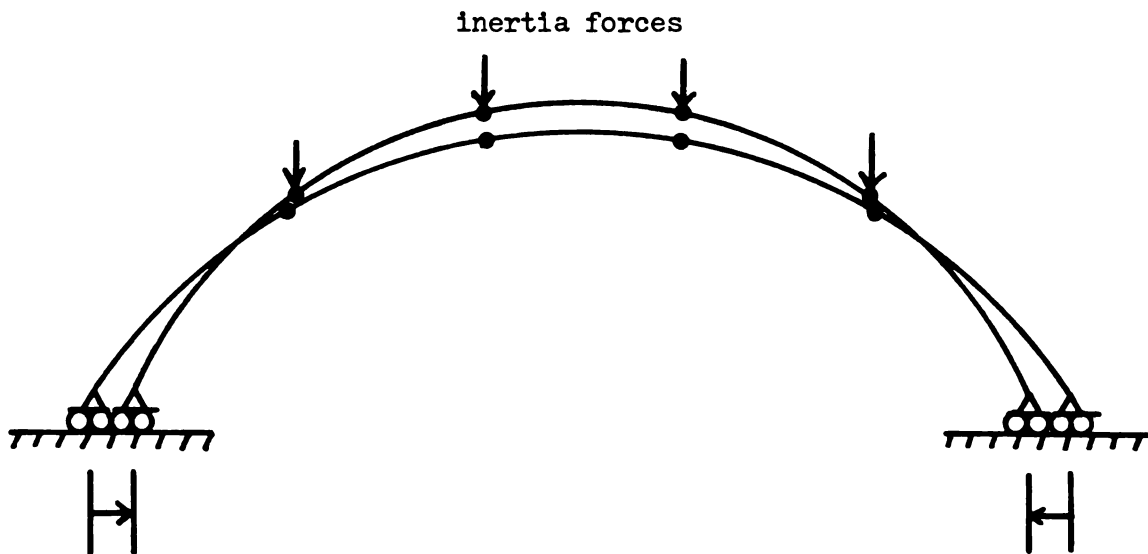


b) NRCB Transfer Mechanisms

Figure 4-1 Deck Longitudinal Force Transfer Mechanisms

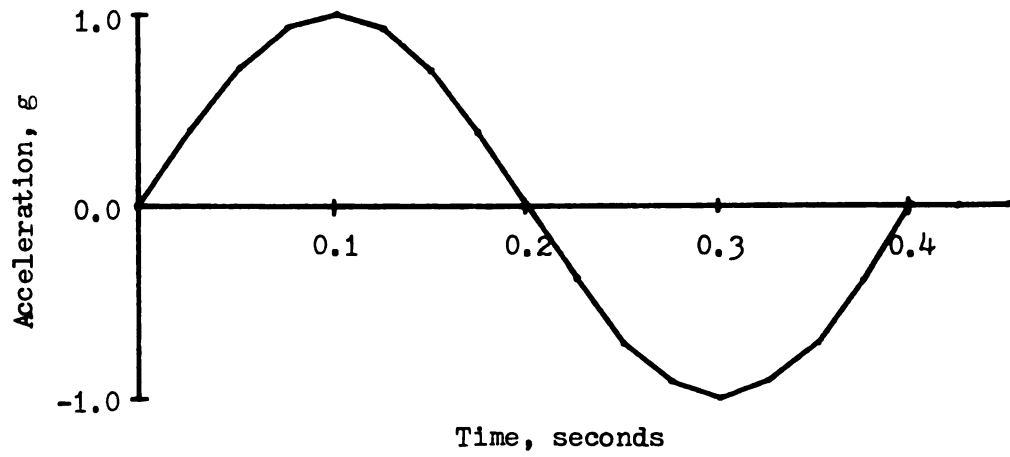


a) Static Pinching

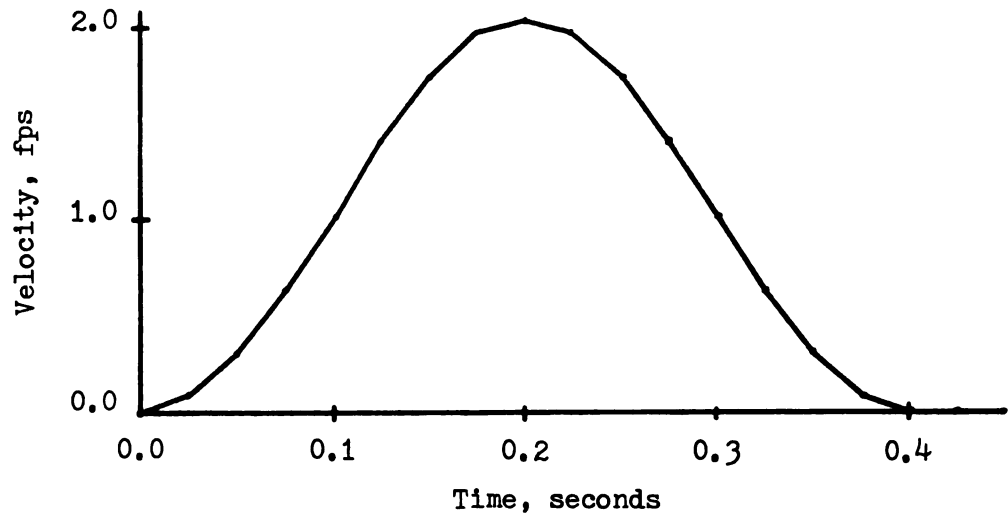


b) Dynamic Pinching

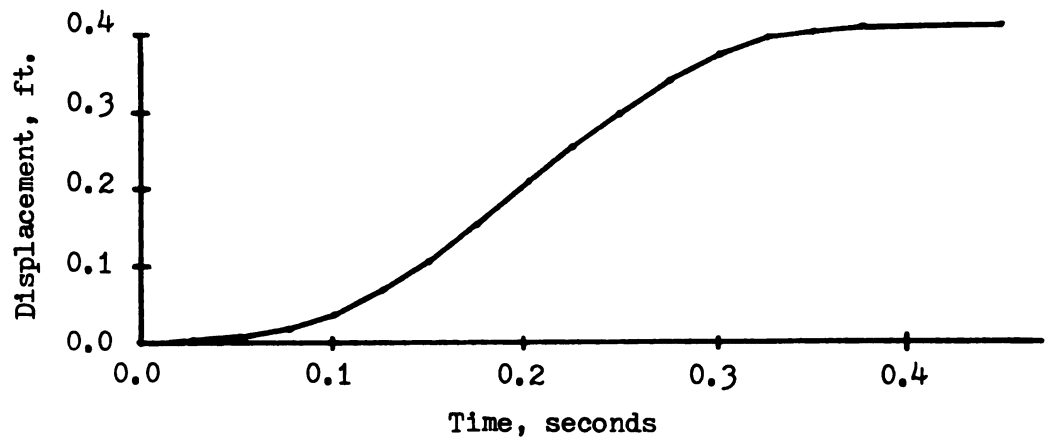
Figure 4-2 Static Versus Dynamic Arch Pinching



a) Test Acceleration



b) Test Velocity



c) Test Displacement

Figure 4-3 Dynamic Arch Pinching Test Motion

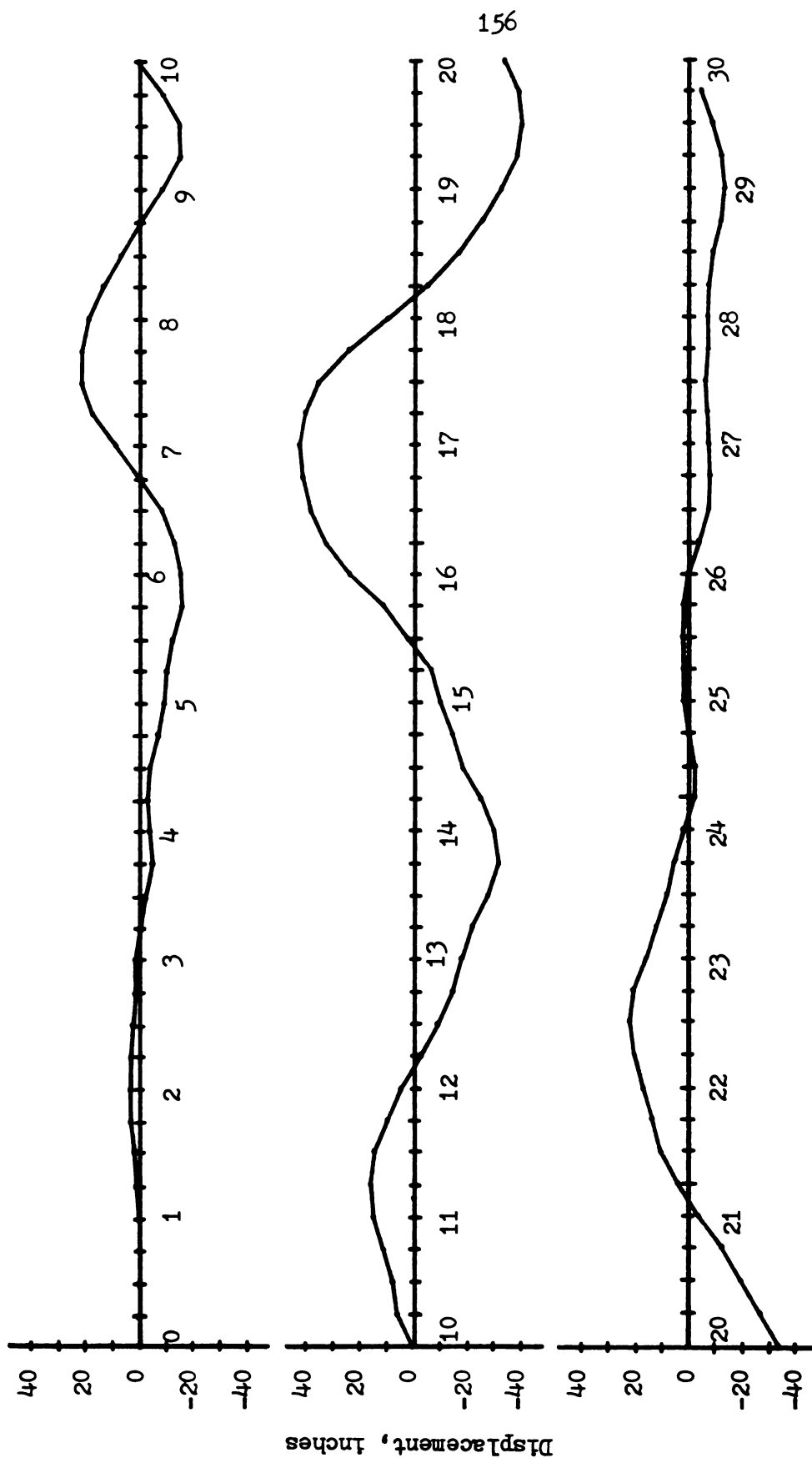
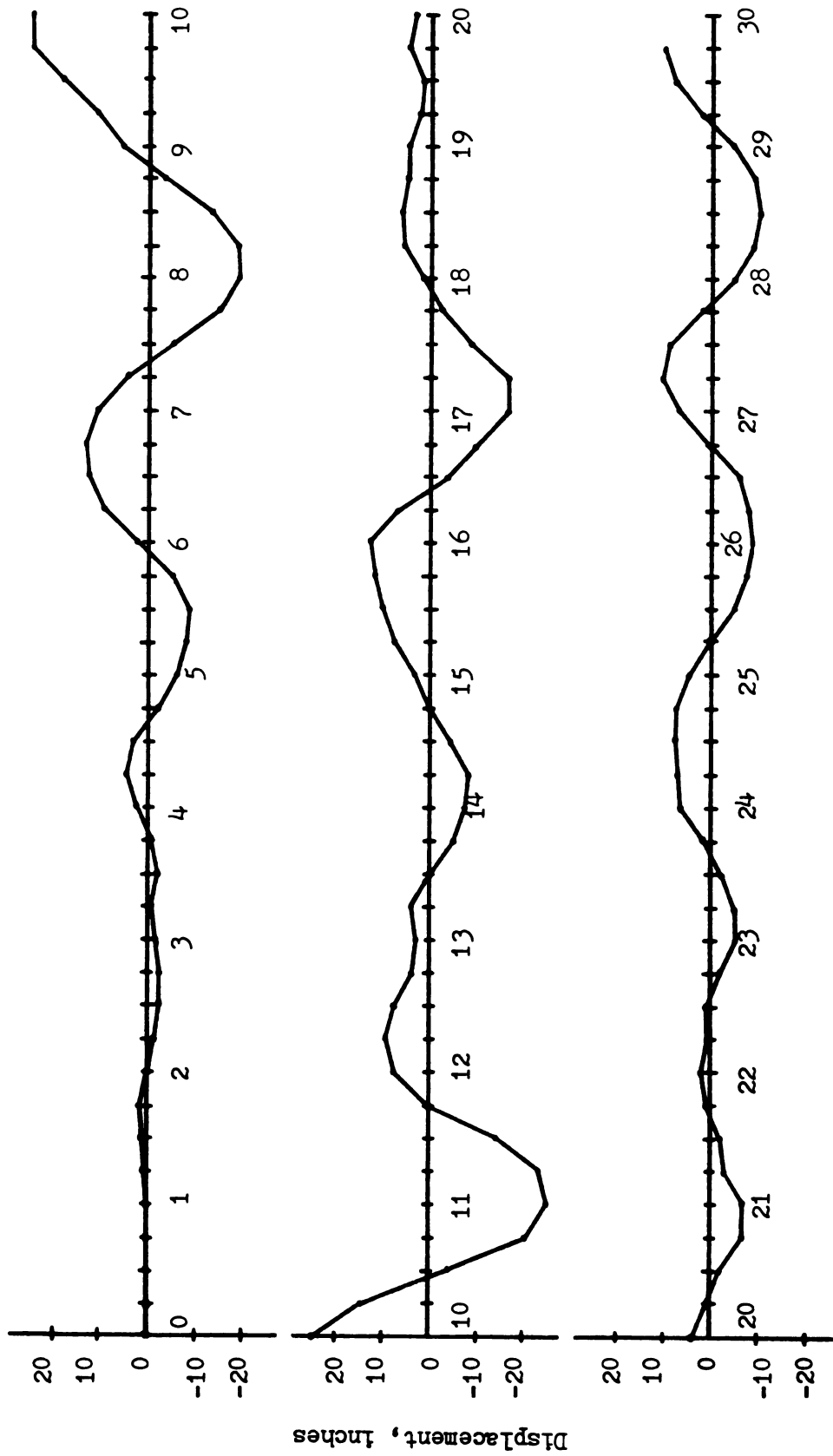


Figure 4-4 NRCB B1-B1 Deck Center Z Displacement



Time, seconds

Figure 4-5 CSCEB B1-B1 Deck Center Z Displacement

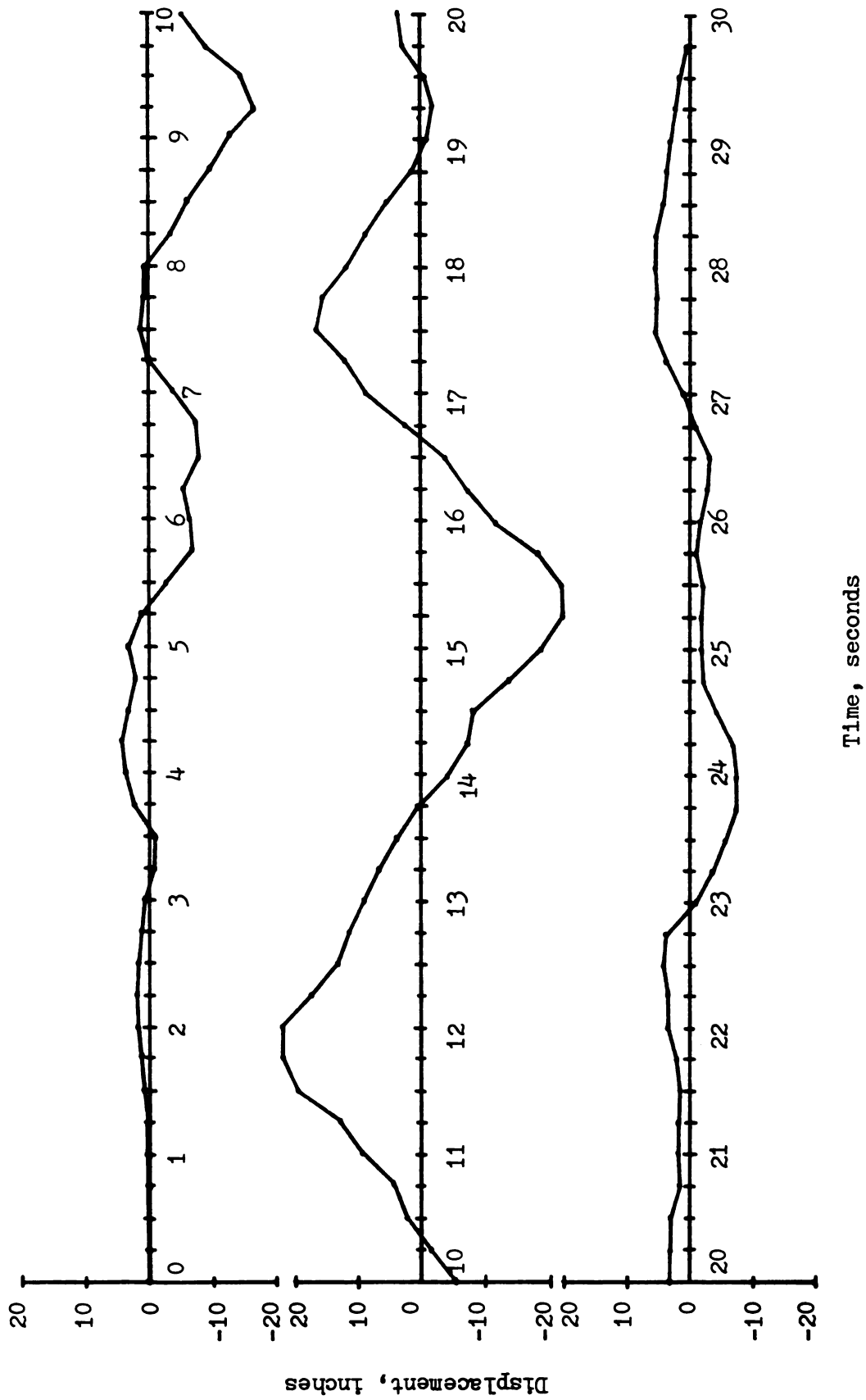


Figure 4-6 Differential B1-B2 Displacement

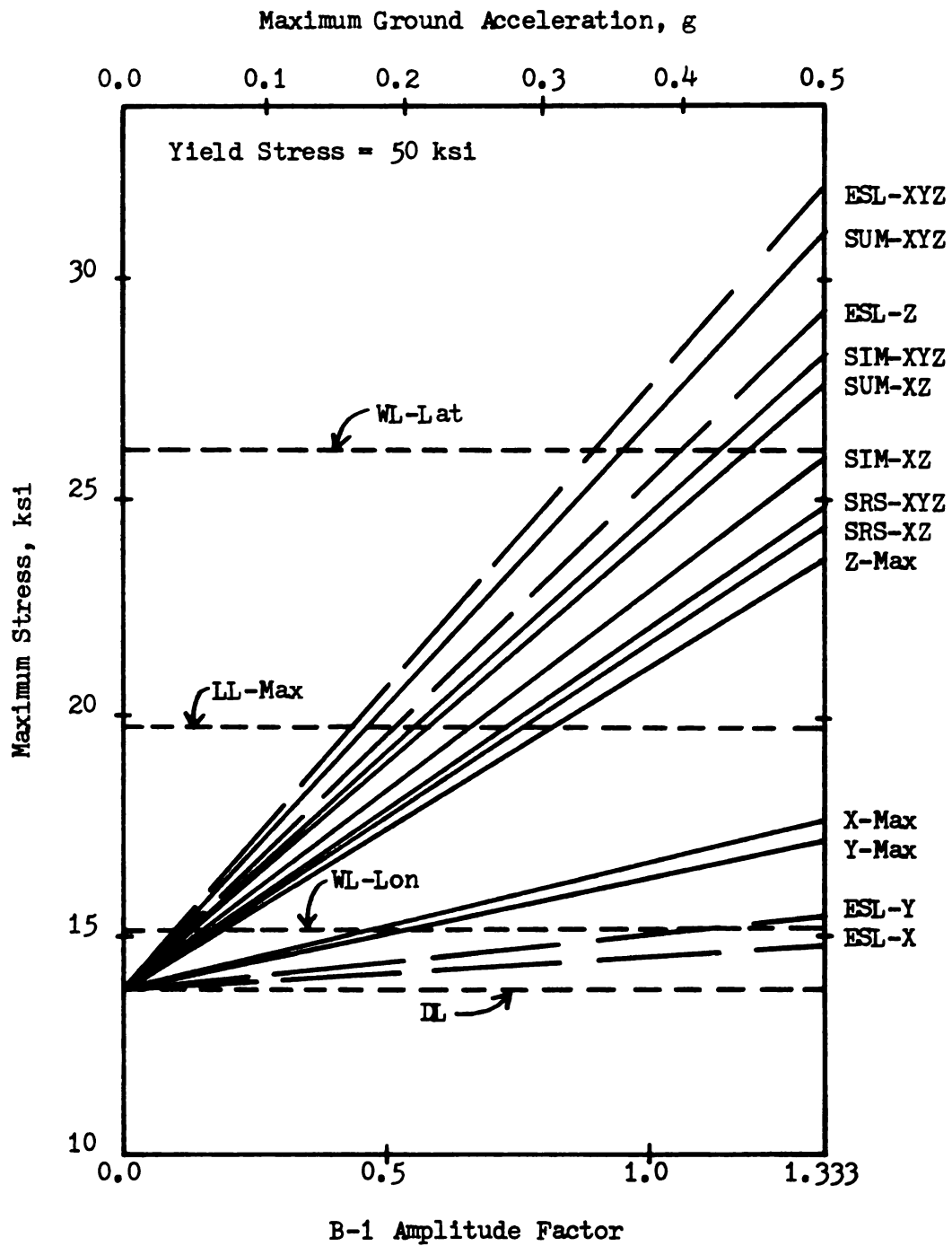


Figure 4-7 NRGB Arch Element 1 (of 14) - Responses At Node I To B1-B1' Loading

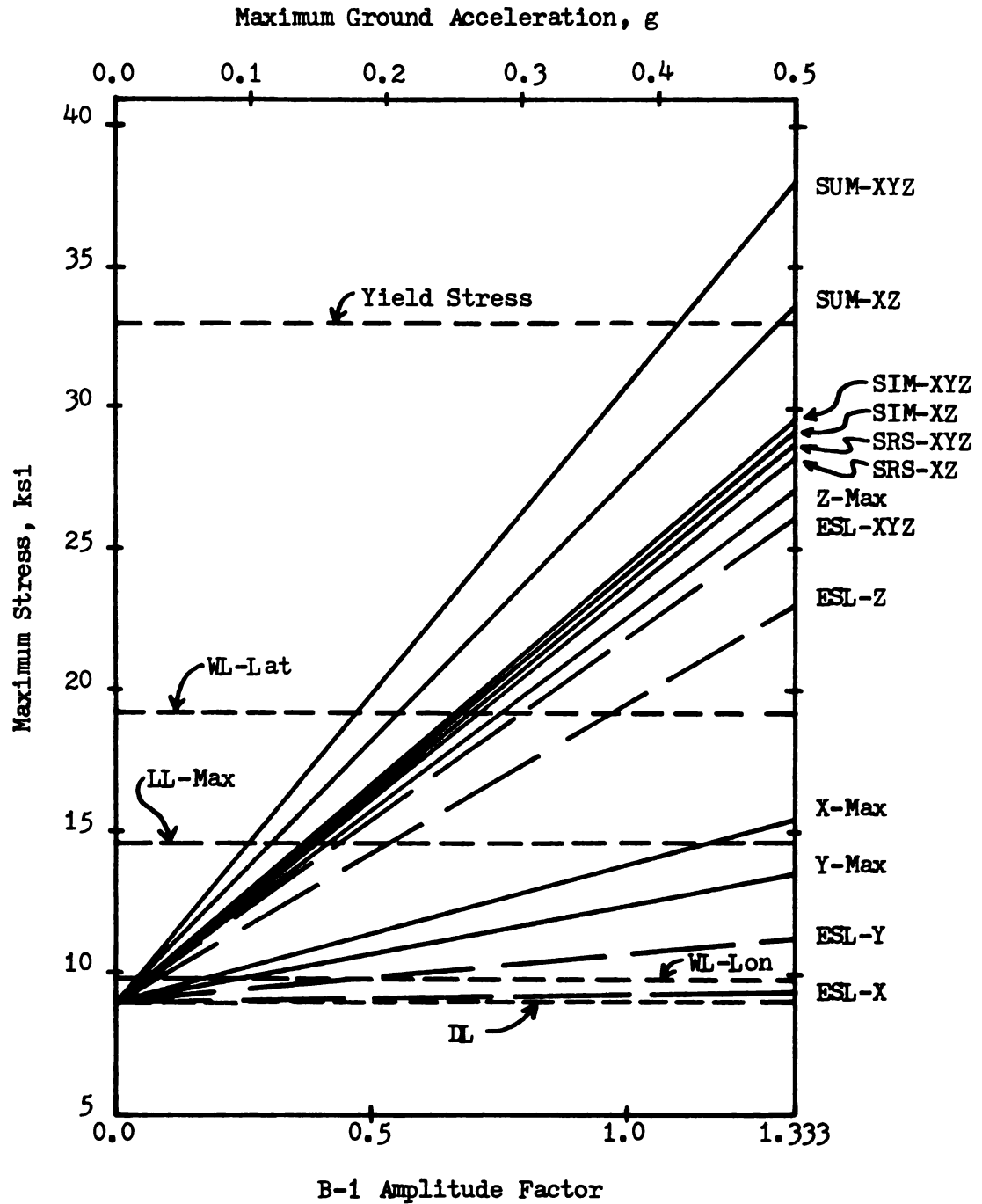


Figure 4-8 CSCB Arch Element 11 (of 11) - Responses At Node J To B1-B1' Loading

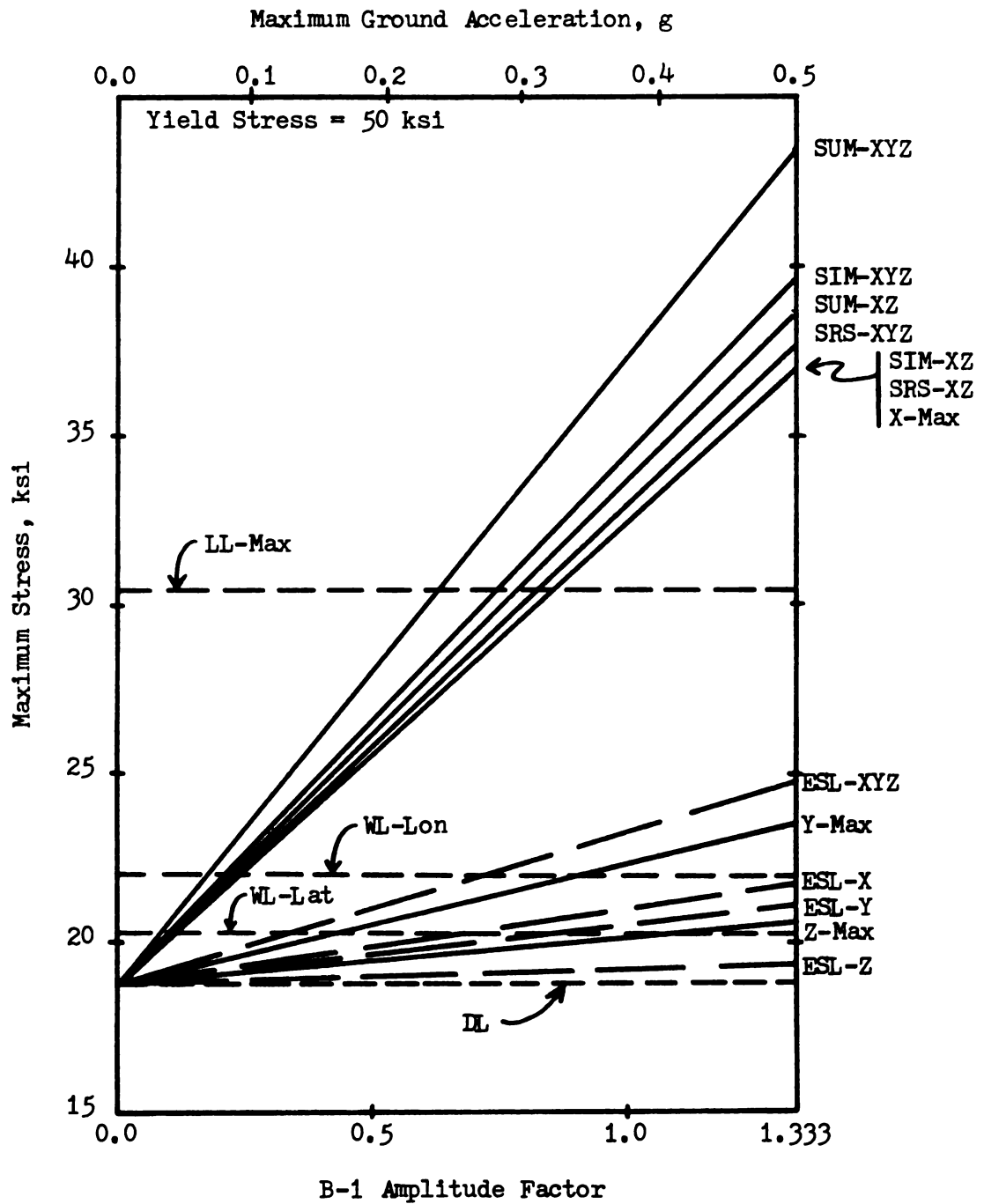


Figure 4-9 NRGB Arch Element 11 (of 14) - Responses At Node I To B1-B1' Loading

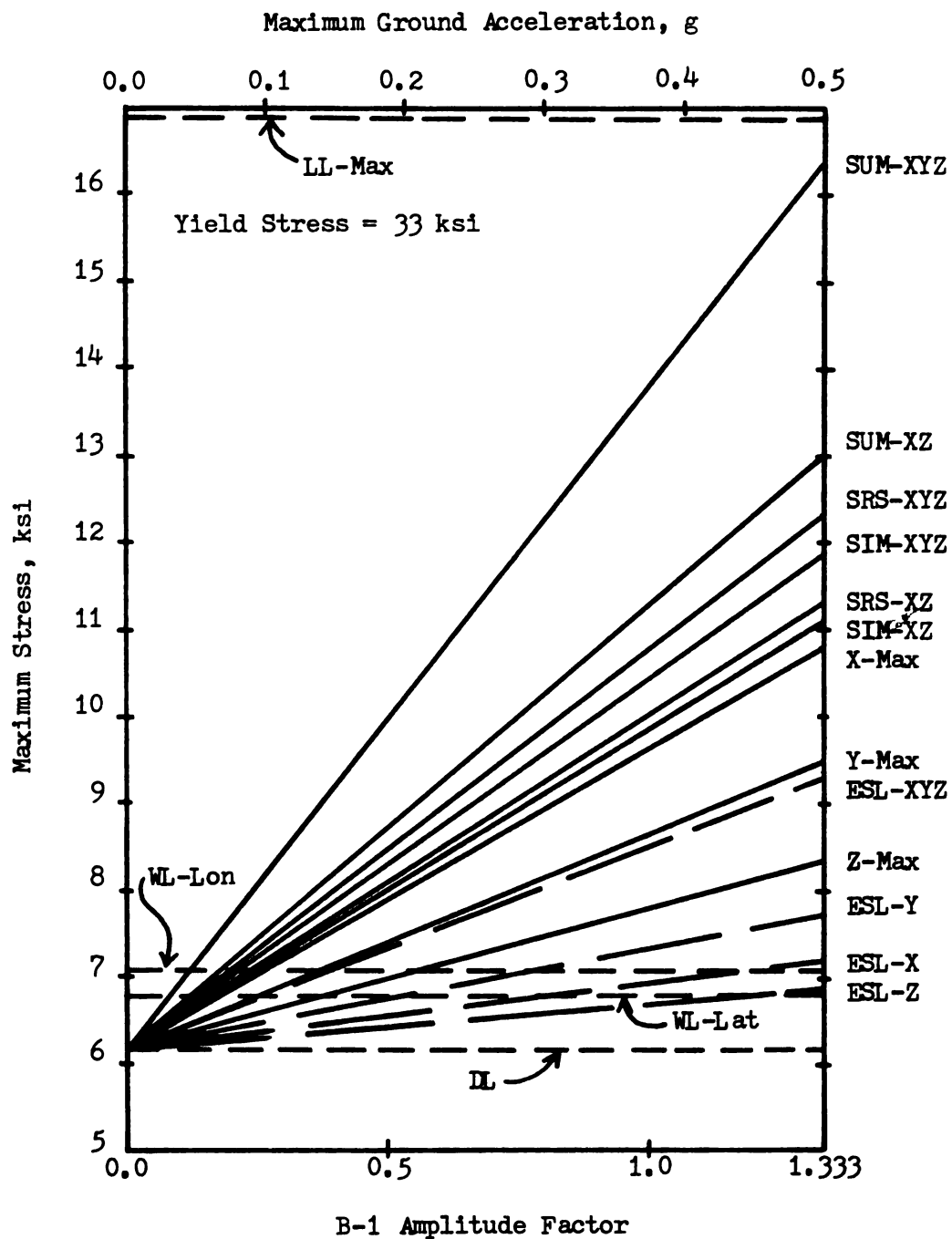


Figure 4-10 CSCB Arch Element 4 (of 11) - Responses At Node I To B1-B1' Loading

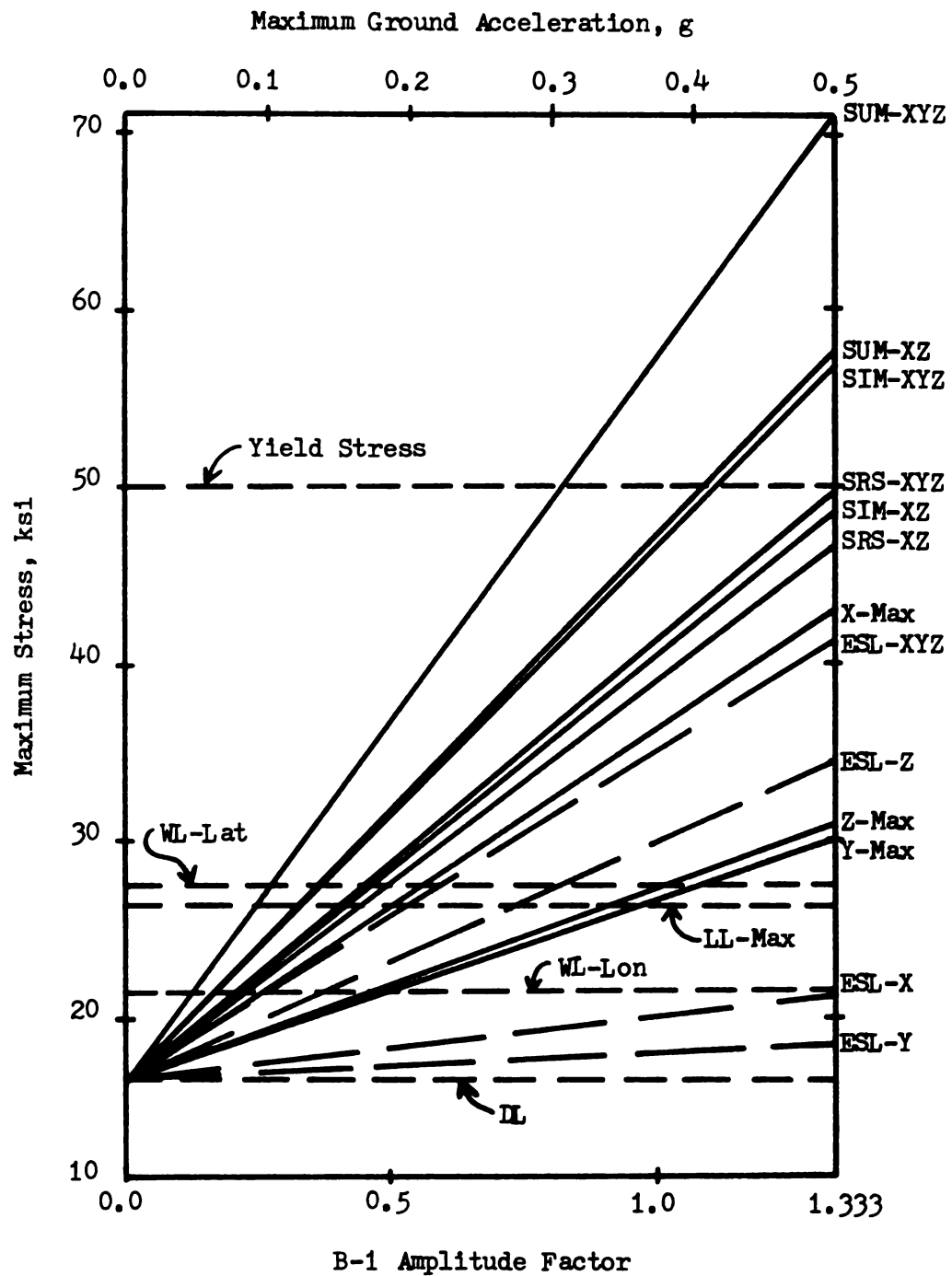


Figure 4-11 NRGB Deck Element 6 (of 14) - Responses At Node J To B1-B1' Loading

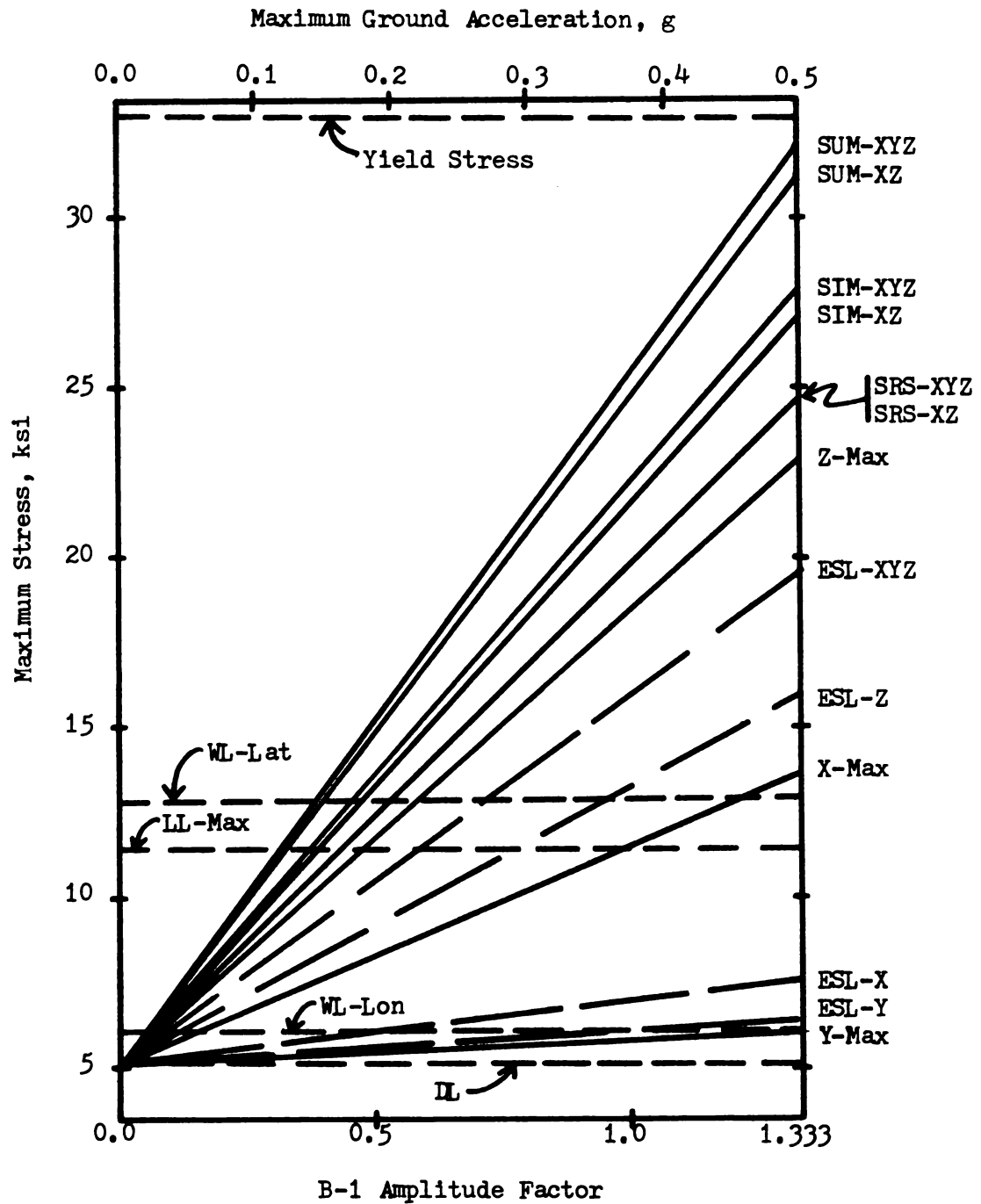


Figure 4-12 CSCB Deck Element 6 (of 11) - Responses At Node I To B1-B1' Loading

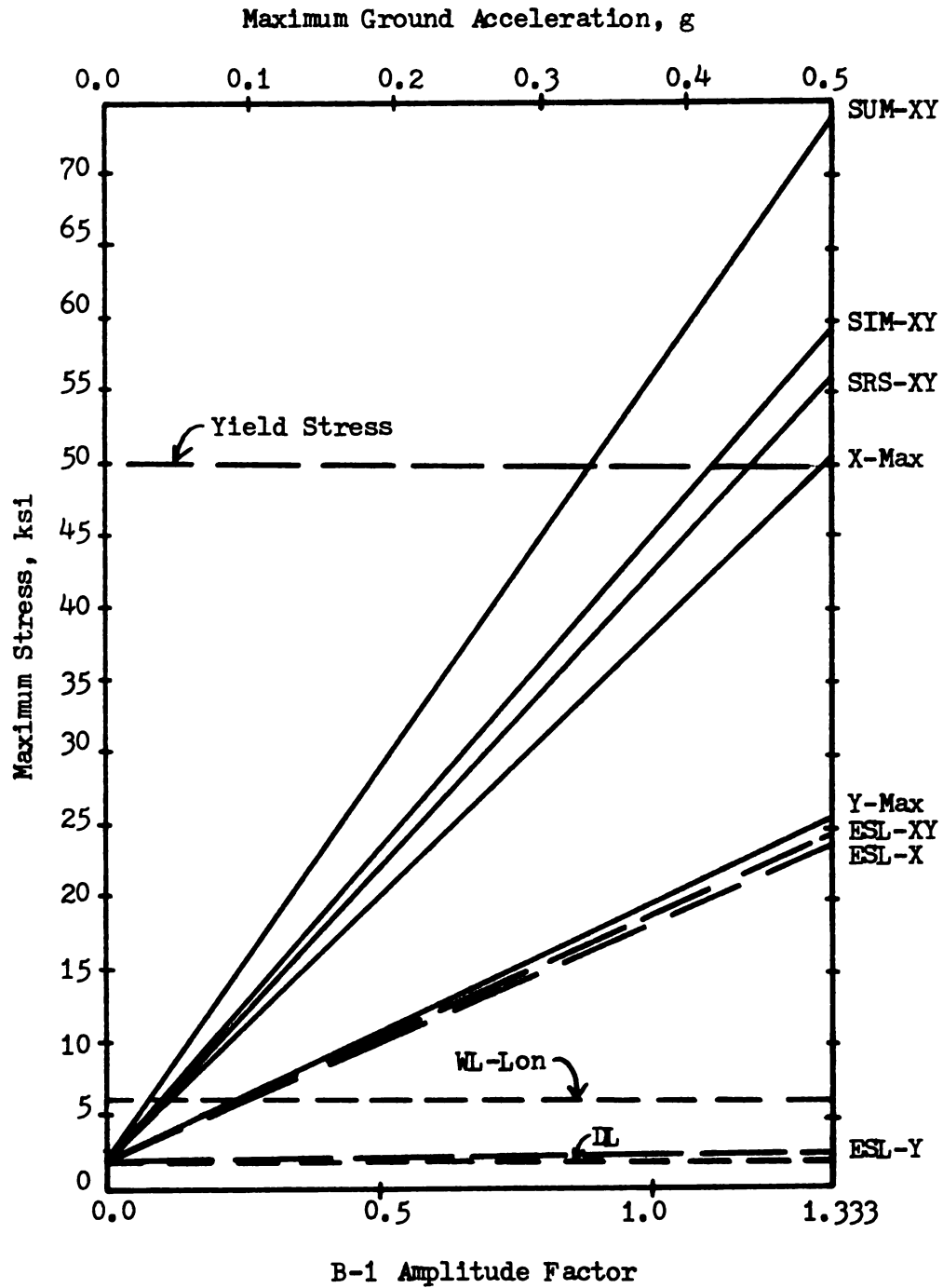


Figure 4-13 NRCB Longitudinal Bracing Truss Element 2 Responses To B1-B1' Loading

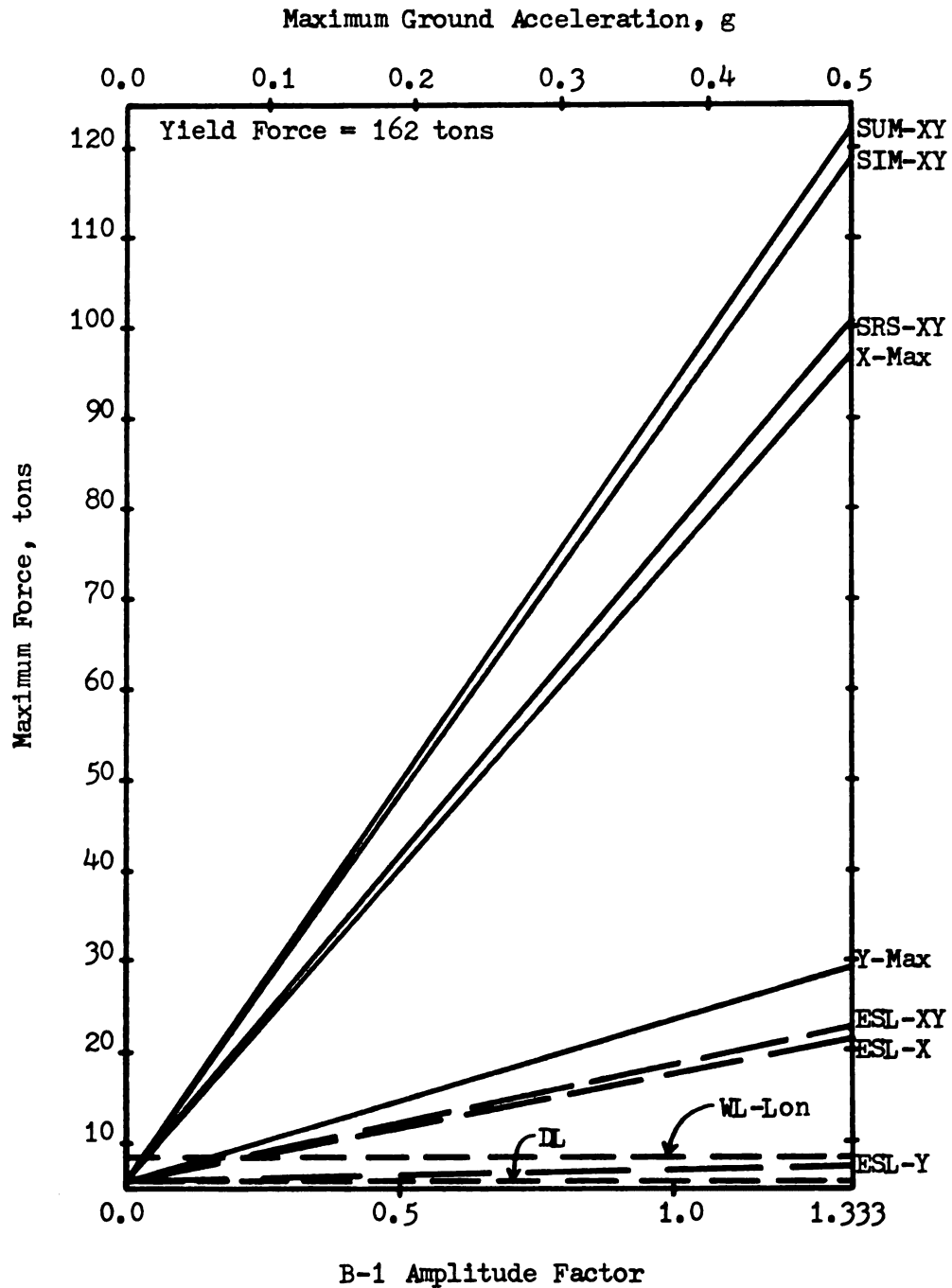


Figure 4-14 CSCB Longitudinal Bracing Truss Element 1 Responses To B1-B1' Loading

CHAPTER V
SUMMARY AND CONCLUSIONS

5.1 SUMMARY OF RESEARCH

The research reported here began as an attempt to answer three questions:

1. How do the responses of long span steel deck arch bridges exposed to unequal seismic support acceleration differ from the responses to uniform support motion?
2. How do the seismic analysis results for the New River Gorge Bridge (NRGB), the world's longest steel deck arch bridge, differ from the responses of a shorter span such as the Cold Springs Canyon Bridge (CSCB)?
3. How do the seismic responses of steel deck arch bridges using time history analysis compare with response spectrum analysis results?

In order to answer these questions it was necessary to create a new finite element program called LINSTRUC. This program incorporates several features that are not found together in any other program in the public domain known to this author. These features include dynamic analysis using time step numerical integration with equal or unequal seismic support acceleration as input, a straight beam element capable of both shear and warping deformations, condensation of structure degrees of freedom and slave nodes.

The models used for NRGB and CSCB were one-plane models i.e models derived by a synthesis of the structural properties in the lateral direction. Thus the deck was represented by one continuous beam while the arch was represented by a series of straight beams connected end to end. This modeling technique necessitated the introduction of "effective" member lengths in order to provide beam element stiffnesses that are "equivalent" to the arch and deck stiffnesses. These one-plane models coupled with the various LINSTRUC features allowed the structure degrees of freedom to be reduced from over 2000 for NRGB to just 34 and from about 250 to 34 for CSCB.

The two ground motions referred to as B-1 and B-2 are artificially generated ground acceleration histories with intensities comparable to the El Centro Earthquake of 1940. The amplitudes of both accelerograms were increased by 33.3% resulting in a maximum ground acceleration of 0.50g for B-1 thus matching the AASHTO Specification requirements for CSCB (discussed below).

The two most important applications of these accelerograms both involved the modified B-1 accelerogram. The first was the application of the modified B-1 accelerogram to all of the bridge supports simultaneously (B1-B1 loading) while the second introduced a time lag between the commencement of the modified B-1 motion at the south bridge supports (arch abutment and deck supports) and the beginning of motion at the north supports (B1-B1' loading). The time lags used in the latter case were based on a wave speed in rock of about 5600 feet per second. Both the B1-B1 and the B1-B1' loadings were applied in the X, Y and Z directions to NRGB and CSCB.

Other combinations of the modified B-1 and B-2 accelerograms were

also applied to the bridge models. One combination applied in the X and Z directions to both bridges was the application of the modified B-1 accelerogram to the south supports and the modified B-2 accelerogram to the north supports. Another combination applied to both bridges in the X direction was similar to the B1-B1' loading but with the time lags doubled. Finally, two combinations applied only in the X direction to NRGB were B-2 applied simultaneously at both bridge supports and B-1 applied with a time lag approximately the same as the fundamental NRGB in-plane period..

The analysis results presented in this report are the stresses or forces for five key elements in each bridge model: an arch element at an abutment, an arch element near a quarter point, a deck element near the center, a longitudinal bracing member and a lateral bracing member. Brief summaries and conclusions for these five types of members are presented in the next section.

5.2 ARCH, DECK AND BRACING SUMMARIES AND CONCLUSIONS

Before characterizing the arch, deck and bracing results, it should be noted that NRGB is located in Zone I of the AASHTO Seismic Risk Map while CSCB is located in Zone III. Thus the peak ground acceleration required by the AASHTO Specifications for seismic analyses of NRGB and CSCB are 0.09g and 0.50g, respectively. In addition, it should also be noted that the AASHTO allowable stress under dead plus earthquake loading is 73.3% of the yield stress ($55\% \times 1.333$). Thus the allowable stress for NRGB is 36.7 ksi while the value for CSCB is 24.2 ksi.

In the following sections, the responses which are referred to are depicted in Figures 4-7 to 4-14 with the B1-B1' responses considered to be functions of the maximum ground acceleration (the top scale in each

figure).

5.2.1 ARCH ELEMENTS NEAR THE ABUTMENTS

At the arch abutments for both bridges, the maximum total arch stresses did not exceed the yield stress under simultaneous combined X, Y and Z applications of B1-B1' loading with a maximum ground acceleration of 0.50g (see Figures 4-7 and 4-8). In addition, the NRGB allowable stress is not exceeded until maximum ground accelerations well in excess of 0.50g are reached while the CSCB allowable stress is surpassed at a approximately 0.36g. Thus considering the locality of each bridge, under a maximum ground acceleration of 0.50g the CSCB arch strength near the abutments may not be adequate with respect to allowable stress design. The NRGB arch strength near the abutments under a maximum ground acceleration of 0.09g would appear to be more than adequate, however.

5.2.2 ARCH ELEMENTS AT THE QUARTER POINTS

Under simultaneous combined X, Y and Z application of the B1-B1' loading with a maximum ground acceleration of 0.50g, neither the NRGB nor the CSCB models had total arch quarter point stresses in excess of the yield stress (see Figures 4-9 and 4-10). The CSCB values at a maximum ground acceleration of 0.50g were also less than the allowable stress, while the NRGB maximum total arch quarter point stress exceeds the allowable stress at a maximum ground acceleration of about 0.42g. In view of the respective AASHTO maximum ground accelerations applicable for NRGB and CSCB, the arch quarter point results for both bridges would appear to fall within the AASHTO allowable stress limits.

5.2.3 DECK ELEMENTS NEAR THE CENTER

Near the center of the deck, the maximum total stress under simultaneous combined X, Y and Z direction Bl-Bl' loading exceeds the yield stress at approximately 0.43g for NRGB (see Figure 4-11). For CSCB, however, the yield stress is not exceeded until maximum ground accelerations greater than 0.50g are reached (see Figure 4-12). The allowable stresses for NRGB and CSCB are exceeded at maximum ground accelerations of about 0.26g and 0.42g, respectively. When compared with the AASHTO maximum site accelerations, however, the NRGB deck design near the center appears to be adequate with respect to staying within the allowable stress under the prescribed maximum ground accelerations while the CSCB design may not be adequate.

5.2.4 LONGITUDINAL BRACING AT THE CROWN

Under simultaneous combined X and Y application of Bl-Bl' loading, the NRGB longitudinal bracing member stresses exceed the yield stress at a maximum ground acceleration of about 0.42g while the CSCB longitudinal cable bracing members do not exceed their breaking strengths until a value well in excess of 0.50g is reached (see Figures 4-13 and 4-14). The allowable stress of the NRGB longitudinal bracing members is exceeded at a maximum ground acceleration of about 0.30g while 73.3% of the CSCB longitudinal cable breaking strength (119 tons) is just reached at 0.50g. Thus under the AASHTO design guidelines, the NRGB and CSCB longitudinal bracing members both seem to be satisfactory.

5.2.5 LATERAL BRACING AT THE CROWN

The CSCB lateral cable bracing forces exceed their breaking strengths under Z direction Bl-Bl' loading at maximum ground accelerations of about 0.24g while the NRGB lateral bent diagonals at

the crown reach their allowable stresses at just over 0.50g. Thus the CSCB lateral cables may be in danger under ground motions similar to Bl-B1' which exceed 1/4 g while the NRGB lateral bent diagonals would be safe even under maximum ground accelerations of 0.50g.

5.3 GENERAL CONCLUSIONS

The following are conclusions regarding NRGB, CSCB and steel deck arch bridges in general.

5.3.1 ONE-PLANE MODELS

The one-plane modeling technique used in the present study proved to be a very effective modeling method. The more important static and modal analysis responses presented in Chapter 3 were generally within 10% of the results based on full three-dimensional modeling analysis. The efficacy of these models made it possible to keep the computing costs of the present research within reasonable bounds.

5.3.2 EFFECTS OF UNEQUAL SEISMIC SUPPORT MOTION

The most important effects of unequal seismic support motion were the increases in arch axial stress under X direction unequal motion. For Bl-B1' loading, NRGB exhibited 8% to 13% increases in arch axial stress compared with results from uniform Bl-B1 loading while CSCB showed 44% to 57% increases.

The CSCB arch axial stresses under Bl-B1' loading were also 22% to 63% greater than the 1982 results. Since the latter were based on the AASHTO Specifications, perhaps provisions for unequal seismic support motion should be considered especially in the longitudinal direction. This is not to imply that costly time history analyses should be undertaken, but perhaps a 20% increase in arch axial stresses derived by response spectrum analysis might be considered.

5.3.3 DECK LONGITUDINAL FORCE TRANSFER MECHANISMS

The one factor that causes the greatest difference in the bridge responses appears to be the differences in their deck longitudinal force transfer mechanisms. If NRGB were built in a higher risk earthquake zone such as California, the AASHTO 0.50g maximum ground acceleration would mean that under X direction ground acceleration, the arch near the quarter points, the deck near the center and the longitudinal bracing members at the crown could all be inadequate with respect to allowable stress design. The latter two member types could in fact have maximum total stresses approaching or surpassing the yield stress. Thus the existence of two NRGB deck expansion joints, one at each end of the main span deck, would seem to leave a California version of NRGB very vulnerable to earthquake damage.

The CSCB members, however, appear to be adequate under X direction ground acceleration. Thus the CSCB deck longitudinal force transfer design with only one deck expansion joint would seem to be more appropriate for earthquake prone regions than the NRGB design.

5.3.4 CSCB LATERAL RESPONSES

In view of the California location of CSCB, several bridge members may be inadequate with respect to allowable stress design under lateral ground motion. These members include the arch near the abutment, the deck near the center and the lateral cable bracing at the crown. In view of the current results and those derived in 1982, perhaps a review of CSCB using current California design criteria should be considered by the State of California Department of Public Works.

5.3.5 RESPONSE SPECTRUM ANALYSIS

The 1982 X and Y direction responses for CSCB were nearly all greater than the B1-B1 results calculated in the current analysis. The Z direction arch quarter point stresses and lateral deck bending stresses at the center derived in the 1982 analysis were slightly higher than the B1-B1 responses in the present study, while the remaining responses were all lower. The smaller 1982 Z direction responses appear to be evidence that the Normalized Rock Spectra (NRS) are not adequate as design spectra in so far as low frequency structure responses are concerned. This conclusion is supported by the AASHTO minimum value of 0.1 for the coefficient C. As discussed in Section 4.5.1, this minimum value for C only applies to structures with low fundamental frequencies.

The Response Coefficient "C" curves in the AASHTO Specifications were derived by modifying the NRS by a number of factors which result in a reduction of the NRS values by a factor of 8. However, the Specifications also impose a minimum value of 0.1 for C which is equivalent to a minimum value of 0.8g for the NRS. Such a 0.8g minimum if applied to the 1982 CSCB model would probably have resulted in all the 1982 Z direction responses being larger than the corresponding values in the present study. Thus response spectrum analysis using the NRS with a minimum ground acceleration of 0.8g would seem to provide a conservative substitute for time history analysis using the B-1 accelerogram.

5.4 FUTURE STUDIES

The following areas would seem worthwhile for future study:

1. similar analyses conducted on other types of arch bridges such as tied through and tied half-through steel deck arches
2. dynamic analyses aimed at determining the effects of soil

structure interaction on arch bridge responses

3. nonlinear seismic analyses of deck arch bridges
4. detailed studies of dynamic arch pinching
5. continued analyses of NRGB and CSCB utilizing a variety of other ground acceleration histories such as the type A, C and D artificially generated accelerograms (ref. 7) and the El Centro north-south, east-west and vertical accelerograms
6. seismic analyses of other complex bridge structures, such as long-span cantilever trusses, utilizing the LINSTRUC program and its special features

Steel deck arch bridges are only one kind of arch bridge and thus they represent only a portion of the arch bridges which actually exist. Two other types of long span steel arches are tied through and tied half-through steel arches. The responses for these types of arches may be quite different from the responses of steel deck arches. Therefore, analyses similar to those performed for this report should be conducted on steel tied through and half-through arches.

As mentioned in Chapter 1, soil structure interaction analyses were not performed on NRGB or CSCB because both bridges are built in deep river valleys with their supports resting on rock. Such soil conditions are common for most steel deck arch bridges. Most through and half-through arches are built in shallow river valleys on deep layers of sediment, however. Thus in the course of analyzing these two types of bridges, soil structure interaction would have to be considered.

Based on the results of the current study, material and geometric nonlinear analyses of deck arch bridges would seem to be justified. The results of the present study indicate that arch and deck stresses could

be quite high under large seismic loading while bracing members could yield or even break. Thus analyses of deck arch bridges including material nonlinearity should be considered. In addition, the 26 and 43 inch maximum lateral displacements of NRGB and CSCB, respectively, under Bl-Bl loading also show a need for geometric nonlinear analyses. Research into nonlinear analysis of arches is currently being conducted at Michigan State University.

The effects of dynamic arch pinching under unequal longitudinal seismic support motion were observed repeatedly in the present study. More detailed studies need to be conducted to evaluate the influence of arch shape and other arch and load parameters on dynamic pinching responses. A study of dyanmic arch pinching is currently underway at Michigan State University.

The B type accelerograms used in the present study represent only two examples of the many different types of earthquake acceleration histories which can occur. Thus even though the time history analyses conducted in the present study were more precise than response spectrum analysis, the results obtained represent only a few samples of NRGB and CSCB seismic responses. Therefore further analyses using the CSCB and NRGB models should be performed to more clearly define the envelope of solutions that exist.

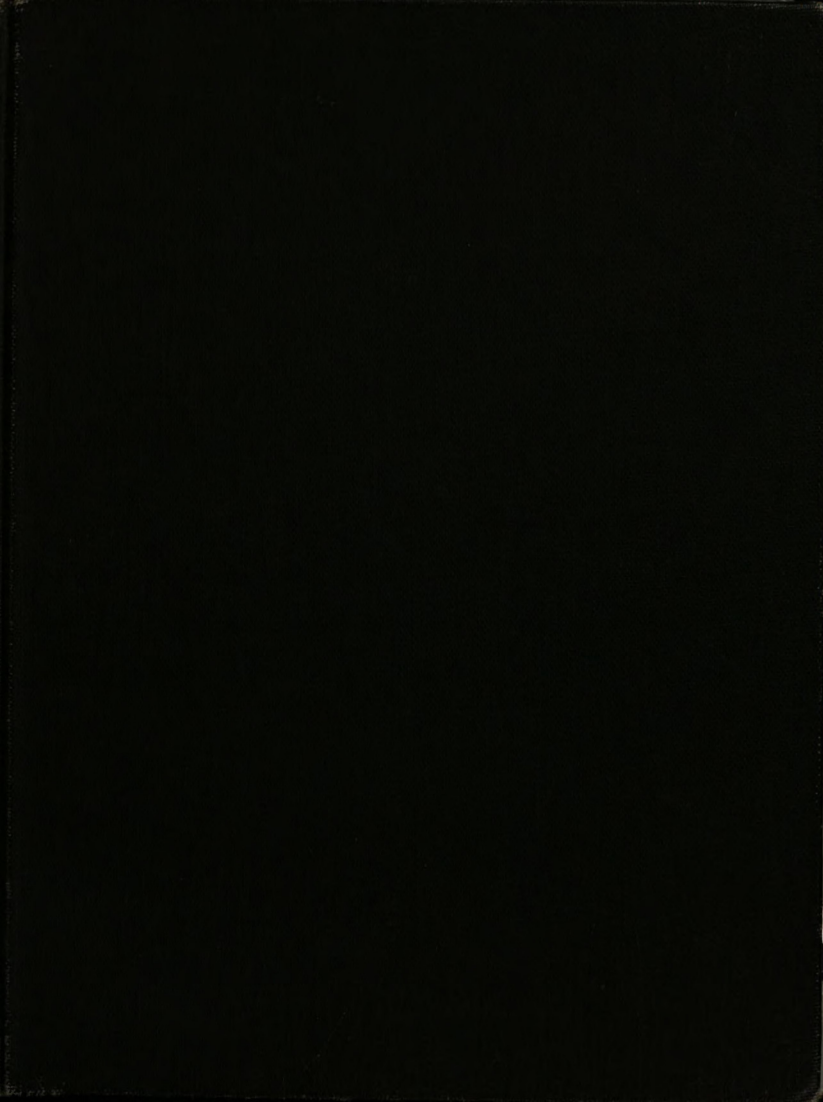
The special features of the LINSTRUC program coupled with the one-plane modeling techniques could also make seismic analyses of other complex structures such as long-span cantilver trusses more efficient and practical. Structures incorporating long-span space trusses could also be more efficiently analyzed with the LINSTRUC program.

100

MICHIGAN STATE UNIV. LIBRARIES



31293106868460



v.2



PLACE IN RETURN BOX to remove this checkout from your record.
TO AVOID FINES return on or before date due.

DATE DUE	DATE DUE	DATE DUE
OCT 31 1991		
029		
FEB 26 1992		
APR 1 1992		
MAY 29 1992		

MSU is An Affirmative Action/Equal Opportunity Institution

UNEQUAL SEISMIC SUPPORT MOTIONS OF STEEL DECK ARCH BRIDGES

Volume II

By

Ralph Alan Dusseau

A DISSERTATION

Submitted to
Michigan State University
in partial fulfillment of the requirements
for the degree of

DOCTOR OF PHILOSOPHY

Department of Civil and Environmental Engineering

1985

3846714

APPENDIX A

LINSTRUC DOCUMENTATION AND DISCUSSION

This appendix contains descriptions and documentation for each subroutine contained in the LINSTRUC program. Each section in this appendix deals with one overlay or one overlay capsule (ovcap) and includes a short commentary on the overlay or ovcap, a list of all data input which may be read by the overlay, a list of all common block variables for those blocks with variables that first appear in the given overlay, a list of miscellaneous variables used in the overlay or ovcap and finally a listing of the overlay or ovcap itself. The overlays are presented in sequential order and are numbered in the section numbers correspond with the overlay numbers in the LINSTRUC program except for the overlay capsules which are discussed in Section A.4 but are only named and not numbered in the program. First, however, a more detailed discussion of what overlays are and how they are used follows.

APPENDIX A

The overlays used in LINSTRUC are essentially groups of one or more subroutines with the overlay system acting as a means of outlining these groups, i.e. organizing them into different levels. There are four levels of overlays allowed by FORTRAN V: the main overlay, the primary overlays, the secondary overlays and the capsules.

In any FORTRAN V program there can only be one main overlay designated OVERLAY(XFILE,0,0,07=un), where XFILE is the name of the core memory file into which the overlays are to be written and un is the

total number of overlays and ovcaps in the program. The main overlay is the highest level of overlays and in addition to standard Fortran operations, the main overlay can call and load into core memory the

primary overlays and the ovcaps. APPENDIX A LINSTRUC program, the main overlay is called LINSTRUC DOCUMENTATION AND DISCUSSION appropriate primary overlay: INITIAL, MAIN or STATUS. A complete listing of

Prog This appendix contains descriptions and documentation for each subroutine contained in the LINSTRUC program. Each section in this can appendix deals with one overlay or one overlay capsule (ovcap) and caps. includes a short commentary on the overlay or ovcap, a list of all data input which may be read by the overlay, a list of all common block variables for those blocks with variables that first appear in the given overlay, a list of miscellaneous variables used in the overlay or ovcap and finally a listing of the overlay or ovcap itself. The overlays are presented in sequential order and all of the section numbers called and correspond with the overlay numbers in the LINSTRUC program except for the overlay capsules which are discussed in Section A.4 but are only named and not numbered in the program. First, however, a more detailed discussion of what overlays are and how they are used follows. y can be

The overlays used in LINSTRUC are essentially groups of one or more subroutines with the overlay system acting as a means of outlining these groups, i.e. organizing them into different levels. There are four the levels of overlays allowed by FORTRAN V: the main overlay, the primary overlays, the secondary overlays and the ovcaps. list order and when a

In any FORTRAN V program there can only be one main overlay designated OVERLAY(XFILE,0,0,OV=nn), where XFILE is the name of the core memory file into which the overlays are to be written and nn is the

total number of overlays and ovcaps in the program. The main overlay is the highest level of overlays and in addition to standard fortran operations, the main overlay can call and load into core memory the primary overlays and the ovcaps. In the LINSTRUC program, the main overlay is called Program MAIN and serves to call the appropriate primary overlay: RESTIFF, EIGEN or STATDYN. A complete listing of Program MAIN is presented at the end of this discussion on overlays.

The primary overlays are the intermediate level of overlays and can call and load their associated secondary overlays and any of the ovcaps. The three primary overlays in LINSTRUC are designated OVERLAY(XFILE,1,0), OVERLAY(XFILE,2,0) and OVERLAY(XFILE,3,0).

The lowest level of overlays are the secondary overlays which can only call and load the ovcaps. Typical designations for the secondary overlays include OVERLAY(XFILE,2,1), OVERLAY(XFILE,2,2), etc.

Finally, the ovcaps are a type of overlay which can be called and loaded by main, primary or secondary overlays or by other ovcaps.

Some other general rules which govern overlays and ovcaps are as follows:

1. Only one main, one primary and one secondary overlay can be loaded into the core memory at any given time with virtually no restrictions on the number of ovcaps. Thus, for example, when a new secondary overlay is called for loading into the core memory, the previous secondary overlay is unloaded.
 2. Overlays can only be loaded in sequential order and when a primary overlay is loaded, only the secondary overlays associated with that primary overlay may be loaded with it.
- As an example of the former, the secondary overlay

OVERLAY(XFILE,2,2) can not be load before the secondary overlay OVERLAY(XFILE,2,1). For an example of the latter rule, if the primary overlay OVERLAY(XFILE,3,0) is in memory then only its associated secondary overlays such as OVERLAY(XFILE,3,1), OVERLAY(XFILE,3,2), etc. may be loaded with it.

3. The first subroutine in a main, primary or secondary overlay must be labelled "PROGRAM" while the remaining subroutines are labelled "SUBROUTINE". All of the subroutines in an ovcap, however, are designated as "SUBROUTINE" and the "name" of the ovcap is the same as the name of the first subroutine in the ovcap.
4. When an overlay is called, it is loaded into memory and operations begin at the first line in the overlay and continue until the return statement in the overlay's "PROGRAM" routine is reached. Ovcaps, however, can be loaded and then called one or more times and then unloaded. Each time an ovcap is called, the operations begin at the first line in the first subroutine and continue until the return statement in the first subroutine is reached.
5. The program and subroutines in each overlay and the subroutines in each ovcap may call other subroutines within the same overlay or ovcap with no loading or unloading of overlays or ovcaps taking place. As in regular fortran programming, the operations in these subroutines begin at line one and continue until the return statement is reached.
6. Overlays are labelled using octal numbering, i.e.

OVERLAY(XFILE,1,7) is followed by OVERLAY(XFILE,1,10).

Overlays are called, however, using decimals, i.e. the

statement CALL OVERLAY(5HXFILE,1,9) calls and loads into

core memory the overlay labelled OVERLAY(XFILE,1,11). Note

also that in the call statement the name XFILE must be

written as the character string 5HXFILE.

All overlays and ovcaps in the LINSTRUC program begin with the same parameter statement which contains the variables that control the sizes of the arrays in the various common blocks. A list of these variables and their definitions is as follows:

VARIABLE NAME	DESCRIPTION
Jn	Variables controlling array sizes in common blocks
n=4	Maximum number of nodal points
n=5	Maximum number of truss elements
n=6	Maximum number of straight beam elements
n=7	Not used
n=8	Maximum number of ground degrees of freedom
n=9	Maximum number of structure degrees of freedom after condensation
n=10	Maximum number of condensed structure degrees of freedom
n=11	Maximum number of degrees of freedom excluding ground degrees of freedom
n=12	Maximum number of degrees of freedom including ground degrees of freedom
n=13	Maximum value of lower bandwidth MBAND1

Before listing Program MAIN, the following outline of the LINSTRUC program is provide for quick reference.

```

OVERLAY(XFILE,0,0,OV=22) INVERSE - invert stiffness matrix
PROGRAM MAIN (INPUT,...
    OVERLAY(XFILE,1,0)
    PROGRAM RESTIFF
    OVERLAY(XFILE,1,1)
    PROGRAM NODDATA - read node data
    OVERLAY(XFILE,1,2)
    PROGRAM ELEMENT
    SUBROUTINE TRUSS - read truss data
    SUBROUTINE SBEAM - read straight beam data
    OVERLAY(XFILE,1,3)
    PROGRAM BAND - calculate bandwidths
    SUBROUTINE INITIAL - initialize program variables
    OVERLAY(XFILE,1,4)
    PROGRAM LOAD - read nodal loads and assemble load vector
    OVERLAY(XFILE,1,5)
    PROGRAM MASS - read nodal masses and assemble mass vector
    OVERLAY(XFILE,1,6)
    PROGRAM DYNLOAD - read damping and dynamic load data
    OVERLAY(XFILE,1,7)
    PROGRAM TRUSSEL - calculate truss element stiffness
    OVERLAY(XFILE,1,10)
    PROGRAM SBEAMEL - calculate straight beam element stiffness
    OVERLAY(XFILE,1,11)
    PROGRAM CONDENS - condense stiffness matrix and load vector
    OVERLAY(XFILE,2,0)
    PROGRAM EIGEN - calculate damping constants Alpha and Beta
    SUBROUTINE EIGENV - calculate eigenvalues and eigenvectors
    OVERLAY(XFILE,3,0)
    PROGRAM STATDYN
    OVERLAY(XFILE,3,1)
    PROGRAM LINSOLN - solve static problem
    SUBROUTINE INVERSE - invert stiffness matrix
    OVERLAY(XFILE,3,2)
    PROGRAM DYNINIT - initialize dynamic solution variables

```

SUBROUTINE INVERSE - invert stiffness matrix

OVERLAY(XFILE,3,3)

PROGRAM DYN SOLN - solve dynamic problem

OVCAP.

SUBROUTINE RECOVER - recover condensed DOF

OVCAP.

SUBROUTINE DISPL - calculate nodal displacements

OVCAP.

SUBROUTINE STRESS - calculate element end forces and stresses

OVCAP.

SUBROUTINE ASSEMBLE - assemble structure stiffness matrix

OVCAP.

SUBROUTINE TRANSFM - transform matrices into global coordinates

Finally, the following is a list of the main overlay in the

LINSTRUC program, Program MAIN:

```

C*****
C*****
C*****
C*****
C      OVERLAY(XFILE,0,0,OV=20)
C      PROGRAM MAIN (INPUT,OUTPUT,DYNLD1,DYNLD2,DISPL,TAPE60=INPUT,
C      +           TAPE61=OUTPUT,TAPE11=DYNLD1,TAPE12=DYNLD2,
C      +           TAPE13=DISPL,TAPE1,TAPE2,TAPE3,TAPE4)
C
C      *****
C      THIS PROGRAM USES THE FINITE ELEMENT METHOD TO ANALYZE
C      TRUSS, STRAIGHT BEAM AND CURVE BEAM ELEMENT FRAMES IN
C      THREE DIMENSIONS
C      *****
C
C      PARAMETER(J4=42,J5=14,J6=55,J7=0,J8=2,J9=34,J10=71,J11=99,
C      +           J12=101,J13=10)
C      COMMON/CB1/NE,NUMNP,NUMEG,IPAR,ISTRESS,ICAL1,ICAL2,ICAL3,ICAL4,
C      +           ICAL5,ICAL6,ICAL7,ICAL8,LINEQL,IDATA
C      COMMON/CB2/NSIZE,NEQ,NCOND,NGDOF,MBAND,MBAND1
C      COMMON/CB3/IA(J4,7),IB(J4,7),IG(J4),X(J4),Y(J4),Z(J4),
C      +           NPRINT(J4)
C      COMMON/CB4/E(2),P(2),NTYPE(2),NEPR(2),MPRINT(J6,2)
C      COMMON/CB5/NITE(J5),NJTE(J5),ATE(J5),LE(J5),SCT(J5,2)
C      COMMON/CB6/NISB(J6),NJSB(J6),NKSJ(J6),NPGS(J6,3),ASB(J6),AGXS(J6),
C      +           AGYS(J6),IXXS(J6),IYYS(J6),KTS(J6),IWS(J6),LSB(J6),
C      +           SCS(J6,16),SES(16),FL(J6,3),ELX(J6),ELY(J6),ELW(J6)
C      COMMON/CB7/SE(16,16),T(14,14)
C      COMMON/CB8/PN(J4,6),R(J11)

```



```

A.1 COMMON/CB9/S(J9,J11),SC(J10,J13),SG(J8,J12)
COMMON/CB10/D(J11),DG(J8),U(J4,7)
COMMON/CB11/NDP(3),ET(40,3),EA(40,3),NIA(J8),AAF(J8),APS(J8),
+ NDPL,NLW(3),FMT,DALPHA,DBETA,DSIGMA,TS,TT,NEAI,NEAG,
all of the over + MODEL,MODE2,DAMP1,DAMP2
REAL IXXS,IYYS,KTS,IWS,LSB,LE
+ INTEGER FMT
C
C.....READ NODE AND ELEMENT DATA AND ASSEMBLE STIFFNESS MATRIX
C
C CALL OVERLAY(5HXFILE,1,0,0)
C
C.....IF DATA CHECK ONLY SKIP ALL FURTHER CALCULATIONS
C
C***** IF(IDATA.EQ.0) GO TO 40
WRITE(61,2030)
GO TO 900
40 CONTINUE
C IF(LINEQL.EQ.2) GO TO 130
C IF(LINEQL.EQ.1) GO TO 140
C IF(DALPHA.NE.0.0) GO TO 140
C IF(DBETA.NE.0.0) GO TO 140
130 CONTINUE
C
C.....SOLVE EIGENPROBLEM
C
C CALL OVERLAY(5HXFILE,2,0,0)
140 IF(LINEQL.EQ.2) GO TO 900
C
C.....PERFORM LINEAR OR DYNAMIC SOLUTION
C
C CALL OVERLAY(5HXFILE,3,0,0)
C
C 900 CONTINUE AND STORE ELEMENT DATA
C
C 2030 FORMAT(' ',15HDATA CHECK ENDS)
C
C END
C*****
C*****
C*****
C.....READ NODAL POINT LOADS AND ASSEMBLE OVER NODAL MASS
C
C CALL OVERLAY(5HXFILE,1,4,0)
GO TO 20
10 CONTINUE
C
C.....READ LIMITED NODAL MASSES AND ASSEMBLE OVER NODAL MASS
C
C CALL OVERLAY(5HXFILE,1,5,0)
20 CONTINUE
IF(LINEQL.NE.3) GO TO 30

```

The following is a listing of Program RESTIFF.

```
C*****
C*****
C*****
OVERLAY(XFILE,1,0)
PROGRAM RESTIFF
C*****
C*****
C*****
PROGRAM TO READ NODE, ELEMENT AND LOAD DATA AND
TO ASSEMBLE STIFFNESS MATRIX AND LOAD VECTOR
C*****
C*****
PARAMETER(J4=42,J5=14,J6=55,J7=0,J8=2,J9=34,J10=71,J11=99,
+ J12=101,J13=10)
COMMON/CB1/NE,NUMNP,NUMEG,IPAR,ISTRESS,ICAL1,ICAL2,ICAL3,ICAL4,
+ ICAL5,ICAL6,ICAL7,ICAL8,LINEQL,IDATA
COMMON/CB4/E(2),P(2),NTYPE(2),NEPR(2),MPRINT(J6,2)
C*****
C.....READ CONTROL AND NODAL POINT DATA
C*****
CALL OVERLAY(5HXFILE,1,1,0)
C*****
C.....READ AND STORE ELEMENT DATA
C*****
CALL OVERLAY(5HXFILE,1,2,0)
C*****
C.....COMPUTE BANDWIDTHS OF STRUCTURE STIFFNESS MATRICES
C*****
CALL OVERLAY(5HXFILE,1,3,0)
IF(LINEQL.NE.1) GO TO 10
C*****
C.....READ NODAL POINT LOADS AND ASSEMBLE INTO LOAD VECTOR -R-
C*****
CALL OVERLAY(5HXFILE,1,4,0)
GO TO 20
10 CONTINUE
C*****
C.....READ LUMPED NODAL MASSES AND ASSEMBLE INTO MASS VECTOR -R-
C*****
CALL OVERLAY(5HXFILE,1,5,0)
20 CONTINUE
IF(LINEQL.NE.3) GO TO 30
C*****
```


C.....READ AND STORE DYNAMIC SOLUTION AND LOAD DATA

C

CALL OVERLAY(5HXFILE,1,6,0)

30 CONTINUE

C

C.....IF DATA CHECK ONLY SKIP ALL FURTHER CALCULATIONS

C

IF(IDATA.EQ.0) GO TO 40

WRITE(61,2030)

GO TO 900

40 CONTINUE

C

C.....COMPUTE ELEMENT LINEAR STIFFNESS AND ASSEMBLE INTO STRUCTURE

C

LINEAR STIFFNESS MATRIX

C

CALL LOVCAP ('TRANSFM')

CALL LOVCAP ('ASSEMBLE')

IF(NTYPE(1).EQ.0) GO TO 160

CALL OVERLAY(5HXFILE,1,7,0)

160 CONTINUE

IF(NTYPE(2).EQ.0) GO TO 170

CALL OVERLAY(5HXFILE,1,8,0)

170 CONTINUE

CALL UOVCAP ('TRANSFM')

CALL UOVCAP ('ASSEMBLE')

C

C.....CONDENSE STRUCTURE STIFFNESS MATRIX

C

CALL OVERLAY(5HXFILE,1,9,0)

900 CONTINUE

C

2030 FORMAT('-',15HDATA CHECK ENDS)

C

RETURN

C

END

C*****

C*****

C*****

C*****

C*****

C*****

C*****

C*****

C*****

C*****

C*****

C*****

C*****

C*****

C*****

C*****

C*****

C*****

C*****

C*****

C*****

C*****

A.1.1 PROGRAM NODDATA

The two main purposes of program NODDATA are to read program control data and to read and process nodal point data. The control data which is read includes the number of equations, the number of elements and the number of element groups. NODDATA also reads and stores the parameters which control solution, stress and print options.

The nodal point data which is read by NODDATA includes the arrays IA, IB and IG and the nodal coordinates X, Y and Z. The arrays IA, IB and IG control the nodal fixity, the slave node and condensation options and the designation of ground degree of freedom nodes. All of the variables which are read by NODDATA and their input formats are as follows:

LINE NAME	NUMBER OF LINES	VARIABLE NAME	FROM COLUMN	TO COLUMN
Title of Problem	1	T1-T8	1	80
Control Line	1	NE	1	5
		NUMNP	6	10
		NUMEG	11	15
		IDATA	16	20
		ISTRESS	21	25
		LINEQL	26	30
		ICAL1	31	35
		ICAL2	36	40
		ICAL3	41	45
		ICAL4	46	50
		ICAL5	51	55
		ICAL6	56	60
		ICAL7	61	65

see the Common Block 1 variables		ICAL8	66	70
VARIABLE NAME				
Node Data	NUMNP	M	1	5
IA		IA(M,1)	6	8
IB		IA(M,2)	9	11
IC		IA(M,3)	12	14
ID		IA(M,4)	15	17
IE		IA(M,5)	18	20
IF		IA(M,6)	21	23
IG		IA(M,7)	24	26
IB(1)		IB(M,1)	27	29
IB(2)		IB(M,2)	30	32
IB(3)		IB(M,3)	33	35
IB(4)		IB(M,4)	36	38
IB(5)		IB(M,5)	39	41
IB(6)		IB(M,6)	42	44
IB(7)		IB(M,7)	45	47
IG(M)		IG(M)	48	50
X(M)		X(M)	51	60
Y(M)		Y(M)	61	70
Z(M)		Z(M)	71	80
Nodal Print Data				
1		NPRINT(1)	1	1
2		NPRINT(2)	2	2
3		:		
4		:		
5		NPRINT(M)	M	M

The control data read by NODDATA is contained in Common Block 1 while the nodal point data is stored in Common Block 3. The following

are the Common Block 1 variables and their definitions:

VARIABLE NAME	DESCRIPTION
NE	Total number of elements in the structure
NUMNP	Total number of nodal points
NUMEG	Total number of element groups
IPAR	Variable identifying different stages of computation: 1 = data input 2 = performing linear solution or eigenvalue solution 3 = performing dynamic solution
ISTRESS	Stress calculation variable: 1 = calculate element end forces and stresses 0 = do not calculate stresses -N = calculate N number of initial yield functions for each element at each end
ICALN	Variable controlling printing: 0 = print 1 = skip N = dynamic solution print increment, used only for ICAL8
n=1	Dynamic load accelerograms being input
n=2	Local and global element stiffness matrices
n=3	Uncondensed and condensed structure stiffness matrices
n=4	Uncondensed and condensed structure load vectors or structure mass vector
n=5	Condensed and recovered global displacement vectors
n=6	Global element nodal displacements
n=7	All eigenvectors calculated
n=8	Dynamic solution print increment
LINEQL	Variable controlling type of solution procedure used: 1 = static solution 2 = eigenvalue/eigenvector solution only 3 = dynamic solution

DATA check variable:
 0 = proceed with solution
 1 = perform data check only

The following is a list of Common Block 3 variables and their definitions:

VARIABLE NAME DESCRIPTION

IA(N,I) Boundary condition code of node N for its Ith degree of freedom:
 For IG(N) = 0 then initially:
 1 = constrained
 0 = free, condensed or slave
 and after processing:
 0 = constrained
 K = equation number for the uncondensed degree of freedom
 -1 = condensed or slave
 For IG(N) = -1 then:
 1 = fixed
 0 = free

IB(N,I) Second boundary condition code of node N for its Ith degree of freedom:
 For IG(N) = 0 then initially:
 0 = free
 M = slave to node M's Ith degree of freedom
 -1 = condensed
 and after processing:
 0 = free
 M = slave to node M's Ith degree of freedom
 -L = Lth condensed degree of freedom
 For IG(N) = -1 after processing:
 B = ground degree of freedom number
 0 = fixed

IG(N) Third boundary condition code for node N:
 0 = normal bridge node
 -1 = ground node

X(N) Global X coordinate of node N

Y(N) Global Y coordinate of node N

Z(N) Global Z coordinate of node N

Finally, the following is a complete listing of Program MODDATA:

NPRINT(N) Nodal displacement print variable:
 0 = print all displacements at node N
 1 = do not print any displacements at node N
 2 = print only X and Y translations at node N
 3 = print X, Y and Z translations at node N

The variables contained in Common Block 2 deal with equation and bandwidth numbers, the former of which are calculated by NODDATA. The following is a list of all Common Block 2 variables and their definitions:

VARIABLE NAME	DESCRIPTION
NSIZE	Total number of degrees of freedom (including condensed and uncondensed structure degrees of freedom but excluding ground degrees of freedom)
NEQ	Total number of uncondensed structure degrees of freedom
NCOND	Total number of condensed structure degrees of freedom
NGDOF	Total number of ground degrees of freedom
MBAND	Upper bandwidth of structure stiffness matrix
MBAND1	Lower bandwidth of structure stiffness matrix

The upper and lower bandwidths are discussed in more detail in the section describing Program BAND.

A list of miscellaneous variables used by the NODDATA subroutine is as follows:

VARIABLE NAME	DESCRIPTION
M	Node number being read

Finally, the following is a complete listing of Program NODDATA:

```

C*****
C*****
C*****
      OVERLAY(XFILE,1,1)
      PROGRAM NODDATA
C
C *****
C      TO READ AND PRINT NODAL POINT DATA; TO CALCULATE EQUATION,
C      CONDENSATION AND GROUND DOF NUMBERS; AND TO STORE THE RESULTS
C      IN ARRAYS -IA-, -IB- AND -IG-
C *****
C
C      REAL M1,M2
      PARAMETER(J4=42,J5=14,J6=55,J7=0,J8=2,J9=34,J10=71,J11=99,
+      J12=101,J13=10)
      COMMON/CB1/NE,NUMNP,NUMEG,IPAR,ISTRESS,ICAL1,ICAL2,ICAL3,ICAL4,
+      ICAL5,ICAL6,ICAL7,ICAL8,LINEQL,IDATA
      COMMON/CB2/NSIZE,NEQ,NCOND,NGDOF,MBAND,MBAND1
      COMMON/CB3/IA(J4,7),IB(J4,7),IG(J4),X(J4),Y(J4),Z(J4),
+      NPRINT(J4)
C
C.....READ CONTROL DATA
C
      READ(60,1110) T1,T2,T3,T4,T5,T6,T7,T8
      WRITE(61,2220)T1,T2,T3,T4,T5,T6,T7,T8
      READ(60,1115) NE,NUMNP,NUMEG,IDATA,ISTRESS,LINEQL,ICAL1,ICAL2,
+      ICAL3,ICAL4,ICAL5,ICAL6,ICAL7,ICAL8
      WRITE(61,2210)NE,NUMNP,NUMEG,IDATA,ISTRESS,LINEQL,ICAL1,ICAL2,
+      ICAL3,ICAL4,ICAL5,ICAL6,ICAL7,ICAL8
C
C.....READ NODAL POINT DATA
C
      WRITE(61,2000)
      WRITE(61,2010)
      WRITE(61,2015)
      DO 100 J=1,NUMNP
      READ(60,1000) M,(IA(M,I),I=1,7),(IB(M,I),I=1,7),IG(M),X(M),Y(M),
+      Z(M)
      WRITE(61,2020)M,(IA(M,I),I=1,7),(IB(M,I),I=1,7),IG(M),X(M),Y(M),
+      Z(M)
100 CONTINUE
C
C.....PROCESS ARRAYS -IA-, -IB- AND -IG- TO FIND EQUATION,
C      CONDENSATION AND GROUND DOF NUMBERS. STORE IN ARRAYS -IA-,
C      -IB- AND -IG-
C
      NEQ=NCOND=NGDOF=0
      DO 125 N=1,NUMNP
      IF(IG(N)) 102,104,125
102 CONTINUE
      DO 103 I=1,3
      IF(IA(N,I).EQ.1) GO TO 103
      NGDOF=NGDOF+1
      IB(N,I)=NGDOF

```



```

103 IA(N,I)=0      NODAL POINT COORDINATE DIMENSION CODES, 32X,
GO TO 125          NODAL POINT COORDINATES/7H NUMBER, 31X, 7HIA(N, I), 32X,
104 CONTINUE
DO 120 I=1,7
2030 IF(IA(N,I).NE.1) GO TO 105      1X, 13, 3F12.5)
2030 IA(N,I)=0      17H GENERATED NODAL DATA //)
2040 GO TO 120      NODAL POINT COORDINATE DIMENSION CODES, 32X,
105 IA(N,I)=-1
IF(IB(N,I)) 110,115,120      1X, 13, 3F12.5)
110 NCOND=NCOND+1      1X, 13, 3F12.5)
2030 IB(N,I)=-NCOND      17H GENERATED NODAL DATA //)
2040 GO TO 120      NODAL POINT COORDINATE DIMENSION CODES, 32X,
115 NEQ=NEQ+1      17H GENERATED NODAL DATA //)
IA(N,I)=NEQ      17H GENERATED NODAL DATA //)
120 CONTINUE
125 CONTINUE
NSIZE=NEQ+NCOND
C110 FORMAT(15I3,3F10.5)
C.....READ AND PROCESS NODE PRINT DATA
C
READ(60,1010) (NPRINT(I),I=1,NUMNP)
DO 128 I=1,NUMNP
2120 IF(NPRINT(I).EQ.0) NPRINT(I)=8      10, 10, 10)
IF(NPRINT(I).EQ.1) NPRINT(I)=0
128 CONTINUE
WRITE(61,2110) (NPRINT(I),I=1,NUMNP)
C
C.....WRITE GENERATED NODAL POINT DATA
C
WRITE(61,2030)
WRITE(61,2040)
DO 230 K=1,NUMNP
IF(IG(K).LT.0) GO TO 230
WRITE(61,2050) K,(IA(K,I),I=1,7),(IB(K,I),I=1,7)
230 CONTINUE
IF(NGDOF.EQ.0) GO TO 245
WRITE(61,2070)
DO 240 L=1,NUMNP
IF(IG(L).GE.0) GO TO 240
WRITE(61,2080) L,(IB(L,I),I=1,3)
240 CONTINUE
245 CONTINUE
WRITE(61,2060) NSIZE,NEQ,NCOND,NGDOF
C
1000 FORMAT(15I3,3F10.5)
1010 FORMAT(55I1)
1020 FORMAT(4E20.10)
C
1110 FORMAT(A10,A10,A10,A10,A10,A10,A10,A10,)
1115 FORMAT(14I5)
C
C
2000 FORMAT('1',32H N O D A L P O I N T D A T A //)
2010 FORMAT(17H INPUT NODAL DATA//)

```



```

0015  FORMAT(6H NDE,27X,36HNODAL POINT BOUNDARY CONDITION CODES,33X,
+       23HNODAL POINT COORDINATES/7H NUMBER,21X,7HIA(N,I),33X,
+       7HIB(N,I)/11X,2(4X,1HX,4X,1HY,4X,1HZ,3X,2HTY,3X,2HTY,3X,
+       2HTZ,4X,1HW,5X),2X,2HTG,7X,4HX(N),8X,4HY(N),8X,4HZ(N))
0020  FORMAT(' ',I4,6X,7I5,5X,7I5,4X,I5,3F12.3)
0030  FORMAT(///22H GENERATED NODAL DATA //)
0040  FORMAT(6H NODE,17X,16HEQUATION NUMBERS,22X,
+       20HCONDENSATION NUMBERS/7H NUMBER,21X,7HIA(N,I),33X,
+       7HIB(N,I)/11X,2(4X,1HX,4X,1HY,4X,1HZ,3X,2HTY,3X,2HTY,3X,
+       2HTZ,4X,1HW,5X))
0050  FORMAT(' ',I4,6X,7I5,5X,7I5)
0060  FORMAT(' ',6HNSIZE=,I3,3X,4HNEQ=,I3,3X,6HNCOND=,I3,3X,6HNGDOF=,I3)
0070  FORMAT(' ',5H NODE,20X,18HGROUND DOF NUMBERS
+       /7H NUMBER,17X,1HX,9X,1HY,9X,1HZ)
0080  FORMAT(' ',I4,10X,3I10)
0090  FORMAT('0 ',9HNPRIINT = ,55I1)
0100  C
0110  FORMAT('0 ',6X,6HNE =,I3/7X,6HNUMNP=,I3/7X,6HNUMEG=,I3/7X,
+       6HIDATA=,I3/5X,8HISTRESS=,I3/6X,7HLINEQL=,I3/7X,
+       6HICAL1=,I3/7X,6HICAL2=,I3/7X,6HICAL3=,I3/7X,6HICAL4=,
+       I3/7X,6HICAL5=,I3/7X,6HICAL6=,I3/7X,6HICAL7=,I3/7X,
+       6HICAL8=,I3)
0120  FORMAT('1 ',A10,A10,A10,A10,A10,A10,A10,A10,A10)
0130  C
0140  C
0150  RETURN
0160  C
0170  END
0180  C*****
0190  C*****
0200  C*****

```

A.1.2 PROGRAM ELEMENT

The two purposes of Program ELEMENT are to read and store the element group material and control data and to call the subroutines TRUSS and SBEAM. If truss elements are part of the structure being analyzed, Program ELEMENT begins by reading and storing the following truss element material and control variables:

LINE NAME	NUMBER OF LINES	VARIABLE NAME	FROM COLUMN	TO COLUMN
Truss Material and Control Line	1	1	1	1
		NTYPE(1)	2	5
		NEPR(1)	6	10
		E(1)	11	20
		P(1)	21	25
		MPRINT(1,1)	26	26
		MPRINT(2,1)	27	27
		:		
		:		
		MPRINT(N,1)	N+25	N+25

Program ELEMENT would then call the subroutine TRUSS which would read and store the following truss element data:

LINE NAME	NUMBER OF LINES	VARIABLE NAME	FROM COLUMN	TO COLUMN
Truss Data	NTYPE(1)	NTE	1	5
		NITE(NTE)	6	10
		NJTE(NTE)	11	15
		ATE(NTE)	16	25
		SCT(NTE,1)	26	35
		SCT(NTE,2)	36	45

If straight beam elements are part of the structure being studied, Program ELEMENT would then read and store the following straight beam element material and control variables:

LINE NAME	NUMBER OF LINES	VARIABLE NAME	FROM COLUMN	TO COLUMN
Straight Beam Material and	1	2	1	1
Control Line		NTYPE(2)	2	5
		NEPR(2)	6	10
		E(2)	11	20
		P(2)	21	25
		MPRINT(1,2)	26	26
		MPRINT(2,2)	27	27
		:		
		:		
		MPRINT(N,2)	N+25	N+25

Finally, Program Element would then call the subroutine SBEAM which would read the following straight beam element data:

LINE NAME	NUMBER OF LINES	VARIABLE NAME	FROM COLUMN	TO COLUMN
Straight Beam Properties -	1	SES(NPR,1)	1	5
Yield Function Coefficients*		SES(NPR,2)	6	10
		SES(NPR,3)	11	15
		SES(NPR,4)	16	20
		SES(NPR,5)	21	25
		SES(NPR,6)	26	30
		SES(NPR,7)	31	35
		SES(NPR,8)	36	40
		SES(NPR,9)	41	45

SES(NPR,10)	46	50
SES(NPR,11)	51	55
SES(NPR,12)	56	60
SES(NPR,13)	61	65
SES(NPR,14)	66	70
SES(NPR,15)	71	75
SES(NPR,16)	76	80

Straight Beam Properties - 3 or 4 lines per property group

Stiffness Constants	1 per property group	NPR	1	5
		ASB(NPR)	6	15
		AGXS(NPR)	16	25
		AGYS(NPR)	26	35
		IXXS(NPR)	36	45
		IYYS(NPR)	46	55
		KTS(NPR)	56	65
		IWS(NPR)	66	75

Effective Beam Lengths	1 per property group	ELX(NPR)	1	10
		ELY(NPR)	11	20
		ELW(NPR)	21	30

Stress Constants 1-8	1 per property group	SCS(NPR,1)	1	10
		SCS(NPR,2)	11	20
		SCS(NPR,3)	21	30
		SCS(NPR,4)	31	40
		SCS(NPR,5)	41	50
		SCS(NPR,6)	51	60

VARIABLE NAME	DESCRIPTION	SCS(NPR,7)	61	70	
		SCS(NPR,8)	71	80	
E(N)	Element group				
P(N)	Stress Constants 9-16*	1 per property group	SCS(NPR,9)	1	10
NTYPE(N)	Number of element types	SCS(NPR,10)	11	20	
NPR(N)	Number of element properties	SCS(NPR,11)	21	30	
NPRINT(I,N)	Number stress print variables	SCS(NPR,12)	31	40	
	0 = calculate and print all stresses for element only for function values for	SCS(NPR,13)	41	50	
	1 = do not calculate	SCS(NPR,14)	51	60	
	function values for	SCS(NPR,15)	61	70	
NPRINT(N,N)	Element group print variables (for element group N:	SCS(NPR,16)	71	80	

Straight Beam Data	NTYPE(2)	NS	1	5
		NISB(NS)	6	10
		NJSB(NS)	11	15
		NKSB(NS)	16	20
		NPGS(NS,1)	21	25
		NPGS(NS,2)	26	30
		NPGS(NS,3)	31	35
		FL(NS,1)	36	45
		FL(NS,2)	46	55
		FL(NS,3)	56	65

* read only if initial yield function values are to be calculated

Common Block 4 contains the element group material and control variables. The following is a list of these Common Block 4 variables and their descriptions:

A list of the variables contained in Common Block 5 is as follows:

VARIABLE NAME	DESCRIPTION
E(N)	Modulus of elasticity of element group N
P(N)	Poisson's ratio of element group N
NTYPE(N)	Number of elements in element group N
NEPR(N)	Number of element property sets in element group N
MPRINT(I,N)	Member stress print variable for element group N: 0 = calculate and print all element end forces and stresses or all yield function values at element ends for element I of group N 1 = do not calculate forces, stresses or yield function values for element I of group N
MPRINT(M,N)	Element group print variable (where M = NTYPE(N) + 1) for element group N: 0 = calculate and print element end forces and stresses or yield function values at element ends for specified elements of group N 1 = do not calculate forces, stresses or yield function values for any elements of group N

The truss element data is contained in Common Block 5. A list of these truss element variables and their definitions is as follows:

VARIABLE NAME	DESCRIPTION
NITE(N)	Node I of truss element N
NJTE(N)	Node J of truss element N
ATE(N)	Axial area of truss element N
LE(N)	Geometric length of truss element N
SCT(N,1)	Yield force for truss element N (used only if yield function values are being calculated)
SCT(N,2)	Dead load force for truss element N (used only if yield function values are being calculated)

Common Block 6 contains the straight beam element data variables. A list of the variables contained in Common Block 6 is as follows:

VARIABLE NAME	DESCRIPTION
NISB(M)	Node I of straight beam element M
NJSB(M)	Node J of straight beam element M
NKSB(M)	Node K of straight beam element M
NPGS(M,L)	Property group associated with section L of straight beam element M
ASB(N)	Axial area of straight beam property group N
AGXS(N)	Local x axis shear area of straight beam property group N
AGYS(N)	Local y axis shear area of straight beam property group N
IXXS(N)	Local x-x moment of inertia of straight beam property group N
IYYS(N)	Local y-y moment of inertia of straight beam property group N
KTS(N)	Torsion constant of straight beam property group N
IWS(N)	Warping constant of straight beam property group N
LSB(M)	Geometric length of straight beam element M
SCS(N,P)	Stress constant P for straight beam property group N: For $ISTRESS = 1$, $P = 1$ and $P = 3$ are the distances from the local x axis to the member extreme fibers at nodes I and J, respectively; while $P = 2$ and $P = 4$ are the distances from the local y axis to the member extreme fibers at nodes I and J, respectively. For $ISTRESS < 0$, $P = 1$ to $P = 4$ are the axial yield force, local x-x yield moment, local y-y yield moment and yield bimoment, respectively, at node I; while $P = 5$ to $P = 8$ are the corresponding values at node J. The values $P = 9$ to $P = 12$ are the dead load axial force, the dead load x-x moment, the dead load y-y moment and the dead load bimoment at node I, respectively; while $P = 13$ to $P = 16$ are the corresponding values at node J.
SES(P)	Straight beam element initial yield function coefficients. The values $P = 9$ to $P = 12$ are the axial force ratio coefficients for yield functions 1 to 4, respectively. The values

P = 13 to P = 16, P = 17 to P = 20 and P = 21 to P = 24 are the corresponding coefficients for the x-x moment ratio, the y-y moment ratio and the bimoment ratio, respectively.

FL(M,J) Fraction of the total length of straight beam element M associated with straight beam property group NPGS(M,J)

ELX(N) Effective member length for property group N with respect to local x bending and local y shear

ELY(N) Effective member length for property group N with respect to local y bending and local x shear

ELW(N) Effective member length for property group N with respect to warping and torsion

The miscellaneous variables used in Program ELEMENT, Subroutine

TRUSS and Subroutine SBEAM are as follows:

VARIABLE NAME	DESCRIPTION
NT	Number of the type of element being read
NTE	Number of the truss element being read
NPR	Number of the straight beam property group being read
NS	Number of straight beam element being processed

Finally, the complete listing of Program ELEMENT and the subroutines

TRUSS and SBEAM is as follows:

```

C*****
C*****
C*****
C      OVERLAY(XFILE,1,2)
C      PROGRAM ELEMENT
C
C      *****
C      TO CALL THE APPROPRIATE ELEMENT SUBROUTINE
C      *****
C      CONTINUE
C      PARAMETER(J4=42,J5=14,J6=55,J7=0,J8=2,J9=34,J10=71,J11=99,
+      J12=101,J13=10)
C      COMMON/CB1/NE,NUMNP,NUMEG,IPAR,ISTRESS,ICAL1,ICAL2,ICAL3,ICAL4,
+      ICAL5,ICAL6,ICAL7,ICAL8,LINEQL,IDATA
C      COMMON/CB4/E(2),P(2),NTYPE(2),NEPR(2),MPRINT(J6,2)

```



```

C
C.....READ CONTROL DATA
C
      NTYPE(1)=NTYPE(2)=N=0
10 IF(N.EQ.NUMEG) GO TO 20
      READ(60,1000) NT,NTYPE(NT),NEPR(NT),E(NT),P(NT),
+           (MPRINT(I,NT),I=1,55)
      NTC=NT-2
      IF(NTC) 11,12,10
11 CALL TRUSS
      N=N+1
      GO TO 10
12 CALL SBEAM
      N=N+1
      GO TO 10
20 CONTINUE
C
1000 FORMAT(I1,I4,I5,F10.5,F5.4,55I1)
C
      RETURN
C
      END
C*****
C*****
C*****
      SUBROUTINE TRUSS
C
C *****
C      TRUSS ELEMENT SUBROUTINE
C *****
C
      PARAMETER(J4=42,J5=14,J6=55,J7=0,J8=2,J9=34,J10=71,J11=99,
+           J12=101,J13=10)
      COMMON/CB4/E(2),P(2),NTYPE(2),NEPR(2),MPRINT(J6,2)
      COMMON/CB5/NITE(J5),NJTE(J5),ATE(J5),LE(J5),SCT(J5,2)
      REAL LE
C
C
C.....PRINT ELEMENT CONTROL DATA
C
      WRITE(61,2000)
      WRITE(61,2020) NTYPE(1),E(1),(MPRINT(I,1),I=1,NTYPE(1))
      WRITE(61,2040)
C
C.....READ ELEMENT DATA
C
      DO 10 I=1,NTYPE(1)
      READ(60,1000) NTE,NITE(NTE),NJTE(NTE),ATE(NTE),(SCT(NTE,K),K=1,2)
      WRITE(61,2060)NTE,NITE(NTE),NJTE(NTE),ATE(NTE),(SCT(NTE,K),K=1,2)
10 CONTINUE
C
1000 FORMAT(3I5,3F10.5)
C
2000 FORMAT('1',27HT R U S S   E L E M E N T S//2X,6HNUMBER,6X,
+       7HMODULUS/4X,2HOF,11X,2HOF/1X,8HELEMENTS,4X,

```

```

+      10HELASTICITY)
2020 FORMAT(' ',I5,E17.6,20X,9HMPRINT = ,35I1)
2040 FORMAT('-',I1X,7HELEMENT,4X,6HNODE I,5X,6HNODE J,12X,4HAREA,11X,
+      11HYIELD FORCE,10X,15HDEAD LOAD FORCE)
2060 FORMAT('0',I5,5X,I5,6X,I5,3(6X,F15.6))
C
      RETURN
C
      END
C*****
C*****
C*****
      SUBROUTINE SBEAM
C
C      *****
C      STRAIGHT BEAM ELEMENT SUBROUTINE
C      *****
C
      PARAMETER(J4=42,J5=14,J6=55,J7=0,J8=2,J9=34,J10=71,J11=99,
+      J12=101,J13=10)
      COMMON/CB1/NE,NUMNP,NUMEG,IPAR,ISTRESS,ICAL1,ICAL2,ICAL3,ICAL4,
+      ICAL5,ICAL6,ICAL7,ICAL8,LINEQL,IDATA
      COMMON/CB4/E(2),P(2),NTYPE(2),NEPR(2),MPRINT(J6,2)
      COMMON/CB6/NISB(J6),NJSB(J6),NKSJ(J6),NPGS(J6,3),ASB(J6),AGXS(J6),
+      AGYS(J6),IXXS(J6),IYYS(J6),KTS(J6),IWS(J6),LSB(J6),
+      SCS(J6,16),SES(16),FL(J6,3),ELX(J6),ELY(J6),ELW(J6)
      REAL IXXS,IYYS,KTS,IWS,LSB
      DIMENSION DUM(7)
C
C      1000 FORMAT(I5,F10.0)
C.....PRINT ELEMENT CONTROL DATA
C
      WRITE(61,2000)
      WRITE(61,2020) NTYPE(2),E(2),P(2), (MPRINT(I,2),I=1,NTYPE(2))
      IF(ISTRESS.GE.0) GO TO 5
      READ(60,1030) (SES(J),J=1,16)
      WRITE(61,2130)
      WRITE(61,2135) (SES(K),K=1,16)
      CONTINUE
      WRITE(61,2040)
C
C.....READ ELEMENT PROPERTY DATA
C
      DO 10 I=1,NEPR(2)
      READ(60,1000) NPR,ASB(NPR),AGXS(NPR),AGYS(NPR),IXXS(NPR),
+      IYYS(NPR),KTS(NPR),IWS(NPR)
      WRITE(61,2060) NPR,ASB(NPR),AGXS(NPR),AGYS(NPR),IXXS(NPR),
+      IYYS(NPR),KTS(NPR),IWS(NPR)
      READ(60,1020) ELX(NPR),ELY(NPR),ELW(NPR)
      READ(60,1020) (SCS(NPR,J),J=1,8)
      IF(ISTRESS.LT.0) READ(60,1020) (SCS(NPR,J),J=9,16)
      CONTINUE
      WRITE(61,2200)
      DO 11 I=1,NPR(2)
      WRITE(61,2210) I,ELX(I),ELY(I),ELW(I)

```

```

11 CONTINUE
1130 IF(ISTRESS.LT.0) GO TO 14
WRITE(61,2110)
DO 12 I=1,NEPR(2)
WRITE(61,2115) I,(SCS(I,K),K=1,4)
12 CONTINUE
GO TO 19
14 CONTINUE
WRITE(61,2120)
DO 16 I=1,NEPR(2)
WRITE(61,2125) I,(SCS(I,K),K=1,8)
16 CONTINUE
WRITE(61,2140)
DO 18 I=1,NEPR(2)
WRITE(61,2125) I,(SCS(I,K),K=9,16)
18 CONTINUE
19 CONTINUE
WRITE(61,2080)
C
C.....READ ELEMENT DATA
C
DO 20 J=1,NTYPE(2)
READ(60,1010) NS,NISB(NS),NJSB(NS),NKS( NS),(NPGS(NS,I),I=1,3),
+ (FL(NS,I),I=1,3)
WRITE(61,2100)NS,NISB(NS),NJSB(NS),NKS( NS),(NPGS(NS,I),I=1,3),
+ (FL(NS,I),I=1,3)
20 CONTINUE
C
1000 FORMAT(I5,7F10.5)
1010 FORMAT(7I5,3F10.5)
1020 FORMAT(8F10.5)
1030 FORMAT(16F5.3)
C
2000 FORMAT('1',43HS T R A I G H T B E A M E L E M E N T S //2X,
+ 6HNUMBER,6X,7HMODULUS,9X,9HPOISSON'S/4X,2HOF,
+ 11X,2HOF,13X,5HRATIO/1X,8HELEMENTS,4X,10HELASTICITY)
2020 FORMAT(' ',I5,2E17.6,20X,9HMPRINT = ,55I1)
2040 FORMAT('0',1X,7HSECTION,6X,5HAXIAL,12X,5HSHEAR,10X,
+ 9HMOMENT OF,8X,9HMOMENT OF,9X,7HTORSION,10X,7HWARPING/2X,
+ 6HNUMBER,7X,4HAREA,13X,6HAREA X,11X,6HAREA Y,9X,
+ 9HINERTIA X,8X,9HINERTIA Y,9X,8HCONSTANT,9X,8HCONSTANT)
2060 FORMAT(' ',I5,7E17.6)
2080 FORMAT('0',1X,7HELEMENT,4X,4HNODE,4X,4HNODE,4X,4HNODE,4X,
+ 14HPROPERTY GROUP,9X,18HFRACTION OF LENGTH/2X,6HNUMBER,6X,
+ 1H1,7X,1HJ,7X,1HK,4X,5HSEC 1,2X,5HSEC 2,2X,5HSEC 3,3X,
+ 5HSEC 1,4X,5HSEC 2,4X,5HSEC 3)
2100 FORMAT(' ',I5,1X,3(3X,I5),2X,3(I5,2X),3(2X,F7.5))
2110 FORMAT('0',1X,7HSECTION,20X,6HNODE I,20X,6HNODE J/2X,6HNUMBER,16X,
+ 3HCXX,10X,3HCYY,10X,3HCXX,10X,3HCYY)
2115 FORMAT(' ',I5,10X,4E13.6)
2120 FORMAT('0',1X,7HSECTION,17X,31HNODE I YIELD FORCES AND MOMENTS,
+ 30X,31HNODE J YIELD FORCES AND MOMENTS/2X,6HNUMBER,10X,
+ 2HP0,12X,3HMX0,12X,3HMY0,12X,3HMY0,13X,2HP0,12X,3HMX0,12X,
+ 3HMY0,12X,3HMY0)

```


A.1.3 PROGRAM BAND

Program BAND serves two main purposes: to calculate the structure stiffness matrix bandwidths and to call the Subroutine INITIAL which initializes the stiffness matrix, load vector and displacement vector arrays. The primary purpose of Program BAND is to calculate the bandwidth MBAND of the upper structure stiffness matrix array S and the bandwidth MBAND1 of the lower structure stiffness matrix array SC both of which are illustrated in Figure 2-3b.

Both Common Block 8 and Common Block 9 variables are initialized by the Subroutine INITIAL. The list of all Common Block 8 variables is as follows:

VARIABLE NAME	DESCRIPTION
PN(N,I)	For LINEQL = 1, PN(N,I) = applied load at node N in the Ith direction For LINEQL = 2 or 3, PN(N,I) = lumped mass at node N in the Ith direction
R(N)	For LINEQL = 1, R(N) = Nth entry in the structure load vector For LINEQL = 2 or 3, R(N) = Nth entry in the structure mass "vector"

The list of all Common Block 9 variables is as follows:

VARIABLE NAME	DESCRIPTION
S(I,J)	I-J entry of the upper structure stiffness matrix in banded format
SC(I,J)	I-J entry of the lower structure stiffness matrix in banded format
SG(I,J)	I-J entry of the ground degree of freedom stiffness matrix in banded format

The following is a list of the miscellaneous variables which are

used by Program BAND and by Subroutine INITIAL:

VARIABLE NAME	DESCRIPTION
IC(N,J)	Fourth boundary condition code: For lower bandwidth MBAND1 calculations: with $IA(N,J) > 0$, then $IC(N,J) = -1$ with $IA(N,J) < 0$ and with $IB(N,J) < 0$, then $IC(N,J) = -IB(N,J)$ For upper bandwidth MBAND calculations: with $IA(N,J) > 0$, then $IC(N,J) = IA(N,J)$ with $IA(N,J) < 0$ and with $IB(N,J) < 0$, then $IC(N,J) = NEQ - IB(N,J)$
KB	Variable controlling type of bandwidth to be calculated: 1 = lower bandwidth MBAND1 2 = upper bandwidth MBAND
MK	Variable controlling number of degrees of freedom per node: 3 = truss element 7 = straight beam element
NI and NJ	Nodes I and J, respectively, of the current element
MB	Bandwidth for current combination of nodes and degrees of freedom
N	Designated bandwidth for stiffness matrix -SG- = NSIZE + NGDOF

The following is the listing of Program BAND and Subroutine

INITIAL:

```

C*****
C*****
C*****
      OVERLAY(XFILE,1,3)
      PROGRAM BAND
C
C *****
C      TO COMPUTE BANDWIDTHS OF STRUCTURE STIFFNESS MATRIX
C *****
C
      PARAMETER(J4=42,J5=14,J6=55,J7=0,J8=2,J9=34,J10=71,J11=99,
+              J12=101,J13=10)
      COMMON/CB1/NE,NUMNP,NUMEG,IPAR,ISTRESS,ICAL1,ICAL2,ICAL3,ICAL4,
+              ICAL5,ICAL6,ICAL7,ICAL8,LINEQL,IDATA

```



```

COMMON/CB2/NSIZE,NEQ,NCOND,NGDOF,MBAND,MBAND1
COMMON/CB3/IA(J4,7),IB(J4,7),IG(J4),X(J4),Y(J4),Z(J4),
+   NPRINT(J4)
COMMON/CB4/E(2),P(2),NTYPE(2),NEPR(2),MPRINT(J6,2)
COMMON/CB5/NITE(J5),NJTE(J5),ATE(J5),LE(J5),SCT(J5,2)
COMMON/CB6/NISB(J6),NJSB(J6),NKSB(J6),NPGS(J6,3),ASB(J6),AGXS(J6),
+   AGYS(J6),IXXS(J6),IYYS(J6),KTS(J6),IWS(J6),LSB(J6),
+   SCS(J6,16),SES(16),FL(J6,3),ELX(J6),ELY(J6),ELW(J6)
REAL IXXS,IYYS,KTS,IWS,LSB,LE
DIMENSION IC(J4,7)
IF(NCOND.EQ.0) GO TO 145

C
C.....DERIVE LOWER BANDWIDTH MBAND1
C
110 MBAND=7
120 KB=1
130 DO 50 I=1,NUMNP
135 DO 40 J=1,7
140 IF(IG(I).LT.0) GO TO 36
145 IF(IA(I,J)) 30,36,36
30 CONTINUE
150 IF(IB(I,J)) 31,36,32
31 CONTINUE
155 IC(I,J)=-IB(I,J)
160 GO TO 40
32 CONTINUE
165 II=IB(I,J)
170 IF(IG(II).LT.0) GO TO 36
175 IF(IA(II,J)) 33,36,36
33 CONTINUE
180 IF(IB(II,J)) 34,36,36
34 CONTINUE
185 IC(I,J)=-IB(II,J)
190 GO TO 40
36 CONTINUE
195 IC(I,J)=-1
40 CONTINUE
50 CONTINUE
60 CONTINUE
200 DO 135 M=1,2
205 IF(NTYPE(M).EQ.0) GO TO 135
135 IF(M.EQ.1) MK=3
140 IF(M.NE.1) MK=7
210 DO 130 K=1,NTYPE(M)
215 IF(M.NE.1) GO TO 70
130 NI=NITE(K)
135 NJ=NJTE(K)
70 GO TO 90
220 CONTINUE
225 IF(M.NE.2) GO TO 80
230 NI=NISB(K)
235 NJ=NJSB(K)
80 GO TO 90
240 CONTINUE

```

```

90  CONTINUE
    DO 120 I=1,MK
    IF(IC(NI,I).LE.0) GO TO 120
    N1=IC(NI,I)
    DO 110 J=1,MK
    IF(IC(NJ,J).LE.0) GO TO 110
    N2=IC(NJ,J)
    MB=N2-N1
    IF(MB) 103,105,105
103  MB=-MB+1
    GO TO 107
105  MB=MB+1
    GO TO 107
107  IF(MB.GT.MBAND) MBAND=MB
110  CONTINUE
120  CONTINUE
130  CONTINUE
135  CONTINUE
C
C.....DERIVE UPPER BANDWIDTH -MBAND-
C
    IF(KB.EQ.2) GO TO 900
    MBAND1=MBAND
    WRITE(61,2010) MBAND1
145  CONTINUE
    MBAND=7
    KB=2
    DO 300 I=1,NUMNP
    DO 200 J=1,7
    IF(IG(I).LT.0) GO TO 158
    IF(IA(I,J)) 150,160,160
150  CONTINUE
    IF(IB(I,J)) 151,160,152
151  CONTINUE
    IC(I,J)=NEQ-IB(I,J)
    GO TO 200
152  CONTINUE
    II=IB(I,J)
    IF(IG(II).LT.0) GO TO 158
    IF(IA(II,J)) 153,156,156
153  CONTINUE
    IF(IB(II,J)) 154,156,156
154  CONTINUE
    IC(I,J)=NEQ-IB(II,J)
    GO TO 200
156  CONTINUE
    IC(I,J)=IA(II,J)
    GO TO 200
158  CONTINUE
    IC(I,J)=-1
    GO TO 200
160  IC(I,J)=IA(I,J)
200  CONTINUE
300  CONTINUE

```



```

GO TO 60
900 CONTINUE
WRITE(61,2000) MBAND
IF(IDATA.EQ.1) GO TO 990
C
C.....INITIALIZE STIFFNESS MATRICES AND LOAD VECTOR
C
CALL INITIAL
990 CONTINUE
C
RETURN
C
2000 FORMAT('-',17HUPPER BANDWIDTH =,I3)
2010 FORMAT('-',17HLOWER BANDWIDTH =,I3)
C
END
C*****
C*****
C*****
SUBROUTINE INITIAL
C
C*****
C TO INITIALIZE STIFFNESS MATRICES -S-, -SC- AND -SG-; AND
C TO INITIALIZE LOAD OR MASS VECTOR -R-
C*****
C
PARAMETER(J4=42,J5=14,J6=55,J7=0,J8=2,J9=34,J10=71,J11=99,
+ J12=101,J13=10)
COMMON/CB2/NSIZE,NEQ,NCOND,NGDOF,MBAND,MBAND1
COMMON/CB8/PN(J4,6),R(J11)
COMMON/CB9/S(J9,J11),SC(J10,J13),SG(J8,J12)
C
C.....SET ARRAYS -S-, -SC-, -SG-, AND -R- EQUAL TO ZERO
C
IF(NGDOF.EQ.0) GO TO 100
DO 90 I=1,NGDOF
N=NGDOF+NSIZE
DO 80 J=1,N
SG(I,J)=0.0
80 CONTINUE
90 CONTINUE
100 CONTINUE
IF(NCOND.EQ.0) GO TO 104
DO 103 I=1,NCOND
DO 102 J=1,MBAND1
SC(I,J)=0.0
102 CONTINUE
103 CONTINUE
104 CONTINUE
DO 106 I=1,NEQ
DO 105 J=1,MBAND
S(I,J)=0.0
105 CONTINUE
106 CONTINUE

```


A.1.4 PROGRAM LOAD

The purpose of Program LOAD is to read the nodal point loads used for static analysis and process them into the load vector array R. The following is a list of the data input for Program LOAD:

LINE	NAME	NUMBER OF LINES	VARIABLE NAME	FROM COLUMN	TO COLUMN
10	Load Data	varies	N	1	5
20	CONTINUE		LN(1)	6	15
25	CONTINUE		LN(2)	16	25
30	CONTINUE		LN(3)	26	35
35	CONTINUE		LN(4)	36	45
40	CONTINUE		LN(5)	46	55
45	CONTINUE		LN(6)	56	65

Next is a list of the miscellaneous variables used in the LOAD program:

VARIABLE NAME	DESCRIPTION
N	Node number of point loads currently being read
LN(K)	Load in Kth direction associated with current node N

Finally, the listing of Program LOAD is as follows:

```

C*****
C*****
C*****
OVERLAY(XFILE,1,4)
PROGRAM LOAD
C
C *****
C   TO READ AND STORE INITIAL LOAD DATA
C *****
C 30 *****
C *****
235 PARAMETER(J4=42,J5=14,J6=55,J7=0,J8=2,J9=34,J10=71,J11=99,
+ J12=101,J13=10)
240 COMMON/CB1/NE,NUMNP,NUMEG,IPAR,ISTRESS,ICAL1,ICAL2,ICAL3,ICAL4,

```

```

+          ICAL5,ICAL6,ICAL7,ICAL8,LINEQL,IDATA
COMMON/CB2/NSIZE,NEQ,NCOND,NGDOF,MBAND,MBAND1
COMMON/CB3/IA(J4,7),IB(J4,7),IG(J4),X(J4),Y(J4),Z(J4),
+          NPRINT(J4)
COMMON/CB8/PN(J4,6),R(J11)
REAL LN(6)
WRITE(61,2015)

C
C.....INITIALIZE NODAL LOAD ARRAY -PN-
C
      DO 20 I=1,NUMNP
      DO 10 J=1,6
      PN(I,J)=0.0
10    CONTINUE
20    CONTINUE
C
C.....READ INITIAL LOAD DATA
C
25    CONTINUE
      READ(60,1000) N,(LN(I),I=1,6)
      IF(N.EQ.0) GO TO 50
      DO 30 K=1,6
      PN(N,K)=LN(K)+PN(N,K)
30    CONTINUE
      WRITE(61,2000) N,(PN(N,I),I=1,6)
      GO TO 25
50    CONTINUE
C
1000  FORMAT(1X,I4,6F10.3)
C
2000  FORMAT(' ',I4,6(E16.8))
2015  FORMAT('1',13HINITIAL LOADS//6H  NODE,42X,14HLOAD DIRECTION//
+        7H NUMBER,10X,1HX,15X,1HY,15X,1HZ,15X,2HTX,14X,2HTY,14X,
+        2HTZ//)
C
      IF(IDATA.EQ.1) GO TO 300
C
C.....PROCESS INITIAL LOADS INTO LOAD VECTOR -R-
C
      DO 280 N=1,NUMNP
      DO 270 I=1,6
      IF(IA(N,I)) 220,270,210
210    CONTINUE
      II=IA(N,I)
      GO TO 260
220    CONTINUE
      IF(IB(N,I).LT.0) GO TO 230
      NN=IB(N,I)
      GO TO 235
230    II=-IB(N,I)+NEQ
      GO TO 260
235    CONTINUE
      IF(IA(NN,I)) 240,270,250
240    CONTINUE

```

```

      II=-IB(NN,I)+NEQ
      GO TO 260
250   CONTINUE
      II=IA(NN,I)
260   R(II)=PN(N,I)+R(II)
270   CONTINUE
280   CONTINUE
C
C.....PRINT LOAD VECTOR -R-
C
      IF(ICAL4.NE.0) GO TO 300
      WRITE(61,2020)
      DO 285 I=1,NSIZE
      WRITE(61,2030) I,R(I)
285   CONTINUE
300   CONTINUE
C
2020  FORMAT('1',44HINITIAL LOADS PROCESSED INTO LOAD VECTOR -R-//)
2030  FORMAT(' ',2HR(',I3,2H)=,F16.6)
C
      RETURN
C
      END
C*****
C*****
C*****

```

A.1.5 PROGRAM MASS ^{Tu For. 214}

Program MASS serves to read the lumped nodal masses used for a dynamic analysis or an eigenvalue/eigenvector analysis and process them into a vector array R which represents the diagonal of the structure mass matrix. The following is a list of the variables which are read by the MASS program:

LINE NAME	NUMBER OF LINES	VARIABLE NAME	FROM COLUMN	TO COLUMN
Mass Data	varies	N	1	5
		MN(1)	6	15
		MN(2)	16	25
		MN(3)	26	35
		MN(4)	36	45
		MN(5)	46	55
		MN(6)	56	65

A list of the Program MASS miscellaneous variables is as follows:

VARIABLE NAME	DESCRIPTION
N	Node number of lumped masses currently being read
MN(K)	Mass in Kth direction associated with current node N

Lastly is a listing of the MASS program itself:

```

C*****
C*****
C*****
  OVERLAY(XFILE,1,5)
  PROGRAM MASS
C
C  *****
C  TO READ AND STORE LUMPED NODAL MASSES
C  *****
C
  PARAMETER(J4=42,J5=14,J6=55,J7=0,J8=2,J9=34,J10=71,J11=99,

```

```

+      J12=101,J13=10)
COMMON/CB1/NE,NUMNP,NUMEG,IPAR,ISTRESS,ICAL1,ICAL2,ICAL3,ICAL4,
+      ICAL5,ICAL6,ICAL7,ICAL8,LINEQL,IDATA
COMMON/CB2/NSIZE,NEQ,NCOND,NGDOF,MBAND,MBAND1
COMMON/CB3/IA(J4,7),IB(J4,7),IG(J4),X(J4),Y(J4),Z(J4),
+      NPRINT(J4)
COMMON/CB8/PN(J4,6),R(J11)
REAL MN(6)
WRITE(61,2010)

C
C.....INITIALIZE NODAL MASS ARRAY -PN-
C
      DO 20 I=1,NUMNP
      DO 10 J=1,6
      PN(I,J)=0.0
10    CONTINUE
20    CONTINUE
C
C.....READ LUMPED NODAL MASS DATA
C
25    CONTINUE
      READ(60,1000) N,(MN(I),I=1,6)
      IF(N.EQ.0) GO TO 50
      DO 30 K=1,6
      PN(N,K)=MN(K)+PN(N,K)
30    CONTINUE
      WRITE(61,2000) N,(PN(N,I),I=1,6)
      GO TO 25
50    CONTINUE
1000  FORMAT(1X,I4,6F10.3)
C
2000  FORMAT(' ',I4,6(E16.8))
2010  FORMAT('1',13HLUMPED MASSES//6H  NODE,27X,14HMASS DIRECTION//
+      7H NUMBER,10X,1HX,15X,1HY,15X,1HZ,15X,2HTX,14X,2HTY,14X,
+      2HTZ//)
C
      IF(IDATA.EQ.1) GO TO 300
C
C.....PROCESS LUMPED NODAL MASSES INTO MASS VECTOR -R-
C
      DO 280 N=1,NUMNP
      IF(IG(N).LT.0) GO TO 280
      DO 270 I=1,6
      IF(IA(N,I)) 220,270,210
210    CONTINUE
      II=IA(N,I)
      GO TO 260
220    CONTINUE
      IF(IB(N,I).LT.0) GO TO 270
      NN=IB(N,I)
      IF(IG(NN).LT.0) GO TO 270
      IF(IA(NN,I)) 270,270,250
250    CONTINUE
      II=IA(NN,I)

```

```

260  R(II)=PN(N,I)+R(II)
270  CONTINUE
280  CONTINUE
C
C.....PRINT MASS VECTOR -R-
C
      IF(ICAL4.NE.0) GO TO 300
      WRITE(61,2020)
      DO 285 I=1,NSIZE
      WRITE(61,2030) I,R(I)
285  CONTINUE
300  CONTINUE
C
2020  FORMAT('1',44HLUMPED MASSES PROCESSED INTO MASS VECTOR -R-//)
2030  FORMAT(' ',2HR(,I3,2H)=,F16.6)
C
      RETURN
C
      END
C*****
C*****
C*****

```


A.1.6 PROGRAM DYNLOAD

Program DYNLOAD serves two purposes: to read and store the dynamic analysis control data, and to read and store the first portions of the ground acceleration histories. The latter segments of ground acceleration history are called the ground acceleration windows and generally include only a small portion of the overall history. As the dynamic solution proceeds, the ground acceleration windows are periodically updated such that the time interval of each window always includes the time associated with the current time step.

The following is a list of all the data input that is read by the DYNLOAD program:

LINE NAME	NUMBER OF LINES	VARIABLE NAME	FROM COLUMN	TO COLUMN
Dynamic Solution Control	1	DALPHA	1	10
		DBETA	11	20
		DSIGMA	21	30
		TS	31	40
		TT	41	50
		MODE1	51	55
		DAMP1	56	65
		MODE2	66	70
		DAMP2	71	80
Dynamic Load Control	1	NEAI	1	5
		NEAG	6	10
		NDP(1)	11	15
		NDP(2)	16	20
		NDP(3)	21	25

		NLW(1)	26	30
		NLW(2)	31	35
		NLW(3)	36	40
		NDPL	41	45
		FMT	46	50
<hr/>				
Dynload Data	varies	ET(J,I)*	varies	varies
		EA(J,I)	varies	varies
<hr/>				
Dynload Generated Data	NEAG	K	1	5
		NIA(K)	6	10
		AAF(K)	11	20
		APS(K)	21	30

* omitted if ground acceleration history time increments are uniform

The variables in Common Block 11 are either read or initialized by Program DYNLOAD. A list of these variables and their descriptions is as follows:

VARIABLE NAME	DESCRIPTION
<hr/>	
NDP(I)	Number of data points in input accelerogram I
ET(J,I)	Time associated with data point J of the window for input accelerogram I
EA(J,I)	Acceleration amplitude associated with data point J of the window for input accelerogram I
NIA(K)	Number of the input accelerogram associated with generated accelerogram K
AAF(K)	Amplitude factor associated with generated accelerogram K
APS(K)	Phase shift associated with generated accelerogram K

NDPL	Number of data points per line of input for all input accelerograms
NLW(I)	Number of lines of data input associated with the window for input accelerogram I
FMT	Input format number
DALPHA	Constant Alpha of damping matrix equation: $C = \text{Alpha} * M + \text{Beta} * K$
DBETA	Constant Beta of damping matrix equation: $C = \text{Alpha} * M + \text{Beta} * K$
DSIGMA	Newmark's Method Constant = 1/4 or 1/6
TS	Time step size to be used in dynamic solution
TT	Total time duration of the dynamic loading
NEAI	Number of earthquake accelerograms input
NEAG	Number of earthquake accelerograms generated
MODE1	Number of first calculated mode used in generating Alpha and Beta in damping matrix equation above
MODE2	Number of second calculated mode used in generating Alpha and Beta in damping matrix equation above
DAMP1	Critical damping ratio for MODE1
DAMP2	Critical damping ratio for MODE2

A listing of the miscellaneous variables used by Program DYNLOAD is as follows:

VARIABLE NAME	DESCRIPTION
NDB	Overall data point number associated with data point 1 of the current line of input
NDE	Overall data point number associated with data point NDPL of the current line of input
ND	Number of tape from which current input accelerogram is to be read
KK	Variable used for current ground acceleration history data point number or for current generated accelerogram number

KKT Previous ground acceleration history data point
 number, used only for generating data point
 times for CALTECH accelerograms

Finally, a listing of the DYNLOAD program itself is as follows:

```

C*****
C*****
C*****
  OVERLAY(XFILE,1,6)
  PROGRAM DYNLOAD
C
C  *****
C  TO READ AND STORE DYNAMIC SOLUTION CONTROL DATA AND
C  DYNAMIC LOADS
C  *****
C
  PARAMETER(J4=42,J5=14,J6=55,J7=0,J8=2,J9=34,J10=71,J11=99,
+           J12=101,J13=10)
  COMMON/CB1/NE,NUMNP,NUMEG,IPAR,ISTRESS,ICAL1,ICAL2,ICAL3,ICAL4,
+           ICAL5,ICAL6,ICAL7,ICAL8,LINEQL,IDATA
  COMMON/CB11/NDP(3),ET(40,3),EA(40,3),NIA(J8),AAF(J8),APS(J8),
+           NDPL,NLW(3),FMT,DALPHA,DBETA,DSIGMA,TS,TT,NEAI,NEAG,
+           MODEL,MODE2,DAMP1,DAMP2
  DIMENSION NN(3)
  INTEGER FMT
C
C.....READ DYNAMIC SOLUTION AND LOAD CONTROL DATA
C
  WRITE(61,2010)
  READ(60,1050) DALPHA,DBETA,DSIGMA,TS,TT,MODEL,DAMP1,MODE2,DAMP2
  WRITE(61,2015)DALPHA,DBETA,DSIGMA,TS,TT
  WRITE(61,2000)
  READ(60,1000) NEAI,NEAG,(NDP(I),I=1,3),(NLW(J),J=1,3),NDPL,FMT
  WRITE(61,2005)NEAI,NEAG,(I,NDP(I),I=1,3),(J,NLW(J),J=1,3),NDPL
  IF(ICAL1.EQ.0) WRITE(61,2020)
C
C.....READ FIRST DYNAMIC LOAD ACCELEROGRAM WINDOWS
C
  DO 100 I=1,NEAI
    IF(ICAL1.EQ.0) WRITE(61,2040) I
    NDB=1
    NDE=NDPL
    ND=10+I
    DO 90 J=1,NLW(I)
      IF(FMT.NE.1) GO TO 10
      READ(ND,1010) (ET(KK,I),EA(KK,I),KK=NDB,NDE)
10    CONTINUE
      IF(FMT.NE.2) GO TO 20
      READ(ND,1020) (ET(KK,I),EA(KK,I),KK=NDB,NDE)
20    CONTINUE
      IF(FMT.NE.3) GO TO 30

```

```

      READ(ND,1030) (EA(KK,I),KK=NDB,NDE)
      DO 25 KK=NDB,NDE
      IF(KK.EQ.1) ET(KK,I)=0.0
      KKT=KK-1
      IF(KK.NE.1) ET(KK,I)=ET(KKT,I)+0.025
25    CONTINUE
30    CONTINUE
      IF(ICALL.EQ.0) WRITE(61,2070) (KK,ET(KK,I),EA(KK,I),KK=NDB,NDE)
      NDB=NDB+NDPL
      NDE=NDE+NDPL
90    CONTINUE
100   CONTINUE
C
C.....READ AND STORE CONTROL DATA FOR GENERATED DYNAMIC LOAD
C      ACCELEROGRAMS
C
      WRITE(61,2050)
      DO 110 KK=1,NEAG
      READ(60,1040) K,NIA(K),AAF(K),APS(K)
      WRITE(61,2060)K,NIA(K),AAF(K),APS(K)
110   CONTINUE
C
1000  FORMAT(10I5)
1010  FORMAT(5(F5.2,F10.4))
1020  FORMAT(3X,4(F8.0,F9.0))
1030  FORMAT(6(1X,F11.7))
1040  FORMAT(2I5,2F10.5)
1050  FORMAT(5F10.5,2(I5,F10.5))
C
2000  FORMAT('-',33HD Y N A M I C   L O A D   D A T A //)
2005  FORMAT('0',6HNEAI =,I3//1X,6HNEAG =,I3//1X,
+          3(4HNDP(,I1,3H) =,I4,10X)//1X,3(4HNLW(,I1,3H) =,I4,10X)//
+          1X,6HNDPL =,I3)
2010  FORMAT('1',42HD Y N A M I C   S O L U T I O N   D A T A //)
2015  FORMAT('0',7HALPHA =,F10.5//1X,6HBETA =,F10.5//1X,7HSIGMA =,
+          F10.5//1X,11HTIME STEP =,F10.5,7HSECONDS//1X,
+          21HTOTAL TIME DURATION =,F10.5,7HSECONDS)
2020  FORMAT('1',27HINITIAL DYNAMIC LOAD WINDOW//)
2040  FORMAT('0',25HDYNAMIC LOAD ACCELEROGRAM,I2//1X,10HDATA POINT,5X,
+          12HTIME,SECONDS,5X,14HACCELERATION,G)
2050  FORMAT('1',27HGENERATED DYNAMIC LOAD DATA//3X,9HGENERATED,9X,
+          5HINPUT,8X,12HACCELEROGRAM,5X,12HACCELEROGRAM/1X,
+          12HACCELEROGRAM,5X,12HACCELEROGRAM,7X,9HAMPLITUDE,10X,
+          5HPHASE/4X,6HNUMBER,11X,6HNUMBER,11X,6HFACTOR,12X,5HSHIFT)
2060  FORMAT('0',1X,I5,12X,I5,12X,F10.5,7X,F10.5)
2070  FORMAT('0',I5,10X,F10.5,10X,F10.5)
C
      RETURN
C
      END
C*****
C*****
C*****

```

A.1.7 PROGRAM TRUSSEL

The primary purposes of Program TRUSSEL are threefold. The first purpose is to calculate the entries in each truss element local stiffness matrix. The second purpose is to call the Subroutine TRANSFM to transform the local element stiffness matrices into global coordinates. Finally, the TRUSSEL program calls the Subroutine ASSEMBLE which assembles the global element stiffness matrices into the structure stiffness matrix. Program TRUSSEL also stores the local element stiffness matrices and the element transformation matrices on tapes for later use by the stress recovery subroutine.

The Common Block 7 variables are used by both Program TRUSSEL and Program SBEAMEL for transferring the local and global element stiffness matrices and to transfer the element transformation matrices. The following is a list of the Common Block 7 variables and their definitions:

VARIABLE NAME	DESCRIPTION
SE(I,J)	Entry I-J of the element stiffness matrix
T(I,J)	Entry I-J of the element transformation matrix

The miscellaneous variables used by the TRUSSEL program are as follows:

VARIABLE NAME	DESCRIPTION
K	Number of the truss element being processed
M	Variable denoting type of element to be transformed or assembled: 1 = truss 2 = straight beam element

Finally, the listing of Program TRUSSEL is as follows:

```

C*****
C*****
C*****
  OVERLAY(XFILE,1,7)
  PROGRAM TRUSSEL T6.FOR subroutine Trusse
C
C *****
C   TRUSS ELEMENT STIFFNESS MATRIX ASSEMBLY PROGRAM
C *****
C
  PARAMETER(J4=42,J5=14,J6=55,J7=0,J8=2,J9=34,J10=71,J11=99,
+           J12=101,J13=10)
  COMMON/CB1/NE,NUMNP,NUMEG,IPAR,ISTRESS,ICAL1,ICAL2,ICAL3,ICAL4,
+           ICAL5,ICAL6,ICAL7,ICAL8,LINEQL,IDATA
  COMMON/CB2/NSIZE,NEQ,NCOND,NGDOF,MBAND,MBAND1
  COMMON/CB3/IA(J4,7),IB(J4,7),IG(J4),X(J4),Y(J4),Z(J4),
+           NPRINT(J4)
  COMMON/CB4/E(2),P(2),NTYPE(2),NEPR(2),MPRINT(J6,2)
  COMMON/CB5/NITE(J5),NJTE(J5),ATE(J5),LE(J5),SCT(J5,2)
  COMMON/CB7/SE(16,16),T(14,14)
  REAL LE
C
C.....CALCULATE ELEMENT STIFFNESS MATRIX
C
  DO 700 K=1,NTYPE(1)
    LE(K)=SQRT((X(NJTE(K))-X(NITE(K)))**2.+(Y(NJTE(K))-Y(NITE(K)))**2.
+           +(Z(NJTE(K))-Z(NITE(K)))**2.)
    DO 400 I=1,14
      DO 300 J=1,14
        SE(I,J)=0.0
300    CONTINUE
400    CONTINUE
    SE(3,3)=SE(10,10)=E(1)*ATE(K)/LE(K)
    SE(3,10)=SE(10,3)=-SE(3,3)
    IF(MPRINT(K,1).NE.0) GO TO 407
    DO 405 I=1,14
      WRITE(1,2130) (SE(I,J),J=1,7)
405    WRITE(1,2130) (SE(I,J),J=8,14)
407    CONTINUE
    IF(ICAL2.NE.0) GO TO 420
    WRITE(61,2100) K
    DO 410 I=1,14
      WRITE(61,2110) I,(SE(I,J),J=1,14)
410    CONTINUE
420    CONTINUE
    M=1
C
C.....TRANSFORM INTO GLOBAL COORDINATES
C
    CALL XOVCAP ('TRANSFM',K,M)
    IF(MPRINT(K,1).NE.0) GO TO 597
    DO 595 I=1,14
      WRITE(2,2130) (T(I,J),J=1,7)
595    WRITE(2,2130) (T(I,J),J=8,14)

```

```

597  CONTINUE
      IF(ICAL2.NE.0) GO TO 650
      WRITE(61,2120) K
      DO 600 I=1,14
      WRITE(61,2110) I,(SE(I,J),J=1,14)
600  CONTINUE
650  CONTINUE
C
C.....ASSEMBLE INTO GLOBAL STIFFNESS MATRIX
C
      CALL XOVCAP ('ASEMBLE',K,M)
700  CONTINUE
C
      RETURN
C
2100  FORMAT('-',13HTRUSS ELEMENT,I4,23H LOCAL STIFFNESS MATRIX/1X,
      +      3HROW,3X,32HCOLUMNS 1 TO 7 / COLUMNS 8 TO 14)
2110  FORMAT(' ',I2,7E18.8/6X,7E18.8)
2120  FORMAT('-',13HTRUSS ELEMENT,I4,24H GLOBAL STIFFNESS MATRIX/1X,
      +      3HROW,3X,32HCOLUMNS 1 TO 7 / COLUMNS 8 TO 14)
2130  FORMAT(' ',7E18.8)
C
      END
C*****
C*****
C*****

```


A.1.8 PROGRAM SBEAMEL

The purposes of the SBEAMEL program are essentially the same as Program TRUSSEL: to calculate the entries of the local element stiffness matrices, to call Subroutine TRANSFM for coordinate transformation of the element stiffness matrices and to call Subroutine ASEMBLE for the assembly of the element stiffness matrices into the global stiffness matrix. Also as in the case of Program TRUSSEL, the SBEAMEL program transfers the local element stiffness matrices and the element transformation matrices via Common Block 7 and stores them on tapes for later use in stress recovery.

The miscellaneous variables used by the SBEAMEL program are as follows:

VARIABLE NAME	DESCRIPTION
K	Number of the straight beam element being processed
DUM(n)	Average stiffnesses for the current straight beam element being processed:
n=1	Axial area
n=2	Local x shear area
n=3	Local y shear area
n=4	Local x-x moment of inertia
n=5	Local y-y moment of inertia
n=6	Torsion constant
n=7	Warping constant
n=8	Effective member length with respect to local x-x bending and local y shear deformation
n=9	Effective member length with respect to local y-y bending and local x shear deformation
n=10	Effective member length with respect to warping and torsion

C1 to C11 Constants used in calculating current beam element stiffness

G Shear modulus

G1 Local x axis shear constant

G2 Local y axis shear constant

* from page 42 of Gere and Weaver (ref. 11)

Lastly, the following is a listing of the SBEAMEL program itself:

```

C*****
C*****
C*****
  OVERLAY(XFILE,1,10) (6 40)
  PROGRAM SBEAMEL beamse
C
C *****
C   STRAIGHT BEAM ELEMENT STIFFNESS MATRIX ASSEMBLY PROGRAM
C *****
C
  PARAMETER(J4=42,J5=14,J6=55,J7=0,J8=2,J9=34,J10=71,J11=99,
+           J12=101,J13=10)
  COMMON/CB1/NE,NUMNP,NUMEG,IPAR,ISTRESS,ICAL1,ICAL2,ICAL3,ICAL4,
+           ICAL5,ICAL6,ICAL7,ICAL8,LINEQL,DATA
  COMMON/CB2/NSIZE,NEQ,NCOND,NGDOF,MBAND,MBAND1
  COMMON/CB3/IA(J4,7),IB(J4,7),IG(J4),X(J4),Y(J4),Z(J4),
+           NPRINT(J4)
  COMMON/CB4/E(2),P(2),NTYPE(2),NEPR(2),MPRINT(J6,2)
  COMMON/CB6/NISB(J6),NJSB(J6),NKSJ(J6),NPCS(J6,3),ASB(J6),AGXS(J6),
+           AGYS(J6),IXXS(J6),IYYS(J6),KTS(J6),IWS(J6),LSB(J6),
+           SCS(J6,16),SES(16),FL(J6,3),ELX(J6),ELY(J6),ELW(J6)
  COMMON/CB7/SE(16,16),T(14,14)
  REAL IXXS,IYYS,KTS,IWS,LSB
  DIMENSION DUM(10)
C
C.....CALCULATE ELEMENT STIFFNESS MATRIX
C
  DO 990 K=1,NTYPE(2)
    LSB(K)=SQRT((X(NJSB(K))-X(NISB(K)))**2.
+           +(Y(NJSB(K))-Y(NISB(K)))**2.+(Z(NJSB(K))-Z(NISB(K)))**2.)
    DO 220 I=1,14
      DO 210 J=1,14
        SE(I,J)=0.0
210    CONTINUE
220    CONTINUE
C
C.....AVERAGE ELEMENT STIFFNESS PROPERTIES

```

```

C
DO 230 I=1,10
  DUM(I)=0.0
230 CONTINUE
  DO 240 I=1,3
    DUM(1)=DUM(1)+ASB(NPGS(K,I))*FL(K,I)
    DUM(2)=DUM(2)+AGXS(NPGS(K,I))*FL(K,I)
    DUM(3)=DUM(3)+AGYS(NPGS(K,I))*FL(K,I)
    DUM(4)=DUM(4)+IXXS(NPGS(K,I))*FL(K,I)
    DUM(5)=DUM(5)+IYYS(NPGS(K,I))*FL(K,I)
    DUM(6)=DUM(6)+KTS(NPGS(K,I))*FL(K,I)
    DUM(7)=DUM(7)+IWS(NPGS(K,I))*FL(K,I)
    DUM(8)=DUM(8)+ELX(NPGS(K,I))*FL(K,I)
    DUM(9)=DUM(9)+ELY(NPGS(K,I))*FL(K,I)
    DUM(10)=DUM(10)+ELW(NPGS(K,I))*FL(K,I)
240 CONTINUE
    IF(DUM(8).EQ.0.0) DUM(8)=LSB(K)
    IF(DUM(9).EQ.0.0) DUM(9)=LSB(K)
    IF(DUM(10).EQ.0.0) DUM(10)=LSB(K)

C
C.....CALCULATE AXIAL STIFFNESS COEFFICIENTS
C
  SE(3,3)=SE(10,10)=E(2)*DUM(1)/LSB(K)
  SE(3,10)=SE(10,3)=-SE(3,3)

C
C.....CALCULATE TORSION AND WARPING STIFFNESS COEFFICIENTS
C
  G=E(2)/(2.*(1.+P(2)))
  IF(DUM(7).EQ.0.0) GO TO 250
  C1=E(2)*DUM(7)/DUM(10)**3.0
  C2=G*DUM(6)/DUM(10)
  SE(4,4)=SE(11,11)=12.0*C1+36.0*C2/30.0
  SE(4,11)=SE(11,4)=-SE(4,4)
  SE(7,7)=SE(14,14)=(DUM(10)**2.0)*(4.0*C1+4.0*C2/30.0)
  SE(4,7)=SE(7,4)=SE(4,14)=SE(14,4)=DUM(10)*(6.0*C1+3.0*C2/30.0)
  SE(7,11)=SE(11,7)=SE(11,14)=SE(14,11)=-SE(4,7)
  SE(7,14)=SE(14,7)=(DUM(10)**2.0)*(2.0*C1-C2/30.0)
  GO TO 260
250 CONTINUE
  SE(4,4)=SE(11,11)=G*DUM(6)/DUM(10)
  SE(4,11)=SE(11,4)=-SE(4,4)
260 CONTINUE

C
C.....CALCULATE LOCAL X SHEAR AND LOCAL Y BENDING STIFFNESS
C      COEFFICIENTS
C
  IF(DUM(2).EQ.0.0) GO TO 270
  G1=6.0*E(2)*DUM(5)/(G*DUM(2)*(DUM(9)**2.0))
  C4=12.0*E(2)*DUM(5)/((DUM(9)**3.0)*(1.0+2.0*G1))
  C5=6.0*E(2)*DUM(5)/((DUM(9)**2.0)*(1.0+2.0*G1))
  C6=4.0*E(2)*DUM(5)*(1.0+G1/2.0)/(DUM(9)*(1.0+2.0*G1))
  C7=2.0*E(2)*DUM(5)*(1.0-G1)/(DUM(9)*(1.0+2.0*G1))
  GO TO 280
270 CONTINUE

```

```

C4=12.0*E(2)*DUM(5)/(DUM(9)**3.0)
C5=6.0*E(2)*DUM(5)/(DUM(9)**2.0)
C6=4.0*E(2)*DUM(5)/DUM(9)
C7=2.0*E(2)*DUM(5)/DUM(9)
280  CONTINUE
      SE(1,1)=SE(8,8)=C4
      SE(1,8)=SE(8,1)=-C4
      SE(1,5)=SE(5,1)=SE(1,12)=SE(12,1)=C5
      SE(8,5)=SE(5,8)=SE(8,12)=SE(12,8)=-C5
      SE(5,5)=SE(12,12)=C6
      SE(5,12)=SE(12,5)=C7
C
C.....CALCULATE LOCAL Y SHEAR AND LOCAL X BENDING STIFFNESS
C          COEFFICIENTS
C
      IF(DUM(3).EQ.0.) GO TO 290
      G2=6.0*E(2)*DUM(4)/(G*DUM(3)*(DUM(8)**2.0))
      C8=12.0*E(2)*DUM(4)/((DUM(8)**3.0)*(1.0+2.0*G2))
      C9=6.0*E(2)*DUM(4)/((DUM(8)**2.0)*(1.0+2.0*G2))
      C10=4.0*E(2)*DUM(4)*(1.0+G2/2.0)/(DUM(8)*(1.0+2.0*G2))
      C11=2.0*E(2)*DUM(4)*(1.0-G2)/(DUM(8)*(1.0+2.0*G2))
      GO TO 300
290  CONTINUE
      C8=12.0*E(2)*DUM(4)/(DUM(8)**3.0)
      C9=6.0*E(2)*DUM(4)/(DUM(8)**2.0)
      C10=4.0*E(2)*DUM(4)/DUM(8)
      C11=2.0*E(2)*DUM(4)/DUM(8)
300  CONTINUE
      SE(2,2)=SE(9,9)=C8
      SE(2,9)=SE(9,2)=-C8
      SE(2,6)=SE(6,2)=SE(2,13)=SE(13,2)=-C9
      SE(9,6)=SE(6,9)=SE(9,13)=SE(13,9)=C9
      SE(6,6)=SE(13,13)=C10
      SE(6,13)=SE(13,6)=C11
C
C.....PRINT ELEMENT STIFFNESS MATRIX
C
      IF(MPRINT(K,2).NE.0) GO TO 915
      DO 910 I=1,14
      WRITE(1,2190) (SE(I,J),J=1,7)
      WRITE(1,2190) (SE(I,J),J=8,14)
910  CONTINUE
915  CONTINUE
      IF(ICAL2.NE.0) GO TO 930
      WRITE(61,2160) K
      DO 920 I=1,14
      WRITE(61,2170) I,(SE(I,J),J=1,14)
920  CONTINUE
930  CONTINUE
      M=2
C
C.....TRANSFORM INTO GLOBAL COORDINATES
C
      CALL XOVCAP ('TRANSFM',K,M)

```

```

      IF(MPRINT(K,2).NE.0) GO TO 945
      DO 940 I=1,14
      WRITE(2,2190) (T(I,J),J=1,7)
      WRITE(2,2190) (T(I,J),J=8,14)
940   CONTINUE
945   CONTINUE
      IF(ICAL2.NE.0) GO TO 960
      WRITE(61,2180) K
      DO 950 I=1,14
      WRITE(61,2170) I,(SE(I,J),J=1,14)
950   CONTINUE
960   CONTINUE
      C
      C.....ASSEMBLE INTO GLOBAL STIFFNESS MATRIX
      C
      CALL XOVCAP ('ASEMBLE',K,M)
990   CONTINUE
      RETURN
      C
2160  FORMAT('-',21HSTRAIGHT BEAM ELEMENT,I4,23H LOCAL STIFFNESS MATRIX/
      +      1X,3HROW,3X,32HCOLUMNS 1 TO 7 / COLUMNS 8 TO 14)
2170  FORMAT('-',I2,7E18.8/6X,7E18.8)
2180  FORMAT('-',21HSTRAIGHT BEAM ELEMENT,I4,
      +      24H GLOBAL STIFFNESS MATRIX/1X,3HROW,3X,
      +      32HCOLUMNS 1 TO 7 / COLUMNS 8 TO 14)
2190  FORMAT('-',7E18.8)
      C
      END
C*****
C*****
C*****

```

A.1.9 PROGRAM CONDENS

The Program CONDENS serves to condense the structure stiffness matrix and load vector as discussed in Section 2.2.3. A listing of the miscellaneous Program CONDENS variables is as follows:

VARIABLE NAME	DESCRIPTION
KP	If ICAL3 = 0, then this variable is used to control printing of structure stiffness matrices: 1 = printing uncondensed matrices 2 = printing condensed matrices
K	Denotes total number of degrees of freedom condensed and currently being condensed
KK	Row number in original structure stiffness matrix of degree of freedom currently being condensed
KKC	Row number in -SC- matrix of degree of freedom currently being condensed
II	Number of first row and column of original structure stiffness matrix (with ground degrees of freedom less than or equal to 0)
LL	Number of last row and column of original structure stiffness matrix excluding degrees of freedom condensed or currently being condensed
NN	Column number in original structure stiffness matrix of entry currently being modified
NNC	Row number in -SC- matrix corresponding to column NN of original structure stiffness matrix
NNG	Row number in -SG- matrix corresponding to column NN of original structure stiffness matrix
J	Column number in banded format corresponding to row KK of original structure stiffness matrix
JJ	Column number in banded format corresponding to column NN of original structure stiffness matrix
MM	Row number in original structure stiffness matrix of entry currently being modified
MMC	Row number in -SC- matrix corresponding to row MM of original structure stiffness matrix

MMG Row number in -SG- matrix corresponding to row MM of
original structure stiffness matrix

K1, K2, K3 & M Variables used to count columns in the printing of the
structure stiffness matrices

DUM Dummy variable used to simplify condensation formulas

Finally, a listing of Program CONDENS is as follows:

```

C*****
C*****
C*****
  OVERLAY(XFILE,1,11)
  PROGRAM CONDENS T12 FOR conden
C
C *****
C   STRUCTURE STIFFNESS MATRIX AND LOAD VECTOR CONDENSATION
C   PROGRAM
C *****
C
  PARAMETER(J4=42,J5=14,J6=55,J7=0,J8=2,J9=34,J10=71,J11=99,
+           J12=101,J13=10)
  COMMON/CB1/NE,NUMNP,NUMEG,IPAR,ISTRESS,ICAL1,ICAL2,ICAL3,ICAL4,
+           ICAL5,ICAL6,ICAL7,ICAL8,LINEQL,IDATA
  COMMON/CB2/NSIZE,NEQ,NCOND,NGDOF,MBAND,MBAND1
  COMMON/CB8/PN(J4,6),R(J11)
  COMMON/CB9/S(J9,J11),SC(J10,J13),SG(J8,J12)
C
C.....WRITE UNCONDENSED STRUCTURE STIFFNESS MATRICES -S-, -SC- AND
C   -SG-
C
  KP=1
  GO TO 805
5   CONTINUE
  KP=2
C
C.....CONDENSE STRUCTURE STIFFNESS MATRIX AND LOAD VECTOR
C
  IF(NCOND.EQ.0) GO TO 900
  DO 120 K=1,NCOND
  LL=NSIZE-K
  KK=LL+1
  KKC=KK-NEQ
  II=1-NGDOF
  DO 110 NN=II,LL
  J=KK-NN+1
  IF(NN.LE.NEQ) GO TO 10
  IF(J.GT.MBAND1) GO TO 110
  NNC=NN-NEQ
  DUM=SC(NNC,J)/SC(KKC,1)
  GO TO 20
10  CONTINUE

```

```

      IF(NN.GT.0) GO TO 15
      NNG=NN+NGDOF
      DUM=SG(NNG,J)/SC(KKC,1)
      GO TO 20
15    CONTINUE
      IF(J.GT.MBAND) GO TO 110
      DUM=S(NN,J)/SC(KKC,1)
20    CONTINUE
      DO 100 MM=II,NN
      JJ=NN-MM+1
      J=KK-MM+1
      IF(MM.LE.NEQ) GO TO 30
      IF(J.GT.MBAND1) GO TO 100
      IF(JJ.GT.MBAND1) GO TO 100
      MMC=MM-NEQ
      SC(MMC,JJ)=SC(MMC,JJ)-SC(MMC,J)*DUM
      GO TO 100
30    CONTINUE
      IF(MM.GT.0) GO TO 35
      MMG=MM+NGDOF
      SG(MMG,JJ)=SG(MMG,JJ)-SG(MMG,J)*DUM
      GO TO 100
35    CONTINUE
      IF(J.GT.MBAND) GO TO 100
      IF(JJ.GT.MBAND) GO TO 100
      S(MM,JJ)=S(MM,JJ)-S(MM,J)*DUM
100   CONTINUE
      IF(LINEQL.EQ.1) R(NN)=R(NN)-R(KK)*DUM
110   CONTINUE
120   CONTINUE
C
C.....WRITE CONDENSED LOAD VECTOR -R-
C
      IF(ICAL4.NE.0) GO TO 800
      IF(LINEQL.NE.1) GO TO 800
      WRITE(61,2170)
      WRITE(61,2180) (I,R(I),I=1,NSIZE)
800   CONTINUE
C
C.....WRITE CONDENSED STRUCTURE STIFFNESS MATRICES -S-, -SC- AND -SG-
C
805   CONTINUE
      IF(ICAL3.NE.0) GO TO 900
      DO 895 K=1,3
      K1=1 ↓
      K2=8 6
      KK=K-2
      IF(KK) 810,820,830
810   CONTINUE
      M=MBAND
      IF(KP.EQ.1) WRITE(61,2005)
      IF(KP.EQ.2) WRITE(61,2010)
      GO TO 840
820   CONTINUE

```



```

      IF(NCOND.EQ.0) GO TO 895
      M=MBAND1
      IF(KP.EQ.1) WRITE(61,2015)
      IF(KP.EQ.2) WRITE(61,2020)
      GO TO 840
830  CONTINUE
      IF(NGDOF.EQ.0) GO TO 895
      M=NSIZE+NGDOF
      IF(KP.EQ.1) WRITE(61,2025)
      IF(KP.EQ.2) WRITE(61,2030)
840  CONTINUE
      K3=M-K1 5
      IF(K3.LE.7) GO TO 860
850  CONTINUE
      WRITE(61,2000) K1,K2
      IF(K.EQ.1) WRITE(61,2090) ((S(I,J),J=K1,K2),I=1,NEQ)
      IF(K.EQ.2) WRITE(61,2090) ((SC(I,J),J=K1,K2),I=1,NCOND)
      IF(K.EQ.3) WRITE(61,2090) ((SG(I,J),J=K1,K2),I=1,NGDOF)
      K1=K1+8
      K2=K2+8
      K3=M-K1 5
      IF(K3.GT.7) GO TO 850
860  CONTINUE
      WRITE(61,2000) K1,M
      IF(KK) 865,870,875
865  CONTINUE
      IF(K3.EQ.0) WRITE(61,2100) ((S(I,J),J=K1,M),I=1,NEQ)
      IF(K3.EQ.1) WRITE(61,2110) ((S(I,J),J=K1,M),I=1,NEQ)
      IF(K3.EQ.2) WRITE(61,2120) ((S(I,J),J=K1,M),I=1,NEQ)
      IF(K3.EQ.3) WRITE(61,2130) ((S(I,J),J=K1,M),I=1,NEQ)
      IF(K3.EQ.4) WRITE(61,2140) ((S(I,J),J=K1,M),I=1,NEQ)
      IF(K3.EQ.5) WRITE(61,2150) ((S(I,J),J=K1,M),I=1,NEQ)
      IF(K3.EQ.6) WRITE(61,2160) ((S(I,J),J=K1,M),I=1,NEQ)
      IF(K3.EQ.7) WRITE(61,2090) ((S(I,J),J=K1,M),I=1,NEQ)
      GO TO 895
870  CONTINUE
      IF(K3.EQ.0) WRITE(61,2100) ((SC(I,J),J=K1,M),I=1,NCOND)
      IF(K3.EQ.1) WRITE(61,2110) ((SC(I,J),J=K1,M),I=1,NCOND)
      IF(K3.EQ.2) WRITE(61,2120) ((SC(I,J),J=K1,M),I=1,NCOND)
      IF(K3.EQ.3) WRITE(61,2130) ((SC(I,J),J=K1,M),I=1,NCOND)
      IF(K3.EQ.4) WRITE(61,2140) ((SC(I,J),J=K1,M),I=1,NCOND)
      IF(K3.EQ.5) WRITE(61,2150) ((SC(I,J),J=K1,M),I=1,NCOND)
      IF(K3.EQ.6) WRITE(61,2160) ((SC(I,J),J=K1,M),I=1,NCOND)
      IF(K3.EQ.7) WRITE(61,2090) ((SC(I,J),J=K1,M),I=1,NCOND)
      GO TO 895
875  CONTINUE
      IF(K3.EQ.0) WRITE(61,2100) ((SG(I,J),J=K1,M),I=1,NGDOF)
      IF(K3.EQ.1) WRITE(61,2110) ((SG(I,J),J=K1,M),I=1,NGDOF)
      IF(K3.EQ.2) WRITE(61,2120) ((SG(I,J),J=K1,M),I=1,NGDOF)
      IF(K3.EQ.3) WRITE(61,2130) ((SG(I,J),J=K1,M),I=1,NGDOF)
      IF(K3.EQ.4) WRITE(61,2140) ((SG(I,J),J=K1,M),I=1,NGDOF)
      IF(K3.EQ.5) WRITE(61,2150) ((SG(I,J),J=K1,M),I=1,NGDOF)
      IF(K3.EQ.6) WRITE(61,2160) ((SG(I,J),J=K1,M),I=1,NGDOF)
      IF(K3.EQ.7) WRITE(61,2090) ((SG(I,J),J=K1,M),I=1,NGDOF)

```

```

895  CONTINUE
900  CONTINUE
    IF(KP.EQ.1) GO TO 5
C
2000 FORMAT('-',7HCOLUMNS,I4,8H THROUGH,I4)
2005 FORMAT('1',42HUNCONDENSED STRUCTURE STIFFNESS MATRIX -S-)
2010 FORMAT('1',40HCONDENSED STRUCTURE STIFFNESS MATRIX -S-)
2015 FORMAT('1',43HUNCONDENSED STRUCTURE STIFFNESS MATRIX -SC-)
2020 FORMAT('1',41HCONDENSED STRUCTURE STIFFNESS MATRIX -SC-)
2025 FORMAT('1',43HUNCONDENSED STRUCTURE STIFFNESS MATRIX -SG-)
2030 FORMAT('1',41HCONDENSED STRUCTURE STIFFNESS MATRIX -SG-)
2090 FORMAT('0',8E16.5)
2100 FORMAT('0',E16.5)
2110 FORMAT('0',2E16.5)
2120 FORMAT('0',3E16.5)
2130 FORMAT('0',4E16.5)
2140 FORMAT('0',5E16.5)
2150 FORMAT('0',6E16.5)
2160 FORMAT('0',7E16.5)
2170 FORMAT('1',25HCONDENSED LOAD VECTOR -R-//)
2180 FORMAT(' ',2HR(,I3,2H)=,F16.6)
C
    RETURN
C
    END
C*****
C*****
C*****

```

A.2 PROGRAM EIGEN

T13.FOR.
T14.FOR
Subroutine
235
EIGEN

The main purpose of Program EIGEN is to prepare the data for and call the Subroutine EIGENV which in turn calculates the structure mode shapes and frequencies as discussed in Section 2.5. The EIGEN program also calculates the damping coefficients Alpha and Beta as discussed in Section 2.1.3. While a listing of all of the variables used by Program EIGEN and Subroutine EIGENV are not presented, the following is a list of the miscellaneous variables used in calculating Alpha and Beta:

VARIABLE NAME	DESCRIPTION
DUM 1 and DUM2	Dummy variables used in searching for the largest modal periods
PERIOD(I)	Period of current mode shape being processed
PI	= 3.14159...
FREQ1 & FREQ2	Angular frequencies of calculated modes with largest and second largest period, respectively; or angular frequencies of MODE1 and MODE2, respectively
I1 & I2	Designates mode numbers which currently have largest and second largest periods, respectively: or designates MODE1 and MODE2, respectively

A listing of the Program EIGEN and Subroutine EIGENV is as follows:

```
C*****
C*****
C*****
  OVERLAY(XFILE,2,0)
  PROGRAM EIGEN
C
C  *****
C    TO SOLVE EIGENPROBLEM FOR MODE SHAPES AND FREQUENCIES
C    AND TO DERIVE DAMPING COEFFICIENTS -DALPHA- AND -DBETA-
C  *****
C
  PARAMETER(J4=42,J5=14,J6=55,J7=0,J8=2,J9=34,J10=71,J11=99,
+           J12=101,J13=10)
  COMMON/CB1/NE,NUMNP,NUMEG,IPAR,ISTRESS,ICAL1,ICAL2,ICAL3,ICAL4,
+           ICAL5,ICAL6,ICAL7,ICAL8,LINEQL
```

```

COMMON/CB2/NSIZE,NEQ,NCOND,NGDOF,MBAND,MBAND1
COMMON/CB8/PN(J4,6),R(J11)
COMMON/CB9/S(J9,J11),SC(J10,J13),SG(J8,J12)
COMMON/CB11/NDP(3),ET(40,3),EA(40,3),NIA(J8),AAF(J8),APS(J8),
+      NDPL,NLW(3),FORM,DALPHA,DBETA,DSIGMA,TS,TT,NEAI,NEAG,
+      MODE1,MODE2,DAMP1,DAMP2
COMMON/CB15/A(J9,J9),B(J9,J9),VALU(J9),N,M,IA
DIMENSION FQCY(J9),PERIOD(J9),D(J9,J9),X(J9,J9),Y(J9),C(J9,J9)

C
C.....SOLVE EIGENPROBLEM FOR FREQUENCIES AND MODE SHAPES
C
      IA=N=NEQ
      M=3

C
C.....INITIALIZE MASS MATRICES -A- AND -D-
C
      DO 2 I=1,NEQ
      DO 1 J=1,NEQ
      IF(I.EQ.J) A(I,J)=D(I,J)=R(I)
      IF(I.NE.J) A(I,J)=D(I,J)=0.0
1      CONTINUE
2      CONTINUE
C
C.....DIAGONALIZE MASS MATRIX -A-
C
      CALL EIGENV solution

C
C.....INITIALIZE STIFFNESS MATRIX -B-
C
      DO 5 I=1,NEQ
      DO 4 J=1,NEQ
      IF(J.GE.I) GO TO 3
      II=I-J+1
      IF(II.GT.MBAND) B(I,J)=0.0
      IF(II.LE.MBAND) B(I,J)=S(J,II)
      GO TO 4
3      CONTINUE
      JJ=J-I+1
      IF(JJ.GT.MBAND) B(I,J)=0.0
      IF(JJ.LE.MBAND) B(I,J)=S(I,JJ)
4      CONTINUE
5      CONTINUE
C
C.....PERFORM ORTHOGONAL TRANSFORMATION OF -B- WITH THE MODAL
C      MATRIX OF -A-
C
      DO 7 I=1,N
      DO 7 K=1,N
      SUM=0.
      DO 6 J=1,N
6      SUM=SUM+B(I,J)*A(J,K)
7      C(I,K)=SUM
      DO 9 K=1,N
      DO 9 I=1,N

```

```

      SUM=0.
      DO 8 J=1,N
      8 SUM=SUM+A(J,I)*C(J,K)
      9 B(I,K)=SUM
10  DO 11 I=1,N
      DO 11 J=1,N
      Y(I)=VALU(I)
      X(I,J)=A(I,J)
11  A(I,J)=B(I,J)/(ABS(SQRT(VALU(I)*VALU(J))))
      CALL EIGENV
      DO 13 I=1,N
      FQCY(I)=SQRT(VALU(I))/(2.*3.141592654)
      PERIOD(I)=1./FQCY(I)
13  CONTINUE
      DO 16 I=1,N
      DO 16 J=1,N
16  B(I,J)=A(I,J)/ABS(SQRT(Y(I)))
      DO 18 I=1,N
      DO 18 K=1,N
      SUM=0.
      DO 17 J=1,N
17  SUM=SUM+X(I,J)*B(J,K)
18  A(I,K)=SUM
C
C.....NORMALIZE EIGENVECTORS WITH RESPECT TO MATRIX A
C
      DO 23 K=1,N
      DO 20 I=1,N
      SUM=0.
      DO 19 J=1,N
19  SUM=SUM+D(I,J)*A(J,K)
20  B(I,K)=SUM
      DO 22 I=1,N
      SM=0.
      DO 21 J=1,N
21  SM=SM+A(J,K)*B(J,K)
22  X(I,K)=A(I,K)/SQRT(SM)
23  CONTINUE
C
C.....PRINT EIGENVALUES AND EIGENVECTORS
C
      WRITE(61,2000)
      DO 25 I=1,N
      WRITE(61,2010) I,VALU(I),FQCY(I),PERIOD(I)
25  CONTINUE
      IF(ICAL7.NE.0) GO TO 40
      DO 30 I=1,N
      WRITE(61,2020) I
      WRITE(61,2030) (X(K,I),K=1,N)
30  CONTINUE
40  CONTINUE
C
2000  FORMAT('1',17HEIGENVALUE NUMBER,9X,10HEIGENVALUE,10X,9HFREQUENCY,
+        12X,6HPERIOD//)

```

```

2010  FORMAT(' ',7X,I3,9X,3(3X,E17.10))
2020  FORMAT('0',11HEIGENVECTOR,1X,I3//)
2030  FORMAT(/1X,10E13.6)
C
      IF(LINEQL.EQ.2) GO TO 900
C
C.....CALCULATE DAMPING COEFFICIENTS -ALPHA- AND -BETA-
C
      IF(MODE1.GT.0) GO TO 150
C
C.....SEARCH FOR TWO LARGEST PERIODS
C
      DUM1=DUM2=0.0
      DO 100 I=1,NEQ
      IF(PERIOD(I).GT.DUM1) GO TO 90
      IF(PERIOD(I).GT.DUM2) GO TO 80
      GO TO 100
80    CONTINUE
      I2=I
      DUM2=PERIOD(I)
      GO TO 100
90    CONTINUE
      I2=I1
      DUM2=DUM1
      I1=I
      DUM1=PERIOD(I)
100   CONTINUE
C
C.....CALCULATE -ALPHA- AND -BETA-
C
      PI=4.*ATAN(1.)
      FREQ1=2.*PI/DUM1
      FREQ2=2.*PI/DUM2
      GO TO 200
150   CONTINUE
      I1=MODE1
      I2=MODE2
      PI=4.*ATAN(1.)
      FREQ1=2.*PI/PERIOD(I1)
      FREQ2=2.*PI/PERIOD(I2)
200   CONTINUE
      WRITE(61,2100) I1,FREQ1,I2,FREQ2
      DBETA=(2.*DAMP1-2.*DAMP2*FREQ2/FREQ1)/(FREQ1-(FREQ2**2.)/FREQ1)
      DALPHA=2.*DAMP2*FREQ2-(FREQ2**2.)*DBETA
      WRITE(61,2110) DALPHA,DBETA
C
2100  FORMAT('0',14HDAMPING MODES:,2X,2(4HMODE,I3,1X,13H(FREQUENCY = ,
+      F17.8,1X,9HRAD/SEC),))
2110  FORMAT('0',8HALPHA = ,F10.9,5X,7HBETA = ,F10.9)
C
900   CONTINUE
C
      RETURN
C

```

END

```

C*****
C*****
C*****
  SUBROUTINE EIGENV T 15. For
C
C *****
C   TO CALCULATE STRUCTURE EIGENVALUES AND EIGENVECTORS
C *****
C
  PARAMETER(J4=42,J5=14,J6=55,J7=0,J8=2,J9=34,J10=71,J11=99,
+           J12=101,J13=10)
  COMMON/CB15/A(J9,J9),B(J9,J9),VALU(J9),N,M,IA
  DIMENSION DIAG(J9),SUPERD(J9),Q(J9),VALL(J9),S(J9),C(J9),D(J9),
+           IND(J9),U(J9)
  DATA COS,SIN/0.0,0.0/
C
C   CALCULATE NORM OF MATRIX
C
  3 ANORM2=0.0
  4 DO 6 I=1,N
  5 DO 6 J=1,N
  6 ANORM2=ANORM2+A(I,J)**2
  7 ANORM=SQRT(ANORM2)
C
C   GENERATE IDENTITY MATRIX
C
  9 IF (M) 10, 45, 10
 10 DO 40 I=1,N
 12 DO 40 J=1,N
 20 IF(I-J) 35, 25, 35
 35 B(I,J)=0.0
 30 GO TO 40
 25 B(I,J)=1.0
 40 CONTINUE
C
C   PERFORM ROTATIONS TO REDUCE MATRIX TO JACOBI FORM
C
 45 IEXIT=1
 50 NN=N-2
 52 IF (NN) 890, 170, 55
 55 DO 160 I=1,NN
 60 II=I+2
 65 DO 160 J=II,N
 70 T1=A(I,I+1)
 75 T2=A(I,J)
 80 CONTINUE
   IF(T2.EQ.0) GO TO 160
   T=SQRT(T1**2+T2**2)
   COS=T1/T
   SIN=T2/T
 90 DO 105 K=I,N
 95 T2=COS*A(K,I+1)+SIN*A(K,J)
100 A(K,J)=COS*A(K,J)-SIN*A(K,I+1)

```

AC(1,2)
AC(1,2)

```

105 A(K,I+1)=T2
110 DO 125 K=I,N
115 T2=COS*A(I+1,K)+SIN*A(J,K)
120 A(J,K)=COS*A(J,K)-SIN*A(I+1,K)
125 A(I+1,K)=T2
128 IF (M) 130, 160, 130
130 DO 150 K=1,N
135 T2=COS*B(K,I+1)+SIN*B(K,J)
140 B(K,J)=COS*B(K,J)-SIN*B(K,I+1)
150 B(K,I+1)=T2
160 CONTINUE
C
C      MOVE JACOBI FORM ELEMENTS AND INITIALIZE EIGENVALUE BOUNDS
C
170 DO 200 I=1,N
180 DIAG(I)=A(I,I)
190 VALU(I)=ANORM
200 VALL(I)=-ANORM
210 DO 230 I=2,N
220 SUPERD(I-1)=A(I-1,I)
    SUPERD(N)=0.
230 Q(I-1)=(SUPERD(I-1))**2
C
C      DETERMINE SIGNS OF PRINCIPAL MINORS
C
235 TAU=0.0
240 I=1
260 MATCH=0
270 T2=0.0
275 T1=1.0
277 DO 450 J=1,N
280 P=DIAG(J)-TAU
290 IF(T2) 300, 330, 300
300 IF(T1) 310, 370, 310
310 T=P*T1-Q(J-1)*T2
320 GO TO 410
330 IF(T1) 335, 350, 350
335 T1=-1.0
340 T=-P
345 GO TO 410
350 T1=1.0
355 T=P
360 GO TO 410
370 IF(Q(J-1)) 380, 350, 380
380 IF(T2) 400, 390, 390
390 T=-1.0
395 GO TO 410
400 T=1.0
C
C      COUNT AGREEMENTS IN SIGN
C
410 IF(T1) 425, 420, 420
420 IF(T) 440, 430, 430
425 IF(T) 430, 440, 440

```



```

430 MATCH=MATCH+1
440 T2=T1
450 T1=T
C
C     ESTABLISH TIGHTER BOUNDS ON EIGENVALUES
C
460 DO 530 K=1,N
465 IF (K-MATCH) 470, 470, 520
470 IF(TAU-VALL(K)) 530, 530, 480
480 VALL(K)=TAU
490 GO TO 530
520 IF(TAU-VALU(K)) 525, 530, 530
525 VALU(K)=TAU
530 CONTINUE
540 IF(VALU(I)-VALL(I)-5.0E-8) 570, 570, 550
550 IF(VALU(I)) 560, 580, 560
560 IF(ABS(VALL(I)/VALU(I)-1.0)-5.0E-8) 570, 570, 580
570 I=I+1
575 IF(I-N) 540, 540, 590
580 TAU=(VALL(I)+VALU(I))/2.0
585 GO TO 260
C
C     JACOBI EIGENVECTORS BY ROTATIONAL TRIANGULARIZATION
C
590 IF (M) 593, 890, 593
593 IEXIT=2
595 DO 610 I=1,N
600 DO 610 J=1,N
610 A(I,J)=0.0
    BETA=0.
615 DO 850 I=1,N
620 IF (I-1) 625, 625, 621
621 IF (VALU(I-1)-VALU(I)-5.0E-7) 730, 730, 622
622 IF (VALU(I-1)) 623, 625, 623
623 IF (ABS(VALU(I)/VALU(I-1)-1.0)-5.0E-7) 730, 730, 625
625 COS=1.0
628 SIN=0.0
630 DO 700 J=1,N
635 IF(J-1) 680, 680, 640
640 CONTINUE
    T=SQRT(T1**2+T2**2)
    COS=T1/T
    SIN=T2/T
650 S(J-1)=SIN
660 C(J-1)=COS
670 D(J-1)=T1*COS+T2*SIN
680 T1=(DIAG(J)-VALU(I))*COS-BETA*SIN
690 T2=UPERD(J)
700 BETA=UPERD(J)*COS
710 D(N)=T1
720 DO 725 J=1,N
725 IND(J)=0
730 SMALLD=ANORM
735 DO 780 J=1,N

```

```

740 IF (IND(J)-1) 750, 780, 780
750 IF (ABS(SMALLD)-ABS(D(J)))780, 780, 760
760 SMALLD=D(J)
770 NN=J
780 CONTINUE
790 IND(NN)=1
800 PRODS=1.0
805 IF (NN-1) 810, 850, 810
810 DO 840 K=2,NN
820 II=NN+1-K
830 A(II+1,I)=C(II)*PRODS
840 PRODS=-PRODS*S(II)
850 A(1,I)=PRODS
C
C   FORM MATRIX PRODUCT OF ROTATION MATRIX WITH JACOBI VECTOR MATRIX
C
855 DO 885 J=1,N
860 DO 865 K=1,N
865 U(K)=A(K,J)
870 DO 885 I=1,N
875 A(I,J)=0.0
880 DO 885 K=1,N
885 A(I,J)=B(I,K)*U(K)+A(I,J)
890 CONTINUE
C
C   RETURN
C
C   END
C*****
C*****
C*****

```

A.3 PROGRAM STATDYN

The sole purpose of Program STATDYN is to call the appropriate secondary overlays for static or dynamic analyses. For static analyses, the secondary overlay Program LINSOLN is called. For dynamic analyses, the secondary overlays Program DYNINIT and Program DYN SOLN are called in that order. The following is a listing of Program STATDYN:

```

C*****
C*****
C*****
  OVERLAY(XFILE,3,0)
  PROGRAM STATDYN
C
C *****
C   LINEAR STATIC OR DYNAMIC SOLUTION PROGRAM
C *****
C
  PARAMETER(J4=42,J5=14,J6=55,J7=0,J8=2,J9=34,J10=71,J11=99,
+           J12=101,J13=10)
  COMMON/CB1/NE,NUMNP,NUMEG,IPAR,ISTRESS,ICAL1,ICAL2,ICAL3,ICAL4,
+          ICAL5,ICAL6,ICAL7,ICAL8,LINEQL,IDATA
  COMMON/CB13/BG(J9,J8),A(J9),V(J9),A0(J9),V0(J9),D0(J9),AG(J8),
+          RE(J9),DV(J9),MLDP(J8),LDP(J8),AG0(J8),VG0(J8),
+          ETB(J8),NDPW(3),TTT(J8),KE(J9,J9),T0,TE,C3,C4,C5,C6,
+          C7,C8,C9,C10,C11,C12,C13,VG(J8),DGO(J8),NCOUNT
  REAL KE
  IF(LINEQL.NE.1) GO TO 10
C
C.....STATIC SOLUTION PROGRAM
C
  IPAR=2
  CALL OVERLAY(5HXFILE,3,1,0)
  GO TO 30
10  CONTINUE
C
C.....DYNAMIC SOLUTION PROGRAM
C
  IPAR=3
  CALL OVERLAY(5HXFILE,3,2,0)
  CALL OVERLAY(5HXFILE,3,3,0)
30  CONTINUE
C
  RETURN
C
  END
C*****
C*****
C*****

```

A.3.1 PROGRAM LINSOLN

The principal purposes of the LINSOLN program are to prepare data for and call the Subroutine INVERSE and then to calculate the structure displacements and call the Subroutines RECOVER, DISPL and STRESS. Program LINSOLN first copies the structure stiffness matrix array S which is in banded format into the array KK which is in standard matrix format. The LINSOLN program then calls the INVERSE subroutine which inverts the stiffness matrix. Next, Program LINSOLN uses the inverted stiffness matrix to calculate the structure displacements as discussed in Section 2.5. Finally, the LINSOLN program calls the subroutines RECOVER, DISPL and STRESS which recover the condensed degrees of freedom, derive the nodal displacements and calculate the element stresses, respectively.

Since the array D which is calculated by Program LINSOLN is contained in Common Block 10, the variables in Common Block 10 and their definitions are listed below:

VARIABLE NAME	DESCRIPTION
D(I)	Ith entry in structure displacement vector
DG(I)	Ith entry in ground displacement vector
U(N,I)	Global displacement of node N in the Ith direction.

A list of the miscellaneous variables used by the LINSOLN program and by the Subroutine INVERSE is as follows:

VARIABLE NAME	DESCRIPTION
KK(I,J)	Matrices used by Program LINSOLN: Before INVERSE is called = I-J entry in structure stiffness matrix After INVERSE is called = I-J entry in inverse of structure stiffness matrix

II	Column in matrix -S- corresponding to row I in matrix -KK-
JJ	Column in matrix -S- corresponding to column J in matrix -KK-
DUM	Dummy variable used in calculating the entries in the structure displacement vector -D-
K(I,J)	Matrices used by Subroutine INVERSE: Before inversion = I-J entry of matrix to be inverted After inversion = I-J entry of matrix inverse
N	Size of matrix -KK- or -K-
I	Number of column currently being reduced
L	Row number of entry currently being processed
J	Column number of entry currently being processed
KK	Current diagonal entry of column being reduced
M	Variable defined as follows: During reduction, M = first row number to be processed in column currently being reduced (forward or backward) After reduction, M = column number of first entry to be replaced in filling in current upper triangle row I
LL	Current row L entry of column being reduced
NN	Number of rows in upper triangle to be filled in

Lastly, the following is a listing of Program LINSOLN and

Subroutine INVERSE:

```

C*****
C*****
C*****
  OVERLAY(XFILE,3,1)
  PROGRAM LINSOLN
C
C  *****
C    TO SOLVE SYSTEM OF LINEAR EQUATIONS S*D=R BY CALLING THE
C    SUBROUTINE -INVERSE-
C  *****
C
  PARAMETER(J4=42,J5=14,J6=55,J7=0,J8=2,J9=34,J10=71,J11=99,
```

```

+          J12=101,J13=10)
COMMON/CB2/NSIZE,NEQ,NCOND,NGDOF,MBAND,MBAND1
COMMON/CB8/PN(J4,6),R(J11)
COMMON/CB9/S(J9,J11),SC(J10,J13),SG(J8,J12)
COMMON/CB10/D(J11),DG(J8),U(J4,7)
REAL KK(J9,J9)

C
C
C.....INITIALIZE MATRIX -KK-
C
      DO 25 I=1,NEQ
      DO 20 J=1,NEQ
      IF(J.GE.I) GO TO 10
      II=I-J+1
      IF(II.GT.MBAND) KK(I,J)=0.0
      IF(II.LE.MBAND) KK(I,J)=S(J,II)
      GO TO 20
10    CONTINUE
      JJ=J-I+1
      IF(JJ.GT.MBAND) KK(I,J)=0.0
      IF(JJ.LE.MBAND) KK(I,J)=S(I,JJ)
20    CONTINUE
25    CONTINUE
C
C.....CALL MATRIX INVERSION SUBROUTINE
C
      CALL INVERSE(NEQ,KK)
C
C.....CALCULATE STRUCTURE DISPLACEMENTS
C
      DO 40 I=1,NEQ
      DUM=0.0
      DO 30 J=1,NEQ
      DUM=KK(I,J)*R(J)+DUM
30    CONTINUE
      D(I)=DUM
40    CONTINUE
C
C.....RECOVER CONDENSED DEGREES OF FREEDOM
C
      CALL XOVCAP ('RECOVER')
      CALL UOVCAP ('RECOVER')
C
C.....IDENTIFY DISPLACEMENTS FOUND FROM SOLUTION OF S*D=R
C
      CALL XOVCAP ('DISPL')
      CALL UOVCAP ('DISPL')
C
C.....COMPUTE NODAL FORCES AND STRESSES DUE TO LINEAR DISPLACEMENTS
C
      IF(ISTRESS.EQ.0) GO TO 900
      CALL XOVCAP ('STRESS')
      CALL UOVCAP ('STRESS')
900  CONTINUE

```

```

C
    RETURN
C
    END
C*****
C*****
C*****
    SUBROUTINE INVERSE(N,K)
C
C    *****
C    MATRIX INVERSION SUBROUTINE FOR AN -N- BY -N- MATRIX -K-
C    *****
C
    PARAMETER(J4=42,J5=14,J6=55,J7=0,J8=2,J9=34,J10=71,J11=99,
+             J12=101,J13=10)
    REAL KK,LL, K(J9,J9)
C
C.....FORWARD REDUCTION
C
    DO 400 I=1,N
        KK=K(I,I)
        K(I,I)=1.0
        DO 100 J=1,N
            K(I,J)=K(I,J)/KK
100    CONTINUE
        IF(I.EQ.N) GO TO 500
        M=I+1
        DO 300 L=M,N
            LL=K(L,I)
            DO 200 J=1,N
                IF(J.NE.I) K(L,J)=K(L,J)-LL*K(I,J)
                IF(J.EQ.I) K(L,J)=-LL*K(I,J)
200    CONTINUE
300    CONTINUE
400    CONTINUE
500    CONTINUE
C
C.....BACKWARD REDUCTION
C
    IF(N.EQ.1) GO TO 1200
    DO 900 I=N,2,-1
        M=I-1
        DO 800 L=M,1,-1
            DO 700 J=1,L
                K(L,J)=K(L,J)-K(I,J)*K(L,I)
700    CONTINUE
800    CONTINUE
900    CONTINUE
C
C.....FILL IN UPPER RIGHT TRIANGLE
C
    NN=N-1
    DO 1100 I=1,NN
        M=I+1

```

```
      DO 1000 J=M,N
      K(I,J)=K(J,I)
1000  CONTINUE
1100  CONTINUE
1200  CONTINUE
C
      RETURN
C
      END
C*****
C*****
C*****
```


A.3.2 PROGRAM DYNINIT

The main task of Program DYNINIT is to initialize the various arrays and variables used by the Program DYN SOLN. This initialization requires matrix inversion, therefore the INVERSE subroutine is also included in the Program DYNINIT overlay. The DYNINIT program was written so that the actual solution overlay which is Program DYN SOLN could be as short as possible. Since Program DYN SOLN would be the secondary overlay which would occupy the core memory longest during a dynamic analysis, it was necessary to make it as short as possible.

Common Block 13 provides the means by which the initialized variables are transferred from Program DYNINIT to Program DYN SOLN. A listing of the Common Block 13 variables is as follows:

VARIABLE NAME	DESCRIPTION
<hr/>	
BG(I,J)	I-J entry of matrix $BG = K_{11}^{-1} * K_{10}$
A(I)	Ith entry in current acceleration vector
V(I)	Ith entry in current velocity vector
A0(I)	Ith entry in previous acceleration vector
V0(I)	Ith entry in previous velocity vector
D0(I)	Ith entry in previous displacement vector
AG(I)	Ith entry in current ground acceleration vector
RE(I)	Ith entry in current equivalent force vector
DV(I)	Ith entry in dummy vector used in calculating -RE-
MLDP(I)	Maximum allowable value of LDP(I) for current accelerogram window
LDP(I)	Data point immediately left of accelerogram time AT (defined as current time T minus phase shift of generated accelerogram I)
AG0(I)	Ith entry in previous ground acceleration vector

VG0(I)	Ith entry in previous ground velocity vector
ETB(I)	Time associated with the first non-zero data point of generated accelerogram I
NDPW(I)	Total number of data points in the window for input accelerogram I
TTT(I)	Time associated with the second non-zero data point of generated accelerogram I
KE(I,J)	Dynamic stiffness matrices: Before inversion of structure stiffness matrix = I-J entry of structure stiffness matrix After inversion = I-J entry of inverse of structure stiffness matrix Before inversion of effective stiffness matrix = I-J entry of matrix Ke After inversion = I-J entry of matrix Ke inverse
T0	Initial time for dynamic loading
TE	End time for dynamic loading
C3 to C8	Constants used in calculating vector -RE-
C9 to C13	Constants used in calculating vectors -V- and -A-
VG(I)	Ith entry in current ground velocity vector
DG0(I)	Ith entry in previous ground displacement vector
NCOUNT	Variable used to determine when results should be printed

A list of the miscellaneous variables used by the DYNINIT program is as follows:

VARIABLE NAME	DESCRIPTION
II and JJ	Row and column number, respectively, in banded format of current entry of matrix -S-, used in converting -S- to unbanded format and in deriving matrix -Ke-
L	Column number in banded format of entry of matrix -SC- currently being processed
C1 and C2	Multipliers of -M11- and -K11- matrices, respectively, used in the formulation of Ke matrix

K	Distance from diagonal of current entry being processed, used in calculating Ke matrix
NA	Generated accelerogram number
DUM	Dummy variable used in calculating matrix -BG-

Finally, the following is a listing of Program DYNINIT and

Subroutine INVERSE:

```

C*****
C*****
C*****
  OVERLAY(XFILE,3,2)
  PROGRAM DYNINIT
C
C *****
C   DYNAMIC VARIABLE INITIALIZATION PROGRAM
C *****
C
  PARAMETER(J4=42,J5=14,J6=55,J7=0,J8=2,J9=34,J10=71,J11=99,
+           J12=101,J13=10)
  COMMON/CB2/NSIZE,NEQ,NCOND,NGDOF,MBAND,MBAND1
  COMMON/CB8/PN(J4,6),R(J11)
  COMMON/CB9/S(J9,J11),SC(J10,J13),SG(J8,J12)
  COMMON/CB10/D(J11),DG(J8),U(J4,7)
  COMMON/CB11/NDP(3),ET(40,3),EA(40,3),NIA(J8),AAF(J8),APS(J8),
+       NDPL,NLW(3),FMT,DALPHA,DBETA,DSIGMA,TS,TT,NEAI,NEAG,
+       MODE1,MODE2,DAMP1,DAMP2
  COMMON/CB13/BG(J9,J8),A(J9),V(J9),A0(J9),V0(J9),D0(J9),AG(J8),
+       RE(J9),DV(J9),MLDP(J8),LDP(J8),AG0(J8),VG0(J8),
+       ETB(J8),NDPW(3),TTT(J8),KE(J9,J9),T0,TE,C3,C4,C5,C6,
+       C7,C8,C9,C10,C11,C12,C13,VG(J8),DG0(J8),NCOUNT
  INTEGER FMT
  REAL KE
C
C.....INVERT CONDENSED STRUCTURE STIFFNESS MATRIX -S-
C
  DO 25 I=1,NEQ
  DO 20 J=1,NEQ
  IF(J.GE.I) GO TO 10
  II=I-J+1
  IF(II.GT.MBAND) KE(I,J)=0.0
  IF(II.LE.MBAND) KE(I,J)=S(J,II)
  GO TO 20
10  CONTINUE
  JJ=J-I+1
  IF(JJ.GT.MBAND) KE(I,J)=0.0
  IF(JJ.LE.MBAND) KE(I,J)=S(I,JJ)
20  CONTINUE
25  CONTINUE

```

```

      CALL INVERSE(NEQ,KE)
C
C.....CALCULATE MATRIX -BG-
C
      DO 50 K=1,NGDOF
      DO 40 I=1,NEQ
      DUM=0.0
      DO 30 J=1,NEQ
      L=J+NGDOF+1-K
      DUM=DUM+KE(I,J)*SG(K,L)
30    CONTINUE
      BG(I,K)=DUM
40    CONTINUE
50    CONTINUE
C
C.....CALCULATE MATRIX -KE- AND INVERT
C
      C1=1.0/(DSIGMA*TS**2.0) +DALPHA/(2.0*DSIGMA*TS)
      C2=1.0+DBETA/(2.0*DSIGMA*TS)
      DO 95 I=1,NEQ
      DO 90 J=1,NEQ
      K=J-I
      IF(K) 60,70,80
60    CONTINUE
      II=I-J+1
      IF(II.GT.MBAND) KE(I,J)=0.0
      IF(II.LE.MBAND) KE(I,J)=S(J,II)*C2
      GO TO 90
70    CONTINUE
      KE(I,J)=S(I,1)*C2+R(I)*C1
      GO TO 90
80    CONTINUE
      JJ=J-I+1
      IF(JJ.GT.MBAND) KE(I,J)=0.0
      IF(JJ.LE.MBAND) KE(I,J)=S(I,JJ)*C2
90    CONTINUE
95    CONTINUE
      CALL INVERSE(NEQ,KE)
C
C.....INITIALIZE VARIABLES AND CONSTANTS
C
      DO 100 NA=1,NEAG
      LDP(NA)=1
      AG(NA)=VG(NA)=DG(NA)=VG0(NA)=DG0(NA)=AG0(NA)=0.0
      ETB(NA)=ET(1,NIA(NA))
      MLDP(NA)=NLW(NIA(NA))*NDPL-1
      TTT(NA)=ETB(NA)+TS
100   CONTINUE
      DO 105 N=1,NEAI
      NDPW(N)=NLW(N)*NDPL
105   CONTINUE
      IF(NEAI.EQ.1) T0=ET(1,1)
      IF(NEAI.EQ.2) T0=MIN(ET(1,1),ET(1,2))
      IF(NEAI.EQ.3) T0=MIN(ET(1,1),ET(1,2),ET(1,3))

```

```

      TE=T0+TT
      DO 110 N=1,NEQ
      A(N)=V(N)=D(N)=A0(N)=V0(N)=D0(N)=0.0
110  CONTINUE
      C3=DALPHA/(2.*DSIGMA*TS)+1./(DSIGMA*TS**2.)
      C4=DALPHA*(1./(2.*DSIGMA)-1.)+1./(DSIGMA*TS)
      C5=DALPHA*TS*(1./(2.*DSIGMA)-2.)/2.+1./(2.*DSIGMA)-1.
      C6=DBETA/(2.*DSIGMA*TS)
      C7=DBETA*(1./(2.*DSIGMA)-1.)
      C8=DBETA*TS*(1./(2.*DSIGMA)-2.)/2.
      C9=1./(2.*DSIGMA*TS)
      C10=(1.-1./(2.*DSIGMA))
      C11=(2.-1./(2.*DSIGMA))*TS/2.
      C12=1./(DSIGMA*TS**2.)
      C13=1./(DSIGMA*TS)
      NCOUNT=-1
C
      RETURN
C
      END
C*****
C*****
C*****
      SUBROUTINE INVERSE(N,K)
C
C      *****
C      MATRIX INVERSION SUBROUTINE FOR AN -N- BY -N- MATRIX -K-
C      *****
C
      PARAMETER(J4=42,J5=14,J6=55,J7=0,J8=2,J9=34,J10=71,J11=99,
+             J12=101,J13=10)
      REAL KK,LL, K(J9,J9)
C
C.....FORWARD REDUCTION
C
      DO 400 I=1,N
      KK=K(I,I)
      K(I,I)=1.0
      DO 100 J=1,N
      K(I,J)=K(I,J)/KK
100  CONTINUE
      IF(I.EQ.N) GO TO 500
      M=I+1
      DO 300 L=M,N
      LL=K(L,I)
      DO 200 J=1,N
      IF(J.NE.I) K(L,J)=K(L,J)-LL*K(I,J)
      IF(J.EQ.I) K(L,J)=-LL*K(I,J)
200  CONTINUE
300  CONTINUE
400  CONTINUE
500  CONTINUE
C
C.....BACKWARD REDUCTION

```

```

C      IF(N.EQ.1) GO TO 1200
      DO 900 I=N,2,-1
      M=I-1
      DO 800 L=M,1,-1
      DO 700 J=1,L
      K(L,J)=K(L,J)-K(I,J)*K(L,I)
700    CONTINUE
800    CONTINUE
900    CONTINUE
C
C.....FILL IN UPPER RIGHT TRIANGLE
C
      NN=N-1
      DO 1100 I=1,NN
      M=I+1
      DO 1000 J=M,N
      K(I,J)=K(J,I)
1000   CONTINUE
1100   CONTINUE
1200   CONTINUE
C
      RETURN
C
      END
C*****
C*****
C*****

```

A.3.3 PROGRAM DYN SOLN

Program DYN SOLN performs the actual dynamic analysis as described in Sections 2.1.1 and 2.1.2. After every n th time step, the DYN SOLN program calls the subroutines RECOVER, DISPL and STRESS which recover the condensed degrees of freedom, derive the nodal displacements and calculate the element stresses, respectively.

As discussed in Section A.1.6, the ground acceleration windows are periodically updated as the dynamic solution progresses. This updating requires the reading from tape of the next portion of the ground acceleration history. The variables which are read are as follows:

LINE NAME	NUMBER OF LINES	VARIABLE NAME	FROM COLUMN	TO COLUMN
Dynload Data	varies	ET(J,I)*	varies	varies
		EA(J,I)	varies	varies

* omitted if ground acceleration history time increments are uniform

The Common Block 13 variables which are used by the DYN SOLN program have already been discussed in Section A.3.2. The following are the miscellaneous variables which are used by the DYN SOLN program:

VARIABLE NAME	DESCRIPTION
KK	Current ground acceleration history data point number
KKT	Previous ground acceleration history data point number, used only for generating data point times for CALTECH accelerograms
T	Current time
NA	Generated accelerogram number
AT	Accelerogram time defined as current time minus phase shift of current generated accelerogram

NR and NL	Numbers of the data points with times immediately right and left, respectively, of time AT
NDB	Window data point number associated with data point 1 of the current line of input
NDE	Window data point number associated with data point NDPL of the current line of input
MM	Previous window data point number associated with current entry being processed
DT	Difference in time between: data points NR and NL, or between the current time and previous time
DA	Difference in acceleration between NR and NL
NN	Number of data points to be renamed in moving previous accelerogram window to new accelerogram window
NRT	Number of the tape from which the current input accelerogram is to be read
DUM	Dummy variable used repeatedly in calculating: matrix -RE- and vector -D-

Finally, the listing of Program DYN SOLN which is as follows:

```

C*****
C*****
C*****
  OVERLAY(XFILE,3,3)
  PROGRAM DYN SOLN
C
C *****
C   DYNAMIC TIME STEP SOLUTION PROGRAM
C *****
C
  PARAMETER(J4=42,J5=14,J6=55,J7=0,J8=2,J9=34,J10=71,J11=99,
+           J12=101,J13=10)
  COMMON/CB1/NE,NUMNP,NUMEG,IPAR,ISTRESS,ICAL1,ICAL2,ICAL3,ICAL4,
+           ICAL5,ICAL6,ICAL7,ICAL8,LINEQL,IDATA
  COMMON/CB2/NSIZE,NEQ,NCOND,NGDOF,MBAND,MBAND1
  COMMON/CB8/PN(J4,6),R(J11)
  COMMON/CB9/S(J9,J11),SC(J10,J13),SG(J8,J12)
  COMMON/CB10/D(J11),DG(J8),U(J4,7)
  COMMON/CB11/NDP(3),ET(40,3),EA(40,3),NIA(J8),AAF(J8),APS(J8),
+           NDPL,NLW(3),FMT,DALPHA,DBETA,DSIGMA,TS,TT,NEAI,NEAG,
+           MODEL,MODE2,DAMP1,DAMP2
  COMMON/CB13/BG(J9,J8),A(J9),V(J9),AO(J9),VO(J9),DO(J9),AG(J8),
+           RE(J9),DV(J9),MLDP(J8),LDP(J8),AG0(J8),VG0(J8),
+           ETB(J8),NDPW(3),TTT(J8),KE(J9,J9),T0,TE,C3,C4,C5,C6,

```



```

+          C7,C8,C9,C10,C11,C12,C13,VG(J8),DGO(J8),NCOUNT
  INTEGER FMT
  REAL KE
C
C.....LOAD SUBROUTINES INVERSE, RECOVER, DISPL AND STRESS
C
  CALL LOVCAP ('RECOVER')
  CALL LOVCAP ('DISPL')
  CALL LOVCAP ('STRESS')
C
C.....BEGIN TIME STEPS AND CALCULATE CURRENT GROUND MOTIONS
C
  DO 900 T=T0,TE,TS
  DO 300 NA=1,NEAG
  AT=T-APS(NA)
  IF(AT.LT.ETB(NA)) GO TO 300
120  CONTINUE
  IF(AT.LT.ET(NDPW(NIA(NA)),NIA(NA))) GO TO 180
  NN=NDPW(NIA(NA))-NDPL
  DO 130 I=1,NN
  MM=I+NDPL
  EA(I,NIA(NA))=EA(MM,NIA(NA))
  ET(I,NIA(NA))=ET(MM,NIA(NA))
130  CONTINUE
  NRT=10+NIA(NA)
  NDB=NN+1
  NDE=NN+NDPL
  IF(FMT.NE.1) GO TO 132
  READ(NRT,1010) (ET(KK,NIA(NA)),EA(KK,NIA(NA)),KK=NDB,NDE)
132  CONTINUE
  IF(FMT.NE.2) GO TO 135
  READ(NRT,1020) (ET(KK,NIA(NA)),EA(KK,NIA(NA)),KK=NDB,NDE)
135  CONTINUE
  IF(FMT.NE.3) GO TO 137
  READ(NRT,1030) (EA(KK,NIA(NA)),KK=NDB,NDE)
  DO 136 KK=NDB,NDE
  KKT=KK-1
  ET(KK,NIA(NA))=ET(KKT,NIA(NA))+0.025
136  CONTINUE
137  CONTINUE
  DO 140 I=1,NEAG
  IF(NIA(I).NE.NIA(NA)) GO TO 140
  LDP(I)=LDP(I)-NDPL
140  CONTINUE
  GO TO 120
180  CONTINUE
  DO 250 NL=LDP(NA),MLDP(NA)
  NR=NL+1
  IF(AT.GE.ET(NR,NIA(NA))) GO TO 250
  IF(AT.LT.TTT(NA)) AGO(NA)=EA(1,NIA(NA))*AAF(NA)
  IF(AT.GE.TTT(NA)) AGO(NA)=AG(NA)
  VGO(NA)=VG(NA)
  DGO(NA)=DG(NA)
  DT=ET(NR,NIA(NA))-ET(NL,NIA(NA))

```

```

DA=EA(NR,NIA(NA))-EA(NL,NIA(NA))
AG(NA)=(EA(NL,NIA(NA))+(AT-ET(NL,NIA(NA))))*DA/DT)*AAF(NA)
IF(AT.LT.TTT(NA)) DT=AT-ETB(NA)
IF(AT.GE.TTT(NA)) DT=TS
VG(NA)=VG0(NA)+(AG0(NA)+AG(NA))*DT/2.
DG(NA)=DG0(NA)+(VG0(NA)+VG(NA))*DT/2.
LDP(NA)=NL
GO TO 300
250 CONTINUE
300 CONTINUE
C
C.....CALCULATE VECTOR -RE-
C
DO 720 I=1,NEQ
DUM=0.0
DO 710 J=1,NEAG
DUM=DUM+BG(I,J)*AG(J)
710 CONTINUE
IF(T.NE.T0) GO TO 715
A0(I)=DUM
GO TO 720
715 CONTINUE
RE(I)=(DUM+C3*D0(I)+C4*V0(I)+C5*A0(I))*R(I)
720 CONTINUE
IF(T.EQ.T0) GO TO 895
DO 730 I=1,NEQ
DV(I)=C6*D0(I)+C7*V0(I)+C8*A0(I)
730 CONTINUE
DO 760 I=1,NEQ
DUM=0.0
DO 750 J=1,NEQ
IF(J.LT.I) GO TO 740
JJ=J-I+1
IF(JJ.GT.MBAND) GO TO 750
DUM=DUM+S(I,JJ)*DV(J)
GO TO 750
740 CONTINUE
II=I-J+1
IF(II.GT.MBAND) GO TO 750
DUM=DUM+S(J,II)*DV(J)
750 CONTINUE
RE(I)=RE(I)+DUM
760 CONTINUE
C
C.....CALCULATE NEW DISPLACEMENT VECTOR -D-
C
DO 780 I=1,NEQ
DUM=0.0
DO 770 J=1,NEQ
DUM=DUM+KE(I,J)*RE(J)
770 CONTINUE
D(I)=DUM
780 CONTINUE
C

```

```

C.....CALCULATE NEW VELOCITY AND ACCELERATION VECTORS -V- AND -A-
C
      DO 790 I=1,NEQ
      V(I)=C9*D(I)-C9*D0(I)+C10*V0(I)+C11*A0(I)
      A(I)=C12*D(I)-C12*D0(I)-C13*V0(I)+C10*A0(I)
790  CONTINUE
C
C.....SET OLD ACCELERATION, VELOCITY AND DISPLACEMENT VECTORS
C      -A0-, -V0- AND -D0- EQUAL TO NEW VECTORS -A-, -V- AND -D-
C
      DO 800 I=1,NEQ
      A0(I)=A(I)
      V0(I)=V(I)
      D0(I)=D(I)
800  CONTINUE
C
C.....CALCULATE ABSOLUTE STRUCTURE DISPLACEMENTS
C
      DO 890 I=1,NEQ
      DUM=0.0
      DO 880 J=1,NGDOF
      DUM=DUM+BG(I,J)*DG(J)
880  CONTINUE
      D(I)=D(I)-DUM
890  CONTINUE
895  CONTINUE
C
C.....RECOVERY COUNTER
C
      NCOUNT=NCOUNT+1
      IF(NCOUNT.NE.ICAL8) GO TO 900
      NCOUNT=0
C
C.....PRINT CURRENT TIME -T-
C
      WRITE(61,2000) T
      WRITE(13,2000) T
C
C.....RECOVER CONDENSED DEGREES OF FREEDOM
C
      CALL XOVCAP ('RECOVER')
C
C.....IDENTIFY NODAL GLOBAL DISPLACEMENTS
C
      CALL XOVCAP ('DISPL')
C
C.....CALCULATE ELEMENT END FORCES AND STRESSES OR
C      CALCULATE VALUES OF YIELD FUNCTIONS AT ELEMENT ENDS
C
      IF(ISTRESS.EQ.0) GO TO 900
      CALL XOVCAP ('STRESS')
900  CONTINUE
C
1010  FORMAT(5(F5.2,F10.4))

```

```
1020  FORMAT(3X,4(F8.0,F9.0))
1030  FORMAT(6(1X,F11.7))
C
2000  FORMAT('-',47HD Y N A M I C   S O L U T I O N   A T   T I M E,3X,
      +      F10.5,3X,13HS E C O N D S)
C
      RETURN
C
      END
C*****
C*****
C*****
```

A.4 OVERLAY CAPSULES

A.4.1 SUBROUTINE RECOVER

The purpose of the Subroutine RECOVER is to recover the condensed degrees of freedom as discussed in Section 2.2.3. The RECOVER subroutine is used only after a static solution is complete or after a specified number of steps in a dynamic analysis have been completed.

The miscellaneous variables used by the Subroutine RECOVER are as follows:

VARIABLE NAME	DESCRIPTION
KKC	Row number in -SC- matrix of degree of freedom currently being recovered
KK	Row number in original structure stiffness matrix of degree of freedom currently being recovered
LL	Number of last row and column of original structure stiffness matrix excluding degrees of freedom yet to be recovered or being recovered
II	Number of first row and column of original structure stiffness matrix (with ground degrees of freedom less than or equal to 0)
NN	Column number in original structure stiffness matrix of entry currently being processed
J	Column number in banded format corresponding to row KK of original structure stiffness matrix
NNC	Row number in -SC- matrix corresponding to column NN of original structure stiffness matrix
NNG	Row number in -SG- matrix corresponding to column NN of original structure stiffness matrix
DUM	Dummy variable used in recovery procedure
N	Lowest displacement vector entry number containing a condensed degree of freedom

The listing of the RECOVER subroutine is as follows:

```

C*****
C*****
C*****
  OVCAP.
  SUBROUTINE RECOVER
C
C  *****
C  TO RECOVER CONDENSED STRUCTURE DEGREES OF FREEDOM
C  *****
C
  PARAMETER(J4=42,J5=14,J6=55,J7=0,J8=2,J9=34,J10=71,J11=99,
+           J12=101,J13=10)
  COMMON/CB1/NE,NUMNP,NUMEG,IPAR,ISTRESS,ICAL1,ICAL2,ICAL3,ICAL4,
+           ICAL5,ICAL6,ICAL7,ICAL8,LINEQL,IDATA
  COMMON/CB2/NSIZE,NEQ,NCOND,NGDOF,MBAND,MBAND1
  COMMON/CB8/PN(J4,6),R(J11)
  COMMON/CB9/S(J9,J11),SC(J10,J13),SG(J8,J12)
  COMMON/CB10/D(J11),DG(J8),U(J4,7)
C
C.....PRINT GROUND DISPLACEMENTS
C
  IF(ICAL5.NE.0) GO TO 10
  IF(NGDOF.EQ.0) GO TO 10
  WRITE(61,2020)
  WRITE(61,2030) (I,DG(I),I=1,NGDOF)
10  CONTINUE
C
C.....PRINT UNCONDENSED DISPLACEMENTS
C
  IF(ICAL5.NE.0) GO TO 15
  IF(IPAR.EQ.2) WRITE(61,2040)
  IF(IPAR.EQ.3) WRITE(61,2050)
  WRITE(61,2010) (I,D(I),I=1,NEQ)
15  CONTINUE
  IF(NCOND.EQ.0) GO TO 120
C
C.....RECOVER CONDENSED DEGREES OF FREEDOM
C
  DO 110 KKC=1,NCOND
  KK=NEQ+KKC
  DUM=0.0
  LL=KK-1
  II=1-NGDOF
  DO 100 NN=II,LL
  J=KK-NN+1
  IF(NN.LE.NEQ) GO TO 20
  NNC=NN-NEQ
  IF(J.GT.MBAND1) GO TO 100
  DUM=DUM+SC(NNC,J)*D(NN)
  GO TO 100
20  CONTINUE
  IF(NN.GT.0) GO TO 30
  NNG=NN+NGDOF
  DUM=DUM+SG(NNG,J)*DG(NNG)

```

```

      GO TO 100
30    CONTINUE
      IF(J.GT.MBAND) GO TO 100
      DUM=DUM+S(NN,J)*D(NN)
100   CONTINUE
      IF(LINEQL.EQ.1) D(KK)=(R(KK)-DUM)/SC(KKC,1)
      IF(LINEQL.NE.1) D(KK)=-DUM/SC(KKC,1)
110   CONTINUE
C
C.....WRITE CONDENSED DISPLACEMENTS
C
      IF(ICAL5.NE.0) GO TO 120
      WRITE(61,2000)
      N=NEQ+1
      WRITE(61,2010) (I,D(I),I=N,NSIZE)
120   CONTINUE
      RETURN
C
2000  FORMAT('-',28HCONDENSED DEGREES OF FREEDOM//)
2010  FORMAT('-',2HD(,I3,2H)=,E25.15)
2020  FORMAT('-',20HGROUND DISPLACEMENTS//)
2030  FORMAT('-',3HDG(,I2,2H)=,E25.15)
2040  FORMAT('1',34HDISPLACEMENTS FROM LINEAR SOLUTION//)
2050  FORMAT('-',35HDISPLACEMENTS FROM DYNAMIC SOLUTION//)
C
      END
C*****
C*****
C*****

```

A.4.2 SUBROUTINE DISPL

The purpose of the DISPL subroutine is to derive the nodal displacements in global coordinates from the displacement vector D. Subroutine DISPL is called only after all of the structure displacements have been recovered by Subroutine RECOVER. The miscellaneous variables used in the DISPL subroutine are as follows:

VARIABLE NAME	DESCRIPTION
NP	Number of current node being processed
I	Node NP degree of freedom which is currently being processed
NE	Equation number associated with degree of freedom I of node NP
NM	Number of node to which node NP is slave in degree of freedom I

A listing of Subroutine DISPL is as follows:

```

C*****
C*****
C*****
  OVCAP.
  SUBROUTINE DISPL
C
C  *****
C    TO RECOVER NODAL DISPLACEMENTS FROM DISPLACEMENT VECTORS -D-
C    AND -DG-
C  *****
C
  PARAMETER(J4=42,J5=14,J6=55,J7=0,J8=2,J9=34,J10=71,J11=99,
+           J12=101,J13=10)
  COMMON/CB1/NE,NUMNP,NUMEG,IPAR,ISTRESS,ICAL1,ICAL2,ICAL3,ICAL4,
+           ICAL5,ICAL6,ICAL7,ICAL8,LINEQL,IDATA
  COMMON/CB2/NSIZE,NEQ,NCOND,NGDOF,MBAND,MBAND1
  COMMON/CB3/IA(J4,7),IB(J4,7),IG(J4),X(J4),Y(J4),Z(J4),
+           NPRINT(J4)
  COMMON/CB10/D(J11),DG(J8),U(J4,7)
C
C.....IDENTIFICATION OF DISPLACEMENTS
C
  IF(ICAL6.EQ.0) WRITE(61,2000)
  IF(LINEQL.EQ.3) WRITE(13,2000)
  DO 230 NP=1,NUMNP

```



```

      DO 220 I=1,7
      * IF(IG(NP).LT.0) GO TO 175
      IF(IA(NP,I)) 160,215,150
150    NE=IA(NP,I)
      U(NP,I)=D(NE)
      IF(NPRINT(NP).LT.I) GO TO 220
C
C.....PRINT NODAL DISPLACEMENTS
C
      IF(IG(1).LT.0) U(NP,I)=U(NP,I)-U(1,I)
      IF(ICAL6.EQ.0) WRITE(61,2020) NE,NP,I,U(NP,I)
      IF(LINEQL.EQ.3) WRITE(13,2020) NE,NP,I,U(NP,I)
      GO TO 220
      / 160    IF(IB(NP,I).LT.0) GO TO 170
      NM=IB(NP,I)
      GO TO 180
      / 170    NE=-IB(NP,I)+NEQ
      U(NP,I)=D(NE)
      IF(NPRINT(NP).LT.I) GO TO 220
C
C.....PRINT NODAL DISPLACEMENTS
C
      IF(IG(1).LT.0) U(NP,I)=U(NP,I)-U(1,I)
      IF(ICAL6.EQ.0) WRITE(61,2020) NE,NP,I,U(NP,I)
      IF(LINEQL.EQ.3) WRITE(13,2020) NE,NP,I,U(NP,I)
      GO TO 220
175    CONTINUE
      * IF(IB(NP,I).EQ.0) GO TO 215
      * IF(IB(NP,I).NE.0) U(NP,I)=DG(IB(NP,I))
      IF(NPRINT(NP).LT.I) GO TO 220
C
C.....PRINT NODAL DISPLACEMENTS
C
      IF(IG(1).LT.0) U(NP,I)=U(NP,I)-U(1,I)
      IF(ICAL6.EQ.0) WRITE(61,2040) IB(NP,I),NP,I,U(NP,I)
      IF(LINEQL.EQ.3) WRITE(13,2040) IB(NP,I),NP,I,U(NP,I)
      GO TO 220
180    * IF(IG(NM).LT.0) GO TO 185
      IF(IA(NM,I)) 190,215,210
185    CONTINUE
      * IF(IB(NM,I).EQ.0) GO TO 215
      IF(IB(NM,I).NE.0) U(NP,I)=DG(IB(NM,I))
      IF(NPRINT(NP).LT.I) GO TO 220
C
C.....PRINT NODAL DISPLACEMENTS
C
      IF(IG(1).LT.0) U(NP,I)=U(NP,I)-U(1,I)
      IF(ICAL6.EQ.0) WRITE(61,2040) IB(NM,I),NP,I,U(NP,I)
      IF(LINEQL.EQ.3) WRITE(13,2040) IB(NM,I),NP,I,U(NP,I)
      GO TO 220
190    NE=-IB(NM,I)+NEQ
      U(NP,I)=D(NE)
      IF(NPRINT(NP).LT.I) GO TO 220
C

```

print (N) - nodal displ.
 print variable
 0 - print all displacement
 at node N
 1 - don't print any
 displacement at
 node N
 2 - print only x, y, z
 3 - print x, y, z and
 node N

GE

C.....PRINT NODAL DISPLACEMENTS

C

IF(IG(1).LT.0) U(NP,I)=U(NP,I)-U(1,I)
 IF(ICAL6.EQ.0) WRITE(61,2020) NE,NP,I,U(NP,I)
 IF(LINEQL.EQ.3) WRITE(13,2020) NE,NP,I,U(NP,I)
 GO TO 220

210 NE=IA(NM,I)
 U(NP,I)=D(NE)
 IF(NPRINT(NP).LT.I) GO TO 220

C

C.....PRINT NODAL DISPLACEMENTS

C

IF(IG(1).LT.0) U(NP,I)=U(NP,I)-U(1,I)
 IF(ICAL6.EQ.0) WRITE(61,2020) NE,NP,I,U(NP,I)
 IF(LINEQL.EQ.3) WRITE(13,2020) NE,NP,I,U(NP,I)
 GO TO 220

215 CONTINUE
 U(NP,I)=0.0

220 CONTINUE

230 CONTINUE

RETURN

C

2000 FORMAT('0',19HNODAL DISPLACEMENTS)

2020 FORMAT(' ',2HD(,I3,4H) = ,2HU(,I2,1H,,I1,4H) = ,F25.15)

2040 FORMAT(' ',3HDG(,I2,4H) = ,2HU(,I2,1H,,I1,4H) = ,F25.15)

C

END

C*****

C*****

C*****

A.4.3 SUBROUTINE STRESS

The major purposes of Subroutine STRESS are: to calculate element end forces and to calculate element end stresses or initial yield function values. To calculate an element's end forces, the STRESS subroutine first uses the corresponding nodal displacements derived by Subroutine DISPL and stores them as a global element end displacement vector. Subroutine STRESS then converts the global element displacements into local displacements using the element's transformation matrix. Finally, the STRESS subroutine multiplies the local element stiffness matrix by the local element displacement vector to get the element end forces.

Element end stresses are calculated from the end forces using standard bending and axial stress formulas. The initial yield function values at the ends of the elements are calculated as discussed in Section 2.2.2. The following is a list of miscellaneous variables used by the STRESS subroutine:

VARIABLE NAME	DESCRIPTION
DS(N)	End displacement N of current element in global coordinates
DL(N)	End displacement N of current element in local coordinates
PI(N) & PJ(N)	End force N of current element at node I or node J. Also used in initial yield function calculations for the end forces due to dynamic loading, and for the sum of the end forces due to dynamic and dead loads.
SI(N) & SJ(N)	End stress N of current element at node I or node J. Also used in initial yield function calculations for the components of the current initial yield function (after each component's force ratio is multiplied by its respective coefficient).
YFI	Value of current initial yield function at node I of

current element being processed

YFJ	Value of current initial yield function at node J of current element being processed
N1	Number of property group at node I of current beam element
N3	Number of property group at node J of current beam element
NYS	Number of initial yield functions to be calculated
K	Variable denoting type of element being processed: 1 = truss element 2 = straight beam element
KK	Number of current type K element being processed
NI	Global node I of current element being processed
NJ	Global node J of current element being processed
IJ	Variable used in deriving global element end displacements from nodal displacements
DUM	Dummy variable used in calculating local element end displacements
II	Variable used in calculating element end forces
YI(I) & YJ(I)	Yield forces of current beam element at nodes I and J, respectively, with I = 1 denoting axial yield force, I = 2 denoting local x-x yield bending moment, I = 3 denoting local y-y yield bending moment and I = 4 denoting yield bimoment
A(I,J)	Initial yield function J coefficients associated with yield force ratio I

Finally, the following is a listing of Subroutine STRESS:

```

C*****
C*****
C*****
  OVCAP.
  SUBROUTINE STRESS
C
C *****
C   TO COMPUTE MEMBER END FORCES AND STRESSES OR
C   TO COMPUTE VALUES OF YIELD FUNCTION AT MEMBER ENDS
C *****
C

```

```

PARAMETER(J4=42,J5=14,J6=55,J7=0,J8=2,J9=34,J10=71,J11=99,
+          J12=101,J13=10)
COMMON/CB1/NE,NUMNP,NUMEG,IPAR,ISTRESS,ICAL1,ICAL2,ICAL3,ICAL4,
+          ICAL5,ICAL6,ICAL7,ICAL8,LINEQL,IDATA
COMMON/CB3/IA(J4,7),IB(J4,7),IG(J4),X(J4),Y(J4),Z(J4),
+          NPRINT(J4)
COMMON/CB4/E(2),P(2),NTYPE(2),NEPR(2),MPRINT(J6,2)
COMMON/CB5/NITE(J5),NJTE(J5),ATE(J5),LE(J5),SCT(J5,2)
COMMON/CB6/NISB(J6),NJSB(J6),NKSJ(J6),NPGS(J6,3),ASB(J6),AGXS(J6),
+          AGYS(J6),IXXS(J6),IYYS(J6),KTS(J6),IWS(J6),LSB(J6),
+          SCS(J6,16),SES(16),FL(J6,3),ELX(J6),ELY(J6),ELW(J6)
COMMON/CB7/SE(16,16),T(14,14)
COMMON/CB10/D(J11),DG(J8),U(J4,7)
REAL IXXS,IYYS,KTS,IWS,LSB,LE
DIMENSION DS(14),DL(14),PI(7),PJ(7),SI(7),SJ(7),YI(4),YJ(4),A(4,4)
C
C.....PROCESS EVERY ELEMENT OF EACH ELEMENT GROUP
C
      IF(ISTRESS.LT.0) NYS=-ISTRESS
      REWIND 1
      REWIND 2
      DO 900 K=1,2
      IF(NTYPE(K).EQ.0) GO TO 900
      NT=NTYPE(K)+1
      IF(MPRINT(NT,K).EQ.1) GO TO 900
      IF(ISTRESS.EQ.1) GO TO 80
      IF(K.EQ.1) GO TO 60
      DO 50 I=1,4
      DO 40 J=1,NYS
      JJ=4*I+J-4
      A(I,J)=SES(JJ)
40    CONTINUE
50    CONTINUE
60    CONTINUE
      IF(K.EQ.1) WRITE(61,2100)
      IF(K.EQ.2) WRITE(61,2110)
      GO TO 90
80    CONTINUE
      IF(K.EQ.1) WRITE(61,2000)
      IF(K.EQ.2) WRITE(61,2010)
90    CONTINUE
      DO 890 KK=1,NTYPE(K)
      IF(MPRINT(KK,K).EQ.1) GO TO 890
      IF(K.EQ.1) NI=NITE(KK)
      IF(K.EQ.1) NJ=NJTE(KK)
      IF(K.EQ.2) NI=NISB(KK)
      IF(K.EQ.2) NJ=NJSB(KK)
      DO 100 I=1,14
      READ(1,1000) (SE(I,J),J=1,7)
100   READ(1,1000) (SE(I,J),J=8,14)
      DO 105 I=1,14
      READ(2,1000) (T(I,J),J=1,7)
105   READ(2,1000) (T(I,J),J=8,14)
C

```

C.....IDENTIFY NODAL DISPLACEMENTS ON EACH ELEMENT

C

```

      DO 110 I=1,7
      DS(I)=U(NI,I)
      IJ=I+7
      DS(IJ)=U(NJ,I)
110   CONTINUE
      DO 120 I=1,14
      DUM=0.0
      DO 115 J=1,14
      DUM=DUM+DS(J)*T(I,J)
115   CONTINUE
120   DL(I)=DUM

```

C

C.....OBTAIN RESULTANT LOADS

C

```

      DO 145 I=1,7
      PI(I)=0.0
      DO 140 J=1,14
      PI(I)=PI(I)+SE(I,J)*DL(J)
140   CONTINUE
145   CONTINUE
      DO 160 I=8,14
      II=I-7
      PJ(II)=0.0
      DO 155 J=1,14
      PJ(II)=PJ(II)+SE(I,J)*DL(J)
155   CONTINUE
160   CONTINUE
      IF(ISTRESS.NE.1) GO TO 300

```

C

C.....WRITE LOCAL ELEMENT END LOADS

C

```

      IF(K.EQ.1) WRITE(61,2035)KK,PI(3),PJ(3)
      IF(K.NE.1) WRITE(61,2030)KK,(PI(I),I=1,7),(PJ(J),J=1,7)
200   CONTINUE

```

C

C.....CALCULATE ELEMENT END STRESSES

C

```

      L=K-2
      IF(L) 210,220,900
210   CONTINUE
      SI(3)=PI(3)/(ATE(KK))
      SJ(3)=PJ(3)/(ATE(KK))
      GO TO 290
220   CONTINUE
      N1=NPGS(KK,1)
      N3=NPGS(KK,3)
      DO 230 I=1,7
      SI(I)=0.0
      SJ(I)=0.0
230   CONTINUE
      IF(ASB(N1).NE.0.0) SI(3)=PI(3)/ASB(N1)
      IF(IXXS(N1).NE.0.0) SI(6)=PI(6)*SCS(N1,1)/IXXS(N1)

```

```

IF(IYYS(N1).NE.0.0) SI(5)=PI(5)*SCS(N1,2)/IYYS(N1)
IF(IWS(N1).NE.0.0) SI(7)=PI(7)*SCS(N1,1)*SCS(N1,2)/IWS(N1)
IF(ASB(N3).NE.0.0) SJ(3)=PJ(3)/ASB(N3)
IF(IXXS(N3).NE.0.0) SJ(6)=PJ(6)*SCS(N3,3)/IXXS(N3)
IF(IYYS(N3).NE.0.0) SJ(5)=PJ(5)*SCS(N3,4)/IYYS(N3)
IF(IWS(N3).NE.0.0) SJ(7)=PJ(7)*SCS(N3,3)*SCS(N3,4)/IWS(N3)
290  CONTINUE
C
C.....WRITE ELEMENT STRESSES
C
      IF(K.EQ.1) WRITE(61,2040) SI(3),SJ(3)
      IF(K.NE.1) WRITE(61,2050) (SI(I),I=1,7),(SJ(J),J=1,7)
      GO TO 890
300  CONTINUE
      IF(ISTRESS.GE.0) GO TO 890
C
C.....CALCULATE VALUE OF YIELD FUNCTION AT NODES -I- AND -J-
C      FOR TRUSS ELEMENTS AND PRINT
C
      L=K-2
      IF(L) 310,320,900
310  CONTINUE
      YFI=(PI(3)+SCT(KK,2))/SCT(KK,1)
      YFJ=-YFI
      WRITE(61,2035) KK,YFI,YFJ
      GO TO 890
C
C.....CALCULATE VALUE OF YIELD FUNCTION AT NODES -I- AND -J-
C      FOR STRAIGHT BEAM ELEMENTS AND PRINT
C
320  CONTINUE
      PI(1)=(PI(3))
      PI(2)=(PI(6))
      PI(3)=(PI(5))
      PI(4)=(PI(7))
      PJ(1)=(PJ(3))
      PJ(2)=(PJ(6))
      PJ(3)=(PJ(5))
      PJ(4)=(PJ(7))
      DO 322 I=1,4
      J=I
      JJ=J+4
      YI(I)=SCS(NPGS(KK,1),J)
      YJ(I)=SCS(NPGS(KK,3),JJ)
      J=J+8
      JJ=JJ+8
      PI(I)=PI(I)+SCS(NPGS(KK,1),J)
      PJ(I)=PJ(I)+SCS(NPGS(KK,3),JJ)
322  CONTINUE
      DO 800 I=1,NYS
      YFI=YFJ=0.0
      DO 700 J=1,4
      SI(J)=(PI(J)/YI(J))*A(J,I)
      SJ(J)=(PJ(J)/YJ(J))*A(J,I)

```

```

      YFI=YFI+SI(J)
      YFJ=YFJ+SJ(J)
700  CONTINUE
      IF(I.EQ.1) WRITE(61,2020) KK,I,(SI(II),II=1,4),YFI
      IF(I.NE.1) WRITE(61,2022) I,(SI(II),II=1,4),YFI
      WRITE(61,2025) (SJ(JJ),JJ=1,4),YFJ
800  CONTINUE
890  CONTINUE
900  CONTINUE
C
1000 FORMAT(1X,7E18.8)
C
2000 FORMAT('0',48HTRUSS ELEMENT LOCAL Z AXIS AXIAL FORCES/STRESSES/
+         1X,7HELEMENT,14X,6HNODE I,10X,6HNODE J)
2010 FORMAT('0',37HSTRAIGHT BEAM ELEMENT FORCES/STRESSES//1X,7HELEMENT,
+         2X,4HNODE,2X,13HLOCAL X SHEAR,4X,13HLOCAL Y SHEAR,4X,
+         13HLOCAL Z AXIAL,3X,15HLOCAL Z TORSION,2X,
+         15HLOCAL Y BENDING,2X,15HLOCAL X BENDING,2X,
+         15HLOCAL Z WARPING)
2020 FORMAT(' ',3X,I4,8X,I1,8X,1HI,5(10X,F10.8))
2022 FORMAT(' ',15X,I1,8X,1HI,5(10X,F10.8))
2025 FORMAT(' ',24X,1HJ,5(10X,F10.8))
2030 FORMAT('0',I4,7X,1HI,E16.6,6(4X,E13.6)/12X,1HJ,E16.6,6(4X,E13.6))
2035 FORMAT(' ',3X,I4,13X,F13.6,3X,F13.6)
2040 FORMAT(' ',14X,F13.6,3X,F13.6)
2050 FORMAT('0',11X,1HI,E16.6,6(4X,E13.6)/12X,1HJ,E16.6,6(4X,E13.6))
2100 FORMAT('0',1X,13HTRUSS ELEMENT,10X,6HNODE I,10X,6HNODE J)
2110 FORMAT('0',3X,5HSBEAM,3X,8HFUNCTION,4X,4HNODE,5X,
+         17HAXIAL FORCE RATIO,3X,16HX-X MOMENT RATIO,4X,
+         16HY-Y MOMENT RATIO,5X,14HBIMOMENT RATIO,6X,
+         14HYIELD FUNCTION)
C
      RETURN
C
      END
C*****
C*****
C*****

```


A.4.4 SUBROUTINE ASEMBLE

The purpose of the Subroutine ASEMBLE is to assemble the element stiffness matrices into the structure stiffness matrix arrays as discussed in Section 2.4.2. The miscellaneous variables used by the ASEMBLE subroutine are as follows:

VARIABLE NAME	DESCRIPTION
K1	Variable denoting upper or lower half of element stiffness matrix: 1 = upper half 2 = lower half
K2	Variable denoting left or right half of element stiffness matrix: 1 = left half 2 = right half
NI	Node I of current element being processed
NJ	Node J of current element being processed
II	Row number of current entry
JJ	Column number of current entry, initially unbanded then transformed into banded format
KK	Modified row number used to place entries in correct row of matrices -SG- or -SC-
MK	Variable controlling number of degrees of freedom per node: 3 = truss element 7 = beam element

A listing of the ASEMBLE subroutine is as follows:

```

C*****
C*****
C*****
  OVCAP.
  SUBROUTINE ASEMBLE(K,M)
C
C  *****
C    TO PROCESS AND ASSEMBLE ELEMENT STIFFNESS MATRICES AND NODAL
C    LOAD VECTORS INTO THEIR CORRESPONDING STRUCTURE ARRAYS.
C  *****
C

```

```

COMMON/CB1/NE,NUMNP,NUMEG,IPAR,ISTRESS,ICAL1,ICAL2,ICAL3,ICAL4,
+   ICAL5,ICAL6,ICAL7,ICAL8,LINEQL,IDATA
COMMON/CB2/NSIZE,NEQ,NCOND,NGDOF,MBAND,MBAND1
PARAMETER(J4=42,J5=14,J6=55,J7=0,J8=2,J9=34,J10=71,J11=99,
+   J12=101,J13=10)
COMMON/CB3/IA(J4,7),IB(J4,7),IG(J4),X(J4),Y(J4),Z(J4),
+   NPRINT(J4)
COMMON/CB5/NITE(J5),NJTE(J5),ATE(J5),LE(J5),SCT(J5,2)
COMMON/CB6/NISB(J6),NJSB(J6),NKSB(J6),NPGS(J6,3),ASB(J6),AGXS(J6),
+   AGYS(J6),IXXS(J6),IYYS(J6),KTS(J6),IWS(J6),LSB(J6),
+   SCS(J6,16),SES(16),FL(J6,3),ELX(J6),ELY(J6),ELW(J6)
COMMON/CB7/SE(16,16),T(14,14)
COMMON/CB8/PN(J4,6),R(J11)
COMMON/CB9/S(J9,J11),SC(J10,J13),SG(J8,J12)
REAL IXXS,IYYS,KTS,IWS,LSB,LE

C
C.....ASSEMBLE ELEMENT STIFFNESS INTO STRUCTURE STIFFNESS
C
  MN=M-2
  IF(MN) 10,20,900
10  CONTINUE
  NI=NITE(K)
  NJ=NJTE(K)
  GO TO 40
20  CONTINUE
  NI=NISB(K)
  NJ=NJSB(K)
40  CONTINUE
  DO 165 K1=1,2
  IF(K1.EQ.1) NP=NI
  IF(K1.EQ.2) NP=NJ
  IF(M.EQ.1) MK=3
  IF(M.EQ.1) MK=7
  DO 160 I=1,MK
  IF(IG(NP).LT.0) GO TO 97
  IF(IA(NP,I)) 105,160,100
97  IF(IB(NP,I).EQ.0) GO TO 160
  II=IB(NP,I)-NGDOF
  GO TO 115
100 II=IA(NP,I)
  GO TO 115
105 IF(IB(NP,I).LT.0) GO TO 110
  NN=IB(NP,I)
  GO TO 111
110 II=-IB(NP,I)+NEQ
  GO TO 115
111 IF(IG(NN).LT.0) GO TO 112
  IF(IA(NN,I)) 113,160,114
112 IF(IB(NN,I).EQ.0) GO TO 160
  II=IB(NN,I)-NGDOF
  GO TO 115
113 II=-IB(NN,I)+NEQ
  GO TO 115
114 II=IA(NN,I)

```

```

115  CONTINUE
      DO 155 K2=1,2
      IF(K2.EQ.1) ND=NI
      IF(K2.EQ.2) ND=NJ
      IF(M.EQ.1) MK=3
      IF(M.NE.1) MK=7
      DO 150 J=1,MK
      IF(IG(ND).LT.0) GO TO 117
      IF(IA(ND,J)) 125,150,120
117  IF(IB(ND,J).EQ.0) GO TO 150
      JJ=IB(ND,J)-NGDOF
      GO TO 145
120  JJ=IA(ND,J)
      GO TO 145
125  IF(IB(ND,J).LT.0) GO TO 130
      NN=IB(ND,J)
      GO TO 132
130  JJ=-IB(ND,J)+NEQ
      GO TO 145
132  IF(IG(NN).LT.0) GO TO 134
      IF(IA(NN,J)) 135,150,140
134  IF(IB(NN,J).EQ.0) GO TO 150
      JJ=IB(NN,J)-NGDOF
      GO TO 145
135  JJ=-IB(NN,J)+NEQ
      GO TO 145
140  JJ=IA(NN,J)
145  CONTINUE
C
C.....IGNORE ENTRIES BELOW AND TO THE LEFT OF THE DIAGONAL.
C      ASSIGN CORRECT ELEMENT STIFFNESS MATRIX ROW AND COLUMN NUMBERS.
C
      IF(JJ.LT.II) GO TO 150
      IF(K1.EQ.1) IE=I
      IF(K1.EQ.2) IE=I+7
      IF(K2.EQ.1) JE=J
      IF(K2.EQ.2) JE=J+7
C
C.....CHANGE -JJ- SUBSCRIPT OF FULL MATRIX TO -JJ- SUBSCRIPT OF
C      BANDED MATRICES.  CHANGE ROW NUMBER -II- AND ASSIGN ENTRIES TO
C      MATRICES -SG-, -SC- OR -S-
C
      JJ=JJ-II+1
      IF(II.GT.0) GO TO 147
      KK=NGDOF+II
      SG(KK,JJ)=SG(KK,JJ)+SE(IE,JE)
      GO TO 150
147  CONTINUE
      IF(II.LE.NEQ) GO TO 149
      KK=II-NEQ
      SC(KK,JJ)=SC(KK,JJ)+SE(IE,JE)  1
      GO TO 150
149  CONTINUE
      S(II,JJ)=S(II,JJ)+SE(IE,JE)

```

150 CONTINUE
155 CONTINUE
160 CONTINUE
165 CONTINUE
900 CONTINUE

C

RETURN

C

END

C*****

C*****

C*****

A.4.5 SUBROUTINE TRANSFM

The Subroutine TRANSFM serves to transform the local element stiffness matrices into global coordinates. The method used for transforming straight beam element local stiffness matrices was discussed in Section 2.4.1 and the method used for truss elements is just a simplified version of the beam element method. No designation of cross-section orientation is necessary for truss elements, thus no K nodes are needed for the truss element transformations. The miscellaneous variables used in the TRANSFM subroutine are as follows:

VARIABLE NAME	DESCRIPTION
ST(I,J)	Entry I-J of intermediate transformation matrix: $ST = SE * T$
NI	Node I of current element
NJ	Node J of current element
NK	Node K of current straight beam element
CX, CY & CZ	Direction cosines of element with respect to global X, Y and Z axes, respectively
CA and SA	Cosine and sine, respectively, of third rotation angle alpha for current element*
L	Length of current element
XPS, YPS & ZPS	Coordinates in a global sense of node K with respect to angle alpha for current element*
CXZ	Quantity $(CX ** 2 + CZ ** 2) ** 0.5$
YPG and ZPG	Coordinates of node K with respect to gamma axes for current element*
* as described on pages 290 to 296 of Gere and Weaver (Ref. 11)	

Lastly, the listing of the TRANSFM subroutine is as follows:

```

C*****
C*****
C*****
      OVCAP.
      SUBROUTINE TRANSFM(K,M)
C
C      *****
C      COORDINATE TRANSFORMATION SUBROUTINE
C      *****
C
      PARAMETER(J4=42,J5=14,J6=55,J7=0,J8=2,J9=34,J10=71,J11=99,
+              J12=101,J13=10)
      COMMON/CB3/IA(J4,7),IB(J4,7),IG(J4),X(J4),Y(J4),Z(J4),
+              NPRINT(J4)
      COMMON/CB5/NITE(J5),NJTE(J5),ATE(J5),LE(J5),SCT(J5,2)
      COMMON/CB6/NISB(J6),NJSB(J6),NKSB(J6),NPGS(J6,3),ASB(J6),AGXS(J6),
+              AGYS(J6),IXXS(J6),IYYS(J6),KTS(J6),IWS(J6),LSB(J6),
+              SCS(J6,16),SES(16),FL(J6,3),ELX(J6),ELY(J6),ELW(J6)
      COMMON/CB7/SE(16,16),T(14,14)
      REAL IXXS,IYYS,KTS,IWS,LSB,LE,L
      DIMENSION ST(14,14)
C
C.....TRUSS ELEMENT DATA PROCESSING
C
      IF(M.EQ.2) GO TO 100
      NI=NITE(K)
      NJ=NJTE(K)
      L=LE(K)
      GO TO 200
C
C.....BEAM ELEMENT DATA PROCESSING
C
100   CONTINUE
      NI=NISB(K)
      NJ=NJSB(K)
      NK=NKSB(K)
      L=LSB(K)
200   CONTINUE
C
C.....THREE DIMENSIONAL COORDINATE TRANSFORMATION
C
C.....INITIALIZE MATRICES -ST- AND -T-
C
      DO 280 I=1,14
      DO 270 J=1,14
      ST(I,J)=T(I,J)=0.0
270   CONTINUE
280   CONTINUE
C
C.....CALCULATE DIRECTION COSINES
C
      CX=(X(NJ)-X(NI))/L
      CY=(Y(NJ)-Y(NI))/L
      CZ=(Z(NJ)-Z(NI))/L

```

```

      CXZ=((CX**2.0+CZ**2.0)**0.5)
      IF(M.EQ.2) GO TO 300
      CA=1.0
      SA=0.0
      GO TO 350
300   CONTINUE
      XPS=X(NK)-X(NI)
      YPS=Y(NK)-Y(NI)
      ZPS=Z(NK)-Z(NI)
      IF(X(NI).NE.X(NJ)) GO TO 320
      IF(Z(NI).NE.Z(NJ)) GO TO 320
      SA=ZPS/((XPS**2.0+ZPS**2.0)**0.5)
      CA=-(XPS*CY)/((XPS**2.0+ZPS**2.0)**0.5)
      GO TO 350
320   CONTINUE
      YPG=-XPS*CX*CY/CXZ+YPS*CXZ-ZPS*CY*CZ/CXZ
      ZPG=-XPS*CZ/CXZ+ZPS*CX/CXZ
      CA=YPG/((YPG**2.0+ZPG**2.0)**0.5)
      SA=ZPG/((YPG**2.0+ZPG**2.0)**0.5)
350   CONTINUE
C
C.....CALCULATE TRANSFORMATION MATRIX -T-
C
      T(3,1)=T(4,4)=T(10,8)=T(11,11)=CX
      T(3,2)=T(4,5)=T(10,9)=T(11,12)=CY
      T(3,3)=T(4,6)=T(10,10)=T(11,13)=CZ
      T(1,2)=T(6,5)=T(8,9)=T(13,12)=CA*CXZ
      T(2,2)=T(5,5)=T(9,9)=T(12,12)=-SA*CXZ
      IF(X(NI).NE.X(NJ)) GO TO 400
      IF(Z(NI).NE.Z(NJ)) GO TO 400
      T(1,1)=T(6,4)=T(8,8)=T(13,11)=-CY*CA
      T(2,1)=T(5,4)=T(9,8)=T(12,11)=CY*SA
      T(1,3)=T(6,6)=T(8,10)=T(13,13)=SA
      T(2,3)=T(5,6)=T(9,10)=T(12,13)=CA
      GO TO 450
400   CONTINUE
      T(1,1)=T(6,4)=T(8,8)=T(13,11)=- (CX*CY*CA+CZ*SA)/CXZ
      T(2,1)=T(5,4)=T(9,8)=T(12,11)= (CX*CY*SA-CZ*CA)/CXZ
      T(1,3)=T(6,6)=T(8,10)=T(13,13)=- (CY*CZ*CA-CX*SA)/CXZ
      T(2,3)=T(5,6)=T(9,10)=T(12,13)= (CY*CZ*SA+CX*CA)/CXZ
450   CONTINUE
      T(7,7)=T(14,14)=1.0
C
C.....CALCULATE INTERMEDIATE MATRIX -ST-
C
      DO 850 I=1,14
      DO 830 J=1,14
      DO 810 LL=1,14
      ST(I,J)=ST(I,J)+SE(I,LL)*T(LL,J)
810   CONTINUE
830   CONTINUE
850   CONTINUE
C
C.....CALCULATE GLOBAL ELEMENT STIFFNESS MATRIX -SE-

```

C

```
      DO 950 I=1,14
      DO 930 J=1,14
      SE(I,J)=0.0
      DO 910 LL=1,14
      SE(I,J)=SE(I,J)+T(LL,I)*ST(LL,J)
910   CONTINUE
930   CONTINUE
950   CONTINUE
      RETURN
```

C

END

```
C*****
C*****
C*****
```


APPENDIX B

APPENDIX B
BRIDGE MODELING DETAILS

This appendix contains details on how NRGB and CSCB were modeled. The first section deals with how the individual bridge members were modeled and how the lumped nodal masses were determined for NRGB. The second section covers the same topics with regards to CSCB. The third section presents actual input listings for four cases of B1-B1' loading: NRGB in the X and Z directions, and CSCB in the X and Z directions. Finally, the fourth section contains listings of the B-1 and B-2 accelerograms.

B.1 NRGB MODELING DETAILS

B.1.1 ARCH DESCRIPTION

The arch in NRGB is a box truss consisting of four 58 inch by 39 inch box girder chords with variable flange and web plate thicknesses connected by simple side trusses, top and bottom lateral K-trusses and transverse V-trusses. The lower arch chord web thicknesses vary from 3 1/4 inches near the abutment to 2 inches at the crown, while the upper arch chord web thicknesses vary from 4 inches near the abutments to 2 3/4 inches at the crown. The lower and upper arch chord cover plate thicknesses vary from 1 3/8 and 1 1/2 inches, respectively, near the abutments to 1 3/16 inches at the crown.

The side trusses are illustrated in Figures 3-1 and B-1 and vary in depth from 53 feet near the abutments to 34 feet near the crown. The

posts and diagonals in the side trusses are box sections that are generally composed of $39 \frac{1}{2}$ by $\frac{7}{16}$ inch web plates and 19 by $\frac{1}{2}$ inch cover plates except for slightly larger plate thicknesses for those members that are fastened to the joints at the bases of the columns.

The top and bottom lateral K-trusses shown in Figure B-2 have a constant width of 72 feet and while the lateral struts have the same cross-sectional area throughout, the lateral diagonals decrease in size from the abutments to the crown. The lateral struts are box sections with $26 \frac{1}{4}$ by $\frac{9}{16}$ inch web plates and 21 by $\frac{5}{8}$ inch cover plates. The lateral diagonals are box sections with web plates that vary in size from $24 \frac{1}{2}$ by $\frac{11}{16}$ inches to $25 \frac{3}{4}$ by $\frac{9}{16}$ inches and with cover plates that vary in size from 26 by $1 \frac{1}{4}$ inches to 18 by $\frac{5}{8}$ inches.

The transverse V-bracing shown in Figure 3-6 occurs only at the panel points and is composed of diagonal sway braces of one cross-sectional area near the abutments and another smaller cross-sectional area near the crown. The sway braces are box sections with $19 \frac{1}{4}$ by $\frac{7}{16}$ inch web plates and 20 by $\frac{7}{8}$ inch cover plates near the abutments and with $19 \frac{1}{2}$ by $\frac{7}{16}$ inch web plates and 18 by $\frac{3}{4}$ inch cover plates near the crown.

The top and bottom chords of each arch side truss are connected at the arch abutments to the hinge connection depicted in Figure B-3. Each of these hinges allows only Z axis rotation with all other displacements restrained.

B.1.2 ARCH MODELING

As discussed earlier in Section 3.1.1, cantilevered segments of the arch were used in determining equivalent straight beam stiffnesses. For the NRGB arch, two cantilevered segments were utilized: one using

the largest (in cross-sectional area) and longest arch members which occur near the arch abutments and the other using the smallest and shortest members near the crown. Each cantilevered segment was composed of three identical subpanels with the arch chords represented by continuous straight beam elements and the remaining members represented by truss elements. The boundary conditions, loads and equations discussed in Section 3.1.1 were then employed to determine the equivalent straight beam stiffnesses of the arch at the crown and near the abutments. Between adjacent panel points in the NRGB one plane models, the arch was represented by a single straight beam element with stiffnesses derived by linear interpolation between the stiffnesses at the crown and those near the arch abutment (see Section 3.1.1)

Because of the box configuration of the NRGB arch cross-section, warping of the arch was assumed to be negligible and twelve degree of freedom straight beam finite elements were used to represent the arch. The hinges at the arch abutments were modeled such that only global Z axis rotations were allowed at these points.

B.1.3 ARCH MASS DISTRIBUTION

The plans for NRGB list a total arch weight of 20,420,840 pounds, but no distribution of this weight is provided. In order to approximate the mass distribution of the NRGB arch, the first step was to calculate the weight of the cantilevered segments of arch at the crown and near the abutments. The weight of each cantilevered segment was then divided by its length to get an approximate weight per foot of arch at the crown and near the abutments. Taking an average of these two weights per foot and multiplying by the total length of the NRGB arch resulted in an approximate arch weight about 20% below the actual weight. This

difference can be attributed to miscellaneous steel such as diaphragms, stiffeners, splice plates, etc., that was not included in the cantilevered segments. The arch weights per foot at the crown and near the abutments were then increased by 20% to account for this miscellaneous steel.

In the NRGB models, arch weights per foot at the intermediate arch nodes were calculated using linear interpolation between the values at the abutment and at the crown. This linear interpolation was much the same as the method used in calculating the arch beam element stiffnesses. Lumped masses at all arch nodal points were then calculated by taking one-half the length of arch on either side of each node times the weight per foot at the given node and then dividing by the gravitational acceleration constant g .

B.1.4 DECK DESCRIPTION

The NRGB deck consists of the following components: two simple side trusses, bottom lateral X-bracing, transverse floorbeam trusses at each subpanel point, nine floor stringers, and a concrete roadway slab. The nine floor stringers (illustrated in Figures 3-6 and B-4) and the concrete roadway slab have expansion joints at every seventh subpanel point and are thus discontinuous at these points. This fact coupled with the relatively weak stringer to floorbeam connections, and the lack of shear connectors between the stringers and the slab led to the assumption that the stringers and slab would not contribute substantially to the deck's overall structural stiffness and thus the stringers and slab were not included in the deck stiffness calculations.

The side trusses illustrated in Figure B-5 are 18 feet deep and consist of six subpanels per panel. These trusses span 129.75 feet between

the bents in the main span, 126.5 feet between the bents in the south approach span and 143.5 feet between the bents in the north approach span. The top and bottom chords are 20 by 13 inch box sections with $\frac{3}{8}$ inch cover plates and web plates that vary in thickness from subpanel to subpanel with a maximum of $1\frac{1}{4}$ inches and a minimum of $\frac{1}{2}$ inch. The verticals and diagonals are either: W14x53, W14x61 or W14x87 wide flange sections, or 12 by 18 inch box sections with web plates that vary in thickness from $\frac{3}{8}$ to $\frac{5}{8}$ inches and with cover plates that vary in thickness from $\frac{7}{8}$ to $1\frac{1}{2}$ inches.

The bottom lateral X-bracing depicted in Figure B-6 spans the 72 feet between the bottom chords of the side trusses and forms three X's per panel. The braces in the main span are box sections composed of $10\frac{1}{2}$ by $\frac{1}{2}$ inch cover plates and 11 by $\frac{5}{16}$ inch web plates, while the braces in the approach spans are box sections composed of $10\frac{1}{2}$ by $\frac{3}{8}$ inch cover plates and $11\frac{1}{4}$ by $\frac{5}{16}$ inch web plates.

The transverse floorbeam trusses shown in Figure 3-6 span the 72 feet between the side trusses and have the same 18 feet of depth as the side trusses. The top chords are box sections with 20 by $\frac{5}{8}$ inch web plates, 21 by $\frac{5}{8}$ inch top cover plates and 15 by $\frac{7}{8}$ inch bottom cover plates. The bottom chords are also box sections with 14 by $\frac{9}{16}$ inch web plates and 12 by $\frac{3}{8}$ inch cover plates. Finally, the inner diagonals are W12x58 sections, the verticals are W12x53 sections and the outer diagonals are W12x65 sections.

The two simple side trusses and the bottom lateral X-bracing form a U-shaped configuration that is continuous over three segments: the south approach span, the main span and the north approach span. At panel points 5 and 19 the top and bottom chords of the deck side trusses

are discontinuous, thus these panel points represent the dividing lines between the approach span deck segments and the main span deck segment. At these points, as illustrated in Figure B-7, the bottom chords of the approach span side trusses are pinned to the top of the bents while the bottom chords of the main span side trusses are attached to the bents by rollers that allow longitudinal motion of the chords at these points. The clearance for relative motion of the deck segments at panel points 5 and 19 is 13.5 inches. At the north and south deck abutments, as shown in Figure B-8, the bottom chords of the deck side trusses are restrained by pins fastened to eyebars embedded in the concrete abutments, while the top chords are not restrained.

B.1.5 DECK MODELING

The equivalent straight beam stiffnesses for the NRGB deck were determined using three cantilever segments which utilized average member stiffnesses in the south approach span, the main span and the north approach span decks, respectively. Each cantilever segment was one panel in length and was composed of six identical subpanels with all side truss and lateral X-bracing truss members represented by truss elements. The equivalent straight beam stiffnesses for each cantilevered segment were derived using the methods described in Section 3.1.1. The three sets of stiffnesses which resulted were then used for all of the straight beam elements representing the south approach span, main span and north approach span decks, respectively.

The deck abutment connections were modeled as semi-rigid with global Z axis rotations and warping displacements allowed but with the remaining degrees of freedom at these nodes restrained. The deck expansion joints at panel points 5 and 19 were modeled such that only Y and Z

axis shear forces and X axis torsional moments would be transferred between the main span deck and the approach span decks at these points.

B.1.6 MAIN SPAN DECK MASS DISTRIBUTION

The weight of the NRGB main span deck was calculated using the bridge plans which break the deck down into its various constituent quantities including: pounds of steel, square feet of concrete slab, linear feet of parapet, etc. The mass of the main span deck was then derived by dividing the total weight by the gravitational acceleration constant g . This total main span deck mass was then lumped in the Y and Z directions at each deck nodal point assuming a uniform distribution along the length of the deck.

In order to keep the total number of degrees of freedom for the in-plane model of NRGB to only 34 (the same as CSCB), deck masses were lumped in the X direction at panel points 5, 8, 11, 13, 16 and 19 only. Because the main span deck is horizontal and parallel with the X axis, it was felt that lumping the deck masses at only 6 points in the X direction would have little affect on the bridge responses.

B.1.7 BENT DESCRIPTIONS

There are 22 bents in NRGB with bents 1 to 5 in the south approach span, bents 6 to 18 in the main span and bents 19 to 22 in the north approach span. The bents in the approach spans are bolted to concrete pedestals at their bases while those in the main span, with the exception of bent 12, are welded to the arch top chords at their bases.

All of the bents except bent 12 consist of two box shaped columns and one box girder cap. The column web plates, which are parallel with the bridge centerline, vary in size from 1 by 142 1/2 inches at the bases of the tallest bents to 5/8 by 47 1/2 inches at the tops of all of

the column bents. The width of the column flange plates varies from 40 to 40 3/4 inchs, but the thickness is constant at 1 1/4 inches. The bent caps are all box girders with 1/2 by 47 inch flange plates and 3/4 by 96 inch web plates.

All of the bents except 11, 12 and 13 have some form of diagonal plate girder cross-bracing with 1 by 22 inch flange plates and with 11/16 by 27 inch webs. In bents 10 and 14 the diagonal cross-bracing takes the form of a V (see Figure B-9a) with the bracing members fastened at their tops to the ends of the bent top strut and at their bases to the center of the top lateral arch strut. Diagonal members forming an X are used as cross-bracing in bents 1, 9, 15 and 22 (see Figure B-9b); while diagonal members forming two X's are utilized in bents 2, 3, 7, 8, 16, 17 and 21. Bents 4, 6, 18 and 20 utilize diagonal members which form three X's; while bents 5 and 19 contain diagonal cross-bracing in the form of four X's.

The connections between the bents (excluding bent 12) and the deck take one of two forms: pins or rollers. The connections at bents 5 and 19, where the deck expansion joints occur, have already been discussed and contain both types of connections. Bents 1, 2, 3, 4, 6, 7, 8, 9, 16, 17, 18, 20, 21, and 22 are connected to the bottom chord of the deck side trusses by pin connections (see Figure B-10a), while bents 10, 11, 13 and 14 are connected by rollers (see Figure B-10b).

As can be seen in Figure B-11, bent 12 consists of two sets of four members with one vertical member, two longitudinal diagonal members and one lateral diagonal member in each set. The primary purpose of the vertical truss members is to transfer vertical forces from the deck side trusses to the arch side trusses. Beginning at the bottom chord of one

deck side truss at panel point 12, each vertical member runs down to the top chord of the arch side truss immediately below. These vertical truss members are fastened to the deck bottom chords by welded connections and to the arch top chords by pin connections. These pins, which rest on top of the arch top chords, prevent the transfer of lateral Z axis moments between the truss support members at bent 12 and the arch top chord.

Bent 12 was the only bent designed to transfer longitudinal X axis forces from the deck to the arch and hence the longitudinal diagonal truss members at bent 12 provide the principal means by which such transfers occur in NRGB. These longitudinal diagonal members run from the bottom chords of the deck side trusses at the adjacent subpanel points to the pin connections described above.

The lateral diagonal members depicted in Figure B-11 run from the quarter points of the deck floorbeam bottom chord to the pin connections described above. These lateral diagonals serve to transfer lateral forces from the deck to the arch at panel point 12.

B.1.8 MAIN SPAN BENT MODELING

All of the bents in the NRGB main span, except bent 12, were modeled as beams with global X axis shear and global Y and Z axis moment releases. The bents with deck roller connections do in effect have such releases, while the bents with deck pin connections are long enough to be assumed to have such releases with little effect on analysis results. This latter assumption is reinforced by the fact that only bent 12 was designed to transfer longitudinal X axis forces from the deck to the arch.

The remaining stiffnesses for the beam elements that represented

the main span bents (except bent 12) in the NRGB models were determined using two-dimensional cantilevered analyses of each bent. All of the bent members were utilized in these analyses with the columns and top struts represented by beam elements and the diagonal bracing represented by truss elements. The bents were fixed at their bases and loaded at their tops in their global Y-Z planes, as shown in Figure B-12, in much the same manner as the cantilevered segments of arch and deck were fixed and loaded. The methods that were then used to derive the axial area, global Z axis shear area, the moment of inertia about the global X axis and the effective member length for the main span bents were the same as the methods used for the cantilevered segments of arch and deck as described in Section 3.1.1.

The bent at panel point 12 was represented in the NRGB models by a single vertical beam element and by two longitudinal diagonal truss elements. The beam element ran between the deck and arch nodes at panel point 12, while the truss elements ran from the arch node at panel point 12 to the deck nodes at panel points 11 and 13. The stiffness constants for the beam element and the axial areas of the truss elements were determined by analyzing one-half the truss system at panel point 12 as illustrated in Figure B-13. In this analysis, the four members shown in Figure B-13 were represented by truss elements which were pinned at their bases to a common free joint and at their tops to separate fixed nodes. Global X, Y and Z axis forces P_X , P_Y and P_Z were then applied in turn at the common free joint resulting in displacements D_X , D_Y and D_Z , respectively.

The moment of inertia about the global X axis and the shear area in the global Z direction for the beam element at panel point 12 were

determined by using PY and PZ and their resulting displacements. First the equivalent X axis rotation $R_m = 2 * D_y / B$ and Z axis translation T_m due to the equivalent X axis moment $M_X = B * P_Y$ were calculated where B is the distance (72 feet) between the vertical truss elements at panel point 12. Then the Z axis translation $T_p = D_Z$ and equivalent X axis rotation R_p due to the shear force P_z were determined. Finally, equations similar to those discussed in Section 3.1.1 were used to derive the equivalent beam moment of inertia I_{XX} , shear area A_Z and the effective length L_{EX} .

The torsion constant for the beam element at panel point 12 was determined by first calculating the Y axis rotation due to load P_X which is $\Phi_{i-Y} = (2 * D_X) / B$ and the torque due to load P_X which is $T_Y = B * P_X$. The torsion constant was then calculated using the formula $K_t = (T_Y * L) / (G * \Phi_{i-Y})$. In the NRGB models, only the beam element used in representing bent 12 was assigned a torsion constant because only bent 12 was designed to transfer longitudinal forces and hence Y axis moments between the deck and the arch.

The axial areas for the longitudinal diagonal truss elements labelled 1 and 2 in Figure 3-7 were determined such that under a global X axis load of $2P_X$, the X axis displacement at their common node (the arch node at panel point 12) would be D_X (the same as in the analysis of bent 12). The total vertical axial area required at bent 12 was determined by $A = (2 * P_Y * L) / (E * D_Y)$. The contribution of the longitudinal diagonal truss elements to the total axial area A was then subtracted from A to get the axial area of the beam element at panel point 12. All other stiffness constants for the beam element at panel point 12 were taken to be zero.

B.1.9 MAIN SPAN BENT MASS DISTRIBUTION

The total weight of each main span bent was determined using the quantities given in the bridge plans and was divided by g to get the total bent mass. In the NRGB models, the mass of each main span bent was divided equally between the arch and deck nodes to which the beam element representing the bent was attached.

B.1.10 APPROACH SPAN MODELING

The approach spans were represented in the NRGB models by translation and rotation springs at the centroid of the deck at bents 5 and 19. Since global X axis axial deck forces and Y and Z axis deck moments are not continuous at these points, the stiffnesses of the corresponding approach span springs were taken to be zero. Since warping bimoments are also discontinuous at these points, no attempt was made at introducing warping springs. Therefore, only a global X axis rotation spring and Y and Z axis translation springs were needed to represent the approach spans at panel points 5 and 19 in the NRGB models.

In order to derive the stiffnesses of these springs, the north and south approach spans were analyzed in their entirety with the bent diagonals represented as truss elements and with the bent columns, top bent struts and deck represented as beam elements. The centroid of the continuous beam that represented the deck in each approach span was connected to the tops of the bent columns using very stiff or virtually rigid elements. Three loads were then applied in turn at the centroid of the deck at bent 5 in the south approach span and at bent 19 in the north approach span. The first load applied to each approach span was a force F_Y in the global Y direction which resulted in a displacement D_Y , the second load was a force F_Z in the Z direction resulting in a

displacement DZ and the third load was a moment MX about the global X axis which resulted in a rotation Phi-X.

The stiffnesses of the Y and Z axis translation springs representing each approach span were determined by $SY = FY / DY$ and $SZ = FZ / DZ$, respectively. The stiffness of the X axis rotation spring was calculated using $RX = MX / \text{Phi-X}$. In practice, three 10 foot beam elements were used to represent these springs at panel point 5 and at panel point 19. The torsion constant of the X direction beam was determined using $Kt = (10 * RX) / G$, while the cross-sectional areas of the Y and Z direction beams were calculated by $A = (10 * SY) / E$ and by $A = (10 * SZ) / E$, respectively. All other stiffness constants for these beams were taken to be zero.

B.1.11 APPROACH SPAN MASS DISTRIBUTION

Since the bents in the approach spans resist translations of the deck in the global Y and Z directions, the assumption was made that under seismic loading the relative motion of the approach span deck in these directions at a given panel point would be primarily resisted by the stiffness of the bent at that panel point i.e. the stiffness of the approach span deck was ignored. Therefore, in the Y and Z directions, the portion of the south approach span mass that was lumped at panel point 5 in the NRGB models included one half the mass of bent 5 and one half the mass of the deck between bents 4 and 5. Similarly, the portion of the north approach span mass that was lumped at panel point 19 in the Y and Z directions included one half the mass of bent 19 and one half the mass of the deck from panel points 19 to 20. Because of the deck expansion joints at panel points 5 and 19, however, none of the mass of either approach span was included in the X direction lumped masses at

these points.

B.2 CSCB MODELING DETAILS

B.2.1 ARCH DESCRIPTION

The arch ribs in CSCB are 9 foot by 3 foot steel box girders with 15/16 inch webs and with flanges varying in thickness from 3 1/2 inches near the quarter points to 1 1/2 inches near the abutments and 2 inches at the crown. The arch ribs are connected by transverse crossframes and by lateral K-bracing.

The crossframes shown in Figure 3-8 are composed of five members each: continuous top and bottom HP section chords, a WT8x18 post and two WT8x25 diagonals. The top and bottom chords are HP10x42 sections for the crossframes from panel points 8 to 15, and are HP10x57 sections for the remaining crossframes.

The arch laterals depicted in Figure B-12 are systems of HP section members that form lateral K-bracing between the crossframe top chords and between the crossframe bottom chords. The top and bottom laterals are HP10x42 sections for those pairs of laterals between panel points 8 and 15, and HP10x57 sections between panel points 6 and 8 and between panel points 15 and 17.

The arch ribs are connected at the abutments to the hinge connections depicted in Figure B-15. As in the case of NRGB, these hinge connections allow Z axis rotations only.

B.2.2 ARCH MODELING

Three cantilevered segments were utilized in determining the equivalent straight beam stiffnesses of the CSCB arch: one using the average member sizes (stiffnesses and lengths) in end panels 6-7 and 16-17, the second using the average member sizes in panels 8-9 and

14-15, and the third using the average members sizes in the center panel 11-12. Each cantilevered segment was composed of four identical subpanels with the arch ribs represented by continuous straight beam elements and the remaining arch members represented by truss elements. The methods described in Section 3.1.1 were followed in determining equivalent straight beam stiffnesses for each cantilevered segment. Between adjacent panel points the arch was modeled using a single straight beam element with stiffnesses derived by linear interpolation between the values for panels 6-7, 8-9, 11-12, 14-15 and 16-17.

Because the arch ribs and the top and bottom laterals give the CSCB arch cross-section a box-like configuration, warping of the arch was assumed to be negligible and twelve degree of freedom straight beam finite elements were used to represent the arch in CSCB. As in the case of NRGB, the hinges at the arch abutments were modeled such that only global Z axis rotations were allowed at these points.

B.2.3 DECK DESCRIPTION

The typical deck cross-section consists of six components: a two-way reinforced concrete roadway slab, four steel floor stringers and a deck lateral. The concrete roadway slab is 7 1/4 inches thick and 34 feet wide with a 1 1/2% tilt for water runoff. The slab is fastened to each floor stringer by trios of 7/8 inch shear connectors spaced every 6 to 18 inches.

All of the floor stringers in the deck are plate girders with 52 by 5/16 inch web plates, 10 inch wide top flange plates and 12 inch wide bottom flange plates. While all four floor stringers at any given cross-section are the same, the thicknesses of the top and bottom flange plates do vary along the length of the deck. The top flange plate

varies from 5/8 inch to 1 inch in thickness while the bottom flange plate varies from 5/8 inch to 1 1/8 inch in thickness. Averaging the top flange plate thicknesses and the bottom flange plate thicknesses over each panel yields four different average floor stringer cross-sections for the CSCB deck.

The deck laterals are illustrated in Figure B-16 and are WT8x18 sections that run in a zig-zag fashion between the two outer floor stringers in a plane 11 inches above the bottom of the stringer web plates.

The expansion connections between the floor stringers and the abutment at panel point 1 which are illustrated in Figure B-17 have curved, selflubricating, bronze bearing plates that allow large global Z axis rotations of the stringers at these points. In addition, these bronze bearing plates have a flat side that allows global X and Z axis translations of the stringers. The clearances for global X axis translation are +8 1/2 and -6 1/2 inches, but the clearances for global Z axis translation are only 1/16 of an inch.

The bearing connections between the stringers and the abutment at panel point 20 are depicted in Figure B-18 and have 2 inch elastomeric bearing pads that allow large global Z axis rotations and some global X axis translations of the stringers at these points. The system of deck laterals ends at panel point 20 with a pin connection at the center of the deck (see Figure B-14) that prevents any global X or Z axis translation of the deck as a whole at this point, but does allow global Y axis rotation.

Between the deck abutments the continuity of the deck is broken at the two towers located at panel points 6 and 17. At these points the

deck floor stringers are connected to the towers by pins located 33 inches from and on either side of the tower centerlines. These pins prevent the transfer of global Z axis moments and bimoments between the approach span and main span decks.

B.2.4 DECK MODELING

Equivalent straight beam stiffnesses for the CSCB deck were calculated based on the composite action of the four floor stringers and the concrete roadway deck. Because there are four average floor stringer cross-sections in the CSCB deck and hence four average deck cross-sections, four sets of deck stiffnesses were calculated.

Because the roadway slab can be expected to crack under only moderate loads, the first step in calculating the stiffnesses of the four CSCB deck cross-sections was making an assumption as to what portion of the cross-sectional area of the roadway slab would be in compression and thus contributing to overall deck stiffness at any given time. Since the portion of the slab area in compression could be anything from 0 to 100%, a compromise value of 50% was chosen. This assumption coupled with a modular ratio of steel to concrete of 10 led to an "effective" modular ratio of 20. Thus the area of concrete was reduced by a factor of 20 and then used in conjunction with the areas of the four floor stringers, the slab reinforcing steel and the deck laterals to calculate the axial area, shear areas, moments of inertia and the torsion constant for each deck cross-section.

In determining the warping constants for the equivalent deck beams each deck cross-section was first converted to a channel section with the concrete roadway slab acting as the channel web and the outside stringers acting as the channel flanges. The first step in this

conversion was to reduce the area of concrete by a factor of 20 and then divide by 28 feet (the distance between the outside stringers) to get an effective channel web thickness w . Next the average distance from the center of the roadway slab to the bottoms of the floor stringers was calculated and used as the channel flange width b . Then an effective channel flange thickness t was calculated by determining the thickness of a rectangular flange with depth b that is required to give a flange moment of inertia equal to 1.33 times the moment of inertia of one floor stringer. The factor of 1.33 was based on 100% of the stiffness of one exterior floor stringer plus 33% of the stiffness of one interior floor stringer. Finally, with all of the channel dimensions determined, the values were substituted into the general warping constant formula for a channel section and thus the warping constants for the four deck cross-sections were determined.

The deck expansion connection at panel point 1 was modeled as semi-rigid with global X axis translations, Y and Z axis rotations, and warping displacements of the deck allowed at this point. The bearing connection at panel point 20 was also modeled as semi-rigid but with only Y and Z axis rotations and warping displacements allowed at this point. The deck joints at panel points 6 and 17 were modeled such that no Z axis moments or warping bimoments could be transferred between the approach span decks and the main span deck at these points.

B.2.5 COLUMN, TOWER AND CABLE DESCRIPTIONS

The columns in CSCB are located at all panel points except 1, 6, 17 and 20 and are 24 1/2 by 25 inch box shapes with 1/2 inch wall thicknesses. The columns at panel points 2, 3, 4 and 5 are in the south approach span, those at panel points 7 to 16 are in the main span and

those at panel points 18 and 19 are in the north approach span. The approach span columns rest on concrete pedestals while the main span columns rest on the arch ribs. The two columns at a given panel point serve to support the ends of the deck floorbeam at that panel point. All of the columns are fastened at both top and bottom by hinged connections as depicted in Figure B-19 that prevent the transfer of moments at these points.

The towers depicted in Figure B-20 are located at panel points 6 and 17 and are each composed of five members: two 48 by 52 1/2 inch box shape columns with 1 1/4 inch wall thicknesses and with their longer sides normal to the centerline of the bridge, two 73 1/2 by 30 inch box girder intermediate struts with 1 1/4 inch flange plates and 1/2 inch webs, and a single composite top strut composed of a 61 3/4 by 30 inch box girder with 7/8 inch flange plates and 5/8 inch webs and topped by a short segment of concrete slab which varies in thickness from 7 1/4 to 12 11/16 inches. The tower columns rest on concrete skewbacks and are anchored to the skewbacks by a system of 29 prestressed 1 3/8 inch rods.

There are four pair of tensioned cables that run between the deck and the arch with two pair lying in the planes of the arch ribs and two pair lying in vertical planes normal to the global X axis. The latter pair of cables are illustrated in Figure B-21 and are located at panel points 11 and 12. They are composed of 1 1/4 inch bridge rope which is tensioned to 2000 psi and has a minimum breaking strength of 96 tons. As can be seen in Figure B-21, these lateral cables run from the center of the crossframe top chord to points on the bottom of the deck floorbeam near where the columns are attached.

The two pair of cables lying in the same vertical planes as the

arch ribs are depicted in Figure B-22 and are located roughly between panel points 11 and 12. These longitudinal cables are composed of 1 5/8 inch bridge rope which is tensioned to 7000 psi and has a minimum breaking strength of 162 tons. Each longitudinal cable begins at a point near where the column at one panel point (11 or 12) is connected to the top cover plate of the arch rib. It then runs through a point midway between the top and bottom flanges of the deck floorbeam at the other panel point. Finally it ends at a point 98 inches from the second panel point where it is fastened to a short plate girder.

B.2.6 MAIN SPAN COLUMN AND CABLE MODELING

Except for the columns at panel points 11 and 12, each pair of main span columns at a given panel point were represented by a single truss element in the CSCB models. Truss elements were chosen because the columns in CSCB (excluding the towers) are hinged at both top and bottom. The cross-sectional area of these truss elements was taken to be twice the cross-sectional area of one column.

The systems of columns and transverse cables at panel points 11 and 12 were each represented by a single beam element in the CSCB models. The stiffnesses of these beam elements were determined in much the same way as the stiffness constants for the beam element representing the bent at panel point 12 in the NRGB models. A pair of truss elements representing one column and one lateral cable as illustrated in Figure B-23a were analyzed in two dimensions. The truss elements were connected at their tops to a common free joint and at their bases to separate fixed nodes. Loads PY and PZ were each applied in turn at the free joint resulting in translations DY and DZ. The axial areas of the equivalent beams at panel points 11 and 12 were determined using

$A = (2 * PY * L) / (E * DY)$ where L is the distance between the arch and deck nodes at panel points 11 and 12 in the one plane models of CSCB.

The moment of inertia about the global X axis and the shear area in the global Z direction for the beam elements at panel points 11 and 12 were determined by using PY and PZ and their resulting displacements. First the equivalent X axis rotation $R_m = 2 * Dy / B$ and Z axis translation T_m due to the equivalent X axis moment $MX = B * PY$ were calculated where B is the distance (26 feet) between the columns at panel points 11 and 12. Then the Z axis translation $T_p = DZ$ and equivalent X axis rotation R_p due to the shear force Pz were determined. Finally, equations similar to those discussed in Section 3.1.1 were used to derive the equivalent beam moment of inertia IXX , shear area AZ and the effective length LEX .

The two pair of longitudinal diagonal cables running between panel points 11 and 12 were represented in the CSCB models by the two truss elements labeled 1 and 2 in Figure 3-9. Each truss element ran from the arch node at one panel point to the deck node at the other panel point and together they formed an X.

Because they transfer longitudinal forces between the deck and the arch, the longitudinal cables in CSCB must also transfer vertical Y axis moments. The torsional stiffnesses of the beam elements at panel points 11 and 12 were used to represent this transfer mechanism. The method used to calculate these torsional stiffnesses was similar to the method used for bent 12 in NRGB.

In calculating the torsional stiffness due to the longitudinal cables, two pair of truss elements (as depicted in Figures B-23b and B-23c) were analyzed in two dimensions. The first pair represented a

column at panel point 11 and a longitudinal cable running from the deck at panel point 11 to the arch at panel point 12. The second pair represented a column at panel point 12 and a cable running from the arch at panel point 11 to the deck at panel point 12. The truss elements in each pair were connected at their tops to a common free joint and at their bases to separate fixed nodes. A load PX was applied at the free joint of each pair of truss elements resulting in translations $DX1$ and $DX2$, respectively. The torque $T = B * PX$ and the average rotation $\Phi-Y = (DX1 + DX2) / B$ were then determined. Then the torsion constants for the beam elements at panel points 11 and 12 were calculated using $Kt = (T * L) / (G * \Phi-Y)$.

B.2.7 APPROACH SPAN MODELING

As in the case of NRGB, the approach spans in CSCB were represented by translations and rotations springs. In CSCB these translation and rotation springs were located at the centroid of the deck at panel points 6 and 17. Because of the Z axis moment and the bimoment releases in the deck at panel points 6 and 17, no Z axis rotation springs or warping springs were needed at these points to represent the approach spans. Between the deck abutments, the deck is continuous with respect to global Z axis shear forces and moments about the Y axis, however, thus it was necessary to include beam elements representing the approach span decks in the CSCB models.

The beam elements used to represent the approach span decks were parallel with the global X axis and had the same length, the average Y axis moment of inertia and the average Z axis shear area as the deck segments that they represented. The remaining stiffnesses (axial, torsional, etc.) of the approach span decks were represented as part of

the stiffnesses of the translation and rotation springs at panel points 6 and 17 as described below.

In order to derive the stiffnesses of the X and Y axis translation springs and X axis rotation springs at panel points 6 and 17, the north and south approach spans were analyzed in their entirety with the tower columns, tower struts and deck represented as beam elements and the remaining columns represented as truss elements. The centroid of the continuous beam that represented the deck in each approach span was fastened to the tops of the columns using virtually rigid elements. Three loads were then applied in turn at the centroid of the deck at panel point 6 in the south approach span and at panel point 17 in the north approach span. The first load applied was a force F_X in the global X direction which resulted in a displacement D_X , the second load was a Y direction force F_Y which resulted in a displacement D_Y and the third load was a moment M_X about the global X axis which resulted in a rotation $\Phi-X$.

The stiffnesses of the X and Y axis translation springs representing each approach span were determined by $S_X = F_X / D_X$ and $S_Y = F_Y / D_Y$, respectively. The stiffness of the X axis rotation spring was calculated using $R_X = M_X / \Phi-X$. In practice, since the approach span decks were represented by beam elements parallel with the global X axis, the X axis translation and rotation springs at panel points 6 and 17 were represented by the axial areas and torsion constants of these beam elements. The axial areas were calculated using $A = (L * S_X) / E$ where L is the length of the given beam element (approach span deck). The torsion constants for these beam elements were determined using $K_t = (L * R_X) / G$. As in the case of NRGB, the Y axis translation

springs at panel points 6 and 17 in CSCB were represented by 10 foot beam elements whose axial areas were determined by the formula

$$A = (10 * SY) / E.$$

Since the approach span decks are represented by beam elements with respect to Z axis translation and Y axis rotation, only the towers were analyzed in deriving the stiffnesses of the Z axis translation springs and Y axis rotation springs at panel points 6 and 17. In this analysis, all of the tower elements were represented by beam elements with the tops of the tower columns connected by virtually rigid elements to a node at the centroid of the deck. Two loads were then applied in turn at the centroid of the deck. The first load was a force FZ applied in the global Z direction which resulted in a displacement DZ and the second load was a moment MY about the Y axis which yielded a rotation Phi-Y.

The stiffnesses of the Z axis translation springs and the Y axis rotation springs were determined using $SZ = FZ / DZ$ and $RY = MY / \text{Phi-Y}$, respectively. In practice, the beam elements used to represent the Y axis translation springs at panel points 6 and 17 were the same elements used to represent the Y axis rotation springs. Additional beam elements at panel point 6 and 17 with lengths of 10 feet each were used to represent the Z axis translation springs. The torsion constants of the Y direction beam elements were determined using $Kt = (10 * RY) / G$, while the axial areas of the Z direction beam elements were calculated by the formula $A = (10 * SZ) / E$. All other stiffness constants for the beam elements representing the CSCB approach spans were taken to be zero.

B.2.8 BRIDGE MASS DISTRIBUTION

Average dead load weights of 3930 pounds per foot, 5335 pounds per foot and 210 pounds per foot for the CSCB arch, deck and columns, respectively, are listed in Reference 14. These dead load weights were the basis for the lumped nodal masses which were used in the 1982 Study of CSCB. These same lumped nodal masses were used in the present study with some modifications for the approach spans.

For the present study, portions of the CSCB approach span deck, tower and column masses were lumped at the deck nodes at panel point 6 for the south approach span and panel point 17 for the north approach span. For the north approach span, half of the deck and tower masses and one-fourth of the column masses were lumped at panel point 17 in the X, Y and Z directions. Similarly, for the south approach span, half of the deck and tower masses and one-fourth of the column masses were lumped at panel point 6 in the Y and Z directions. Because of the deck expansion joint at panel point 1, all of the mass of the south approach span deck was lumped in the X direction at panel point 6 along with half of the mass of the tower at panel point 6 and half the mass of the columns in the south approach span.

B.3 INPUT LISTINGS

The following pages contain input listings for Bl-Bl' loading of the NRGB in-plane model in the X direction, the NRGB out-of-plane model in the Z direction, the CSCB in-plane model in the X direction and the CSCB out-of-plane model in the Z direction. Figures B-24 and B-25 depict the NRGB and CSCB models with the node numbers and element numbers used in the analyses labelled.

NEW RIVER GORGE BRIDGE - ACCELEROGRAM B1 APPLIED WITH PHASE SHIFT IN X DIRECTION

[illegible]

2	0.996022	0.303590	0.118200	1304.52	80.6544	12.8040	82337.9
132.834	129.712	142.650					
7082.35	254965.0	63741.2	2294682.0	7082.35	254965.0	63741.2	2294682.0
0.5		-30093.3		-0.5		16904.7	
3	0.996022	0.303590	0.118200	1304.52	80.6544	12.8040	82337.9
132.834	129.712	142.650					
7082.35	254965.0	63741.2	2294682.0	7082.35	254965.0	63741.2	2294682.0
0.0		-16904.7		0.0		17306.0	
4	0.0000000	0.000000	0.000000	0.00	0.0000	347.4750	
0.							
1.	1.	1.	1.	1.	1.	1.	1.
0.							
5	0.0850942	0.000000	0.000000	0.00	0.0000	0.0000	
0.							
1.	1.	1.	1.	1.	1.	1.	1.
0.							
6	0.0026701	0.000000	0.000000	0.00	0.0000	0.0000	
0.							
1.	1.	1.	1.	1.	1.	1.	1.
0.							
7	0.0000000	0.000000	0.000000	0.00	0.0000	352.7310	
0.							
1.	1.	1.	1.	1.	1.	1.	1.
0.							
8	0.0886640	0.000000	0.000000	0.00	0.0000	0.0000	
0.							
1.	1.	1.	1.	1.	1.	1.	1.
0.							
9	0.0028963	0.000000	0.000000	0.00	0.0000	0.0000	
0.							
1.	1.	1.	1.	1.	1.	1.	1.
0.							
10	3.52903	0.00000	0.549991	3459.75	0.0000	0.0000	
269.390							
28030.2	1009086.	1.	1.	17414.1	626906.	1.	1.
2271.1				-2271.1			
11	3.43683	0.00000	0.587033	3438.65	0.0000	0.0000	
197.438							
22800.0	820798.	1.	1.	18119.1	652287.	1.	1.
2132.8				-2132.8			
12	3.39486	0.00000	0.802843	3201.43	0.0000	0.0000	
131.003							
20580.8	740908.	1.	1.	16976.6	611157.	1.	1.
2042.2				-2042.2			
13	4.06142	0.00000	0.791567	3115.42	0.0000	0.0000	
83.0217							
17297.9	622723.	1.	1.	17297.9	622723.	1.	1.
1966.4				-1966.4			
14	4.91382	0.00000	1.530670	5805.94	0.0000	0.0000	
85.5870							
16695.4	601033.	1.	1.	16695.4	601033.	1.	1.
1912.6				-1912.6			
15	5.92216	0.00000	0.182354	2655.29	0.0000	0.0000	
19.4527							

16335.9	588094.	1.	1.	16335.9	588094.	1.	1.
1886.2				-1886.2			
16	3.04191	0.00000	0.768549	6020.25	0.0000	3960.9600	
69.5167							
12260.2	441366.	1.	1.	12260.2	441366.	1.	1.
1832.3				-1832.3			
17	14.4280	0.483997	1.621630	24946.8	9774.56	1355.360	
128.052	92.631						
129725.3	4670120.	2678184.		1.	103620.4	3730340.	2678184.
35514.6		0.0			-35514.6		43978.5
18	13.8356	0.482150	1.536830	23921.4	8823.50	1277.170	
241.505	174.633						
103620.4	3730340.	2678184.		1.	97931.5	3525540.	2368498.
32699.1		43978.5			-32699.1		-73519.4
19	13.0770	0.479784	1.428250	22608.4	7605.71	1177.040	
226.545	163.726						
97931.5	3525540.	2368498.		1.	92643.4	3335160.	2096060.
30385.1		73519.4			-30385.1		-102759.0
20	12.3660	0.477567	1.326480	21377.8	6464.36	1083.190	
212.524	153.503						
92643.4	3335160.	2096060.		1.	87643.4	3155160.	1853374.
28599.5		102759.0			-28599.5		-92526.7
21	11.6891	0.475456	1.229600	20206.3	5377.82	993.854	
199.176	143.771						
87643.4	3155160.	1853374.		1.	82849.3	2982580.	1634933.
27345.6		92526.7			-27345.6		-45173.6
22	11.0364	0.473421	1.136170	19076.6	4329.99	907.700	
186.305	134.386						
82849.3	2982580.	1634933.		1.	78198.3	2815140.	1435822.
26552.8		45173.6			-26552.8		5065.7
23	10.3989	0.471433	1.044920	17973.2	3306.59	823.553	
173.733	125.219						
78198.3	2815140.	1435822.		1.	73624.3	2650480.	1251613.
26178.9		-5065.7			-26178.9		18784.3
24	10.3989	0.471433	1.044920	17973.2	3306.59	823.553	
173.733	125.219						
73624.3	2650480.	1251613.		1.	78198.3	2815140.	1435822.
26178.9		-18784.3			-26178.9		5057.5
25	11.0364	0.473421	1.136170	19076.6	4329.99	907.700	
186.305	134.386						
78198.3	2815140.	1435822.		1.	82849.3	2982580.	1634933.
26552.7		-5057.5			-26552.7		-45190.3
26	11.6891	0.475456	1.229600	20206.3	5377.82	993.854	
199.176	143.771						
82849.3	2982580.	1634933.		1.	87643.4	3155160.	1853374.
27345.5		45190.3			-27345.5		-92552.5
27	12.3660	0.477567	1.326480	21377.8	6464.36	1083.190	
212.524	153.503						
87643.4	3155160.	1853374.		1.	92643.4	3335160.	2096060.
28599.5		92552.5			-28599.5		-102791.0
28	13.0770	0.479784	1.428250	22608.4	7605.71	1177.040	
226.545	163.726						
92643.4	3335160.	2096060.		1.	97931.5	3525540.	2368498.
30385.0		102791.0			-30385.0		-73578.7

29	13.8356	0.482150	1.536830	23921.4	8823.50	1277.170	
	241.505	174.633					
	97931.5	3525540.	2368498.	1.	103620.4	3730340.	2678184. 1.
	32699.6		73578.7		-32699.6		-43917.1
30	14.4280	0.483997	1.621630	24946.8	9774.56	1355.360	
	128.052	92.631					
103620.4	3730340.	2678184.		1.	129725.3	4670120.	2678184. 1.
	35514.0	43917.1			-35514.0		0.0
-31	0.996022	0.303590	0.118200	1304.52	80.6544	12.8040	82337.9
	132.834	129.712	142.650				
	7082.35	254965.0	63741.2	2294682.0	7082.35	254965.0	63741.2 2294682.0
	0.0		-17306.0		0.0		16981.4
-32	0.996022	0.303590	0.118200	1304.52	80.6544	12.8040	82337.9
	132.834	129.712	142.650				
	7082.35	254965.0	63741.2	2294682.0	7082.35	254965.0	63741.2 2294682.0
	-0.1		-16981.4		0.1		18622.8
-33	0.996022	0.303590	0.118200	1304.52	80.6544	12.8040	82337.9
	132.834	129.712	142.650				
	7082.35	254965.0	63741.2	2294682.0	7082.35	254965.0	63741.2 2294682.0
	-0.1		-18622.8		0.1		20889.0
-34	0.996022	0.303590	0.118200	1304.52	80.6544	12.8040	82337.9
	132.834	129.712	142.650				
	7082.35	254965.0	63741.2	2294682.0	7082.35	254965.0	63741.2 2294682.0
	-155.6		-20889.0		155.6		20579.3
-35	0.996022	0.303590	0.118200	1304.52	80.6544	12.8040	82337.9
	132.834	129.712	142.650				
	7082.35	254965.0	63741.2	2294682.0	7082.35	254965.0	63741.2 2294682.0
	-155.6		-20579.3		155.6		20888.9
36	0.996022	0.303590	0.118200	1304.52	80.6544	12.8040	82337.9
	132.834	129.712	142.650				
	7082.35	254965.0	63741.2	2294682.0	7082.35	254965.0	63741.2 2294682.0
	-0.1		-20888.9		0.1		18622.5
-37	0.996022	0.303590	0.118200	1304.52	80.6544	12.8040	82337.9
	132.834	129.712	142.650				
	7082.35	254965.0	63741.2	2294682.0	7082.35	254965.0	63741.2 2294682.0
	-0.1		-18622.5		0.1		16981.2
-38	0.996022	0.303590	0.118200	1304.52	80.6544	12.8040	82337.9
	132.834	129.712	142.650				
	7082.35	254965.0	63741.2	2294682.0	7082.35	254965.0	63741.2 2294682.0
	0.0		-16981.2		0.0		17303.6
-39	0.996022	0.303590	0.118200	1304.52	80.6544	12.8040	82337.9
	132.834	129.712	142.650				
	7082.35	254965.0	63741.2	2294682.0	7082.35	254965.0	63741.2 2294682.0
	0.0		-17303.6		0.0		16918.2
-40	0.996022	0.303590	0.118200	1304.52	80.6544	12.8040	82337.9
	132.834	129.712	142.650				
	7082.35	254965.0	63741.2	2294682.0	7082.35	254965.0	63741.2 2294682.0
	0.5		-16918.2		-0.5		29986.6
-41	0.996022	0.303590	0.118200	1304.52	80.6544	12.8040	82337.9
	132.834	129.712	142.650				
	7082.35	254965.0	63741.2	2294682.0	7082.35	254965.0	63741.2 2294682.0
	0.0		-29986.6		0.0		0.0
1	8	10	1	1	1	1	1.
2	10	12	1	2	2	2	1.

3	12	14	1	3	3	3	1.
4	14	16	1	31	31	31	1.
5	16	18	1	32	32	32	1.
6	18	20	1	33	33	33	1.
7	20	22	1	34	34	34	1.
8	22	24	1	35	35	35	1.
9	24	26	1	36	36	36	1.
10	26	28	1	37	37	37	1.
11	28	30	1	38	38	38	1.
12	30	32	1	39	39	39	1.
13	32	34	1	40	40	40	1.
14	34	36	1	41	41	41	1.
15	9	10	1	10	10	10	1.
16	11	12	1	11	11	11	1.
17	13	14	1	12	12	12	1.
18	15	16	1	13	13	13	1.
19	17	18	1	14	14	14	1.
20	19	20	1	15	15	15	1.
21	21	22	1	16	16	16	1.
22	23	24	1	15	15	15	1.
23	25	26	1	14	14	14	1.
24	27	28	1	13	13	13	1.
25	29	30	1	12	12	12	1.
26	31	32	1	11	11	11	1.
27	33	34	1	10	10	10	1.
28	4	8	1	4	4	4	1.
29	5	8	1	5	5	5	1.
30	6	8	5	6	6	6	1.
31	36	40	1	7	7	7	1.
32	36	41	1	8	8	8	1.
33	36	42	41	9	9	9	1.
34	7	9	1	17	17	17	1.
35	9	11	1	18	18	18	1.
36	11	13	1	19	19	19	1.
37	13	15	1	20	20	20	1.
38	15	17	1	21	21	21	1.
39	17	19	1	22	22	22	1.
40	19	21	1	23	23	23	1.
41	21	23	1	24	24	24	1.
42	23	25	1	25	25	25	1.
43	25	27	1	26	26	26	1.
44	27	29	1	27	27	27	1.
45	29	31	1	28	28	28	1.
46	31	33	1	29	29	29	1.
47	33	35	1	30	30	30	1.
9	62.8167	62.8167					
33	62.8167	62.8167					
11	65.9538	65.9538					
31	65.9538	65.9538					
13	57.0212	57.0212					
29	57.0212	57.0212					
15	49.9338	49.9338					
27	49.9338	49.9338					
17	44.4994	44.4994					

25	44.4994	44.4994					
19	40.6756	40.6756					
23	40.6756	40.6756					
21	36.7035	36.7035					
8	98.9825	79.0403					
10		70.5313					
12		66.2353					
14	190.7242	63.4213					
16		61.0676					
18		59.3990					
20	146.4268	58.5766					
22		56.9024					
24	146.4268	58.5766					
26		59.3990					
28		61.0676					
30	190.7242	63.4213					
32		66.2353					
34		70.5313					
36	98.9825	77.5134					
0							
0.101699	0.0215163		0.25	0.025		30.0	
1	2 2000	0	0	6	0	0	6 3
1	1	1.333					
2	1	1.333		0.3			

NEW RIVER GORGE BRIDGE - ACCELEROGRAM B1 APPLIED WITH PHASE SHIFT IN Z DIRECTION

49	42	2	0	-4	3	0	1	1	1	1	1	10					
1	1	1	0	1	1	1	1	0	0	0	0	0	-1	48.250	0.0000		
2	1	1	0	1	1	1	1	0	0	1	0	0	0	58.250	-10.0000		
3	1	1	0	1	1	1	1	0	0	1	0	0	0	58.250	0.0000	10.	
4	1	1	0	1	1	1	1	0	0	1	0	0	0	-10.000	414.2410		
5	1	1	0	1	1	1	1	0	0	1	0	0	0	0.000	404.2410		
6	1	1	0	1	1	1	1	0	0	1	0	0	0	0.000	414.2410	10.	
7	1	1	0	1	1	1	1	0	0	1	0	0	0	58.250	0.0000		
8	1	1	0	0	0	1	0	0	0	0	-1	-1	0	-1	0.000	414.2410	
9	1	1	0	0	0	1	1	0	0	0	-1	-1	0	0	129.750	64.0696	
10	1	1	0	0	0	1	0	0	0	0	-1	-1	0	-1	129.750	414.8900	
11	1	1	0	0	0	1	1	0	0	0	-1	-1	0	0	259.500	160.6157	
12	1	1	0	0	0	1	0	0	0	0	-1	-1	0	-1	259.500	415.5400	
13	1	1	0	0	0	1	1	0	0	0	-1	-1	0	0	389.250	236.5676	
14	1	1	0	0	0	1	0	0	0	0	-1	-1	0	-1	389.250	416.1900	
15	1	1	0	0	0	1	1	0	0	0	-1	-1	0	0	519.000	294.6259	
16	1	1	0	0	0	1	0	0	0	0	-1	-1	0	-1	519.000	416.8400	
17	1	1	0	0	0	1	1	0	0	0	-1	-1	0	0	648.750	336.3683	
18	1	1	0	0	0	1	0	0	0	0	-1	-1	0	-1	648.750	417.4820	
19	1	1	0	0	0	1	1	0	0	0	-1	-1	0	0	778.500	361.6971	
20	1	1	0	0	0	1	0	0	0	0	-1	-1	0	-1	778.500	417.9920	
21	1	1	0	0	0	1	1	0	0	0	-1	-1	0	0	908.250	370.0000	
22	1	1	0	0	0	1	0	0	0	0	-1	-1	0	-1	908.250	418.1880	
23	1	1	0	0	0	1	1	0	0	0	-1	-1	0	0	1038.000	361.6971	
24	1	1	0	0	0	1	0	0	0	0	-1	-1	0	-1	1038.000	417.9920	
25	1	1	0	0	0	1	1	0	0	0	-1	-1	0	0	1167.750	336.3683	
26	1	1	0	0	0	1	0	0	0	0	-1	-1	0	-1	1167.750	417.4820	
27	1	1	0	0	0	1	1	0	0	0	-1	-1	0	0	1297.500	294.6259	
28	1	1	0	0	0	1	0	0	0	0	-1	-1	0	-1	1297.500	416.8400	
29	1	1	0	0	0	1	1	0	0	0	-1	-1	0	0	1427.250	236.5676	
30	1	1	0	0	0	1	0	0	0	0	-1	-1	0	-1	1427.250	416.1900	
31	1	1	0	0	0	1	1	0	0	0	-1	-1	0	0	1557.000	160.6157	
32	1	1	0	0	0	1	0	0	0	0	-1	-1	0	-1	1557.000	415.5400	
33	1	1	0	0	0	1	1	0	0	0	-1	-1	0	0	1686.750	64.0696	
34	1	1	0	0	0	1	0	0	0	0	-1	-1	0	-1	1686.750	414.8900	
35	1	1	0	1	1	1	1	0	0	37	0	0	0	0	1758.250	0.0000	
36	1	1	0	0	0	1	0	0	0	0	-1	-1	0	-1	1816.500	414.2410	
37	1	1	0	1	1	1	1	0	0	0	0	0	0	-1	1768.250	0.0000	
38	1	1	0	1	1	1	1	0	0	37	0	0	0	0	1758.250	-10.0000	
39	1	1	0	1	1	1	1	0	0	37	0	0	0	0	1758.250	0.0000	10.
40	1	1	0	1	1	1	1	0	0	37	0	0	0	0	1826.500	414.2410	
41	1	1	0	1	1	1	1	0	0	37	0	0	0	0	1816.500	404.2410	
42	1	1	0	1	1	1	1	0	0	37	0	0	0	0	1816.500	414.2410	10.
111111333																	

2	0.996022	0.303590	0.118200	1304.52	80.6544	12.8040	82337.9
132.834	129.712	142.650					
7082.35	254965.0	63741.2	2294682.0	7082.35	254965.0	63741.2	2294682.0
0.5		-30093.3		-0.5		16904.7	
3	0.996022	0.303590	0.118200	1304.52	80.6544	12.8040	82337.9
132.834	129.712	142.650					
7082.35	254965.0	63741.2	2294682.0	7082.35	254965.0	63741.2	2294682.0
0.0		-16904.7		0.0		17306.0	
4	0.0000000	0.000000	0.000000	0.00	0.0000	347.4750	
0.							
1.	1.	1.	1.	1.	1.	1.	1.
0.							
5	0.0850942	0.000000	0.000000	0.00	0.0000	0.0000	
0.							
1.	1.	1.	1.	1.	1.	1.	1.
0.							
6	0.0026701	0.000000	0.000000	0.00	0.0000	0.0000	
0.							
1.	1.	1.	1.	1.	1.	1.	1.
0.							
7	0.0000000	0.000000	0.000000	0.00	0.0000	352.7310	
0.							
1.	1.	1.	1.	1.	1.	1.	1.
0.							
8	0.0886640	0.000000	0.000000	0.00	0.0000	0.0000	
0.							
1.	1.	1.	1.	1.	1.	1.	1.
0.							
9	0.0028963	0.000000	0.000000	0.00	0.0000	0.0000	
0.							
1.	1.	1.	1.	1.	1.	1.	1.
0.							
10	3.52903	0.00000	0.549991	3459.75	0.0000	0.0000	
269.390							
28030.2	1009086.	1.	1.	17414.1	626906.	1.	1.
2271.1				-2271.1			
11	3.43683	0.00000	0.587033	3438.65	0.0000	0.0000	
197.438							
22800.0	820798.	1.	1.	18119.1	652287.	1.	1.
2132.8				-2132.8			
12	3.39486	0.00000	0.802843	3201.43	0.0000	0.0000	
131.003							
20580.8	740908.	1.	1.	16976.6	611157.	1.	1.
2042.2				-2042.2			
13	4.06142	0.00000	0.791567	3115.42	0.0000	0.0000	
83.0217							
17297.9	622723.	1.	1.	17297.9	622723.	1.	1.
1966.4				-1966.4			
14	4.91382	0.00000	1.530670	5805.94	0.0000	0.0000	
85.5870							
16695.4	601033.	1.	1.	16695.4	601033.	1.	1.
1912.6				-1912.6			
15	5.92216	0.00000	0.182354	2655.29	0.0000	0.0000	
19.4527							

16335.9	588094.	1.	1.	16335.9	588094.	1.	1.
1886.2				-1886.2			
16	3.04191	0.00000	0.768549	6020.25	0.0000	3960.9600	
69.5167							
12260.2	441366.	1.	1.	12260.2	441366.	1.	1.
1832.3				-1832.3			
17	14.4280	0.483997	1.621630	24946.8	9774.56	1355.360	
128.052	92.631						
129725.3	4670120.	2678184.		1.	103620.4	3730340.	2678184.
35514.6		0.0			-35514.6		43978.5
18	13.8356	0.482150	1.536830	23921.4	8823.50	1277.170	
241.505	174.633						
103620.4	3730340.	2678184.		1.	97931.5	3525540.	2368498.
32699.1		43978.5			-32699.1		-73519.4
19	13.0770	0.479784	1.428250	22608.4	7605.71	1177.040	
226.545	163.726						
97931.5	3525540.	2368498.		1.	92643.4	3335160.	2096060.
30385.1		73519.4			-30385.1		-102759.0
20	12.3660	0.477567	1.326480	21377.8	6464.36	1083.190	
212.524	153.503						
92643.4	3335160.	2096060.		1.	87643.4	3155160.	1853374.
28599.5		102759.0			-28599.5		-92526.7
21	11.6891	0.475456	1.229600	20206.3	5377.82	993.854	
199.176	143.771						
87643.4	3155160.	1853374.		1.	82849.3	2982580.	1634933.
27345.6		92526.7			-27345.6		-45173.6
22	11.0364	0.473421	1.136170	19076.6	4329.99	907.700	
186.305	134.386						
82849.3	2982580.	1634933.		1.	78198.3	2815140.	1435822.
26552.8		45173.6			-26552.8		5065.7
23	10.3989	0.471433	1.044920	17973.2	3306.59	823.553	
173.733	125.219						
78198.3	2815140.	1435822.		1.	73624.3	2650480.	1251613.
26178.9		-5065.7			-26178.9		18784.3
24	10.3989	0.471433	1.044920	17973.2	3306.59	823.553	
173.733	125.219						
73624.3	2650480.	1251613.		1.	78198.3	2815140.	1435822.
26178.9		-18784.3			-26178.9		5057.5
25	11.0364	0.473421	1.136170	19076.6	4329.99	907.700	
186.305	134.386						
78198.3	2815140.	1435822.		1.	82849.3	2982580.	1634933.
26552.7		-5057.5			-26552.7		-45190.3
26	11.6891	0.475456	1.229600	20206.3	5377.82	993.854	
199.176	143.771						
82849.3	2982580.	1634933.		1.	87643.4	3155160.	1853374.
27345.5		45190.3			-27345.5		-92552.5
27	12.3660	0.477567	1.326480	21377.8	6464.36	1083.190	
212.524	153.503						
87643.4	3155160.	1853374.		1.	92643.4	3335160.	2096060.
28599.5		92552.5			-28599.5		-102791.0
28	13.0770	0.479784	1.428250	22608.4	7605.71	1177.040	
226.545	163.726						
92643.4	3335160.	2096060.		1.	97931.5	3525540.	2368498.
30385.0		102791.0			-30385.0		-73578.7

29	13.8356	0.482150	1.536830	23921.4	8823.50	1277.170	
	241.505	174.633					
	97931.5	3525540.	2368498.	1.	103620.4	3730340.	2678184. 1.
	32699.6		73578.7		-32699.6		-43917.1
30	14.4280	0.483997	1.621630	24946.8	9774.56	1355.360	
	128.052	92.631					
103620.4	3730340.	2678184.		1.	129725.3	4670120.	2678184. 1.
	35514.0		43917.1		-35514.0		0.0
31	0.996022	0.303590	0.118200	1304.52	80.6544	12.8040	82337.9
	132.834	129.712	142.650				
7082.35	254965.0	63741.2	2294682.0	7082.35	254965.0	63741.2	2294682.0
	0.0		-17306.0		0.0		16981.4
32	0.996022	0.303590	0.118200	1304.52	80.6544	12.8040	82337.9
	132.834	129.712	142.650				
7082.35	254965.0	63741.2	2294682.0	7082.35	254965.0	63741.2	2294682.0
	-0.1		-16981.4		0.1		18622.8
33	0.996022	0.303590	0.118200	1304.52	80.6544	12.8040	82337.9
	132.834	129.712	142.650				
7082.35	254965.0	63741.2	2294682.0	7082.35	254965.0	63741.2	2294682.0
	-0.1		-18622.8		0.1		20889.0
34	0.996022	0.303590	0.118200	1304.52	80.6544	12.8040	82337.9
	132.834	129.712	142.650				
7082.35	254965.0	63741.2	2294682.0	7082.35	254965.0	63741.2	2294682.0
	-155.6		-20889.0		155.6		20579.3
35	0.996022	0.303590	0.118200	1304.52	80.6544	12.8040	82337.9
	132.834	129.712	142.650				
7082.35	254965.0	63741.2	2294682.0	7082.35	254965.0	63741.2	2294682.0
	-155.6		-20579.3		155.6		20888.9
36	0.996022	0.303590	0.118200	1304.52	80.6544	12.8040	82337.9
	132.834	129.712	142.650				
7082.35	254965.0	63741.2	2294682.0	7082.35	254965.0	63741.2	2294682.0
	-0.1		-20888.9		0.1		18622.5
37	0.996022	0.303590	0.118200	1304.52	80.6544	12.8040	82337.9
	132.834	129.712	142.650				
7082.35	254965.0	63741.2	2294682.0	7082.35	254965.0	63741.2	2294682.0
	-0.1		-18622.5		0.1		16981.2
38	0.996022	0.303590	0.118200	1304.52	80.6544	12.8040	82337.9
	132.834	129.712	142.650				
7082.35	254965.0	63741.2	2294682.0	7082.35	254965.0	63741.2	2294682.0
	0.0		-16981.2		0.0		17303.6
39	0.996022	0.303590	0.118200	1304.52	80.6544	12.8040	82337.9
	132.834	129.712	142.650				
7082.35	254965.0	63741.2	2294682.0	7082.35	254965.0	63741.2	2294682.0
	0.0		-17303.6		0.0		16918.2
40	0.996022	0.303590	0.118200	1304.52	80.6544	12.8040	82337.9
	132.834	129.712	142.650				
7082.35	254965.0	63741.2	2294682.0	7082.35	254965.0	63741.2	2294682.0
	0.5		-16918.2		-0.5		29986.6
41	0.996022	0.303590	0.118200	1304.52	80.6544	12.8040	82337.9
	132.834	129.712	142.650				
7082.35	254965.0	63741.2	2294682.0	7082.35	254965.0	63741.2	2294682.0
	0.0		-29986.6		0.0		0.0
1	8	10	1	1	1	1	1.
2	10	12	1	2	2	2	1.

3	12	14	1	3	3	3	1.
4	14	16	1	31	31	31	1.
5	16	18	1	32	32	32	1.
6	18	20	1	33	33	33	1.
7	20	22	1	34	34	34	1.
8	22	24	1	35	35	35	1.
9	24	26	1	36	36	36	1.
10	26	28	1	37	37	37	1.
11	28	30	1	38	38	38	1.
12	30	32	1	39	39	39	1.
13	32	34	1	40	40	40	1.
14	34	36	1	41	41	41	1.
15	9	10	1	10	10	10	1.
16	11	12	1	11	11	11	1.
17	13	14	1	12	12	12	1.
18	15	16	1	13	13	13	1.
19	17	18	1	14	14	14	1.
20	19	20	1	15	15	15	1.
21	21	22	1	16	16	16	1.
22	23	24	1	15	15	15	1.
23	25	26	1	14	14	14	1.
24	27	28	1	13	13	13	1.
25	29	30	1	12	12	12	1.
26	31	32	1	11	11	11	1.
27	33	34	1	10	10	10	1.
28	4	8	1	4	4	4	1.
29	5	8	1	5	5	5	1.
30	6	8	5	6	6	6	1.
31	36	40	1	7	7	7	1.
32	36	41	1	8	8	8	1.
33	36	42	41	9	9	9	1.
34	7	9	1	17	17	17	1.
35	9	11	1	18	18	18	1.
36	11	13	1	19	19	19	1.
37	13	15	1	20	20	20	1.
38	15	17	1	21	21	21	1.
39	17	19	1	22	22	22	1.
40	19	21	1	23	23	23	1.
41	21	23	1	24	24	24	1.
42	23	25	1	25	25	25	1.
43	25	27	1	26	26	26	1.
44	27	29	1	27	27	27	1.
45	29	31	1	28	28	28	1.
46	31	33	1	29	29	29	1.
47	33	35	1	30	30	30	1.
9					62.8167		
33					62.8167		
11					65.9538		
31					65.9538		
13					57.0212		
29					57.0212		
15					49.9338		
27					49.9338		
17					44.4994		

25	44.4994
19	40.6756
23	40.6756
21	36.7035
8	79.0403
10	70.5313
12	66.2353
14	63.4213
16	61.0676
18	59.3990
20	58.5766
22	56.9024
24	58.5766
26	59.3990
28	61.0676
30	63.4213
32	66.2353
34	70.5313
36	77.5134

0				
0.0612283	0.0366152	0.25	0.025	30.0
1 2 2000 0	0 6	0 0	6 3	
1 1 1.333				
2 1 1.333	0.3			

COLD SPRINGS CANYON BRIDGE - BI APPLIED WITH PHASE SHIFT IN X DIRECTION

40	42	2	0	-4	3	1	1	1	1	1	1	1	10			
1	0	1	1	1	1	1	1	0	0	0	0	0	-1	-10.000	109.970	
2	0	0	1	1	1	1	1	1	0	0	0	0	0	0.000	99.970	
3	0	0	1	1	1	1	1	1	0	0	0	0	0	0.000	109.970	
4	0	0	1	1	1	1	1	1	0	0	0	0	0	-319.040	246.524	
5	0	0	1	1	1	1	1	1	0	0	0	0	0	-10.749	236.524	
6	0	0	1	1	1	1	1	1	0	0	0	0	0	-10.749	246.524	
7	0	0	1	1	1	0	1	1	0	0	0	-1	0	0.000	109.970	
8	0	0	1	1	1	0	1	0	0	0	0	0	-1	0	-10.749	246.524
9	1	1	1	1	1	1	0	0	0	0	0	0	0	0	0.000	
10	1	1	1	1	1	1	0	0	0	0	0	0	0	0	0.000	
11	1	1	1	1	1	1	0	0	0	0	0	0	0	0	0.000	
12	0	0	1	1	1	0	1	0	13	0	0	0	-1	0	63.636	241.641
13	0	0	1	1	1	0	1	0	0	0	0	0	-1	0	63.636	146.016
14	0	0	1	1	1	0	1	0	15	0	0	0	-1	0	127.273	237.475
15	0	0	1	1	1	0	1	0	0	0	0	0	-1	0	127.273	174.957
16	0	0	1	1	1	0	1	0	17	0	0	0	-1	0	190.909	233.255
17	0	0	1	1	1	0	1	0	0	0	0	0	-1	0	190.909	194.585
18	0	0	1	1	1	0	1	0	19	0	0	0	-1	0	254.545	229.030
19	0	0	1	1	1	0	1	0	0	0	0	0	-1	0	254.545	205.214
20	0	0	1	1	1	0	1	0	21	0	0	0	-1	0	318.182	224.804
21	0	0	1	1	1	0	1	0	0	0	0	0	-1	0	318.182	207.989
22	0	0	1	1	1	0	1	0	0	0	0	0	-1	0	381.818	203.766
23	0	0	1	1	1	0	1	0	22	0	0	0	-1	0	381.818	220.579
24	0	0	1	1	1	0	1	0	0	0	0	0	-1	0	445.455	192.544
25	0	0	1	1	1	0	1	0	24	0	0	0	-1	0	445.455	216.353
26	0	0	1	1	1	0	1	0	0	0	0	0	-1	0	509.091	173.466
27	0	0	1	1	1	0	1	0	26	0	0	0	-1	0	509.091	212.128
28	0	0	1	1	1	0	1	0	0	0	0	0	-1	0	572.727	145.387
29	0	0	1	1	1	0	1	0	28	0	0	0	-1	0	572.727	207.898
30	0	0	1	1	1	0	1	0	0	0	0	0	-1	0	636.364	107.993
31	0	0	1	1	1	0	1	0	30	0	0	0	-1	0	636.364	203.612
32	1	1	1	1	1	1	1	0	0	0	0	0	0	0	0.000	
33	1	1	1	1	1	1	1	0	0	0	0	0	0	0	0.000	
34	1	1	1	1	1	1	1	0	0	0	0	0	0	0	0.000	
35	0	0	1	1	1	0	1	0	0	0	0	0	-1	0	710.749	198.617
36	0	0	1	1	1	0	1	40	40	0	0	0	-1	0	700.000	63.490
37	0	0	1	1	1	1	1	40	40	0	0	0	0	0	891.770	198.617
38	0	0	1	1	1	1	1	40	40	0	0	0	0	0	710.749	188.617
39	0	0	1	1	1	1	1	40	40	0	0	0	0	0	710.749	198.617
40	0	1	1	1	1	1	1	0	0	0	0	0	0	-1	710.000	63.490
41	0	0	1	1	1	1	1	40	40	0	0	0	0	0	700.000	53.490
42	0	0	1	1	1	1	1	40	40	0	0	0	0	0	700.000	63.490

11111122111222222222222222222211122111111

1 10 10 4176000. 0.30011111111

1	20	22	0.01440	324.0	10.5
2	21	23	0.01440	324.0	1.4
3	12	13	0.66667	3168.0	0.0
4	14	15	0.66667	3168.0	0.0
5	16	17	0.66667	3168.0	0.0
6	18	19	0.66667	3168.0	0.0
7	25	24	0.66667	3168.0	0.0
8	27	26	0.66667	3168.0	0.0

9	29	28	0.66667	3168.0	0.0			
10	31	30	0.66667	3168.0	0.0			
2	30	29	4176000.	0.3101010110111111111010101011				
1.	1.	1.	1.	1.	1.	-1.	-1.	-1.
1	2.22743	0.45139	1.58889	225.82070	8.32026	0.12616	720.68500	
	0.0							
	10584.7	76579.0	10645.1	36383.6	10584.7	76579.0	10645.1	36383.6
	-0.88	0.0	0.0	0.0	0.88	0.0	2520.97	0.0
2	2.20146	0.45139	1.55139	222.52117	7.63122	0.12587	702.85200	
	0.0							
	10461.3	75459.9	9514.4	35655.0	10461.3	75459.9	9514.4	35655.0
	-0.65	0.0	-2520.97	0.0	0.65	0.0	1804.81	0.0
3	2.16674	0.45139	1.52778	219.20443	7.43470	0.12577	683.99200	
	0.0							
	10296.3	74335.1	9254.5	34811.1	10296.3	74335.1	9254.5	34811.1
	0.40	0.0	-1804.81	0.0	-0.40	0.0	2110.64	0.0
4	0.66667	0.00000	0.0207236	274.62400	0.00000	1.60388		
	20.3633							
	3168.0	41184.0	1.	1.	3168.0	41184.0	1.	1.
	-341.9	0.0	0.	0.	341.9	0.0	0.	0.
5	0.0090299	0.00000	1.53984	220.60150	0.00000	3434.6680		
	0.0							
	1.	1.	1.	1.	1.	1.	1.	1.
	0.							
6	0.2496470	0.00000	0.00000	0.00000	0.00000	1.3291		
	0.0							
	1.	1.	1.	1.	1.	1.	1.	1.
	0.							
7	0.0017058	0.00000	0.00000	0.00000	0.00000	0.0000		
	0.0							
	1.	1.	1.	1.	1.	1.	1.	1.
	0.							
8	2.1743400	0.00000	1.54832	221.58380	0.00000	2017.0020		
	0.0							
	1.	1.	1.	1.	1.	1.	1.	1.
	0.							
9	0.2498810	0.00000	0.00000	0.00000	0.00000	1.3291		
	0.0							
	1.	1.	1.	1.	1.	1.	1.	1.
	0.							
10	0.0017058	0.00000	0.00000	0.00000	0.00000	0.0000		
	0.0							
	1.	1.	1.	1.	1.	1.	1.	1.
	0.							
11	4.75185	2.80981	0.382418	997.0290	57.03870	33.04680		
	93.0467	75.4193						
	21087.0	247193.0	51589.7	1.0	25839.0	302898.0	72657.0	1.0
	5440.84	0.0	0.0	0.0	-5440.84	0.0	2711.71	0.0
12	5.54941	2.81146	0.342304	1165.3500	74.75980	37.61510		
	88.6584	71.7706						
	25839.0	302898.0	72657.0	1.0	28215.0	330751.0	83206.9	1.0
	5146.71	0.0	2711.71	0.0	-5146.71	0.0	2734.98	0.0
13	6.34697	2.81311	0.302190	1333.6800	92.48080	42.18340		
	84.2702	68.122						

28215.0	330751.0	83206.9	1.0	30591.0	358603.0	93769.6	1.0
4935.18	0.0	-2734.98	0.0	-4935.18	0.0	2836.51	0.0
14	5.96023	2.81270	0.281749	1184.2200	83.81180	39.95440	
77.4461	66.6803						
30591.0	358603.0	93769.6	1.0	28215.0	330751.0	83206.9	1.0
4789.22	0.0	-2836.51	0.0	-4789.22	0.0	-155.29	0.0
15	5.57349	2.81229	0.261309	1034.7500	75.14290	37.72530	
70.6220	65.2387						
28215.0	330751.0	83206.9	1.0	25839.0	302898.0	72657.0	1.0
4722.86	0.0	155.29	0.0	-4722.86	0.0	-3136.46	0.0
16	5.18675	2.81188	0.240868	885.2850	66.47390	35.49630	
63.7979	63.7970						
25893.0	302898.0	72657.0	1.0	25839.0	302898.0	72657.0	1.0
4724.87	0.0	3136.46	0.0	-4724.87	0.0	-3638.02	0.0
17	5.57349	2.81229	0.261309	1034.7500	75.14290	37.72530	
70.6220	65.2387						
25839.0	302898.0	72657.0	1.0	28215.0	330751.0	83206.9	1.0
4803.98	0.0	3638.02	0.0	-4803.98	0.0	-1388.59	0.0
18	5.96023	2.81270	0.281749	1184.2200	83.81180	39.95440	
77.4461	66.6803						
28215.0	330751.0	83206.9	1.0	30591.0	358603.0	93769.6	1.0
4943.59	0.0	1388.59	0.0	-4943.59	0.0	1017.57	0.0
19	6.34697	2.81311	0.302190	1333.6800	92.48080	42.18340	
84.2702	68.122						
30591.0	358603.0	93769.6	1.0	28215.0	330751.0	83206.9	1.0
5163.80	0.0	-1017.57	0.0	-5163.80	0.0	906.25	0.0
20	5.54941	2.81146	0.342304	1165.3500	74.75980	37.61510	
88.6584	71.7706						
28215.0	330751.0	83206.9	1.0	25839.0	302898.0	72657.0	1.0
5441.75	0.0	-906.25	0.0	-5441.75	0.0	-3810.61	0.0
21	4.75185	2.80981	0.382418	997.0290	57.03870	33.04680	
93.0467	75.4193						
25839.0	302898.0	72657.0	1.0	21087.0	247193.0	51589.7	1.0
5801.13	0.0	3810.61	0.0	-5801.13	0.0	0.0	0.0
22	2.16674	0.45139	1.52778	219.20443	7.43470	0.12577	683.99200
0.0							
10296.3	74335.1	9254.5	34811.1	10296.3	74335.1	9254.5	34811.1
-0.28	0.0	-2110.64	0.0	0.28	0.0	1761.49	0.0
23	2.16674	0.45139	1.52778	219.20443	7.43470	0.12577	683.99200
0.0							
10296.3	74335.1	9254.5	34811.1	10296.3	74335.1	9254.5	34811.1
-0.25	0.0	-1761.49	0.0	0.25	0.0	1435.69	0.0
24	2.16674	0.45139	1.52778	219.20443	7.43470	0.12577	683.99200
0.0							
10296.3	74335.1	9254.5	34811.1	10296.3	74335.1	9254.5	34811.1
-9.95	0.0	-1435.69	0.0	9.95	0.0	1398.84	0.0
25	2.16674	0.45139	1.52778	219.20443	7.43470	0.12577	683.99200
0.0							
10296.3	74335.1	9254.5	34811.1	10296.3	74335.1	9254.5	34811.1
-8.29	0.0	-1398.84	0.0	8.29	0.0	1643.80	0.0
26	2.16674	0.45139	1.52778	219.20443	7.43470	0.12577	683.99200
0.0							
10296.3	74335.1	9254.5	34811.1	10296.3	74335.1	9254.5	34811.1
-8.22	0.0	-1643.80	0.0	8.22	0.0	1954.68	0.0

27	2.16674	0.45139	1.52778	219.20443	7.43470	0.12577	683.99200
	0.0						
10296.3	74335.1	9254.5	34811.1	10296.3	74335.1	9254.5	34811.1
-8.91	0.0	-1954.68	0.0	8.91	0.0	1598.06	0.0
28	2.20146	0.45139	1.55139	222.52117	7.63122	0.12587	702.85200
	0.0						
10461.3	75459.9	9514.4	35655.0	10461.3	75459.9	9514.4	35655.0
-7.64	0.0	-1598.06	0.0	7.64	0.0	2456.90	0.0
29	2.22743	0.45139	1.58889	225.82070	8.32026	0.12616	720.68500
	0.0						
10584.7	76579.0	10645.1	36383.6	10584.7	76579.0	10645.1	36383.6
-7.50	0.0	-2456.90	0.0	7.50	0.0	0.0	0.0

1	8	12	1	1	1	1	1.
2	12	14	1	2	2	2	1.
3	14	16	1	3	3	3	1.
4	16	18	1	22	22	22	1.
5	18	20	1	23	23	23	1.
6	20	23	1	24	24	24	1.
7	23	25	1	25	25	25	1.
8	25	27	1	26	26	26	1.
9	27	29	1	27	27	27	1.
10	29	31	1	28	28	28	1.
11	31	35	1	29	29	29	1.
12	20	21	4	4	4	4	1.
13	23	22	4	4	4	4	1.
14	4	8	1	5	5	5	1.
15	5	8	1	6	6	6	1.
16	6	8	5	7	7	7	1.
17	35	37	1	8	8	8	1.
18	35	38	1	9	9	9	1.
19	35	39	38	10	10	10	1.
20	7	13	1	11	11	11	1.
21	13	15	1	12	12	12	1.
22	15	17	1	13	13	13	1.
23	17	19	1	14	14	14	1.
24	19	21	1	15	15	15	1.
25	21	22	1	16	16	16	1.
26	22	24	1	17	17	17	1.
27	24	26	1	18	18	18	1.
28	26	28	1	19	19	19	1.
29	28	30	1	20	20	20	1.
30	30	36	1	21	21	21	1.

8	62.42900	36.18900
12	11.97700	11.97700
13	8.35800	8.35800
14	10.88600	10.88600
15	8.50660	8.50660
16	10.73100	10.73100
17	8.20120	8.20120
18	10.64300	10.64300
19	7.43880	7.43880
20	10.61900	10.61900
21	6.87580	6.87580
23	10.61900	10.61900

22	6.91880	6.91880
25	10.64300	10.64300
24	7.58740	7.58740
27	10.73100	10.73100
26	8.47340	8.47340
29	10.88600	10.88600
28	8.87360	8.87360
31	11.97700	11.97700
30	8.76400	8.76400
35	25.16600	25.16600

0

0.173871	0.0132199	0.25	0.025	30.0
1	2 2000	0	0 6	0 0 6 3
1	1	1.333	0.125	
2	1	1.333		

COLD SPRINGS CANYON BRIDGE - B1 APPLIED WITH PHASE SHIFT IN Z DIRECTION

40	42	2	1	-4	3	1	1	1	1	1	1	1	10		
1	1	1	0	1	1	1	1	0	0	0	0	0	-1	-10.000	109.970
2	1	1	0	1	1	1	1	0	0	1	0	0	0	0.000	99.970
3	1	1	0	1	1	1	1	0	0	1	0	0	0	0.000	109.970
4	1	1	0	1	0	1	1	0	0	1	0	-1	0	-319.040	246.524
5	1	1	0	1	1	1	1	0	0	1	0	0	0	-10.749	236.524
6	1	1	0	1	1	1	1	0	0	1	0	0	0	-10.749	246.524
7	1	1	0	1	1	1	1	0	0	1	0	0	0	0.000	109.970
8	1	1	0	0	0	1	0	0	0	0	-1	-1	0	-10.749	246.524
9	1	1	1	1	1	1	1	0	0	0	0	0	0	0.000	
10	1	1	1	1	1	1	1	0	0	0	0	0	0	0.000	
11	1	1	1	1	1	1	1	0	0	0	0	0	0	0.000	
12	1	1	0	0	0	1	0	0	0	0	13	-1	0	63.636	241.641
13	1	1	0	0	0	1	1	0	0	0	-1	-1	0	63.636	146.016
14	1	1	0	0	0	1	0	0	0	0	15	-1	0	127.273	237.475
15	1	1	0	0	0	1	1	0	0	0	-1	-1	0	127.273	174.957
16	1	1	0	0	0	1	0	0	0	0	17	-1	0	190.909	233.255
17	1	1	0	0	0	1	1	0	0	0	-1	-1	0	190.909	194.585
18	1	1	0	0	0	1	0	0	0	0	19	-1	0	254.545	229.030
19	1	1	0	0	0	1	1	0	0	0	-1	-1	0	254.545	205.214
20	1	1	0	0	0	1	0	0	0	0	-1	-1	0	318.182	224.804
21	1	1	0	0	0	1	1	0	0	0	-1	-1	0	318.182	207.989
22	1	1	0	0	0	1	1	0	0	0	-1	-1	0	381.818	203.766
23	1	1	0	0	0	1	0	0	0	0	-1	-1	0	381.818	220.579
24	1	1	0	0	0	1	1	0	0	0	-1	-1	0	445.455	192.544
25	1	1	0	0	0	1	0	0	0	0	24	-1	0	445.455	216.353
26	1	1	0	0	0	1	1	0	0	0	-1	-1	0	509.091	173.466
27	1	1	0	0	0	1	0	0	0	0	26	-1	0	509.091	212.128
28	1	1	0	0	0	1	1	0	0	0	-1	-1	0	572.727	145.387
29	1	1	0	0	0	1	0	0	0	0	28	-1	0	572.727	207.898
30	1	1	0	0	0	1	1	0	0	0	-1	-1	0	636.364	107.993
31	1	1	0	0	0	1	0	0	0	0	30	-1	0	636.364	203.612
32	1	1	1	1	1	1	1	0	0	0	0	0	0	0.000	
33	1	1	1	1	1	1	1	0	0	0	0	0	0	0.000	
34	1	1	1	1	1	1	1	0	0	0	0	0	0	0.000	
35	1	1	0	0	0	1	0	0	0	0	-1	-1	0	710.749	198.617
36	1	1	0	1	1	1	1	0	0	40	0	0	0	700.000	63.490
37	1	1	0	1	0	1	1	0	0	40	0	-1	0	891.770	198.617
38	1	1	0	1	1	1	1	0	0	40	0	0	0	710.749	188.617
39	1	1	0	1	1	1	1	0	0	40	0	0	0	710.749	198.617
40	1	1	0	1	1	1	1	0	0	0	0	0	0	-1	710.000
41	1	1	0	1	1	1	1	0	0	40	0	0	0	700.000	53.490
42	1	1	0	1	1	1	1	0	0	40	0	0	0	700.000	63.490

11111133111333333333333333333311133111111

1 10 10 4176000. 0.311111111111

1	20	22	0.01440	324.0	10.5
2	21	23	0.01440	324.0	1.4
3	12	13	0.66667	3168.0	0.0
4	14	15	0.66667	3168.0	0.0
5	16	17	0.66667	3168.0	0.0
6	18	19	0.66667	3168.0	0.0
7	25	24	0.66667	3168.0	0.0
8	27	26	0.66667	3168.0	0.0

```

9 29 28 0.66667 3168.0 0.0
10 31 30 0.66667 3168.0 0.0
2 30 29 4176000. 0.3010101101100011111101010110110
1. 1. 1. 1. 1. 1. -1. -1. -1. 1. 1. -1. 1. -1. 1. -1.
1 2.22743 0.45139 1.58889 225.82070 8.32026 0.12616 720.68500
0.0
10584.7 76579.0 10645.1 36383.6 10584.7 76579.0 10645.1 36383.6
-0.88 0.0 0.0 0.0 0.88 0.0 2520.97 0.0
2 2.20146 0.45139 1.55139 222.52117 7.63122 0.12587 702.85200
0.0
10461.3 75459.9 9514.4 35655.0 10461.3 75459.9 9514.4 35655.0
-0.65 0.0 -2520.97 0.0 0.65 0.0 1804.81 0.0
3 2.16674 0.45139 1.52778 219.20443 7.43470 0.12577 683.99200
0.0
10296.3 74335.1 9254.5 34811.1 10296.3 74335.1 9254.5 34811.1
0.40 0.0 -1804.81 0.0 -0.40 0.0 2110.64 0.0
4 0.66667 0.00000 0.0207236 274.62400 0.00000 1.60388
20.3633
3168.0 41184.0 1. 1. 3168.0 41184.0 1. 1.
-341.9 0.0 0. 0. 341.9 0.0 0. 0.
5 0.0090299 0.00000 1.53984 220.60150 0.00000 3434.6680
0.0
1. 1. 1. 1. 1. 1. 1. 1.
0.
6 0.2496470 0.00000 0.00000 0.00000 0.00000 1.3291
0.0
1. 1. 1. 1. 1. 1. 1. 1.
0.
7 0.0017058 0.00000 0.00000 0.00000 0.00000 0.0000
0.0
1. 1. 1. 1. 1. 1. 1. 1.
0.
8 2.1743400 0.00000 1.54832 221.58380 0.00000 2017.0020
0.0
1. 1. 1. 1. 1. 1. 1. 1.
0.
9 0.2498810 0.00000 0.00000 0.00000 0.00000 1.3291
0.0
1. 1. 1. 1. 1. 1. 1. 1.
0.
10 0.0017058 0.00000 0.00000 0.00000 0.00000 0.0000
0.0
1. 1. 1. 1. 1. 1. 1. 1.
0.
11 4.75185 2.80981 0.382418 997.0290 57.03870 33.04680
93.0467 75.4193
21087.0 247193.0 51589.7 1.0 25839.0 302898.0 72657.0 1.0
5440.84 0.0 0.0 0.0 -5440.84 0.0 2711.71 0.0
12 5.54941 2.81146 0.342304 1165.3500 74.75980 37.61510
88.6584 71.7706
25839.0 302898.0 72657.0 1.0 28215.0 330751.0 83206.9 1.0
5146.71 0.0 2711.71 0.0 -5146.71 0.0 2734.98 0.0
13 6.34697 2.81311 0.302190 1333.6800 92.48080 42.18340
84.2702 68.122

```

28215.0	330751.0	83206.9	1.0	30591.0	358603.0	93769.6	1.0
4935.18	0.0	-2734.98	0.0	-4935.18	0.0	2836.51	0.0
14	5.96023	2.81270	0.281749	1184.2200	83.81180	39.95440	
77.4461	66.6803						
30591.0	358603.0	93769.6	1.0	28215.0	330751.0	83206.9	1.0
4789.22	0.0	-2836.51	0.0	-4789.22	0.0	-155.29	0.0
15	5.57349	2.81229	0.261309	1034.7500	75.14290	37.72530	
70.6220	65.2387						
28215.0	330751.0	83206.9	1.0	25839.0	302898.0	72657.0	1.0
4722.86	0.0	155.29	0.0	-4722.86	0.0	-3136.46	0.0
16	5.18675	2.81188	0.240868	885.2850	66.47390	35.49630	
63.7979	63.7970						
25893.0	302898.0	72657.0	1.0	25839.0	302898.0	72657.0	1.0
4724.87	0.0	3136.46	0.0	-4724.87	0.0	-3638.02	0.0
17	5.57349	2.81229	0.261309	1034.7500	75.14290	37.72530	
70.6220	65.2387						
25839.0	302898.0	72657.0	1.0	28215.0	330751.0	83206.9	1.0
4803.98	0.0	3638.02	0.0	-4803.98	0.0	-1388.59	0.0
18	5.96023	2.81270	0.281749	1184.2200	83.81180	39.95440	
77.4461	66.6803						
28215.0	330751.0	83206.9	1.0	30591.0	358603.0	93769.6	1.0
4943.59	0.0	1388.59	0.0	-4943.59	0.0	1017.57	0.0
19	6.34697	2.81311	0.302190	1333.6800	92.48080	42.18340	
84.2702	68.122						
30591.0	358603.0	93769.6	1.0	28215.0	330751.0	83206.9	1.0
5163.80	0.0	-1017.57	0.0	-5163.80	0.0	906.25	0.0
20	5.54941	2.81146	0.342304	1165.3500	74.75980	37.61510	
88.6584	71.7706						
28215.0	330751.0	83206.9	1.0	25839.0	302898.0	72657.0	1.0
5441.75	0.0	-906.25	0.0	-5441.75	0.0	-3810.61	0.0
21	4.75185	2.80981	0.382418	997.0290	57.03870	33.04680	
93.0467	75.4193						
25839.0	302898.0	72657.0	1.0	21087.0	247193.0	51589.7	1.0
5801.13	0.0	3810.61	0.0	-5801.13	0.0	0.0	0.0
22	2.16674	0.45139	1.52778	219.20443	7.43470	0.12577	683.99200
0.0							
10296.3	74335.1	9254.5	34811.1	10296.3	74335.1	9254.5	34811.1
-0.28	0.0	-2110.64	0.0	0.28	0.0	1761.49	0.0
23	2.16674	0.45139	1.52778	219.20443	7.43470	0.12577	683.99200
0.0							
10296.3	74335.1	9254.5	34811.1	10296.3	74335.1	9254.5	34811.1
-0.25	0.0	-1761.49	0.0	0.25	0.0	1435.69	0.0
24	2.16674	0.45139	1.52778	219.20443	7.43470	0.12577	683.99200
0.0							
10296.3	74335.1	9254.5	34811.1	10296.3	74335.1	9254.5	34811.1
-9.95	0.0	-1435.69	0.0	9.95	0.0	1398.84	0.0
25	2.16674	0.45139	1.52778	219.20443	7.43470	0.12577	683.99200
0.0							
10296.3	74335.1	9254.5	34811.1	10296.3	74335.1	9254.5	34811.1
-8.29	0.0	-1398.84	0.0	8.29	0.0	1643.80	0.0
26	2.16674	0.45139	1.52778	219.20443	7.43470	0.12577	683.99200
0.0							
10296.3	74335.1	9254.5	34811.1	10296.3	74335.1	9254.5	34811.1
-8.22	0.0	-1643.80	0.0	8.22	0.0	1954.68	0.0

27	2.16674	0.45139	1.52778	219.20443	7.43470	0.12577	683.99200
	0.0						
10296.3	74335.1	9254.5	34811.1	10296.3	74335.1	9254.5	34811.1
-8.91	0.0	-1954.68	0.0	8.91	0.0	1598.06	0.0
28	2.20146	0.45139	1.55139	222.52117	7.63122	0.12587	702.85200
	0.0						
10461.3	75459.9	9514.4	35655.0	10461.3	75459.9	9514.4	35655.0
-7.64	0.0	-1598.06	0.0	7.64	0.0	2456.90	0.0
29	2.22743	0.45139	1.58889	225.82070	8.32026	0.12616	720.68500
	0.0						
10584.7	76579.0	10645.1	36383.6	10584.7	76579.0	10645.1	36383.6
-7.50	0.0	-2456.90	0.0	7.50	0.0	0.0	0.0
1	8	12	1	1	1	1	1.
2	12	14	1	2	2	2	1.
3	14	16	1	3	3	3	1.
4	16	18	1	22	22	22	1.
5	18	20	1	23	23	23	1.
6	20	23	1	24	24	24	1.
7	23	25	1	25	25	25	1.
8	25	27	1	26	26	26	1.
9	27	29	1	27	27	27	1.
10	29	31	1	28	28	28	1.
11	31	35	1	29	29	29	1.
12	20	21	4	4	4	4	1.
13	23	22	4	4	4	4	1.
14	4	8	1	5	5	5	1.
15	5	8	1	6	6	6	1.
16	6	8	5	7	7	7	1.
17	35	37	1	8	8	8	1.
18	35	38	1	9	9	9	1.
19	35	39	38	10	10	10	1.
20	7	13	1	11	11	11	1.
21	13	15	1	12	12	12	1.
22	15	17	1	13	13	13	1.
23	17	19	1	14	14	14	1.
24	19	21	1	15	15	15	1.
25	21	22	1	16	16	16	1.
26	22	24	1	17	17	17	1.
27	24	26	1	18	18	18	1.
28	26	28	1	19	19	19	1.
29	28	30	1	20	20	20	1.
30	30	36	1	21	21	21	1.
8							36.18900
12							11.97700
13							8.35800
14							10.88600
15							8.50660
16							10.73100
17							8.20120
18							10.64300
19							7.43880
20							10.61900
21							6.87580
23							10.61900

22					6.91880				
25					10.64300				
24					7.58740				
27					10.73100				
26					8.47340				
29					10.88600				
28					8.87360				
31					11.97700				
30					8.76400				
35					25.16600				
0									
0.142583	0.0165368				0.25	0.025		30.0	
1	2	2000	0	0	6	0	0	6	3
1	1		1.333						
2	1		1.333		0.125				

B.4 B-1 AND B-2 ACCELEROGRAMS

The following pages contain listings of the B-1 and B-2 accelerograms. These listings show ground acceleration only since the time steps used are a uniform 0.025 seconds. Each line is labelled on the far right with the name of the accelerogram and the line number.

0.0	-0.0094661	-0.0183128	-0.0270858	-0.0366823	-0.0457688	B-1	1
-0.0522596	-0.0572962	-0.0520235	-0.0523379	-0.0798364	-0.0980104	B-1	2
-0.1056126	-0.1292132	-0.1432429	-0.1450879	-0.1347314	-0.1140900	B-1	3
-0.0829798	-0.0693467	-0.0823783	-0.1271849	-0.1286079	-0.0733230	B-1	4
-0.0653459	-0.1249650	-0.1873516	-0.1804321	-0.1379664	-0.0892742	B-1	5
-0.0686886	-0.0435507	-0.0145651	-0.0324445	-0.0887651	-0.1045456	B-1	6
-0.1274030	-0.0670890	-0.0204241	-0.1379957	-0.2647585	-0.3131646	B-1	7
-0.3292329	-0.6903815	-0.8562267	-0.3486637	-0.2789336	-0.3698072	B-1	8
-0.1453372	-0.1185893	-0.1069940	-0.4906658	-0.7109529	-0.2352922	B-1	9
-0.2037920	-0.4732444	-1.0952864	-1.1960030	-0.4668612	-0.0476186	B-1	10
0.3362817	0.5084810	0.1908463	0.4431558	0.9733272	0.7077292	B-1	11
0.3841354	0.0119325	-0.1575539	0.2440161	0.2436705	0.9359490	B-1	12
1.5477753	1.2363443	0.4791695	-0.0466715	0.4957108	0.3797427	B-1	13
-0.1083094	-0.1674902	0.0807674	0.3817823	0.2412108	0.1200086	B-1	14
0.2223201	0.9638374	1.1268196	-0.0097126	0.4660605	1.7274961	B-1	15
1.3275080	-0.5597236	-1.8591776	-1.8144236	-1.3649826	-0.5854431	B-1	16
-0.3627311	-0.0237781	0.4801950	0.2404780	0.2263615	-0.0918869	B-1	17
-0.9976104	-0.6456296	-0.2522434	-0.0407066	0.6850653	0.7959874	B-1	18
0.2208754	-0.7410934	-1.0479927	-1.8623829	-1.8236008	0.3898934	B-1	19
0.9567263	0.6170982	0.2662278	-1.0427685	-2.7575655	-2.2683811	B-1	20
0.3988355	2.7793703	3.3515940	5.2111015	5.6261463	1.6291447	B-1	21
1.1434212	2.3633270	2.1351643	2.7388935	0.7256407	-2.4084167	B-1	22
-1.7637177	-0.0536901	1.1864653	2.5340462	0.7007682	-3.1222496	B-1	23
-4.9839907	-7.1363668	-6.8638430	-2.3975410	1.9918938	3.0353327	B-1	24
-0.0672250	-0.1486553	0.9871831	1.2483845	3.1627913	1.4009256	B-1	25
-1.1511450	-4.5231171	-7.3470125	-6.5618963	-2.2464209	0.8254650	B-1	26
-1.0514565	-1.0449800	1.3922262	2.2835760	0.4950622	1.3750134	B-1	27
4.5017262	3.5072556	1.3675604	1.0207901	0.9883710	-1.8859444	B-1	28
-4.3148060	-3.8190136	-2.7135553	-0.8353882	2.5011101	6.0630398	B-1	29
7.5901070	6.9605274	8.7946110	9.0899029	5.5427828	1.7237616	B-1	30
-2.1985502	-4.7267065	-3.9595919	-3.6670799	-2.8470154	-0.2288637	B-1	31
3.4452639	3.4334631	2.1767044	-0.6732395	-3.6307116	-4.9000187	B-1	32
-3.9138613	-0.4568446	0.8450176	1.1570091	2.5403357	3.7379761	B-1	33
4.7961578	3.2029123	-0.3922077	-2.7418375	-2.0279770	1.7908602	B-1	34
5.2782383	2.7740755	-0.2546852	-0.8331050	-1.3057766	-0.2550101	B-1	35
0.4867291	-0.3226222	-1.2401571	3.4445362	4.0087519	1.7116184	B-1	36
-1.3853207	-6.0952997	-6.0143757	-2.3509722	-1.0707998	-1.6329565	B-1	37
-0.7881445	0.5773309	1.1785822	2.8603897	3.8188086	1.4146795	B-1	38
1.2508068	-2.0222435	-6.8744135	-9.3492184	-11.3995476	-7.9140377	B-1	39
-2.5919838	-2.9338112	-2.2791882	0.3430501	0.5027267	2.4210262	B-1	40
2.9508057	1.3933372	3.0880680	4.2375364	1.8024244	-0.8612049	B-1	41
0.3015324	1.4606066	0.3665355	-0.1481841	0.8711592	1.4324818	B-1	42
-1.7260504	-2.9011574	-1.8167152	-0.8236058	-1.4287224	-2.2249966	B-1	43
-0.6208572	1.1958132	-0.7281052	-3.2726879	-2.7396059	-1.9150314	B-1	44
-2.9417191	-3.2554026	-0.8069473	3.5093822	3.8780508	-0.1674487	B-1	45
-2.2725277	-2.4829254	-4.9810171	-5.4129725	-2.0368366	-1.4322634	B-1	46
-1.2901649	1.1012869	2.2553453	2.8305731	5.0237818	4.0952740	B-1	47
3.9536448	3.4968596	0.6534820	-1.8306704	-2.1825275	-1.5875053	B-1	48
-3.0638113	0.3204570	6.0173473	3.1701612	-0.0658927	-0.7503650	B-1	49
-0.1136736	4.3601685	7.5474463	9.7777472	10.8700724	9.5250368	B-1	50
2.8834820	-3.3335886	-5.6376972	-6.6536493	-5.3525515	-4.7630911	B-1	51
-4.8150053	-6.6375113	-3.5718527	-1.2505569	0.3886688	4.0926352	B-1	52
3.8453169	5.1838913	6.9000330	3.1048803	0.7649112	2.0052309	B-1	53
-0.2100675	-2.4957409	-1.2915592	0.7341078	3.3209772	6.1809187	B-1	54

5.7165327	6.1706963	5.9668331	3.1743898	-0.0908955	-4.8514662	B-1	55
-8.0529642	-7.7916794	-4.7598515	-4.2018814	-4.7372284	-0.1676329	B-1	56
4.4122677	3.3859978	1.6231871	1.1671343	-0.1242615	0.9292835	B-1	57
6.2810526	7.8082800	5.6417828	4.5626163	-2.7432213	-7.3955297	B-1	58
-5.9664984	-4.6988459	-0.6674881	2.3859615	1.8542624	2.2867718	B-1	59
2.4389191	0.6770183	0.3628359	1.2811899	2.1813831	2.5841751	B-1	60
3.4131622	2.2181587	2.9819975	5.1407909	0.6611040	-4.3762007	B-1	61
-5.7609091	-5.2350998	-5.2835894	-5.7467852	-5.4740562	-7.3011360	B-1	62
-6.8486042	-7.1866474	-12.0773020	-10.8582716	-7.0269423	-3.8429337	B-1	63
0.2752368	2.2851219	-1.1167221	-2.8797417	-1.3285370	-0.7285811	B-1	64
0.3454608	-0.5664703	-2.8727961	-5.8496418	-5.1124516	-1.9800129	B-1	65
-1.3146057	-0.0490406	0.9661641	1.6250439	2.8643494	2.8645477	B-1	66
0.7620558	-0.4091212	0.0262492	-0.1605179	-0.5397772	-1.0464449	B-1	67
1.2722597	4.5095072	6.3180923	6.8741913	5.8527069	3.5247564	B-1	68
1.2858076	0.9162301	2.0630131	1.2823524	1.0196218	1.9989891	B-1	69
0.6213171	-0.2227809	1.2022257	2.7083797	3.2670765	4.1732807	B-1	70
0.3745143	-2.4420719	-1.2561054	0.0226932	-1.3306322	-6.9202070	B-1	71
-9.3743687	-6.2259769	-1.8002205	-0.6713756	-3.9148178	-3.2883625	B-1	72
-2.0992365	-4.2374668	-2.8388329	0.9977880	3.8949366	4.3599691	B-1	73
4.4884529	5.4002485	1.1993170	-0.9982921	2.0865383	4.4207163	B-1	74
4.6197996	1.8907309	1.5040321	2.8174658	0.0799072	-2.7003384	B-1	75
-4.2411098	-6.8762684	-8.6307878	-9.6154327	-5.9658079	-1.9072666	B-1	76
-1.1970358	0.4175081	2.1512089	5.3067150	8.2708797	4.3914328	B-1	77
1.4167356	1.3299942	2.7557507	0.7853079	-1.7864637	-0.0236865	B-1	78
0.5214843	3.3689070	7.8410149	9.4370365	9.3699379	4.6723566	B-1	79
0.8950686	1.8129911	3.9040785	2.6486692	-0.8924710	-2.7216425	B-1	80
-2.4595461	1.5964174	3.8584232	4.8082542	7.1468029	5.1523485	B-1	81
3.9142494	4.7259979	1.4441671	-1.3304033	-2.5317125	-2.7784052	B-1	82
1.0535641	1.1106577	0.3380719	0.8486171	-0.9144692	-1.0925398	B-1	83
0.7763810	-0.4498553	-1.7590580	-2.3423882	-6.5370998	-6.4945812	B-1	84
0.0847720	1.6454754	-1.2003117	-1.7538424	-2.0122938	-2.1933451	B-1	85
-2.1204996	-5.5936556	-4.9112463	-2.8097715	-4.2659206	-1.5242510	B-1	86
-1.5594893	-2.4099083	-2.0347147	-1.7490587	0.2434590	-0.4394326	B-1	87
0.3781525	3.5656242	4.6680908	3.6268120	0.4012301	-2.6005697	B-1	88
-2.2122717	1.3937969	4.0230503	3.0578480	1.4077778	1.8030787	B-1	89
4.4074125	4.0343571	2.1669149	1.0747013	0.5401323	1.8980198	B-1	90
1.6420927	-1.7291307	-2.2113619	-0.6734264	-0.7479523	-0.6300684	B-1	91
-0.3751858	-0.1592451	-1.8377485	-3.3079844	-6.0279512	-5.5634375	B-1	92
-0.4848879	1.6283550	2.5671692	4.5777721	4.1220474	3.2340031	B-1	93
1.5716124	0.8859414	3.2535887	2.6905642	2.8819666	5.6937666	B-1	94
3.2923365	-1.8513622	-6.4989824	-8.3530779	-7.7426863	-3.8667259	B-1	95
-0.8167638	-1.0108643	-0.1710520	0.2061262	-2.0994816	-4.8559179	B-1	96
-4.4030590	-3.8199768	-2.7399387	2.4601021	11.0674944	11.9160900	B-1	97
6.5750599	2.1856012	1.9175358	2.4475574	0.7711055	1.7274466	B-1	98
0.5746776	-4.3049650	-2.8528891	-1.1714859	-1.1123476	-2.1097260	B-1	99
-6.0537758	-7.9423552	-8.0007629	-6.9014502	-6.6261768	-2.5226736	B-1	100
2.0097504	1.6668501	4.0753422	8.2200203	7.3756437	4.0433207	B-1	101
2.9494610	1.1824350	-1.8226967	-3.9378729	-3.0098267	-3.7528858	B-1	102
-3.6012373	-0.8865713	-0.4316775	-1.6635513	-2.2495375	-0.7896591	B-1	103
0.6038710	0.5028344	-0.9118696	-4.1738596	-7.9505835	-6.6339321	B-1	104
-2.8178005	-1.2531013	-1.6033163	-1.3186312	-3.5359640	-5.9365921	B-1	105
-7.5668192	-7.4777832	-1.2609367	3.0688133	4.8775082	4.7695169	B-1	106
1.9213009	0.3726618	-0.0135745	1.7094240	3.3202610	2.9366407	B-1	107
3.7848492	5.2848539	1.9475212	-0.7252479	0.8288842	3.4539547	B-1	108

5.3349161	3.4879408	1.8069439	3.2512407	3.0155582	1.5619612	B-1 109
0.6398215	0.1069221	-1.4585361	-1.1639404	-0.8431773	-3.0834951	B-1 110
-4.0174284	-5.9067984	-3.7339821	0.1787401	1.0981407	2.5126686	B-1 111
5.8290720	5.0727215	1.6774750	0.7851654	0.0018649	-1.2531748	B-1 112
-0.5590881	-0.5289268	0.2371995	1.6837578	1.3016157	0.7569663	B-1 113
0.0068534	-0.6360039	1.5159454	3.0381279	2.8265772	0.7852588	B-1 114
-1.1952982	-0.4000469	-1.2426033	-2.4364462	-4.0131235	-6.8890038	B-1 115
-7.4777403	-6.0694094	-5.9107437	-3.6240826	-0.2083678	1.7047176	B-1 116
4.9844284	8.6637125	7.8470793	6.3447971	5.1262913	2.9080105	B-1 117
3.7967577	4.1833611	1.6420164	-0.6193379	0.8660924	2.6362047	B-1 118
2.2209492	2.3564119	3.2278204	2.3268795	0.7623380	0.2899454	B-1 119
0.9565205	1.5271626	1.8788576	1.3639288	-1.3566418	-3.0544453	B-1 120
-5.5687618	-6.4206123	-3.8515339	-0.2858191	0.8218505	0.7722017	B-1 121
0.8862540	0.1943608	1.1418762	3.4493961	3.9887066	4.9171715	B-1 122
5.8660126	4.6521769	3.5326204	2.3022308	-0.9671527	-5.6073494	B-1 123
-6.6593761	-3.9726143	-1.9728775	0.0730397	1.6922646	2.0177040	B-1 124
1.3387699	-0.0927198	-0.1176546	-0.3516683	-2.9094982	-2.9466019	B-1 125
-1.5051880	-1.2546434	-0.7808530	-1.6456642	-3.3692818	-4.2526207	B-1 126
-4.2141428	-3.1926098	-0.4593280	1.3902349	2.3571854	4.3011847	B-1 127
5.0304956	5.3621740	1.7497988	-2.7357512	-3.6650515	-3.5877323	B-1 128
-2.8319283	-3.9688158	-4.9994516	-3.1311159	-3.1471958	-2.4835730	B-1 129
-1.5953083	-2.7382803	-4.4681826	-4.4027672	-1.8807106	-1.5067005	B-1 130
-2.3138323	-3.2532549	-4.0877800	-0.9413010	1.7118759	0.3074641	B-1 131
0.0848060	0.8997577	2.5810957	3.4607821	4.2320900	5.1577110	B-1 132
4.1799355	2.0799198	-0.7950696	-1.8817444	-1.8714952	-0.8121209	B-1 133
-0.8420810	-0.6341919	0.7665504	0.8866572	1.8479080	2.0425940	B-1 134
-0.3763520	-2.7252216	-2.9413023	-1.9257107	-0.6916439	0.2487203	B-1 135
-0.6623580	-2.9836197	-2.3053303	2.0073891	4.4449625	4.7341099	B-1 136
6.0197544	6.4747372	3.6383314	1.7323294	1.8694334	1.4452286	B-1 137
0.4931180	0.3515125	1.6074705	-0.2264276	-4.2152672	-5.0478420	B-1 138
-3.5144720	-2.7747965	-3.3739843	-2.9038382	-2.7240782	-1.6398306	B-1 139
-0.9298539	0.6225616	1.3978777	-0.4019704	-2.6274252	-3.4007940	B-1 140
-1.5268507	-0.3018402	1.2680626	4.3330870	5.9724512	4.0441046	B-1 141
2.1226721	0.7773629	0.6920518	1.3983555	0.0280065	-2.5148649	B-1 142
-4.5583172	-4.0532618	-1.4824886	1.7140446	4.4636335	4.7713194	B-1 143
3.1476831	1.9196777	0.3340089	-0.0769393	0.4109266	-0.1500707	B-1 144
-0.5211774	-0.7700450	-1.4788771	-2.1385279	-0.7801316	0.9156306	B-1 145
0.9639432	0.0995193	0.0160277	0.8718136	1.6638193	1.1129770	B-1 146
1.0416317	2.4784899	4.4950180	4.7413254	1.8530512	-1.0247622	B-1 147
-0.8610840	0.1512152	0.4268911	0.8908091	0.4818408	0.1070611	B-1 148
-0.2939623	-2.7963705	-3.8741379	-4.1051197	-4.3816624	-1.3814602	B-1 149
1.8122387	3.0425024	4.2781992	4.4450941	3.2772512	0.4832808	B-1 150
-0.5302337	0.0017544	-0.3174685	0.7571126	2.4285660	3.7153273	B-1 151
3.6104536	2.1896906	1.7515955	3.5741396	3.0321732	1.9378138	B-1 152
2.9036331	1.4771299	-0.9384248	-3.2120504	-4.9646816	-4.2963419	B-1 153
-4.1179142	-5.2467251	-3.2420483	-0.1638049	1.8531303	2.3763266	B-1 154
2.2954330	1.3951168	-1.3908615	-2.6236086	-2.8318043	-2.3525553	B-1 155
-1.5061026	-0.3454750	1.7866564	2.0692406	0.2348522	-0.9504263	B-1 156
-2.4689560	-3.1515064	-2.0682726	-0.9478286	0.1956422	0.1536900	B-1 157
0.8253291	-0.0843188	-1.3418274	0.0936280	-0.2488770	-0.6702236	B-1 158
-0.8261374	-1.4766541	-1.1747208	-1.4795856	-0.6397970	-1.0341988	B-1 159
-0.0930408	2.6919622	2.3571520	0.6076113	-0.4881456	-0.3264416	B-1 160
1.4520121	1.9436893	0.9407203	-0.3105197	-0.6099294	0.2620976	B-1 161
-0.6744406	-2.4804621	-2.2036324	-2.1585960	-2.6133795	-2.3982677	B-1 162

-1.9054098	-2.2111330	-2.7235155	-2.2100267	-1.4718666	-1.8727064	B-1 163
-1.5784245	0.0015882	0.5803904	0.7181500	0.4684021	-0.0206508	B-1 164
-0.2278005	0.1532755	-0.2742020	-1.8777447	-2.3953915	-1.3092499	B-1 165
0.1335123	0.6064045	1.4251137	2.6959743	2.6153030	2.1588850	B-1 166
1.4710903	0.4791629	0.2403666	-0.1474457	0.2206828	1.7639999	B-1 167
1.3422422	-0.3246164	-0.5227845	-0.4552790	-1.3490620	-1.4481716	B-1 168
-0.1242559	0.4634610	0.0895509	-0.4580410	-1.3336363	-1.5404854	B-1 169
-1.3728819	-1.9938927	-1.7173548	-0.5336783	-0.2093508	-0.4982952	B-1 170
-0.8522261	-0.5830910	0.9855202	2.8268976	3.0067873	2.6091690	B-1 171
1.9595585	1.5961180	1.3902798	0.7569323	2.0776958	2.7035007	B-1 172
1.5072012	0.5162550	-0.7243622	-1.7940226	-1.2503185	-0.4551535	B-1 173
0.1213362	0.9867110	1.2626276	2.3345423	3.6877289	3.3325815	B-1 174
1.8443232	0.9514546	1.3973131	1.0733356	-0.2739895	-1.4069118	B-1 175
-2.4621906	-3.0060844	-1.8544540	-0.5845272	-0.4454938	-1.9877996	B-1 176
-1.9437885	-1.1644955	-1.3381433	-1.6641626	-2.9616823	-3.4066715	B-1 177
-2.0845938	-1.0956097	-0.4385667	0.5521469	1.0743771	1.7103033	B-1 178
1.5847893	0.9791900	1.5636492	1.6505499	0.7079785	-0.2078966	B-1 179
-1.7457428	-3.0146923	-2.4180603	-1.3938637	-0.4956250	-0.1269904	B-1 180
-0.1072348	0.8812334	1.6057825	0.9945974	0.7536944	1.0809355	B-1 181
1.1563902	0.4154674	0.2100316	1.6026573	2.9805794	3.0114622	B-1 182
1.9431715	0.8465530	1.3290052	1.7334166	1.1306858	0.6492631	B-1 183
0.7459421	0.9457843	0.4452246	0.5687535	0.1342375	-0.2724438	B-1 184
0.5207704	0.4261082	0.6789343	2.0757685	2.4709063	2.1699486	B-1 185
1.9110785	0.7639669	-0.7208657	-1.6485853	-2.3810349	-1.4701223	B-1 186
0.0960010	0.5156639	-0.2584622	-1.0283365	-1.2812939	-0.7327472	B-1 187
-0.2267203	-0.2118162	-0.2777174	-0.9558793	-1.0534344	-0.5437497	B-1 188
0.3464371	1.4973269	2.3021231	2.1397791	2.3714628	2.3579292	B-1 189
1.6245556	1.5700598	0.6626243	-1.1851950	-2.5218906	-2.5062571	B-1 190
-1.5625134	-0.9801031	-1.2876339	-1.2267380	-0.8671952	-0.2013265	B-1 191
-0.0181608	0.5301251	0.7899933	0.2352818	-0.0847210	-1.2329216	B-1 192
-1.0164909	0.1200681	0.6349530	0.2952720	-0.0031632	-0.7672698	B-1 193
-1.5135860	-1.4293957	-1.1801395	-0.9341795	-1.1180353	-0.6738136	B-1 194
0.5135373	1.3824673	1.2749586	1.2064314	0.8170877	0.3325981	B-1 195
-0.2697856	-1.4680204	-1.6349688	-0.9094760	-0.4284047	-0.3560836	B-1 196
0.0885726	0.9087130	1.1395626	0.5908508	0.1130108	0.1246090	B-1 197
0.6692793	1.1419907	0.6485804	0.4963492	0.3116745	-0.4924986	B-1 198
-0.7052194	-0.4566765	-0.2216459	0.2304038	0.1959717	-0.2237166	B-1 199
-0.3287164	-0.1730170	0.3365650	0.1263474	-0.3135347	-0.5741517	B-1 200
-1.3854256	-1.9819164	-1.1786919	-0.5149963	-0.5194088	0.3299457	B-1 201
0.8593372	0.2181805	-0.9451743	-1.3503857	-1.2827158	-1.8655605	B-1 202
-2.1266298	-0.6916060	1.1488113	2.3404226	2.3470564	1.2569256	B-1 203
1.1392870	0.8893011	-0.1653194	-0.3471727	0.1547401	0.5952567	B-1 204
0.3591638	0.3415818	0.6806387	0.6720989	0.9795290	0.3934325	B-1 205
-1.0089025	-1.5773106	-1.4608135	-0.4792073	0.0630476	-0.4128793	B-1 206
-1.2047071	-1.6058588	-1.0236626	-0.9362710	-1.3983831	-1.1161461	B-1 207
-0.2981585	0.0268309	-0.4325933	-0.6856309	-0.1427141	0.4087568	B-1 208
0.7296557	0.6901585	0.8078359	0.4647546	-0.1922230	0.1727090	B-1 209
0.0595888	-0.5735682	-0.9976605	-0.9484904	-0.8729458	-0.5461490	B-1 210
0.3281130	0.8425871	1.0213699	0.6896788	0.8347140	1.0798206	B-1 211
0.5374383	0.1026420	0.0555947	-0.0850364	-0.0359703	0.0471663	B-1 212
0.0812424	0.0324586	-0.4469337	-0.3066691	0.3813187	0.9306518	B-1 213
1.3336630	1.1454477	-0.1225458	-1.2582788	-0.8447891	-0.7971885	B-1 214
-0.8345978	0.1761302	0.2769535	0.2267165	1.2160139	0.7361757	B-1 215
0.3078305	0.3786125	0.3696308	1.2518206	0.9887618	0.0503786	B-1 216

-0.0633460	-0.9225520	-1.2523537	-0.5025275	-0.4429508	-0.5002376	B-1	217
0.1771075	0.8143465	0.7478627	0.0037912	-0.6280987	-0.9438902	B-1	218
-1.7065992	-1.9725924	-1.5220480	-0.5258231	0.0328731	-0.2527656	B-1	219
0.0019537	0.5147149	-0.2168746	-0.9676230	-0.9865476	-0.4828219	B-1	220
0.1746052	0.2141476	-0.2782007	-0.5168791	-0.3438716	-0.5952671	B-1	221
-0.6549343	0.3432342	0.9051022	1.2656832	1.0081415	0.3367963	B-1	222
0.5366263	1.0415106	1.3809576	0.9213471	0.0410853	-0.0376208	B-1	223
-0.0556995	-0.1867086	0.0030055	0.0798421	0.3487458	0.5535803	B-1	224
0.3427083	0.8482309	0.7812656	0.1150399	0.2899341	0.6670358	B-1	225
0.8425578	0.3415894	0.0856709	0.2993993	0.5761809	0.4711359	B-1	226
-0.0357843	0.0548308	0.4499204	0.1283879	-0.3456289	-0.5164797	B-1	227
-0.3425931	0.2012085	0.9422113	1.4514112	1.2709408	1.0025663	B-1	228
0.8968050	0.0308836	-0.7712783	-1.0343065	-1.0199375	-0.8341134	B-1	229
0.1433411	0.9731147	1.0046377	0.8943529	-0.1920474	-1.2272511	B-1	230
-1.0170393	-0.3647470	-0.1020782	-0.2332101	0.3261065	0.7616148	B-1	231
0.5963596	0.9690534	0.6497456	-0.2992142	-0.8977928	-0.7886496	B-1	232
-0.3720367	-0.2128879	-0.2121543	-0.3402910	-0.7047284	-1.3237362	B-1	233
-1.1008301	-0.2012160	-0.0024173	-0.2738855	-0.0479953	0.5706542	B-1	234
0.6535821	-0.1381240	-0.6690603	-0.6827595	-0.2728082	0.4661927	B-1	235
0.1961181	-0.2422277	-0.1089137	-0.0806230	-0.1696111	-0.0331101	B-1	236
0.3765531	0.4615989	0.1160598	0.0717914	0.0251445	-0.2321827	B-1	237
-0.0419861	0.2287419	0.5134619	1.3317633	1.7259808	1.2870493	B-1	238
0.8648186	0.2082791	-0.4660208	-0.0912675	0.8179583	1.0723019	B-1	239
0.4712945	-0.0234533	-0.2053330	-0.2121184	-0.5982962	-0.7653370	B-1	240
-0.3591411	-0.0837502	0.0395301	0.2371014	0.1390740	0.0571933	B-1	241
0.0825143	-0.2482284	-0.5382456	-1.0018902	-0.9661649	-0.5068918	B-1	242
-0.6593854	-0.5012036	-0.0364594	-0.0932541	-0.2604839	-0.0976506	B-1	243
0.0814133	-0.0973248	-0.0168898	0.4189122	0.6042271	0.3977657	B-1	244
-0.2987638	-0.7721923	-0.5265577	-0.3416923	-0.7266303	-1.3187466	B-1	245
-1.5285387	-1.3107443	-0.9799039	-0.7861738	-0.2897103	0.3918660	B-1	246
0.4940642	0.4847255	0.3940822	0.1942796	0.0747913	-0.1069137	B-1	247
0.0262379	-0.0112687	-0.3045011	-0.4283764	-0.4685532	-0.5183890	B-1	248
-0.2863356	0.0996345	-0.1257119	-0.0757270	-0.2910370	-0.5764349	B-1	249
-0.2799723	-0.3967912	-0.4047115	-0.3176290	-0.3274699	-0.5181237	B-1	250
-0.4345556	-0.1938632	-0.4053593	-0.5023528	-0.1211644	0.1811961	B-1	251
0.1336313	0.3756872	0.6134496	0.8046037	0.8123466	0.6414419	B-1	252
0.4859549	0.4162041	0.9000033	0.9730713	0.5636611	0.5044868	B-1	253
0.4022329	0.1756335	0.1282784	-0.0518545	-0.5764434	-0.8500760	B-1	254
-0.9887355	-0.8583476	-0.5442700	-0.3208045	0.1200908	0.3583744	B-1	255
0.1310478	-0.0425885	-0.3345906	-0.6391757	-0.5787539	-0.3255739	B-1	256
-0.0487035	0.0509858	0.4785396	0.8967324	1.3689623	1.5001612	B-1	257
1.3886995	1.1333961	0.7117299	0.2224635	-0.2224334	-0.1309534	B-1	258
0.0513229	0.0517053	0.0662855	0.0453864	0.1902316	0.2598541	B-1	259
0.1931002	0.0349335	-0.1670181	-0.3784764	-0.3030460	0.1677122	B-1	260
0.0973239	-0.4166403	-0.4927139	-0.1195176	0.1433222	0.1102403	B-1	261
-0.1171947	-0.1019328	0.2514247	0.6908970	0.5479620	-0.1132497	B-1	262
-0.4888594	-0.3376877	-0.2458555	-0.5086226	-0.6212575	-0.4509448	B-1	263
0.1455893	0.5683936	0.6905060	0.4205683	-0.0175404	0.0542415	B-1	264
0.4748534	0.8582145	0.9215246	0.7897251	0.5992764	0.2060516	B-1	265
-0.1223664	-0.2183428	-0.1622826	0.1303264	0.3364866	0.1094358	B-1	266
-0.0323245	-0.0373310	-0.1209274	-0.1480840	-0.1345330	-0.0328996	B-1	267
0.0791934	-0.2668500	-0.4134893	-0.3795303	-0.6092911	-0.5097179	B-1	268
-0.4045699	-0.5980838	-0.5955390	-0.3071856	-0.0087957	0.1945298	B-1	269
0.3120409	-0.0258517	-0.5193805	-0.6654136	-0.4581335	-0.3528373	B-1	270

-0.6309239	-0.7337320	-0.4191000	-0.1753710	-0.1371581	0.0128097	B-1	271
0.1087437	-0.1430587	-0.2931181	0.0370751	0.3230103	0.4614384	B-1	272
0.2134961	-0.2382477	-0.5359964	-0.4853269	-0.2746966	-0.0513776	B-1	273
0.3010819	0.2652135	-0.0194922	-0.1246874	0.1150002	0.4442379	B-1	274
0.3992491	0.1399484	0.0640533	0.0330762	0.1349522	0.3417064	B-1	275
0.3844593	0.4223502	0.3598427	0.4642051	0.6044641	0.1911183	B-1	276
-0.0813472	-0.0455629	-0.0845548	0.1713938	0.5863675	0.5897800	B-1	277
0.6200876	0.6633721	0.3907565	0.2357132	-0.0462777	-0.3349172	B-1	278
-0.3087653	-0.2299449	-0.2662344	-0.1869975	-0.3808041	-0.4605536	B-1	279
-0.4483284	-0.4430425	-0.1628691	-0.1083282	-0.0573160	0.0692778	B-1	280
0.2948499	0.4218318	0.3729866	0.0227999	-0.4399397	-0.6201283	B-1	281
-0.6875505	-0.7728032	-0.7134212	-0.3091789	0.0546211	0.2253765	B-1	282
0.2085131	0.0780348	0.0484561	0.2759025	0.7275066	0.7829209	B-1	283
0.5933021	0.2882968	0.3047249	0.5999232	0.4978034	0.3316407	B-1	284
0.2851194	0.1910427	-0.1053944	-0.1718461	0.0193062	0.3120579	B-1	285
0.2197044	-0.0218547	0.1320261	0.2123526	0.1965383	0.1579080	B-1	286
-0.0379900	-0.2624997	-0.1867369	-0.0040631	-0.0923279	0.0591573	B-1	287
0.2197121	0.2175997	0.1697839	-0.0176235	0.1659558	0.3022944	B-1	288
0.0626095	-0.1466289	-0.1455582	0.0017280	0.1776957	0.2477450	B-1	289
0.0400995	-0.1111808	-0.1151665	0.0084558	-0.0790149	-0.3714871	B-1	290
-0.4286247	-0.3820175	-0.2701039	-0.3279732	-0.4848652	-0.5452642	B-1	291
-0.4298088	-0.2498327	-0.2426035	-0.2265587	-0.1453145	-0.1996977	B-1	292
-0.1489206	0.0712861	0.0540640	-0.1823018	-0.2330458	-0.2063934	B-1	293
-0.2438481	-0.1933014	-0.0630873	0.0413110	0.0358806	-0.0136690	B-1	294
0.2604697	0.5243056	0.4782771	0.4012386	0.2797579	0.3077691	B-1	295
0.1102375	-0.1539789	-0.1434014	-0.2198783	-0.3131570	-0.3689698	B-1	296
-0.3054377	-0.0798477	0.0749007	0.2805275	0.4386848	0.3920218	B-1	297
0.2588134	0.1324935	0.1576124	0.0950237	-0.0160721	0.0880372	B-1	298
0.1576625	0.0538147	-0.0670409	-0.0793360	-0.1621118	-0.3303773	B-1	299
-0.4848558	-0.2624451	0.1221936	0.1389106	0.1209311	0.3774860	B-1	300
0.4578134	0.3015135	0.2256004	0.2931134	0.4735513	0.2275966	B-1	301
-0.1787382	-0.2842450	-0.0772784	0.2041857	0.2866217	0.0457792	B-1	302
-0.1433939	0.0191031	-0.0055664	-0.3987364	-0.4826491	-0.3556209	B-1	303
-0.2857945	-0.2490858	-0.1248413	0.0635481	0.0787967	-0.0513644	B-1	304
-0.2660918	-0.2502482	-0.2004248	-0.1157538	-0.0746241	-0.0913458	B-1	305
-0.0006166	0.0752001	0.0275315	-0.2236704	-0.3293103	-0.2141910	B-1	306
-0.0598910	-0.0719387	-0.1025437	-0.0246195	-0.1813443	-0.3338020	B-1	307
-0.3000829	-0.2172589	-0.2216496	-0.3575028	-0.1269847	0.1089486	B-1	308
0.1350825	0.1250415	0.0683798	0.0594699	-0.0266789	0.0234420	B-1	309
-0.0563916	-0.1663128	-0.0577041	0.1615981	0.3347483	0.3707318	B-1	310
0.4586038	0.4973926	0.6262102	0.5531431	0.3963767	0.1607068	B-1	311
-0.2430634	-0.2830552	-0.0570630	0.1552566	0.1622450	-0.0477262	B-1	312
-0.0946281	0.0157737	0.0549866	-0.0420248	-0.0909144	0.0163289	B-1	313
0.1922145	0.3292046	0.1843423	-0.0741832	-0.1995580	-0.2026882	B-1	314
-0.0450181	0.0566758	0.1373243	0.0961021	-0.0170494	-0.1299232	B-1	315
-0.4356367	-0.5911549	-0.4414372	-0.3455297	-0.4330797	-0.2798401	B-1	316
-0.1614262	-0.2225042	-0.2332591	-0.0386406	0.0836332	-0.0248092	B-1	317
-0.0054238	0.0535777	0.1234145	0.1147104	0.0392421	0.1545285	B-1	318
0.2259498	0.3247080	0.3672607	0.4757797	0.5810570	0.4688573	B-1	319
0.3607624	0.1314973	0.0054360	-0.0392204	-0.2636858	-0.4410728	B-1	320
-0.5587491	-0.5716580	-0.3219404	0.0425102	0.1961360	0.1121128	B-1	321
0.1812981	0.2791573	0.1921588	0.1507657	0.1897689	0.2288552	B-1	322
0.2501991	0.1015844	0.0018554	-0.0216111	-0.0473098	0.1391014	B-1	323
0.0714987	-0.1741765	-0.2457583	-0.3197657	-0.3932984	-0.2347190	B-1	324

-0.0195498	0.1112809	0.1766344	0.1344500	0.1401390	0.1674346	B-1 325
0.0844595	0.0481757	0.0587560	-0.1211209	-0.1402079	-0.0067750	B-1 326
0.0574274	0.2021084	0.2458715	0.1921371	-0.0082178	-0.1076918	B-1 327
0.0199860	0.1905196	0.3694060	0.4276181	0.2764823	0.1685771	B-1 328
0.1462266	0.1513501	0.1457187	0.1213145	-0.0093150	-0.1525126	B-1 329
-0.1399484	-0.1311148	-0.0194308	0.0985449	-0.0067259	-0.1613243	B-1 330
-0.2085425	-0.1794094	-0.0162647	0.0301443	-0.1874630	-0.1759989	B-1 331
0.0081243	0.1724136	0.1848211	0.1142732	-0.0869003	-0.2525248	B-1 332
-0.3253360	-0.3117916	-0.2260961	-0.3982680	-0.3634884	-0.1897576	B-1 333
-0.2154534	-0.2425478	-0.0696970	0.0	0.0	0.0	B-1 334

0.0	-0.0061329	-0.0128305	-0.0203420	-0.0285589	-0.0351186	B-2	1
-0.0399824	-0.0462333	-0.0590364	-0.0771453	-0.0914308	-0.0947857	B-2	2
-0.0971096	-0.0725628	-0.0276429	-0.0088146	-0.0382950	-0.0720246	B-2	3
-0.0574813	-0.0129872	0.0330799	0.0248631	-0.0242871	-0.0832064	B-2	4
-0.1287420	-0.1366397	-0.1517147	-0.2198613	-0.2749281	-0.3020980	B-2	5
-0.2764757	-0.2297617	-0.1147113	0.0008914	0.1328315	0.1342289	B-2	6
0.0558147	0.1184402	0.0964278	-0.0200257	-0.2894733	-0.3948545	B-2	7
-0.3866613	-0.2580383	-0.0931107	-0.1864357	-0.2556389	-0.1759413	B-2	8
0.0499867	0.3506797	0.4126962	0.4023189	0.2512642	-0.2080770	B-2	9
-0.9708155	-1.4936895	-1.1845884	-0.7198440	-0.2445440	0.4062602	B-2	10
0.4109946	-0.0588089	-0.3005465	0.2110523	0.1970057	-0.0819638	B-2	11
0.7990175	0.8724084	0.3268137	0.5273764	0.4539872	0.5447478	B-2	12
0.9078047	1.0218039	1.3072195	1.0029840	0.0079345	-0.1611119	B-2	13
0.1471086	-0.0654517	0.1044068	0.2322951	0.4270120	0.5563148	B-2	14
1.0345936	0.8366714	0.3029072	0.6122466	-0.5167214	-1.5705614	B-2	15
-1.2319603	-1.0115614	-0.9065063	-0.7015548	-1.4663105	-2.4175339	B-2	16
-2.4173794	-2.3322506	-1.6326189	-0.9227503	0.1009272	1.0991554	B-2	17
0.8537962	-0.2281650	-1.4283247	-1.0302954	-0.9038067	-0.9214821	B-2	18
1.2581186	2.5442934	1.4230824	1.6322117	1.3715649	0.2740414	B-2	19
0.2790506	-1.9803972	-2.9072905	-1.4504108	-2.1304712	-2.7043753	B-2	20
-1.5821466	-0.5751536	-0.0308052	0.9711035	2.9161739	5.5394745	B-2	21
7.1876125	4.5619812	0.2186714	0.0459444	2.3253832	3.1360502	B-2	22
1.8703098	0.7787454	0.9359320	1.9069967	2.6491489	2.9788160	B-2	23
2.3976622	1.9295168	2.7606983	2.6467943	1.4104900	1.1687489	B-2	24
-0.3214239	-2.7994289	-2.6823702	-3.2056522	-5.3095560	-5.6894722	B-2	25
-1.7430506	-0.2423269	-1.0382881	-1.2506266	-3.6772490	-2.1503649	B-2	26
0.1708782	0.1764786	-0.8876939	-1.1586723	-2.0806446	-4.4486132	B-2	27
-2.3467617	1.2463741	2.6662064	2.9260788	-0.3523245	-2.3545218	B-2	28
-1.5402212	0.1823471	2.4885969	0.8595686	-2.3553228	-1.9951696	B-2	29
-0.9959911	0.2630843	2.3216496	3.8327427	4.3923721	1.8533583	B-2	30
-1.0700550	-2.8227692	-1.9368448	-0.0766996	2.7414560	6.4597092	B-2	31
8.8590326	10.1360388	8.4261818	4.8422451	2.5293407	-0.6279787	B-2	32
-3.4295387	-6.7949791	-8.7336369	-4.9466009	0.4363204	2.1775827	B-2	33
-1.0960321	-3.9013615	-3.7525625	-2.6696997	-1.6864176	-2.1694059	B-2	34
-2.1164408	-1.1391048	-1.5542440	-1.6505032	-2.7243061	-2.2090435	B-2	35
-2.1673326	-3.2830276	-3.6454782	-0.9912708	2.7616043	3.3567686	B-2	36
1.4500275	1.6196785	4.6850796	3.1138020	0.1224297	0.5983557	B-2	37
-1.7360325	-6.1764145	-6.3698826	-5.5593119	-3.8169575	-2.2077732	B-2	38
-2.3465462	-0.4230272	1.3297205	3.8170214	6.7932596	5.5325718	B-2	39
5.0509396	5.1499205	3.2727003	3.2855310	3.7020597	3.3101511	B-2	40
4.1294832	3.2908840	-0.6890076	-4.3395195	-3.7148676	-4.3889713	B-2	41
-7.0397158	-7.9261055	-5.1208706	-3.2599888	-2.9030352	-3.1611156	B-2	42
-3.6862059	-1.4539194	-1.6935644	-4.6100130	-2.5947466	3.2607489	B-2	43
6.3826990	6.5714550	4.8162441	0.4105697	1.4584265	2.5059090	B-2	44
-0.1333820	-1.1013288	-2.0978537	-2.2388096	0.7351031	2.7199507	B-2	45
1.3424568	2.0359631	3.3557405	2.8078566	1.9856377	4.7618647	B-2	46
8.0518579	7.8170033	7.0871010	3.8886089	1.2592678	-0.0851875	B-2	47
-4.0130377	-5.9486103	-6.4449215	-5.4326982	-2.4182749	0.7842202	B-2	48
1.9034357	1.0096207	1.1889400	0.9218041	1.0012608	-0.0474363	B-2	49
-2.5313730	-5.3890324	-5.8614244	-2.0268059	1.7958784	5.5998030	B-2	50
4.9115086	0.5593024	-3.0686054	-5.5212975	-5.1781301	-2.4305573	B-2	51
0.9935323	1.7450552	2.9205675	4.2744055	3.3871107	0.9237767	B-2	52
0.6408376	1.5221415	-0.1933712	-0.5640143	1.9913406	0.5663692	B-2	53
-4.9942474	-8.5243950	-7.3001070	-4.7285252	-3.1321144	-1.1012497	B-2	54

0.8377610	1.5233850	1.7583342	1.9581280	3.0974255	1.0134144	B-2	55
1.1517305	0.2801781	-2.5185843	-2.3552732	-1.6818371	0.4025785	B-2	56
1.7966604	1.8893270	0.8001761	1.7981930	0.8869613	0.6361003	B-2	57
3.0186586	2.3487549	0.5074300	-1.1737814	-2.0340796	-4.4685059	B-2	58
-7.4303904	-5.5736151	-2.5641518	1.8138847	7.4668655	8.2441816	B-2	59
6.6378431	5.7747803	3.3400574	2.2958899	0.4651181	-0.3748534	B-2	60
0.3805331	-1.9328957	-2.6708164	-2.6391249	-3.7561064	-2.0794573	B-2	61
1.1371326	1.4155006	-2.9543629	-4.0167847	-1.1673164	0.2484154	B-2	62
1.4547148	4.4832945	6.7606907	4.3405800	0.8415881	2.3806906	B-2	63
5.4452114	4.7178211	2.2520771	-0.9235066	-6.2698698	-5.1228085	B-2	64
-0.9963461	-3.0341673	-6.1066322	-8.9551048	-8.3009949	-7.1035337	B-2	65
-3.9314518	1.3183804	2.7333355	3.1300020	3.0194263	2.3782806	B-2	66
2.1433840	-0.1388785	-2.5059977	-2.6901655	0.2325662	5.0591087	B-2	67
8.0169001	5.4851112	1.8658590	0.1715298	-0.5890020	0.0283568	B-2	68
0.2198301	2.0752544	2.0486031	0.9884701	2.6323023	3.0908632	B-2	69
5.0549316	5.6557531	2.3652639	-1.9309053	-4.5576982	-4.8361616	B-2	70
-6.1840296	-4.9268923	-3.3426180	-3.5896044	-0.4099323	5.1796532	B-2	71
5.0308151	2.2650299	-0.7136856	-3.2949486	-3.1768036	-1.2775993	B-2	72
0.6559852	2.2670412	3.7794828	4.0509567	-0.0970312	-0.9418477	B-2	73
4.0628147	4.9541740	2.4844341	-1.8871641	-4.3934250	-3.1045971	B-2	74
-2.3656292	-2.0852757	-3.1576157	-1.6752739	1.4320726	0.2597304	B-2	75
0.1838230	2.5165510	5.5276403	7.7132740	4.5483246	1.2253094	B-2	76
-1.6249666	-3.8410921	-3.9485769	-4.9172525	-6.3107653	-5.7421064	B-2	77
-4.0050268	-2.5643177	-1.7716265	-3.5969734	-0.1744692	2.9969225	B-2	78
1.9125338	2.0589361	2.3151283	3.6666517	2.3429890	3.7859211	B-2	79
5.1919117	0.7283469	-3.9970264	-5.5656080	-4.5821075	-2.8284578	B-2	80
-0.4297588	0.9805856	-1.3262281	-5.7210102	-7.6143866	-6.2856293	B-2	81
-4.1812954	1.5202675	3.3125086	0.4984199	-0.5137517	1.3152742	B-2	82
3.1231890	3.0324020	4.6035709	6.2020817	3.9681520	5.1288319	B-2	83
5.1873398	-2.2606525	-3.5485506	0.9441715	2.5096731	1.2637701	B-2	84
0.1161362	-1.4602699	-4.0036497	-5.9744740	-4.8715410	-4.0048208	B-2	85
-5.5147734	-4.8061905	-3.2047195	-3.5847673	-2.3537407	1.2563972	B-2	86
1.1508455	1.9000130	5.6365356	2.2309427	-4.6806412	-7.9512205	B-2	87
-6.4430265	-2.1472673	-0.1119239	1.8582258	5.1834755	7.8537807	B-2	88
5.2815905	2.8756819	3.3087788	0.9198221	-2.0223255	-3.2339840	B-2	89
-2.1451654	-1.1259937	-0.0187217	1.2368393	0.9908959	0.5937307	B-2	90
-0.6073582	0.2838890	1.1071081	-0.3026994	-0.4622031	1.2349453	B-2	91
4.7428493	2.1762981	-2.7527657	-4.7479572	-4.8194780	-4.3110056	B-2	92
-4.3611917	-4.8782234	-5.2268133	-5.5194540	-2.2514277	2.3713150	B-2	93
5.3180389	5.4644794	3.9997444	3.7725649	3.3918037	4.8920660	B-2	94
7.0231152	5.3168097	2.6450205	2.7802296	5.0572805	4.8106165	B-2	95
1.5762730	-3.1545401	-7.5438862	-7.4204674	-3.3115387	-1.2854004	B-2	96
-2.4797802	-4.1434708	-4.3417559	-1.6077318	0.6012866	0.4096368	B-2	97
-1.3997116	-2.9845324	-3.5751743	-3.3083639	-2.5267162	-1.0384283	B-2	98
-1.1924477	-1.6117964	-0.0534134	-0.5599946	-1.6452284	-3.2352276	B-2	99
-4.6246748	-2.2496176	-0.0141024	1.9519091	3.0815830	2.1305962	B-2	100
2.0392485	3.0233564	2.5817289	0.8742970	-1.6322060	0.3108691	B-2	101
3.1169214	4.5016737	5.8350716	5.7827425	8.2297707	7.1221828	B-2	102
2.1203241	-0.7980072	-1.4398289	-1.2309380	-0.7565621	-2.6636372	B-2	103
-3.3300962	-2.4303045	0.3072857	5.2949295	4.5382557	1.1159697	B-2	104
1.3811092	3.1611376	2.3650608	1.9783850	1.3180046	-1.2257652	B-2	105
-0.9293846	3.6176548	5.2497759	2.4988585	1.3965530	1.0131493	B-2	106
-2.4597950	-1.6136026	2.4122829	3.3452368	1.6589746	-1.5215168	B-2	107
-2.4861164	-4.5376091	-4.2499905	-2.4261799	-1.6243792	-1.1239614	B-2	108

2.6202688	8.8232832	9.1727324	5.0851965	0.2077078	-1.1104050	B-2 109
-0.1577049	-1.0238905	-1.3709612	-2.1743259	-0.6873268	0.3053584	B-2 110
-1.8940058	-0.7829077	1.7810049	5.0455379	7.5622988	9.2304754	B-2 111
8.3915091	4.8673439	1.5954189	-0.3675402	-0.3550752	0.4785274	B-2 112
-0.6134137	-2.6582308	-4.6914473	-3.8766947	-2.4692116	-3.4379559	B-2 113
-6.8682632	-7.1430120	-1.7433443	0.8388827	1.5861216	1.4951525	B-2 114
1.0091200	1.7018919	1.5540562	-0.1437545	-0.1331044	-2.2733479	B-2 115
-5.1708822	-6.9692240	-4.9256315	-1.5482569	-2.2593699	-2.8932819	B-2 116
-3.0907574	-1.3690434	-1.3867941	-1.4871531	-0.0693297	0.4069967	B-2 117
2.0662909	0.5237193	-2.4990616	-1.9216824	0.1124083	0.7184786	B-2 118
0.3636697	-0.7518881	-2.8893042	-1.3814363	-0.8268757	-4.1282215	B-2 119
-2.4162893	-1.6750126	-3.9307318	-3.4347248	-2.7613354	-1.1810913	B-2 120
1.0850077	0.6659272	-1.4712439	-1.5114088	1.3258944	3.2600689	B-2 121
3.6747904	4.5396872	3.8822470	2.0900841	0.5207043	0.4921464	B-2 122
3.2452860	2.4667444	0.2396830	0.0683703	0.6737598	1.6167850	B-2 123
1.6488523	0.7249807	-0.6943322	-2.4175243	-3.9475832	-6.2628946	B-2 124
-6.5767145	-5.8381395	-3.9932318	-1.3940821	-1.4586582	-0.7328057	B-2 125
0.9051381	1.9474916	3.0855618	5.8551149	6.3791380	4.2255087	B-2 126
3.8196716	2.5582972	1.7356405	0.3543887	-1.2289715	1.1587667	B-2 127
1.8924236	0.1361760	-0.8020627	-1.9266272	-1.6888103	-1.3311481	B-2 128
-1.8251238	-0.9282864	0.4077285	1.0991106	1.4626188	1.3196478	B-2 129
-0.5194135	-3.3393230	-3.3553686	-1.6757479	0.4857283	3.2802362	B-2 130
3.1035776	2.9831038	0.7881369	-3.0200911	-1.9330454	-1.5100460	B-2 131
-0.4030318	-0.5329654	-1.9425735	0.1394866	0.6892436	0.8250363	B-2 132
0.6436108	-0.5562752	-2.4709997	-2.6606064	-1.7854338	-2.9479666	B-2 133
-3.8165970	-2.3758707	-0.0046750	1.2907763	-0.4480999	-2.0810080	B-2 134
-2.1396112	-2.4757547	-1.8070965	0.8688675	3.4704914	3.8910112	B-2 135
1.4778118	-0.0289318	0.1822876	0.0408152	0.4499865	1.2720718	B-2 136
3.9173069	4.6844301	2.4817438	-0.7121304	-1.6802549	-0.3138717	B-2 137
-0.3485759	-0.4366452	-1.3178225	-2.1600285	-1.8687048	-1.7207813	B-2 138
-0.9266084	0.7426684	1.7768393	2.2571573	2.0365992	-0.3657830	B-2 139
-1.9179659	-1.5768127	-2.6631842	-3.5409689	-2.1511507	-0.4992349	B-2 140
-0.0468188	0.1810148	0.2622251	-0.5897478	1.0757484	4.5026493	B-2 141
5.1438456	4.5213175	2.1920328	-0.3279582	-1.5155668	-1.5158701	B-2 142
-1.5718927	-1.5604115	-2.3372059	-3.5682764	-2.4420424	-0.2631297	B-2 143
1.5268097	2.1685705	3.7495070	4.3807278	3.1880884	4.7619114	B-2 144
5.6388607	3.9794264	1.7461452	-1.1304274	-1.9276495	-0.8039607	B-2 145
1.3759403	2.5044489	2.5334282	2.7369070	2.0990419	0.3961859	B-2 146
-1.2715330	-1.0089369	-0.3589504	-0.5655326	-1.2259712	-3.0460615	B-2 147
-1.6652489	1.0009623	0.4115036	-2.1328707	-2.9973154	-1.2736635	B-2 148
0.3652230	2.2844362	2.4949274	0.9153417	-0.9986690	-1.3205643	B-2 149
-0.0697849	1.5580072	1.3580427	-0.1380296	0.3571138	1.4490328	B-2 150
1.5038471	1.4393005	2.1371078	2.6018124	1.6481409	-0.7167864	B-2 151
-2.8142872	-3.7599545	-5.3825293	-6.2480602	-5.5687752	-4.5997868	B-2 152
-3.4020329	-2.4244270	-1.6959496	-2.1900682	-1.6123371	-0.3615820	B-2 153
-0.0223551	1.2579088	2.7195053	3.3509731	4.3354836	4.0757227	B-2 154
2.0517139	0.3633997	-1.6207170	-2.5171442	-2.7719460	-2.5528545	B-2 155
-1.0660667	0.8504915	1.4457722	0.7384900	0.1468452	0.0601459	B-2 156
-0.3089353	-0.6125129	-0.3442333	-0.4865847	0.0149022	0.2218527	B-2 157
-0.3987420	-1.3949432	-2.6370802	-1.3457060	1.2162371	0.4994615	B-2 158
-0.8143314	1.0916338	3.5964079	3.3595037	2.2298527	2.6231594	B-2 159
1.7373981	0.7251582	2.0662088	2.9419861	2.5876780	1.4433699	B-2 160
0.6488343	0.3887679	0.1806304	-0.2946346	-0.5781752	-0.9710920	B-2 161
-1.6143894	-1.9797783	-0.6862853	0.2531348	0.3980612	0.5352968	B-2 162

0.9913350	0.6568888	0.1663043	1.5008974	2.2446232	1.1340294	B-2 163
-0.4570269	-1.9353237	-3.0732727	-3.2727528	-1.8144360	-0.6262649	B-2 164
-0.4366358	-0.8898318	-0.9218060	-1.0583344	-2.5576181	-2.8524380	B-2 165
-2.0033178	-1.8308144	-1.6730623	-0.8496585	0.5219214	0.7877932	B-2 166
-0.1111383	-0.6730866	-0.4200302	-0.0182599	-0.5789627	0.0458028	B-2 167
0.8453576	0.2901636	-0.1774417	-1.0217314	-2.0037565	-2.7275190	B-2 168
-2.1636229	-0.4740233	0.2693475	0.5574291	0.2487817	-0.2287183	B-2 169
0.0475950	-0.0754220	-0.0564822	1.0222397	1.1592836	0.6036029	B-2 170
1.1752148	2.8305178	3.7096386	3.0463219	1.4444275	0.1481643	B-2 171
0.7796848	1.2557716	-0.2807985	-1.6248798	-1.3940668	-0.8178166	B-2 172
-0.9682169	-0.7939969	-0.3671918	0.0990123	0.3613270	-0.2885328	B-2 173
-0.1253540	-0.2625754	-0.4280091	-0.1410871	0.4579031	0.9408458	B-2 174
0.5351608	0.0307694	-0.8201631	-0.6259882	0.3083196	1.2638893	B-2 175
0.9142388	0.8418978	2.0195856	3.0877542	2.8403015	1.9762955	B-2 176
1.0456419	-1.0677853	-2.5066051	-2.3812952	-1.1301527	-0.3245551	B-2 177
-0.0956233	0.4230658	1.1362877	1.2570095	0.8929223	0.9944122	B-2 178
1.7137041	1.6700745	0.6415514	-0.6575338	-0.6335508	-0.3415478	B-2 179
-0.8312637	-0.4781583	0.5306652	1.1635199	1.4583635	2.9973898	B-2 180
2.6375332	1.5716944	2.3671970	2.0248623	0.9989692	0.0770386	B-2 181
-0.7202255	-0.3895724	0.2266948	0.0996948	-0.2617311	-0.7893606	B-2 182
-0.5723585	0.1306503	0.3268090	-0.3388935	-1.0402765	-0.9306716	B-2 183
-0.9857044	-0.1837833	0.2843753	-0.3012642	0.1535881	-0.1717243	B-2 184
0.0560564	0.6320975	0.8725454	0.7578934	0.2830467	-0.4558710	B-2 185
-1.2236967	-0.4551525	0.2814217	0.0285117	-0.6082968	-1.1868505	B-2 186
-0.6449554	0.0657066	-0.2070166	-0.6272536	-0.3016258	0.6167837	B-2 187
0.3252650	-0.8014084	-0.7960261	-0.6015482	-1.3769083	-1.5703382	B-2 188
-0.9175087	-0.3527060	0.0155037	-0.2996306	-0.5823932	0.0709236	B-2 189
0.3769978	-0.1316890	-0.5210848	1.0849218	2.5681181	1.1308985	B-2 190
-0.2779223	-0.1671408	-0.4871173	-0.8903568	-1.1800070	-2.3222427	B-2 191
-2.3215084	-1.5182571	-0.8356138	-0.0638710	-0.1870503	0.1046787	B-2 192
1.0986471	1.3545580	1.2088032	0.8078217	0.1186886	-0.3581487	B-2 193
-0.7400085	-1.0292139	-0.9802240	-0.6798351	-0.6542780	-0.8937769	B-2 194
-1.9613075	-2.3610010	-0.8230836	0.0595558	-0.0779762	0.3767720	B-2 195
1.3481302	1.5098467	1.1976528	0.2691104	-0.3111542	-0.1601657	B-2 196
-0.2843969	-0.8247635	-1.3864021	-1.2462158	-0.9703348	-0.6403730	B-2 197
-0.3693720	-0.0424101	1.3875036	2.3711061	2.1211615	1.9865265	B-2 198
1.7951679	0.7636232	-0.0846663	-0.6195834	-1.3834305	-1.0392323	B-2 199
-0.1464694	0.0795380	-1.2163353	-2.8658237	-3.2009583	-2.6463137	B-2 200
-1.7337027	-1.5085697	-2.3060684	-1.5233593	-0.4675713	-0.4541667	B-2 201
-0.0940493	0.4899123	0.8292968	0.0626813	-0.3826849	-0.6078596	B-2 202
-0.7017162	0.1564652	0.2067522	0.0324180	0.5189829	1.0128708	B-2 203
0.9596252	0.0887378	-0.7404466	-0.0926688	0.9145277	1.0407143	B-2 204
0.2639219	0.4320193	1.5368977	1.4212646	0.6025963	-0.3211462	B-2 205
-0.0630760	0.4562441	0.8338650	0.7040654	0.7200733	0.9110992	B-2 206
0.5179150	0.6286454	0.4027663	0.0492672	0.3497534	1.0574484	B-2 207
1.4522762	1.6046953	1.2518139	0.5056548	0.4719772	0.5647989	B-2 208
0.5683399	0.6304168	0.4188215	0.5706561	0.4304113	-0.0148389	B-2 209
0.0637624	0.5710782	1.2390690	1.0330544	0.4140370	0.5810721	B-2 210
0.7504132	0.7822174	1.1314001	0.9699948	0.2554907	0.0731038	B-2 211
-0.2031507	-0.6140718	-0.8184246	-0.7993357	-0.4562894	-0.0863281	B-2 212
0.2408755	0.8873464	1.1180382	0.7028276	0.3053122	0.2201625	B-2 213
0.0241653	-0.5934607	-0.0835662	1.0171804	0.5563082	0.0480454	B-2 214
0.2422900	0.0109694	-0.5492641	-1.1143427	-1.4520350	-2.1078396	B-2 215
-2.7655821	-2.0183506	-0.3718213	0.7010902	0.8919243	0.7625487	B-2 216

0.5162956	0.8495340	0.6174296	0.2802867	-0.7186249	-2.0328388	B-2 217
-1.8798561	-1.5449495	-1.3699074	-1.3420372	-0.9742780	-0.2507561	B-2 218
0.8596110	0.8773450	0.5079116	-0.0687783	0.1905168	1.0092010	B-2 219
0.6017550	0.7402558	0.9720089	0.8602352	0.3775039	-0.4588020	B-2 220
-0.6997815	-0.8921055	-1.1099977	-1.2083006	-1.0224533	-0.2853809	B-2 221
0.2807957	0.3057994	-0.3234541	-0.8950969	-0.4561818	-0.0709623	B-2 222
0.2846774	0.7280316	0.8724708	0.8553053	0.6500270	0.1296201	B-2 223
0.0550744	-0.1237554	-0.6183568	-1.0815344	-1.6532240	-1.4790773	B-2 224
-0.8442358	0.4376112	0.8117489	0.0858145	0.0472446	0.5027173	B-2 225
0.1531065	-0.7961168	-1.2979984	-0.8485746	-0.3113884	-0.3924259	B-2 226
-0.4834026	-0.1867152	0.0533483	0.3139606	0.4324896	0.1756731	B-2 227
0.0214383	-0.3875073	-0.4947289	0.2973360	0.9541211	0.9724386	B-2 228
0.9757218	1.6999655	2.2437611	1.6650190	0.7609321	0.4914089	B-2 229
0.5504491	0.4145828	-0.2105793	-0.9836053	-1.1293125	-1.0224295	B-2 230
-1.3437862	-1.5105152	-1.2983990	-0.3939216	0.2680700	0.4213502	B-2 231
0.4208054	-0.3368077	-0.6149169	-0.6429639	-0.7520466	-0.5968646	B-2 232
-0.1225288	0.3341345	0.4339276	0.4127698	0.6222991	0.6739506	B-2 233
0.1544549	0.0822008	0.1366208	-0.2226996	-0.2278232	0.3524322	B-2 234
0.8527152	0.9174398	0.3045370	0.0162345	0.2693674	0.1884705	B-2 235
0.0899361	0.0257837	0.1092629	0.3594395	0.5068502	0.3201199	B-2 236
0.0363272	-0.0996175	-0.0294568	0.0148134	-0.3695316	-0.6271204	B-2 237
-0.6057218	-0.4258581	-0.4023471	-0.1600137	0.5647054	0.6874741	B-2 238
0.4403881	0.1235732	0.3545426	1.0087585	1.0003128	0.0264428	B-2 239
-0.7625468	-1.0578241	-0.8396751	-0.1847578	0.0065871	-0.0985656	B-2 240
-0.3754992	-0.3473389	-0.0847465	0.5485539	0.8367658	-0.0585719	B-2 241
-0.4980347	-0.3486410	0.0989971	0.4521385	0.4286578	0.5903485	B-2 242
0.5215673	0.2552471	-0.0036703	-0.5642692	-0.6958647	-0.4179547	B-2 243
-0.2711605	-0.2376887	-0.1233805	0.0120552	0.2377586	0.4875517	B-2 244
0.7217363	0.8363041	0.5271554	-0.0286854	-0.4783801	-0.6726956	B-2 245
-0.5168924	0.0900032	0.5660245	0.5811316	0.3885517	-0.0639333	B-2 246
-0.3478563	-0.0656547	0.1944156	0.1298043	0.0172080	0.1444232	B-2 247
0.2849353	-0.1196281	-0.2029648	0.0364443	-0.0476101	-0.2047174	B-2 248
-0.3064471	-0.0601337	0.3850551	0.7257588	0.7015595	0.8369840	B-2 249
1.0444183	0.8636534	0.8828406	0.5780572	0.3215598	0.5747476	B-2 250
0.4788277	0.0840166	-0.1331384	0.0596153	0.3215580	0.0841497	B-2 251
0.0990831	0.3896706	0.0383517	-0.9809887	-1.2963438	-1.1422424	B-2 252
-1.1168318	-0.9055648	-0.3920538	0.1423052	0.2577522	0.1098258	B-2 253
0.1554492	0.1905780	0.1957847	0.3473586	0.2952304	0.2065813	B-2 254
0.0495977	-0.3821619	-0.1788449	-0.1064473	-0.6826423	-0.8654767	B-2 255
-0.5997759	-0.1926243	-0.0161212	0.0299129	-0.0457688	-0.0876397	B-2 256
-0.0493163	-0.0194365	-0.2057050	-0.0571404	0.0252823	-0.2388407	B-2 257
-0.4290439	-0.5462000	-0.5881871	-0.5151644	-0.0246534	0.4730744	B-2 258
0.4938460	0.7790570	0.6984161	0.1402287	0.0810885	0.2869559	B-2 259
0.3808154	0.3781168	0.4419886	0.3274190	0.3099937	0.3810458	B-2 260
0.1917121	0.0594009	0.1920370	0.2514181	0.2558910	0.2189652	B-2 261
-0.0884735	-0.3814754	-0.4962302	-0.9333740	-1.2982206	-0.9750448	B-2 262
-0.6594289	-0.5619010	-0.2432334	-0.2750131	-0.4028882	-0.1898085	B-2 263
-0.0006676	0.0404064	0.1074576	0.2518572	-0.0532369	-0.6785443	B-2 264
-1.1278925	-1.1318979	-1.0074310	-0.8453302	-0.4609095	-0.2647744	B-2 265
-0.4592865	-0.7680744	-0.4077861	0.2550704	0.1158898	0.0154763	B-2 266
0.0979131	0.2894828	0.3067899	0.2469971	0.0747431	-0.0538563	B-2 267
0.0367219	-0.0545418	-0.0065569	0.1917925	0.2667668	0.0996392	B-2 268
-0.1346200	-0.5727032	-0.7111238	-0.2846991	0.0746751	-0.0492738	B-2 269
-0.1261793	0.2799657	0.4543499	0.1895829	-0.0833046	-0.0764031	B-2 270

0.1227469	-0.2551772	-0.2711558	-0.0103990	0.0043133	0.2885017	B-2	271
0.3595027	0.1800686	-0.1320063	-0.5406554	-0.6638989	-0.4408688	B-2	272
-0.0436537	0.1931635	0.3197526	0.6574280	0.6301014	0.3492926	B-2	273
0.2894497	0.2831450	0.0119655	-0.1649040	-0.1742691	-0.2036965	B-2	274
-0.3123884	-0.4771753	-0.5740800	-0.7484387	-0.5948544	-0.1576616	B-2	275
0.2455317	0.2196411	-0.1307721	-0.0874584	-0.0651627	-0.0470803	B-2	276
0.0212494	-0.0454392	-0.2431805	-0.3849739	-0.3222407	-0.1306702	B-2	277
0.1392854	0.1586993	0.2661493	0.4834602	0.5734190	0.7520288	B-2	278
0.7811769	0.5453520	0.0789526	0.0803850	0.2245929	0.0224099	B-2	279
-0.0201966	0.2017013	0.5165808	0.3233379	-0.0419021	-0.2131835	B-2	280
-0.3986108	-0.1720689	0.2790695	0.4132013	0.4963728	0.6228203	B-2	281
0.5634496	0.2677999	0.0169767	0.0050187	0.1796182	0.4790543	B-2	282
0.7509429	0.9053742	0.9180970	0.9508398	0.8034225	0.4803517	B-2	283
0.3880682	0.3384299	0.2271424	0.0526240	-0.1220935	0.0384489	B-2	284
0.2492407	0.1291707	0.1735741	0.1400390	-0.2245561	-0.5237381	B-2	285
-0.5638537	-0.5689867	-0.4456609	-0.2052782	-0.1539261	-0.0070252	B-2	286
0.0315276	0.2503776	0.6844610	0.7581314	0.5502254	0.2936828	B-2	287
-0.0312509	-0.2836454	-0.2460321	-0.0228386	0.1082234	0.2088277	B-2	288
0.0209529	-0.1924440	-0.0807797	0.0546287	0.1760735	0.3040932	B-2	289
0.5193540	0.5781374	0.3440973	-0.0334189	-0.2241567	-0.1712899	B-2	290
-0.2507769	-0.3241670	-0.1752048	0.0178076	0.0280367	-0.2767996	B-2	291
-0.3224003	-0.1002549	-0.1811290	-0.2581629	0.0114396	0.0558335	B-2	292
-0.0273228	0.0344925	0.0660617	0.0254900	-0.0088741	-0.1584688	B-2	293
-0.2898595	-0.4990470	-0.6346471	-0.3145894	0.0025221	0.0272652	B-2	294
-0.2074178	-0.4441227	-0.4285426	-0.3278939	-0.3215184	-0.2039705	B-2	295
-0.0859362	-0.1181635	-0.0991341	-0.0907671	0.0162487	0.0752870	B-2	296
0.0019735	0.1060564	0.2223549	0.2194853	0.1619304	0.2508411	B-2	297
0.3756334	0.2697895	0.0483881	-0.2057211	-0.4704362	-0.5481999	B-2	298
-0.5137612	-0.2444552	0.0409087	0.0750546	0.0682693	0.2029949	B-2	299
0.2205430	-0.0274900	-0.1130127	0.0737328	0.0711380	-0.1130646	B-2	300
-0.1481671	-0.1119173	0.0260736	-0.0082216	-0.1136414	-0.0263352	B-2	301
0.0138446	-0.0706479	0.0702636	0.1001095	-0.0659323	-0.0782038	B-2	302
-0.0368824	0.0059403	-0.0374480	0.0437726	0.0825039	0.0702173	B-2	303
0.1540980	0.1458679	0.0178482	-0.1311064	-0.0271236	0.0899427	B-2	304
-0.0008375	-0.0580393	-0.0661325	-0.2494267	-0.5122183	-0.4971263	B-2	305
-0.2970179	-0.0611582	-0.0076484	-0.0168369	-0.1545520	-0.3339173	B-2	306
-0.4105914	-0.4266711	-0.3906876	-0.2563131	0.0699067	0.2625008	B-2	307
0.2369040	0.1819534	0.2032604	0.0612592	-0.0821621	-0.0389655	B-2	308
-0.0424611	-0.0026807	0.1626623	0.1969972	0.2435941	0.2033879	B-2	309
0.1829126	0.1983474	0.1674346	0.1601128	0.1136377	-0.0144555	B-2	310
-0.1181540	-0.0376558	0.0231436	-0.0751728	-0.1192617	-0.0537968	B-2	311
-0.0918180	-0.1824831	-0.1857795	-0.2405007	-0.0864499	0.1673250	B-2	312
0.0773086	0.0824142	0.3101779	0.3112572	0.2593555	0.3618132	B-2	313
0.1849306	0.0006997	0.1382374	0.0934884	-0.1004333	-0.0779177	B-2	314
-0.0928661	-0.1308448	0.0014976	0.1808665	0.2856567	0.3484502	B-2	315
0.3790346	0.2581893	0.0997109	0.0030783	0.0987790	0.2125027	B-2	316
0.1881202	0.1450756	0.0112725	-0.1654535	-0.2792358	-0.2965524	B-2	317
-0.0782925	0.1757827	0.2570525	0.2163373	0.2052348	0.1892354	B-2	318
0.2199812	0.1704987	-0.0514088	0.0137379	0.0314700	-0.0932769	B-2	319
-0.0829619	-0.0778960	-0.1930842	-0.2071978	-0.1233616	-0.0972701	B-2	320
0.0919511	0.1859655	0.0750594	0.0774634	0.1216516	0.1126425	B-2	321
0.1048704	-0.0084369	-0.1262558	-0.1290300	-0.0510443	-0.0325993	B-2	322
0.0448321	-0.0141675	-0.1374716	-0.0755665	-0.1103876	-0.1230236	B-2	323
-0.1134555	-0.1666858	-0.2108794	-0.1949595	-0.0615321	0.1796088	B-2	324

0.3270734	0.2817097	0.1300838	-0.0294691	0.0021095	-0.1223220	B-2 325
-0.2415175	-0.0098108	-0.0353820	-0.0233730	0.1531603	0.0846255	B-2 326
0.0154725	0.0585171	0.1040016	0.0456092	-0.0774720	-0.1254060	B-2 327
-0.1797721	-0.1387784	0.0344321	0.0911372	0.1176299	0.1912116	B-2 328
0.3144280	0.2682145	0.1435563	0.2013492	0.2477044	0.2565539	B-2 329
0.2911059	0.2517902	0.0010944	-0.1368408	-0.1814265	-0.3677621	B-2 330
-0.4800929	-0.5361806	-0.4139020	-0.2984286	-0.2534944	-0.1666348	B-2 331
-0.1191701	-0.2272972	-0.4280960	-0.4037201	-0.2963446	-0.1901750	B-2 332
-0.0540848	0.0747440	0.2527580	0.3131249	0.1640013	0.0392799	B-2 333
-0.0680578	-0.2041574	-0.2931238	0.0	0.0	0.0	B-2 334

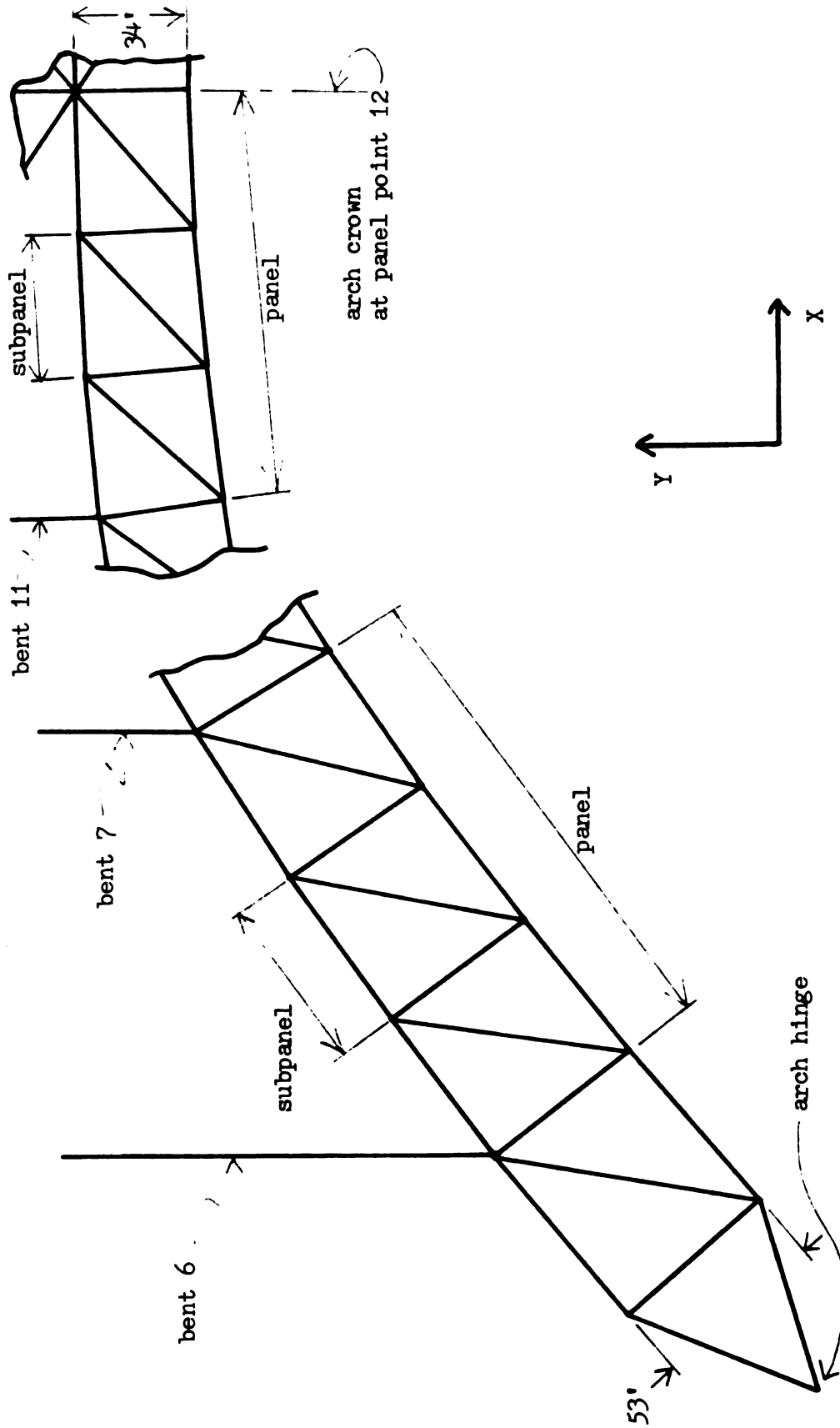


Figure B-1 NRCB Arch Side Trusses

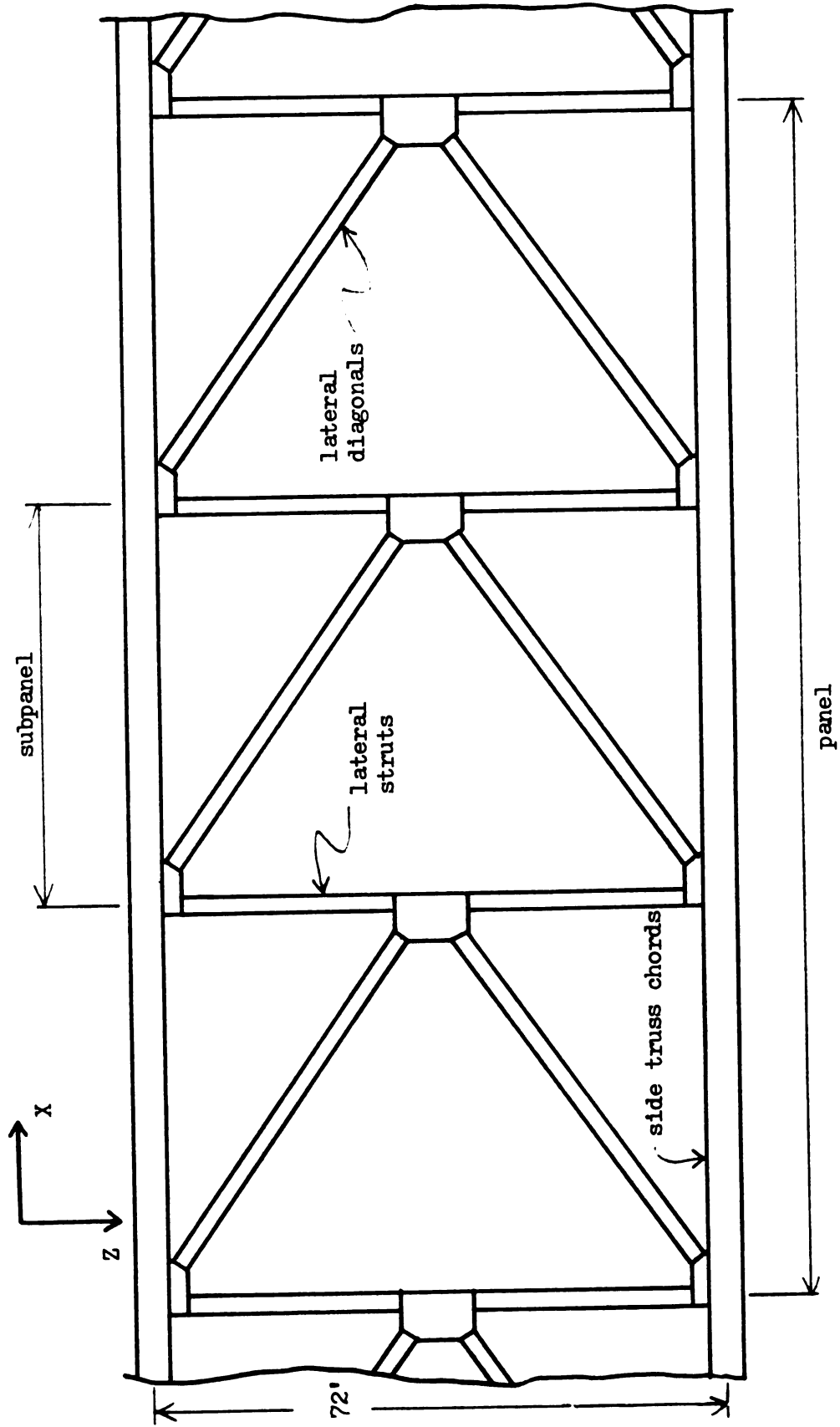
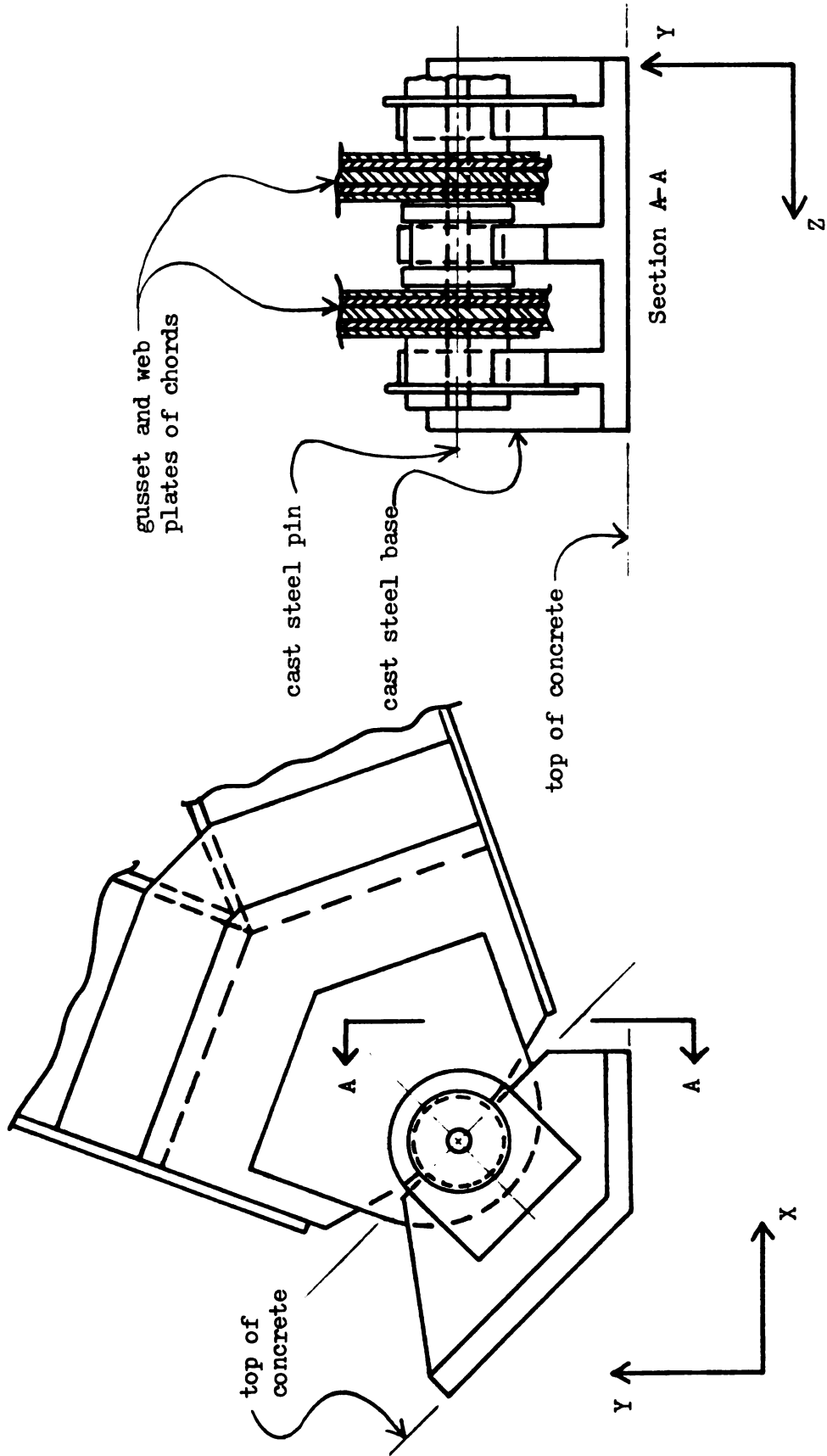


Figure B-2 NRCB Arch Lateral K-bracing



Figures B-3 NRCB Arch Hinges

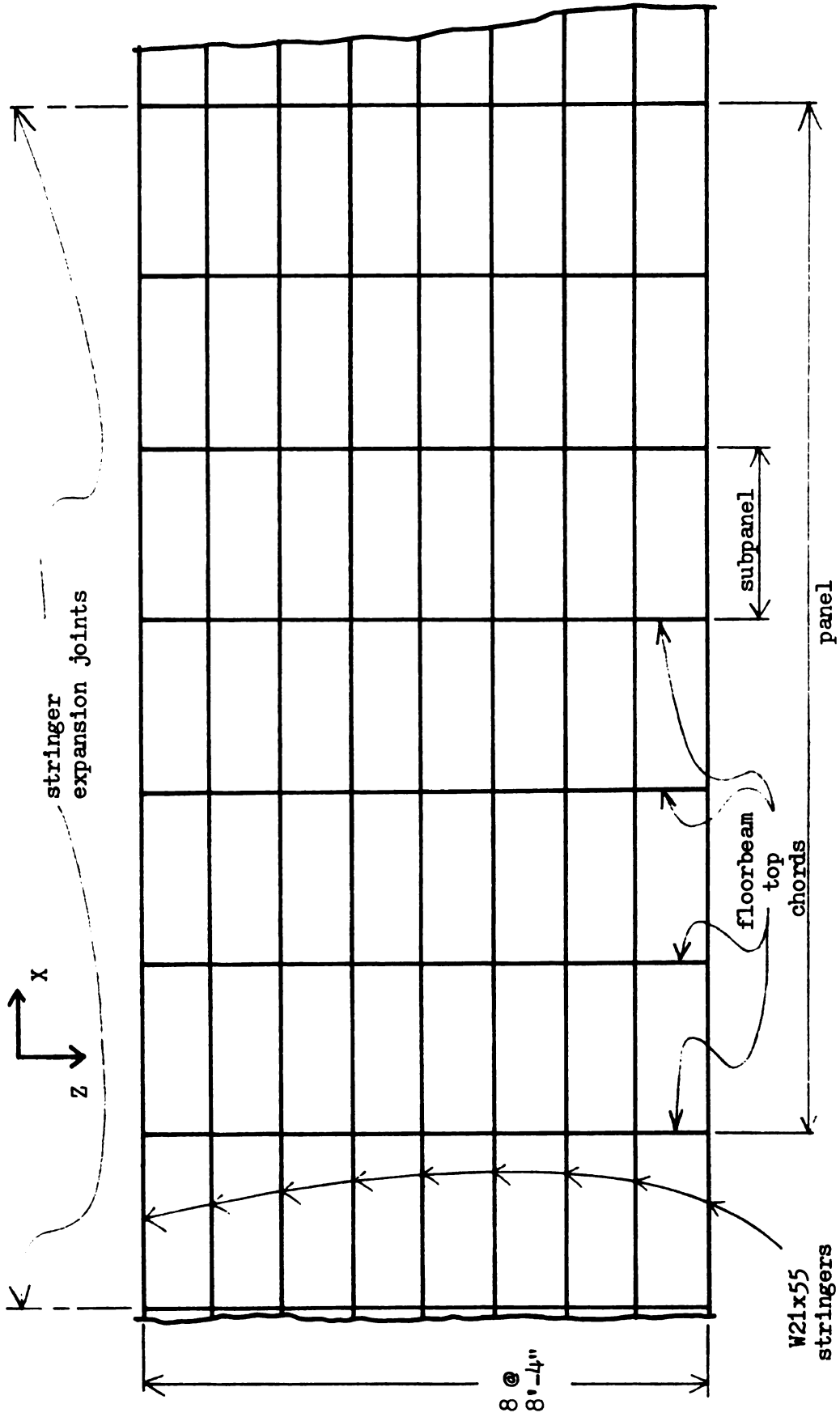


Figure B-4 NRCB Deck Floor Stringers

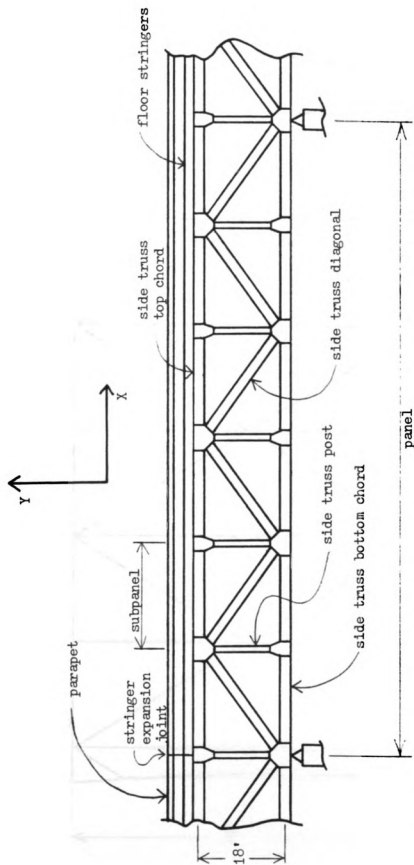


Figure B-5 NRCB Deck Side Truss

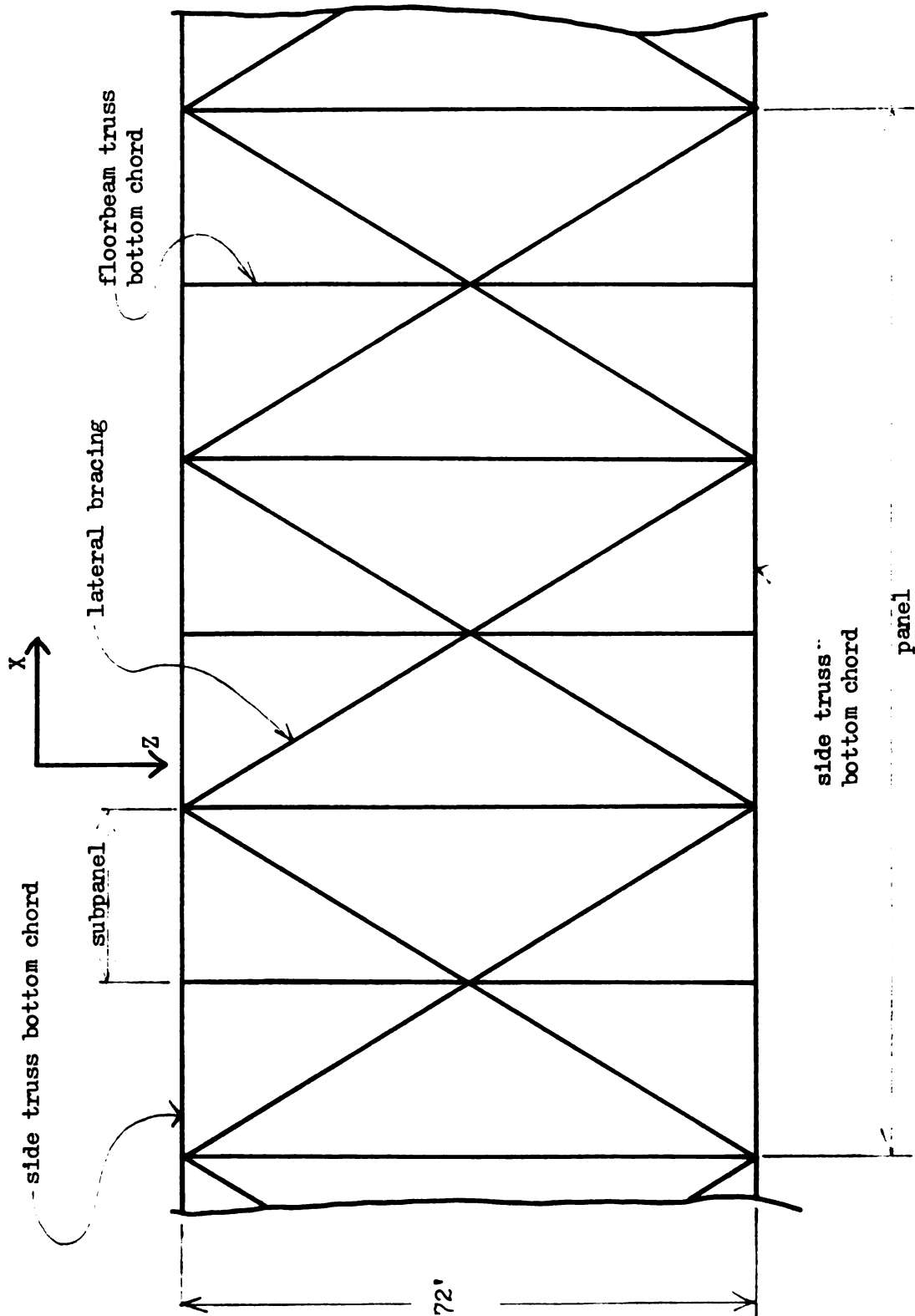


Figure B-6 NRGB Deck Lateral X-bracing

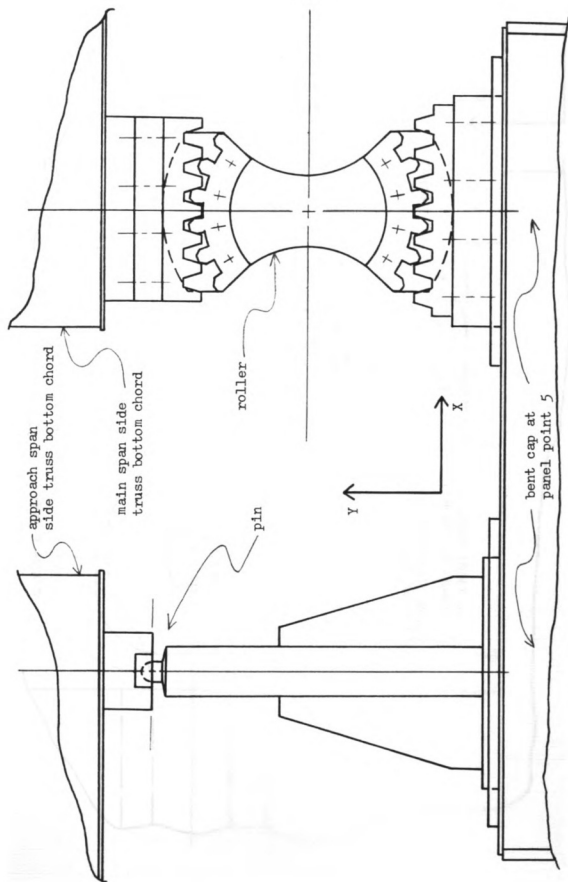


Figure B-7 NRCB Deck Expansion Joint Connections

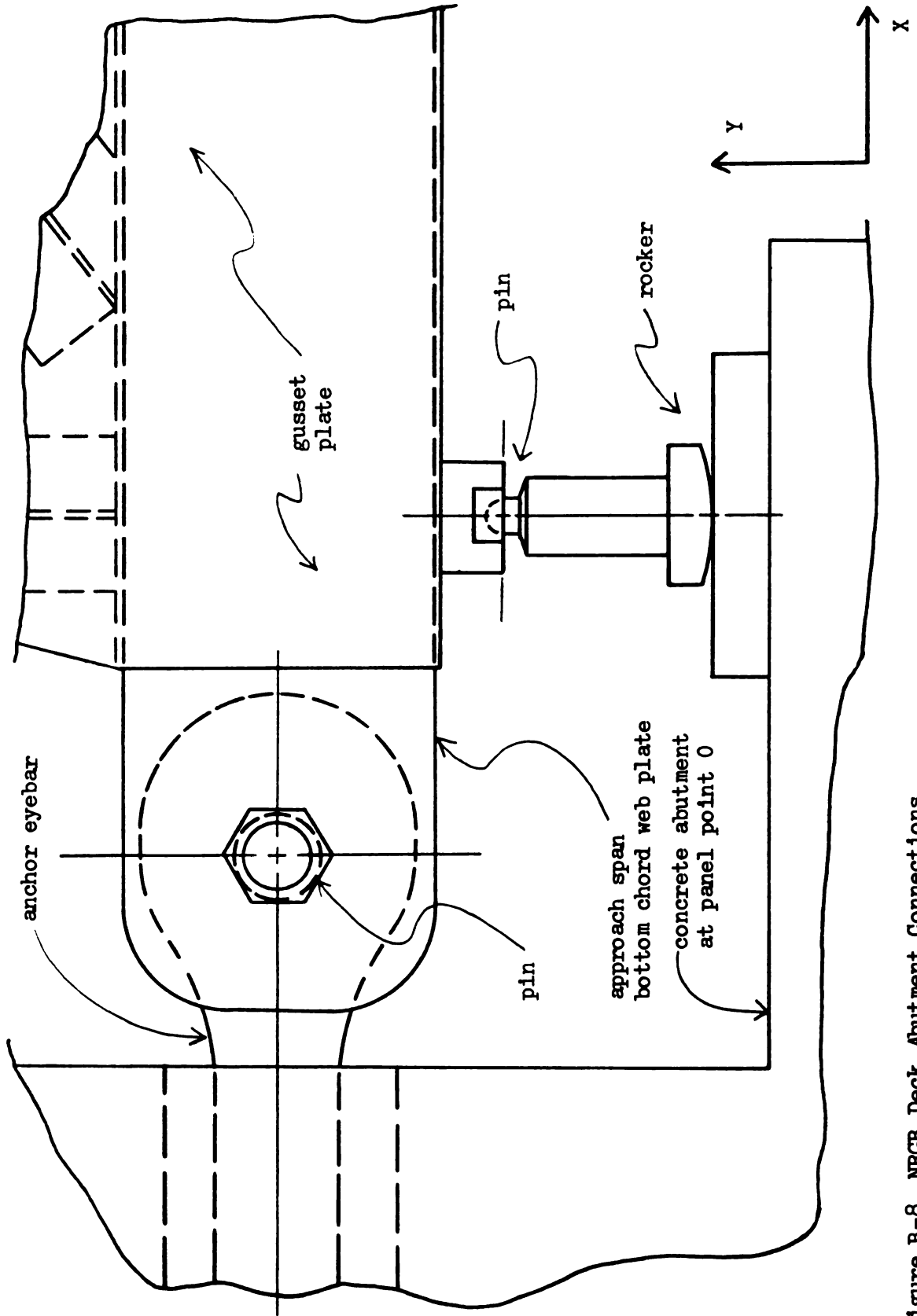
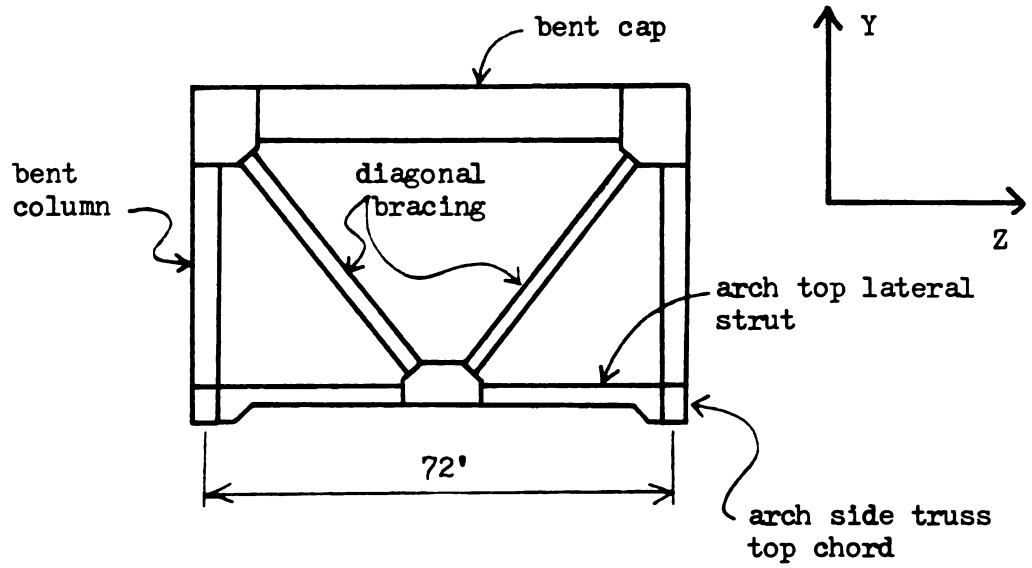
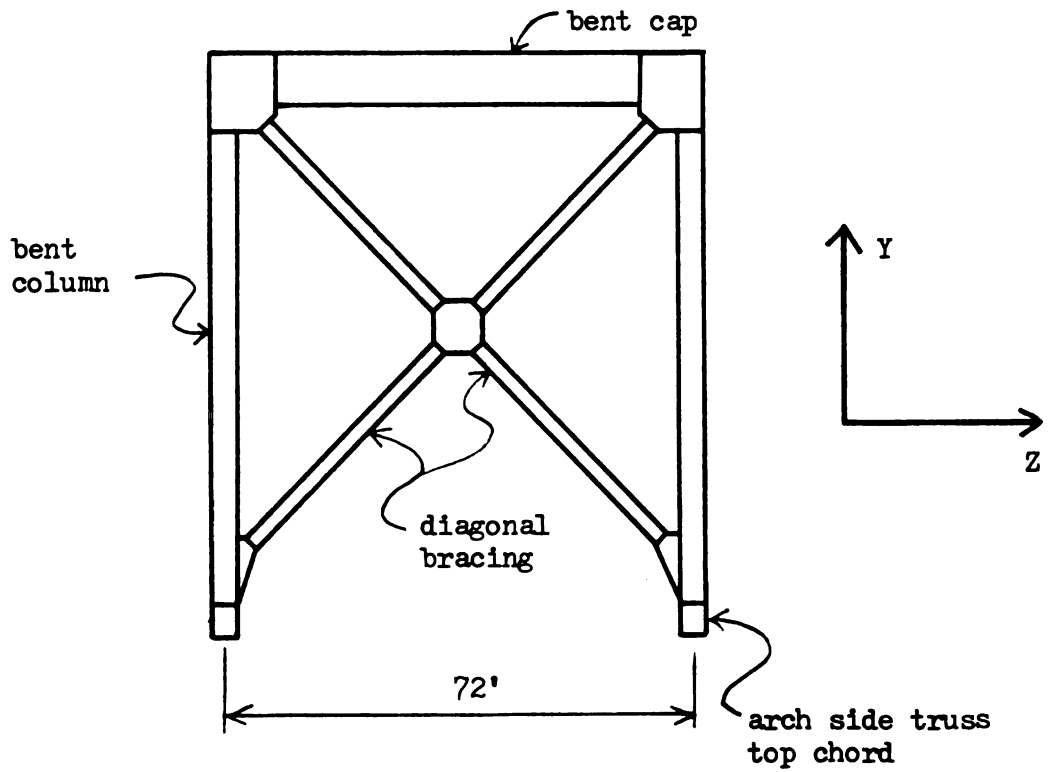


Figure B-8 NRCB Deck Abutment Connections

351



a) Bent 10



b) Bent 9

Figure B-9 NRGB Typical Bents

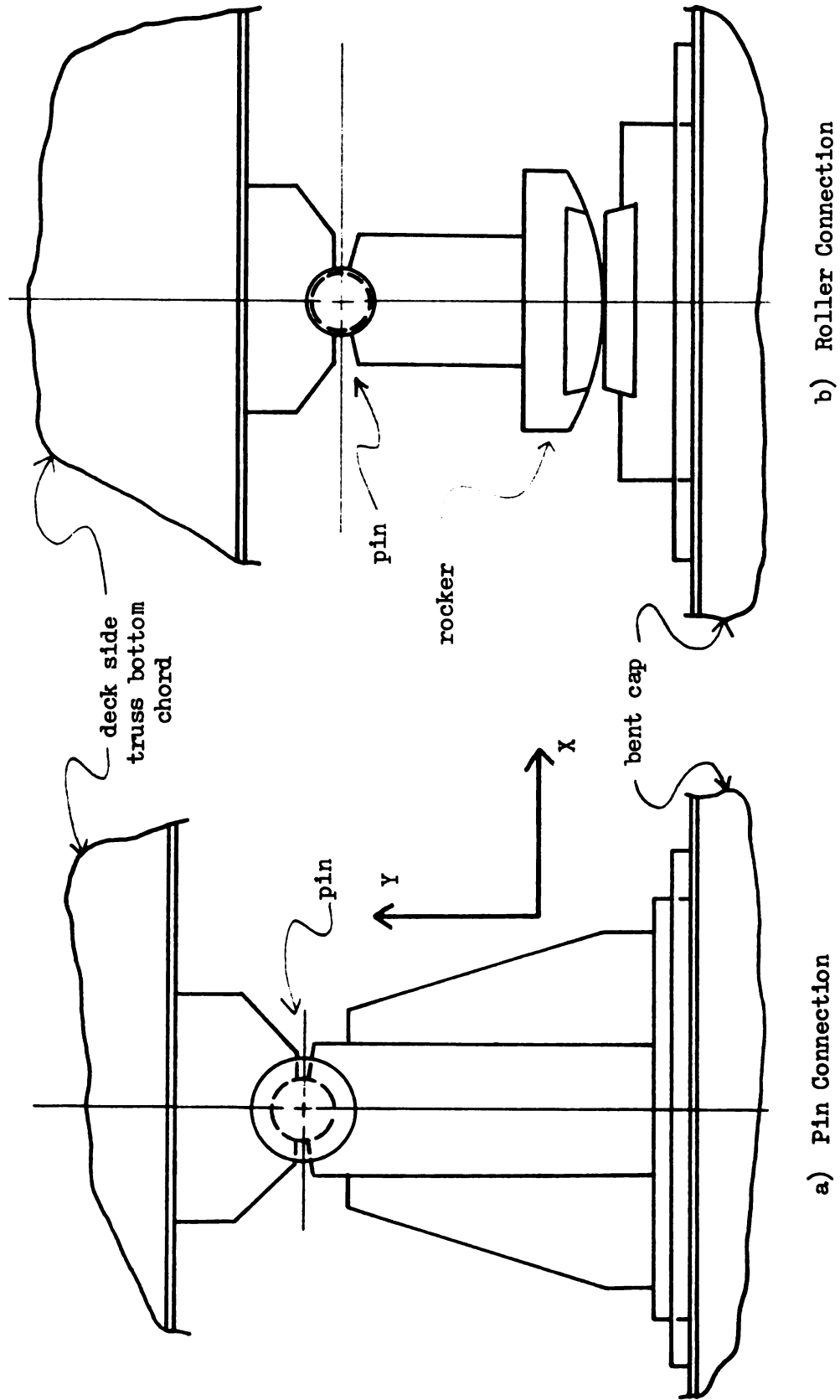


Figure B-10 NRCB Bent Cap to Deck Connections

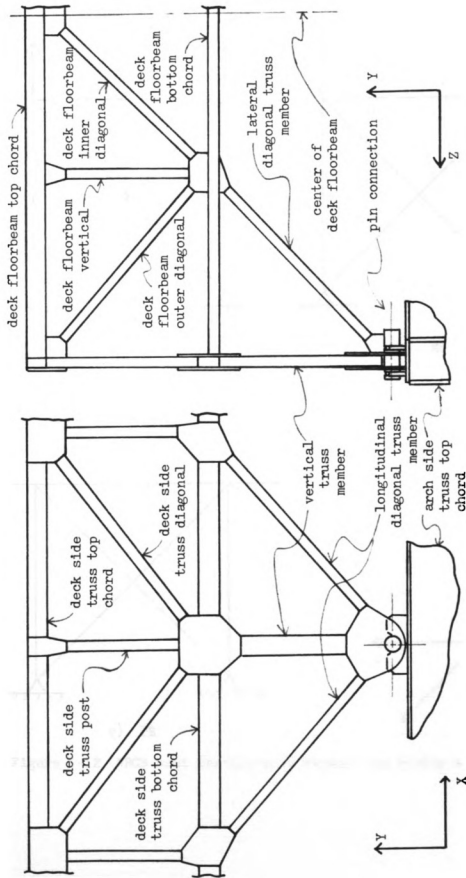
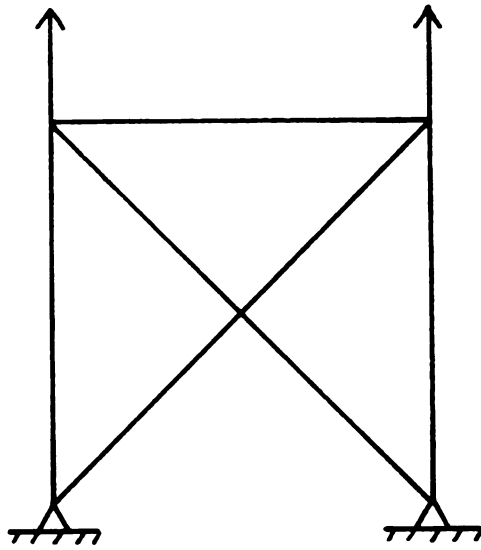
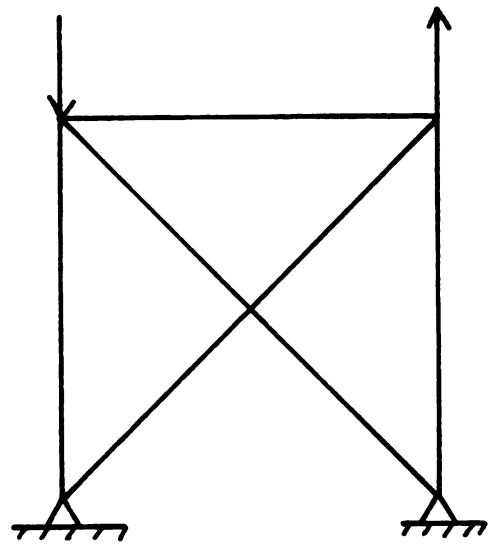


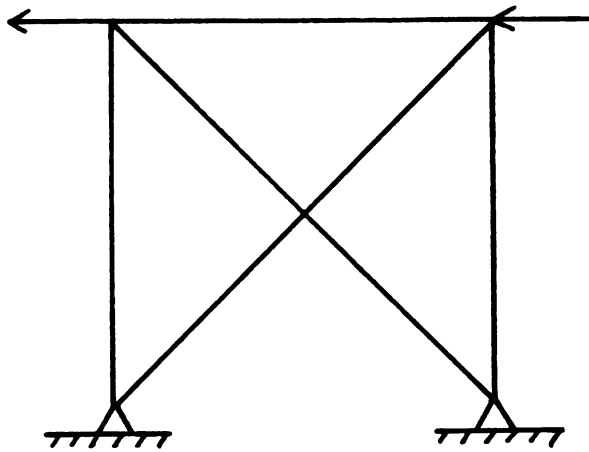
Figure B-11 NRCB Bent 12



a) PY



b) MX



c) PZ

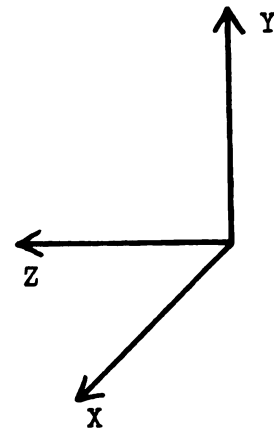


Figure B-12 NRGB Bent Cantilevered Segment End Fixity and End Loads

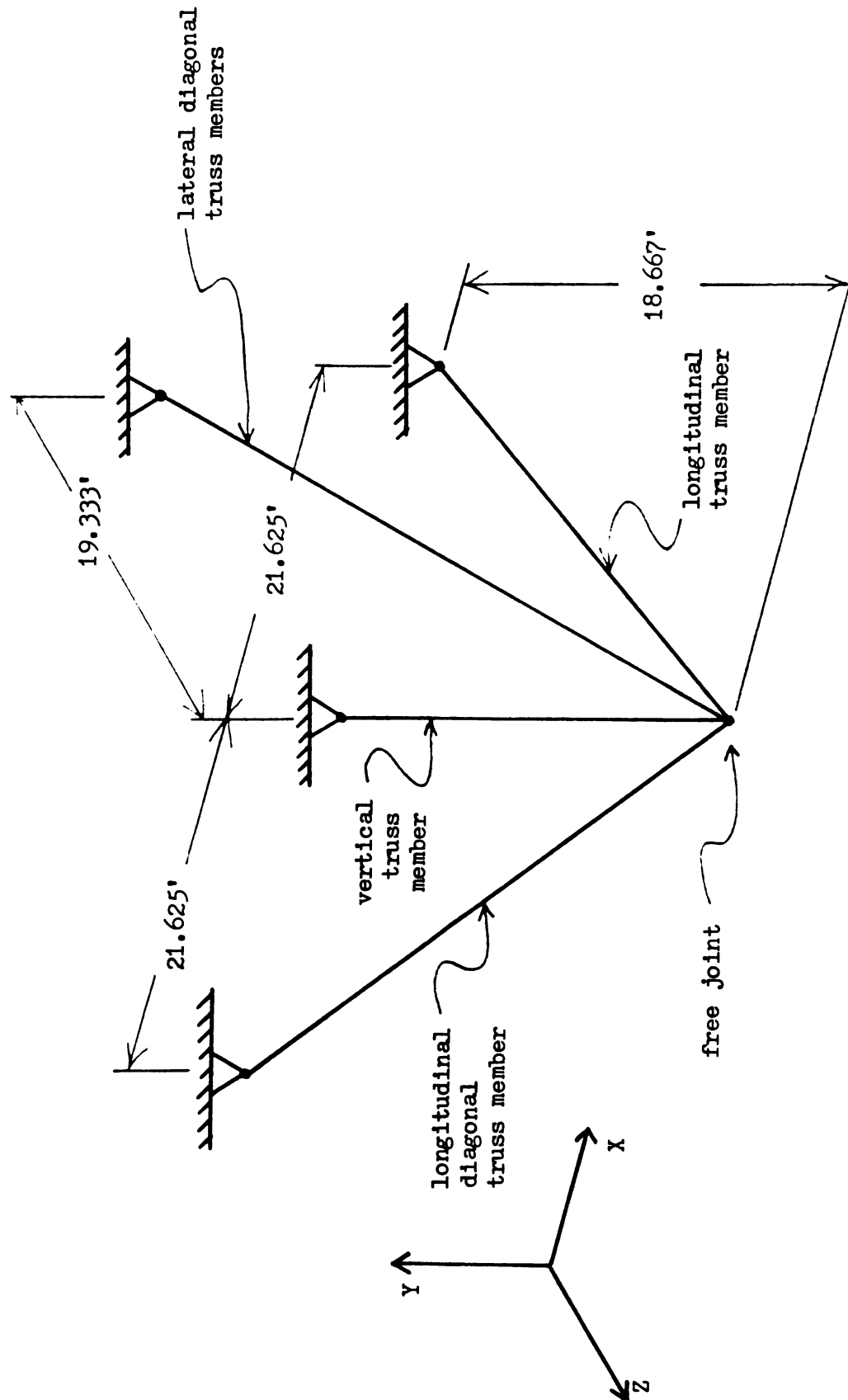


Figure B-13 NRCB Bent 12 Model

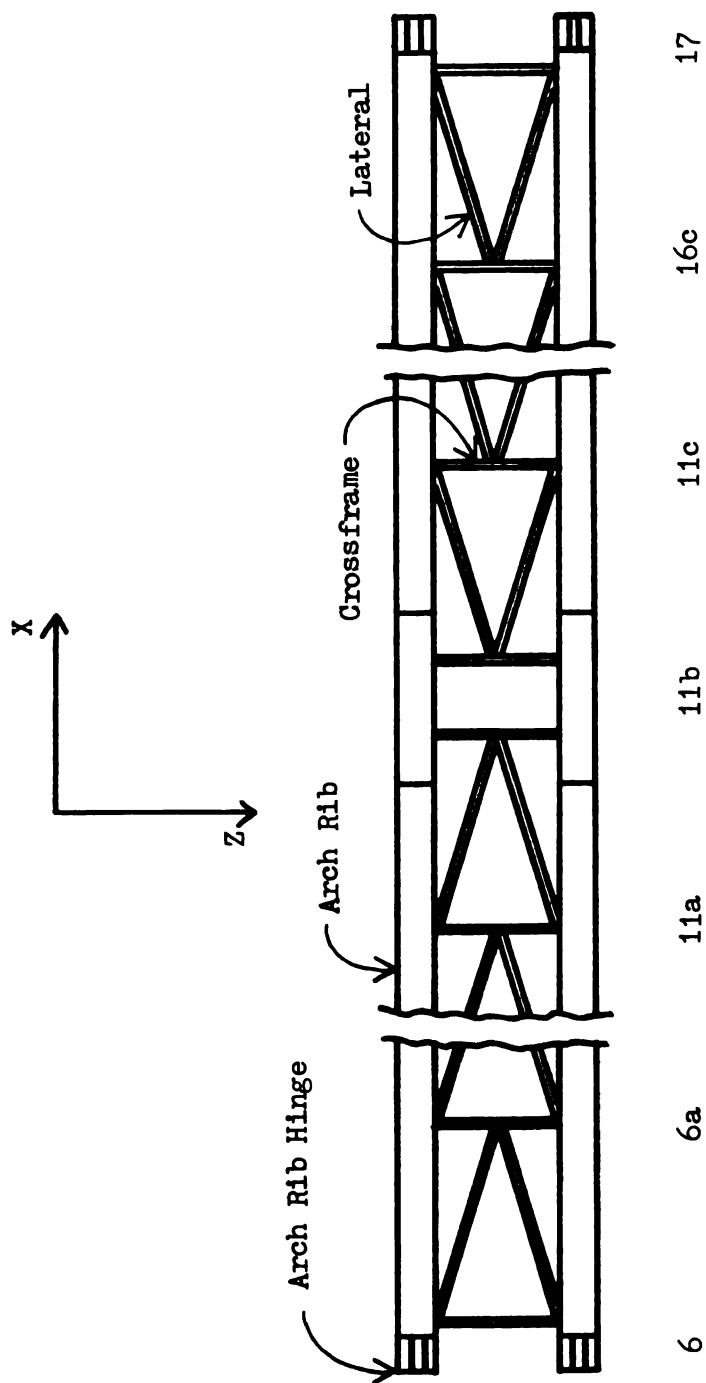


Figure B-14 CSCB Arch Lateral K-bracing

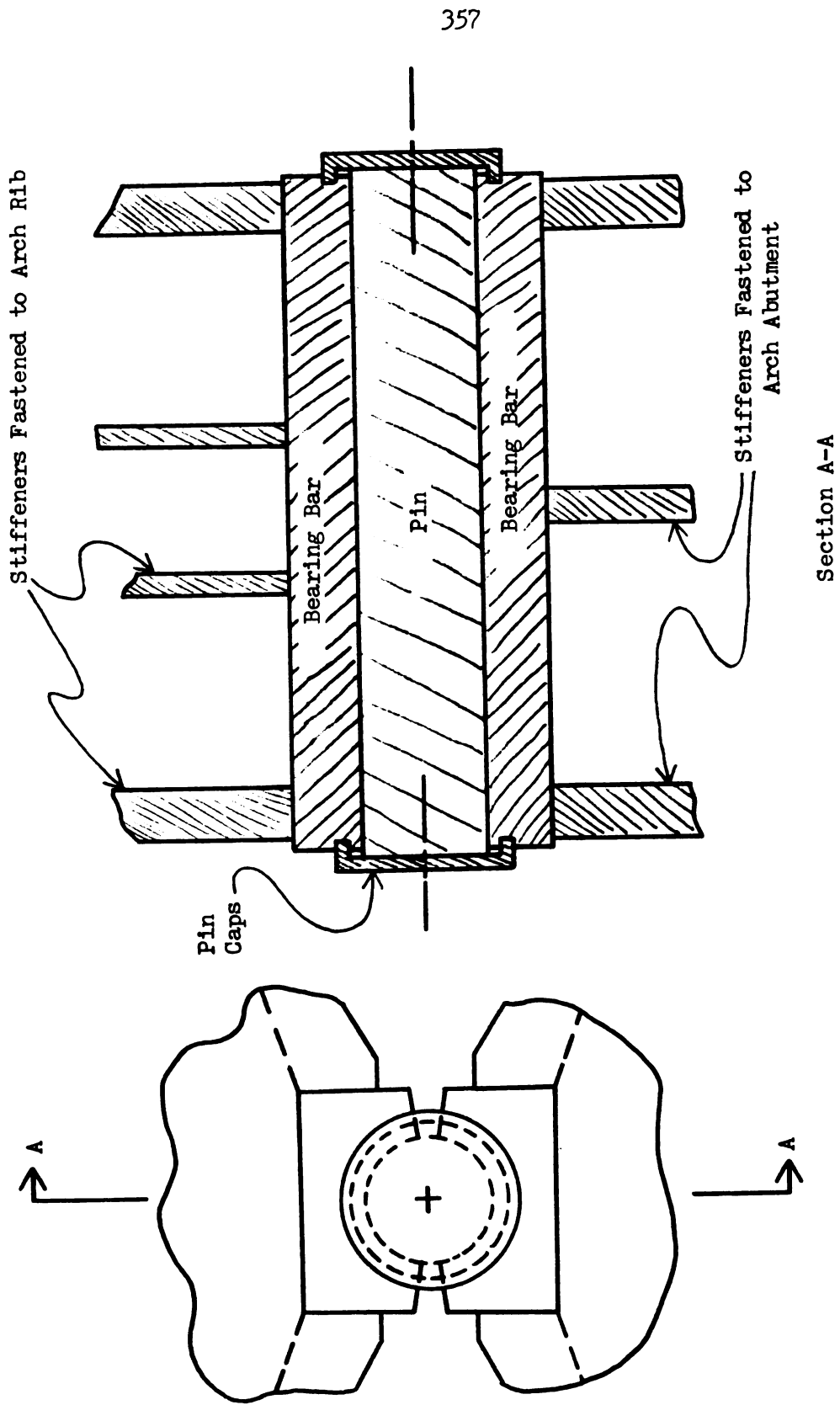


Figure B-15 GSCB Arch Hinges

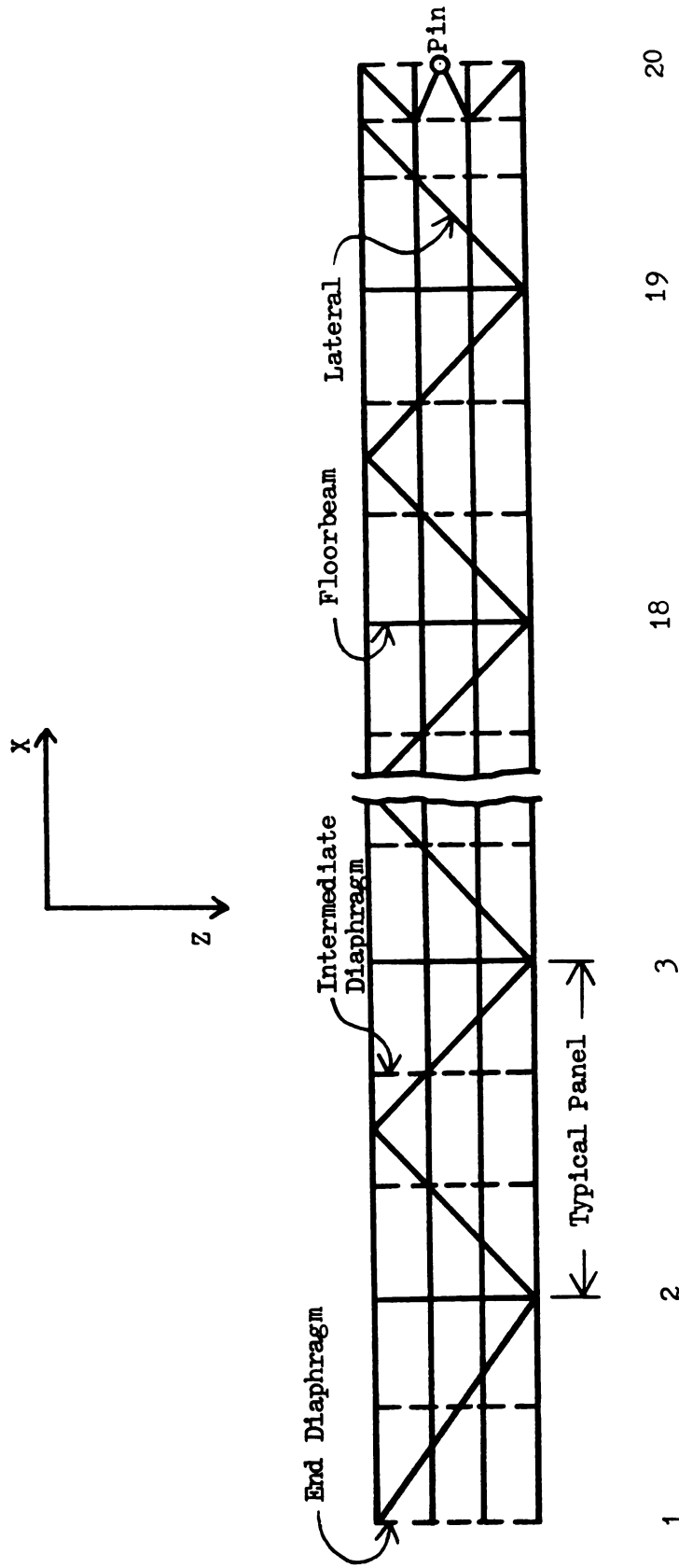


Figure B-16 CSCB Deck Lateral Bracing

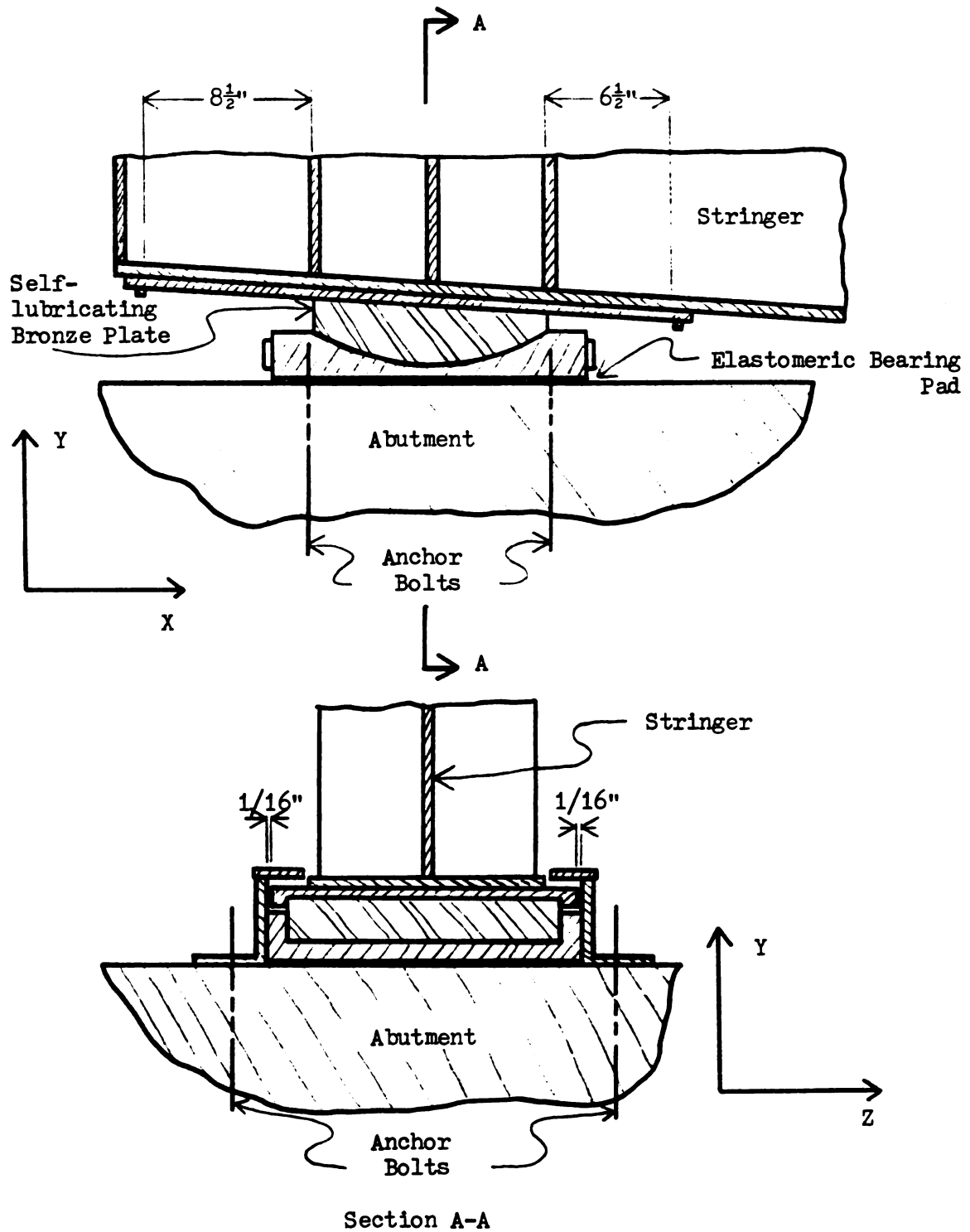


Figure B-17 CSCB Deck Expansion Connections at Panel Point 1

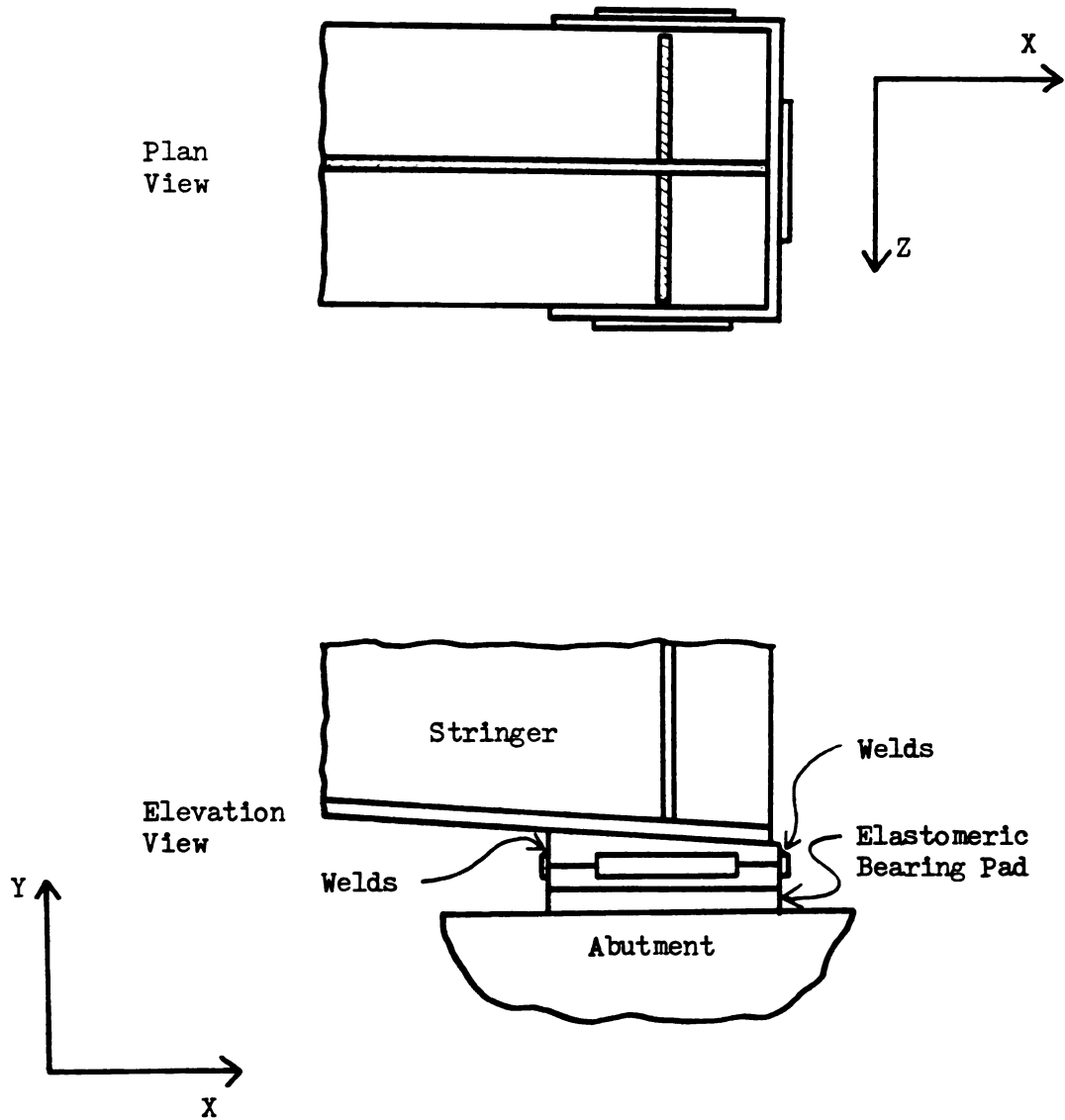


Figure B-18 CSCB Deck Bearing Connections at Panel Point 20

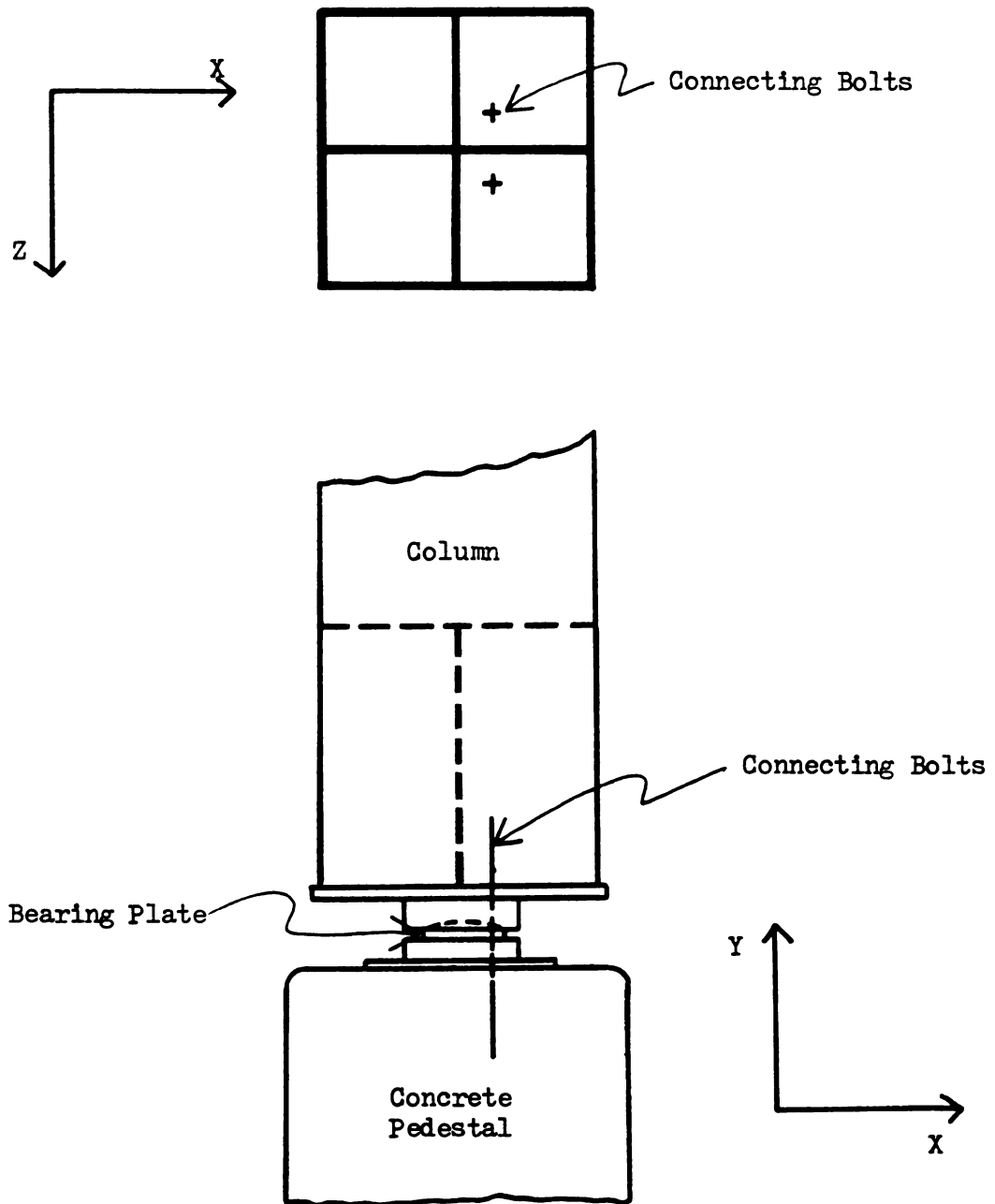


Figure B-19 CSCB Column Cross-section and Pedestal Connections

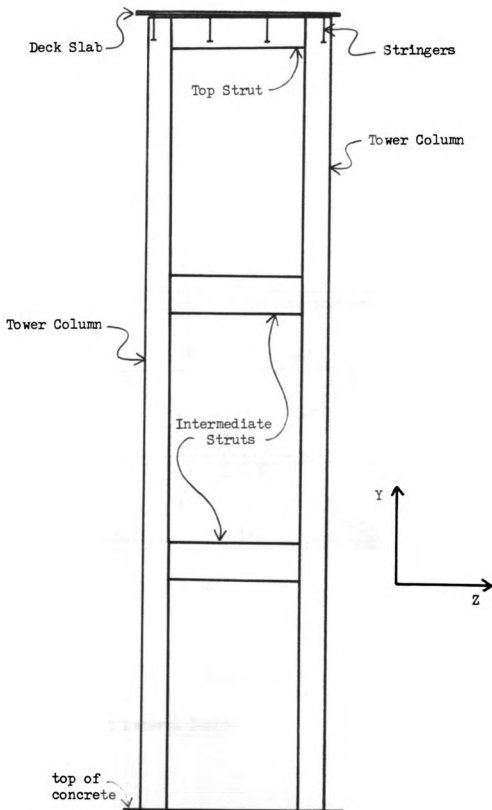


Figure B-20 CSCB Tower Elevation View

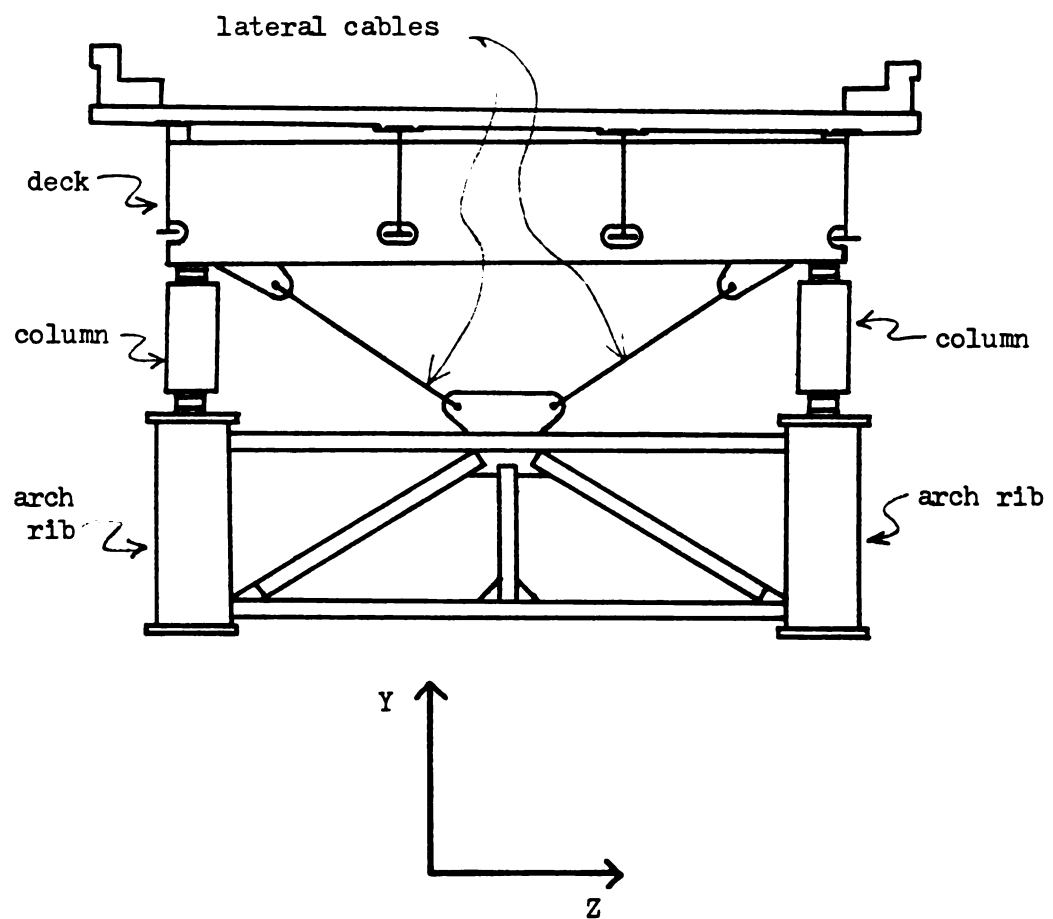


Figure B-21 CSCB Lateral Cables

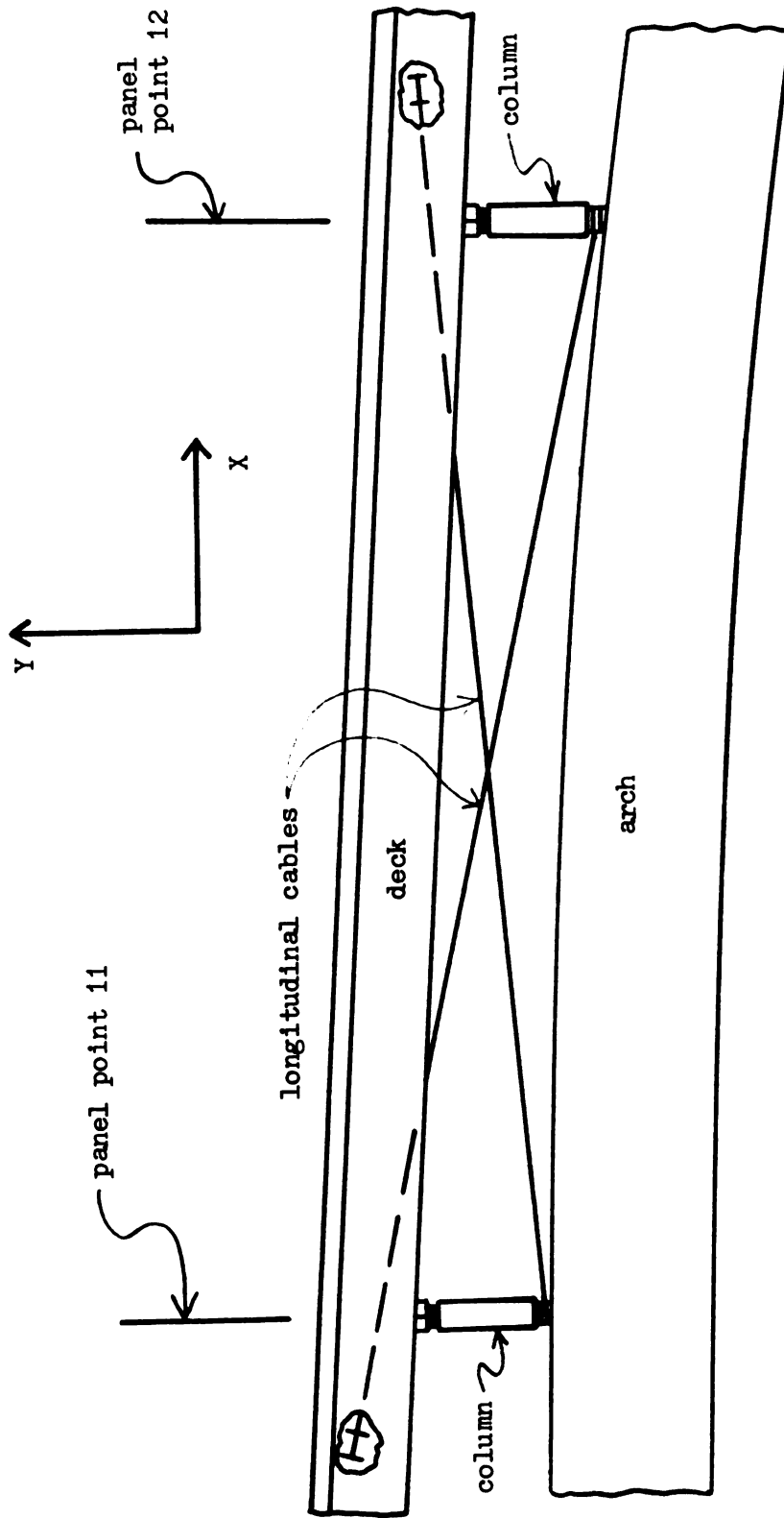


Figure B-22 CSCB Longitudinal Cables

The diagram shows a cable structure. A vertical column is positioned 14' from the left edge. The cable is supported by a pin support at the bottom of the column and a roller support at the right end. The horizontal distance between the column and the roller support is 63.635'. The cable is labeled 'longitudinal cable'. The top of the column is labeled 'free joint'. The diagram also shows 'panel point 11' at the column base and 'panel point 12' at the roller support. A coordinate system with X and Y axes is shown on the left.

Diagram illustrating the Longitudinal Cable Model 2. The model shows a cable supported by a column and a free joint. The horizontal distance between the support points is 63.635'. The vertical distance between the support points is 5.6'. The cable is labeled "longitudinal cable". The support points are labeled "panel point 11" and "panel point 12". The column is labeled "column". The free joint is labeled "free joint". A coordinate system (X, Y) is shown at the bottom right.

c) Longitudinal Cable Model 2

Figure B-23 CSCB Cable Models

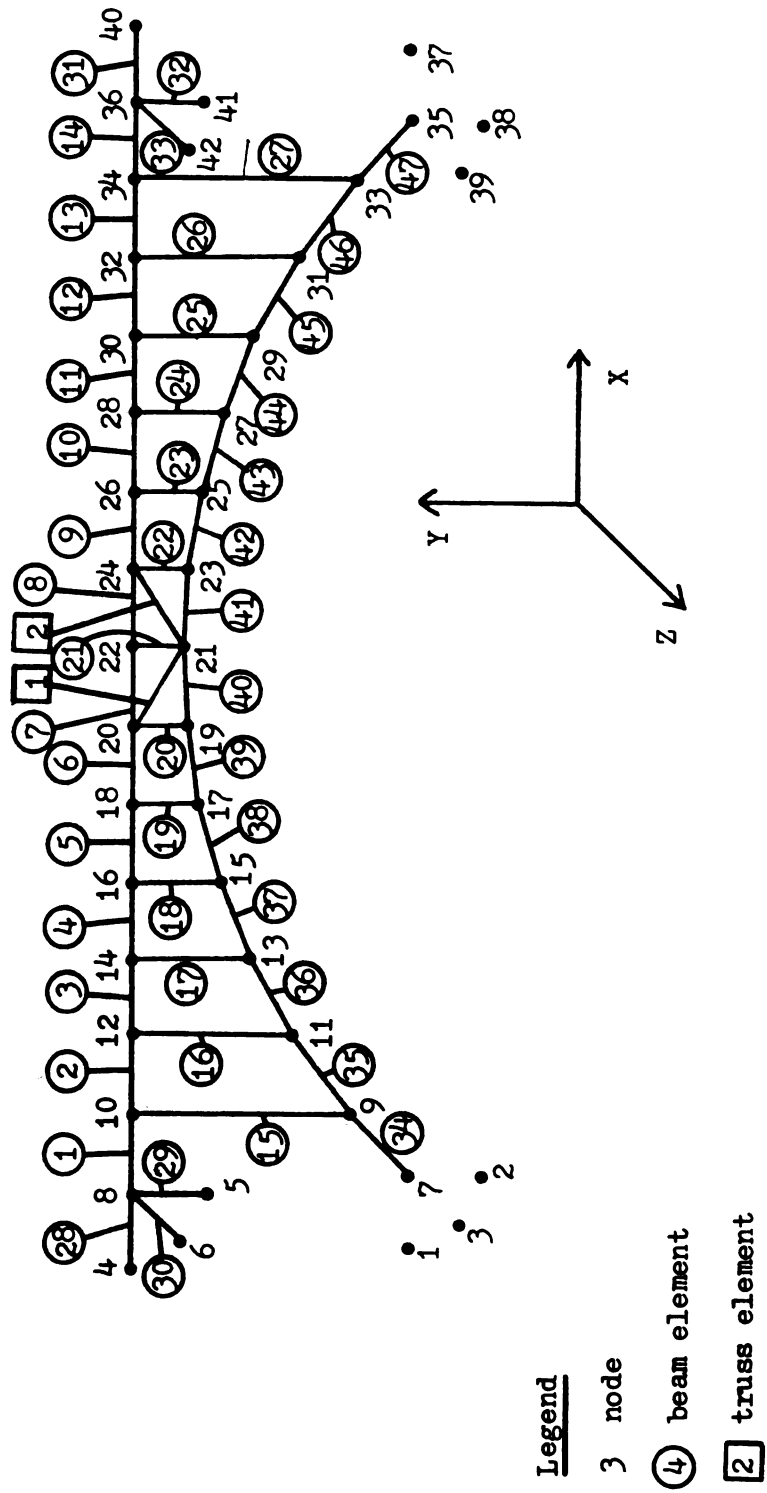


Figure B-24 NRGB Node and Element Numbers

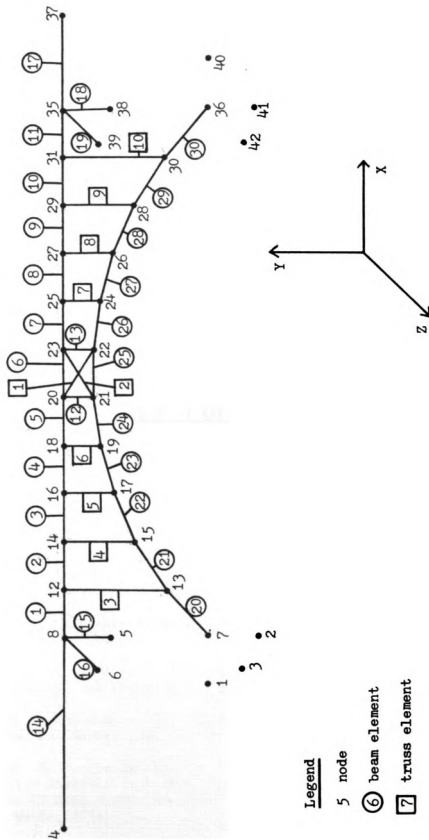


Figure B-25 CSCE Node and Element Numbers

LIST OF REFERENCES

LIST OF REFERENCES

1. Tseng, W. S. and Penzien, J., "Seismic Response of Long Multi-span Highway Bridges", Earthquake Engineering and Structural Dynamics, Volume 4, pages 25-48, 1975.
2. Abdel-Ghaffer, A. M., "Dynamic Analyses of Suspension Bridge Structures", California Institute of Technology, Report No. EERL 76-01, Earthquake Engineering Research Laboratory, Pasadena, California, May 1976.
3. Dusseau, R. A., "Seismic Analyses of Two Steel Deck Arch Bridges", M. S. Thesis, Department of Civil and Sanitary Engineering, Michigan State University, East Lansing, Michigan, March 1982.
4. Dusseau, R. A. and Wen, R. K., "Seismic Responses of Two Deck Arch Bridges", American Society of Civil Engineers, Meeting Preprint 82-010, Las Vegas, Nevada, April 1982.
5. Gates, J. M., "Factors Considered in the Development of the California Seismic Design Criteria", Proceedings of a Workshop on Earthquake Resistance of Highway Bridges, pages 142-162, Applied Technology Council, Palo Alto, California, January 1979.
6. AASHTO, "Standard Specifications for Highway Bridges", American Association of State Highway and Transportation Officials, 13th Edition, Washington, D.C., 1984.
7. Jennings, P. C., Housner, G. W., and Tsai, N. C., "Simulated Earthquake Motions", California Institute of Technology, Earthquake Engineering Research Laboratory, Pasadena, California, April 1968.
8. Bathe, K. J., "Finite Element Procedures in Engineering Analysis", Prentice-Hall, Inc., Englewood Cliffs, New Jersey, 1982.
9. Clough, R. W. and Penzien, J., "Dynamics of Structures", McGraw-Hill Book Company, New York, 1975.
10. Chen, W. F. and Atsuta, T., "Theory of Beam-Columns, Volume 2: Space Behavior and Design", McGraw-Hill, Inc., 1977.
11. Davidson, B. J. and Medland, I. C., "A Finite Element Approach To Stability Analysis in Frames (Including Warping Effects)", Finite Element Methods in Engineering, pages 621-637, University of New South Wales, 1974.

12. Gere, J. M. and Weaver, W., "Analysis of Framed Structures", D. Van Nostrand Reinhold Company, New York, New York, 1965.
13. Cook, D. C., "Concepts and Applications of Finite Element Analysis", John Wiley & Sons, Inc., New York, New York, 1974.
14. Merritt, F. S., "Structural Steel Designer's Handbook", McGraw-Hill Book Company, New York, 1972.
15. Newmark, N. M. and Rosenblueth, E., "Fundamentals of Earthquake Engineering", Prentice-Hall, Inc., Englewood Cliffs, New Jersey, 1971.

MICHIGAN STATE UNIV. LIBRARIES



31293107001954